

The impact and deformation of press-fit metal acetabular components

Hothi, Hardip Singh

The copyright of this thesis rests with the author and no quotation from it or information derived from it may be published without the prior written consent of the author

For additional information about this publication click this link.

<http://qmro.qmul.ac.uk/jspui/handle/123456789/3117>

Information about this research object was correct at the time of download; we occasionally make corrections to records, please therefore check the published record when citing. For more information contact scholarlycommunications@qmul.ac.uk

Queen Mary University of London
School of Engineering and Materials Science

**The Impact and Deformation of
Press-Fit Metal Acetabular
Components**

By

Hardip Singh Hothi

Thesis submitted for the degree of Doctor of Philosophy

June 2012

Abstract

Early failure of some metal-on-metal (MoM) hip implants are extensively reported but not fully explained. These arthroplasties commonly utilise large-diameter, thin-walled acetabular cups that have the advantage of minimal removal of acetabular bone and a reduced chance of dislocation; however they may deform during insertion which involves impaction. The role of diametrical cup deformation as a factor to unsatisfactory implant performance has not been widely reported. The aim of this thesis was to investigate the extent to which deformations may occur in clinically relevant situations and to assess the significance of a range of variables on the deformation generated.

2D axisymmetric finite element (FE) models established a method of simulating impaction using different momentums. Experimentally validated 3D foam models showed that deformation is clearly influenced by the orientation of the cup, the support of the underlying bone and the geometry of the component itself.

CT scans of the pelvis from 8 similarly sized female patients from two discrete age populations were used to develop clinically relevant FE models. Cup deformations were found to occur due to pinching between the iliac and ilial regions and were significant when compared to typical minimum diametrical clearances of 80-120 μm . In young pelvis models deformations of 34–63 μm were found to be significantly greater than in the older pelvis models, $p < 0.001$. Surprisingly, small changes in the cup version increased deformations by up to 40% from the surgeon identified optimal position and were 30% greater when an eccentricity was introduced into the reamed acetabulum.

The local deformations estimated in the acetabular cups may cause localised reductions in the fluid-film thickness, resulting in regions where boundary, rather than mixed lubrication takes place. This may help explain why failure and high wear rates are sometimes found in young patients with acetabular components positioned in clinically optimal positions.

Table of Contents

ABSTRACT	2
TABLE OF CONTENTS	3
LIST OF FIGURES	7
LIST OF TABLES	12
ACKNOWLEDGEMENTS	14
CHAPTER 1: INTRODUCTION	15
CHAPTER 2: LITERATURE REVIEW	18
2.1 Anatomical Reference Planes and Terms	18
2.2 Anatomy of the Hip Joint	19
2.2.1 Function of the Hip	19
2.2.2 The Hip Joint	20
2.2.3 Structure of the Pelvis	21
2.2.4 Bone Structure in the Pelvis	22
2.3 Common Indicators for a Hip Replacement	23
2.4 History of Hip Arthroplasty	24
2.4.1 Total Hip Replacement	26
2.4.2 Hip Resurfacing	27
2.4.3 Failure of Early Hip Resurfacing Designs	28
2.4.4 Re-Introduction of Metal-on-Metal Bearings	29
2.5 Modern Hip Replacement Acetabular Components	30
2.5.1 Cup-Head Articulating Surfaces	31
2.5.2 Orientation of Acetabular Cups	31
2.5.3 Current Cementless Designs	33
2.5.4 Supplementary Fixation	33
2.5.5 Press-Fit Fixation	34
2.5.5.1 <i>Incidence of Polar Gaps</i>	35
2.5.5.2 <i>Influence of Interference Size on Fixation Stability</i>	36
2.5.5.3 <i>Effect of Press-Fit Fixation on Surrounding Bone</i>	37
2.6 Recent Metal-on-Metal Designs	38
2.6.1 Causes of Failure of Hip Replacements	40
2.6.2 Indicators for Revision Surgery	43
2.7 Implant Tribology	44
2.8 Concerns Surrounding the use of Metal-on-Metal Implants	50
2.8.1 Uncertainty of the Factors Causing MoM Problems	53
2.9 Deformation of Acetabular Cups	54

2.9.1	Experimental Methods	54
2.9.2	Finite Element Modelling	62
2.9.3	Finite Element Models of Acetabular Cups and Shells	65
2.10	Aims and Objectives	69
CHAPTER 3: 2D FOAM MODEL DEVELOPMENT AND METHODS		70
3.1	Introduction	70
3.2	Static Implicit 2D Model Development	71
3.2.1	Meshing of Static Implicit 2D Model	73
3.2.2	Boundary Conditions and Interaction Properties in Static 2D Model	76
3.3	Application of Load in Static 2D Model	77
3.3.1	Results	79
3.3.2	Discussion	85
3.4	Development of Dynamic 2D Axisymmetric Model	86
3.4.1	Single Cup Impact	86
3.4.2	Multiple Cup Impacts	88
3.4.3	Definition of Material Properties	89
3.4.4	Addition of Rigid Cap between Cup and Impactor	90
3.5	Simulation Parameters	92
3.5.1	Method	92
3.5.2	Results	93
3.5.2	Discussion	96
3.6	Introduction of Plasticity into Foam Model	100
3.6.1	Method	100
3.6.2	Results	100
3.6.3	Discussion	101
3.7	Introduction of Viscoelastic Properties into Foam Model	102
3.7.1	Results	102
3.7.2	Discussion	102
3.8	Conclusions	103
CHAPTER 4: EXPERIMENTAL VALIDATION AND 3D CUP-FOAM MODEL DEVELOPMENT		104
4.1	Introduction	104
4.2	Experimental Cup Impaction Study	105
4.2.1	Experimental Methods	105
4.2.2	Impaction of the Cup	107
4.2.3	Results of Experimental Study	111
4.2.4	Discussion	116
4.3	Preliminary Finite Element Simulations using a 3D Cup Design	118
4.3.1	Preliminary FE Model Development	119

4.4	Development and Validation of a 3D FE Cup Impaction Model	123
4.4.1	Preliminary Model Development using Static Cup Insertion Loads	123
4.4.2	Development of a 3D Cup Impaction Model	124
4.4.3	Meshing and Material Property Definition of 3D FE Cup Impaction Model	126
4.4.4	Validation of Model using the Coefficient of Friction	129
4.4.5	Results	130
4.5	Influence of Cup Support and Misalignment on Deformation	135
4.5.1	Methods for Varying Cup Support and Alignment	136
4.5.2	Results: Influence of Varying Cup Support and Alignment on Deformation	138
4.5.3	Discussion	141
4.6	Influence of Impaction Method on Deformation	145
4.6.1	Methods	145
4.6.2	Results	146
4.7	Influence of the Geometry of the Cup on Deformation	146
4.7.1	Taguchi Design of Experiment to investigate the influence of cup geometry	147
4.7.2	Results	149
4.7.3	Discussion	151
4.8	Conclusions	153
CHAPTER 5: DEVELOPMENT OF ANATOMICALLY CORRECT FE MODELS OF THE PELVIS		154
5.1	Introduction	154
5.2	Development of FE Pelvis Model	154
5.2.1	Selection of Patient CT Data	156
5.2.2	Creation of 3D Model	157
5.2.3	Cup Size Selection and Reaming of Acetabulum	160
5.2.4	Initial Meshing of Pelvis Models	163
5.2.5	Definition of Pelvis Material Properties	165
5.2.6	Development of Impaction Model	168
5.2.7	Definition of Boundary Conditions	170
5.2.8	Definition of Contact Behaviour	171
5.2.8.1	<i>Tangential Condition: Sliding Formulation</i>	171
5.2.8.2	<i>Tangential Condition: Coefficient of Friction</i>	172
5.2.8.3	<i>Normal Condition</i>	172
5.2.9	Mesh Refinement	173
5.3	Influence of Cup Orientation	176
5.3.1	Simulation of the Cup Impaction in Surgeon Defined Orientations	176
5.4	Variation of Cup Orientation in Acetabular Cavity	181
5.4.1	Results: Influence of Cup Position on Deformation	182
5.4.2	Discussion	187
5.5	Introduction of an Eccentricity in the Cavity during Hand Reaming	190

5.5.1	Results.....	191
5.5.2	Discussion	192
5.6	Definition of Time Dependent Properties in the Pelvis Cavity	192
5.6.1	Results.....	194
5.6.2	Discussion	195
5.7	Influence of the Material and Geometry of the Acetabular Component.....	196
5.7.1	Methods	196
5.7.2	Results	197
5.7.3	Discussion	198
5.8	Conclusions	199
CHAPTER 6: DISCUSSION, CONCLUSIONS AND RECOMMENDATIONS FOR FUTURE WORK.....		200
6.1	Significance of Cup Deformation	209
6.2	Recommendations for Future Work	210
APPENDIX: PUBLICATIONS AND PRESENTATIONS OF THE WORK OF THE THESIS		212
REFERENCES		213

List of Figures

Figure 2.1	Reference planes used to describe the human anatomy	18
Figure 2.2	Terms used to describe different regions of the body	19
Figure 2.3	Key features of the hip joint	20
Figure 2.4	Structure of the pelvis	21
Figure 2.5	Key bony regions of the right hemi-pelvis	21
Figure 2.6	(a) Total hip replacement (THR) and (b) Hip resurfacing replacement	24
Figure 2.7	The evolution of Total Hip Replacement designs	26
Figure 2.8	The Charnley press-fit Teflon-on-Teflon design	27
Figure 2.9	(a) Angle of cup abduction and (b) cup version	32
Figure 2.10	Distribution of acetabular cup orientations in 105 patients with MoM implants	32
Figure 2.11	Large surface area contact between cup and bone shown by dark patches on reverse of cup lined by a pressure sensitive film after impaction into cadaveric models	35
Figure 2.12	Incidence of polar gap at insertion and bone growth across gap after several years ..	36
Figure 2.13	Highest strains visible at periphery of acetabular bone	37
Figure 2.14	Number of MoM implanted by head size	38
Figure 2.15	Schematic representing a peak above the articulating surface of a component, indicating roughness	45
Figure 2.16	(a) Lambda value greater than 3, indicating full fluid-film lubrication, (b) lambda values between 1 and 3, indicating mixed lubrication and (c) lambda ration less than 1 indicating boundary lubrication	46
Figure 2.17	The coefficient of friction is related to the film thickness and therefore mode of lubrication	47
Figure 2.18	Influence of femoral head diameter on volumetric wear rates	48
Figure 2.19	Measurement of points on articulating surface of cup to determine sphericity	49
Figure 2.20	Radial Clearance determined by calculating the difference between the outer radius of the head and the inner radius of the cup	49
Figure 2.21	Distribution of strain gauges within the various acetabular cups	56
Figure 2.22	Pinching in the pelvis simulated in experimental foam models by (a) Jin et al [2006] and (b) Schmidig et al [2010]	57
Figure 2.23	Compressive loads applied to cup along diameter using custom load platens	59
Figure 2.24	Radial deformation observed by Springer et al. [2012] for different cup designs following rim loading with a 1000 N load	61
Figure 2.25	Calculated stiffness values for different cup sizes by various manufacturers	62
Figure 2.26	Elements are connected together at nodes to form a mesh	63
Figure 2.27	Finite element simulation of the rim loading used experimentally	65
Figure 2.28	2D finite element model of insertion of press-fit cup with interference	66
Figure 2.29	Finite element model created of pelvis and hammer	67

Figure 3.1	Construction of cup 'part' in Abaqus CAE	71
Figure 3.2	Cross-sectional dimensions of acetabular cup in foam cavity	72
Figure 3.3	(a) the sharp corner at the point of contact between cup and cavity and (b) the introduction of a fillet to allow cup to move properly into the cavity	73
Figure 3.4	Axisymmetric finite element model of the acetabular cup and foam cavity	74
Figure 3.5	A schematic representation of the load impulses applied to the acetabular cup	78
Figure 3.6	Deformation of 60mm Cup with 0.5mm Interference	80
Figure 3.7	Deformation of 60mm Cup at different interferences (Friction = 0.3)	81
Figure 3.8	Polar Gap Remaining with 1mm Interference at different coefficients of friction	83
Figure 3.9	Polar Gap Remaining with different interferences (Friction = 0.3)	83
Figure 3.10	Contact Area (%) - 1mm Interference	84
Figure 3.11	Axisymmetric finite element model of the acetabular cup, foam cavity and impactor	87
Figure 3.12	Axisymmetric finite element model of the cup, foam cavity and impactors	88
Figure 3.13	Axisymmetric finite element model of cup impaction with rigid cap	91
Figure 3.14	Definition of Multi-point constraint between cup and cap	91
Figure 3.15	Polar gap observed after impaction at 1.5 m/s at different interferences with a coefficient of friction of 0.3	93
Figure 3.16	Cup Deformation observed after impaction of Co-Cr cup at 1 m/s with an interference of 1mm and a friction coefficient of 0.3 *Cup fully seated at this point and locked cap released from cup and removed	96
Figure 3.17	Diametrical cup deformation after impaction at 1m/s with 1mm interference and coefficient of friction of 0.3 - comparison of viscoelastic and elastic foam after polar impaction	102
Figure 4.1	CoCrMo Cup impacted into foam cavity representing the human acetabulum	105
Figure 4.2	Cross-sectional dimensions, in mm, of the acetabular cup and foam cavity	106
Figure 4.3	Height of cup rim above cavity surface measured after each impact to determine polar gap	106
Figure 4.4	Foam block with a reamed cavity and a hole at the base to allow for removal of the cup	107
Figure 4.5	Impact Testing System used to perform impaction of cups into foam cavities clamped to rigid surface	108
Figure 4.6	CMM used to measure inner diameter of cups before and after insertion	109
Figure 4.7	Cup inserted into foam cavities by impacting on its rim using a free cap	109
Figure 4.8	Cup inserted into foam cavities by impacting on the cups inner polar surface	110
Figure 4.9	Mean polar gap remaining following impacts required to insert cups using impaction at the pole, around the rim (free rim) and on to a locked rim, with an impact velocity of 1 ms ⁻¹ and an interference of 1 mm. Arrows indicate that subsequent impacts reduce the polar gap remaining by less than 10 µm	114

Figure 4.10	Out of “Roundness” plots determined using a CMM for a cup measured (a) immediately after impaction and (b) 24 hours after impaction. Cup deformations were recorded as the maximum reduction in diameter in each measurement 115
Figure 4.11	Change in deformation of a period of 24 hours following impaction in Airex foam ... 116
Figure 4.12	Titanium acetabular shells subjected to rim loading 118
Figure 4.13	Showing (a) the direction of the point loads applied at the cup rim and (b) the resulting unrealistic deformations that were observed 119
Figure 4.14	Showing the area on the rim where the opposing pressure was applied (in red)..... 120
Figure 4.15	Mesh convergence achieved by increasing the number of elements in model 121
Figure 4.16	Graph showing the deformations observed as the rim point load was increased 122
Figure 4.17	Displacement control applied to the central node of the cup 123
Figure 4.18	(a) Rim impaction using rigid cap and (b) Polar impaction 124
Figure 4.19	Cross-section of the 3D cup impaction process 125
Figure 4.20	Mesh convergence achieved using (a) the polar gap remaining and (b) the diametrical deformation. Red line indicates the minimum number of elements for accuracy to within 1% 127
Figure 4.21	Stress in cup with (a) no hourglass control and (b) enhanced hourglass control 129
Figure 4.22	Comparison of experimental polar gap remaining with that observed in the FE model with varying coefficients of friction under free rim conditions 130
Figure 4.23	Difference in the polar gap remaining between the experimental and FE model ($P_a - P_b$) using coefficients of friction between (a) 0.3 and 0.1 and (b) 0.8 and 0.9, for each successive impact, using an interference of 1 mm and impact velocity of 1 ms^{-1} 131
Figure 4.24	The relationship between the mean polar gap remaining after each impact (1 – 10), as measured experimentally compared with that observed in the FE model, under all test parameters 133
Figure 4.25	Final diametrical deformations after the final impact for each test parameter, measured experimentally compared with that estimated in the FE model 134
Figure 4.26	Foam cavity partitioned into three segments to model non-uniform support and orientation of cup with respect to cavity varied during impaction, with (a) opposing pinch points and (b) pinch points at 150° to each other 137
Figure 4.27	Maximum reduction and expansion of diameter recorded after a change in shape of the cup 137
Figure 4.28	The ratio of deformation with variable cup support ($\Delta\phi_{e0}$) compared to the uniformly supported and aligned cup ($\Delta\phi_0$) as a function of cup orientation. The greatest eccentricity of the deformed cup with varying support is displayed in italics 140
Figure 4.29	Cross-section showing the position of the seated component at (a) 0° and (b) 15° relative to the cavity after impaction. Pinching of the cup in the simulations occurred in a direction perpendicular to the red circle when a tilt was introduced. The contact area between the foam and cup in each model is highlighted 143

Figure 4.30	Schematic of the right hemi-pelvis, indicating the position of the pinch points more likely to be observed anatomically [Adapted from Tortora et al 2006]. Rotations of the cup about the central axis simulated changes in the version of the cup.....	144
Figure 4.31	Orientation of cup with respect to cavity varied during impaction	145
Figure 4.32	Maximum cup deformations observed with increasing cup orientation	146
Figure 4.33	Development of a Taguchi Design of Experiment	147
Figure 5.1	Flowchart summarising the steps involved in the development and simulation of the 3D pelvis models	155
Figure 5.2	Typical DICOM image of the pelvis	156
Figure 5.3	DICOM images imported into Mimics 14.01. Unmodified scans are visible in the (a) coronal, (b) transverse and (c) sagittal planes	157
Figure 5.4	Segmentation of bone (yellow) from surrounding soft tissue	158
Figure 5.5	Initial 3D model created from segmented bone in CT scans	158
Figure 5.6	Femoral head and shaft removed from model to leave the acetabular region fully exposed.....	159
Figure 5.7	Cropped 3D model of the right pelvis with acetabular region visible with (a) artefacts present and (b) wrap function applied to smooth the outer surface	159
Figure 5.8	Rapid prototype model created of the cropped right pelvis	160
Figure 5.9	Cross-sectional geometry of the CoCrMo cup selected by the orthopaedic surgeons	161
Figure 5.10	Region of acetabular cavity to be reamed was identified within 3-Matic 5.1.....	162
Figure 5.11	(a) Boolean subtraction of a 55 mm diameter sphere used to create (b) a hemispherical reamed cavity	162
Figure 5.12	Typical element distribution mesh generated by 3-Matic	163
Figure 5.13	Elements that fail the defined criteria are highlighted	164
Figure 5.14	(a) Mesh density increased to 10,000 elements and (b) further increased to 15,000 elements, thereby reducing the number of poorly shaped elements	164
Figure 5.15	Relationships established from previous studies between apparent density and stiffness.....	166
Figure 5.16	Variation in the apparent bone density, gcm^{-3} determined from the CT data in a young pelvis model	167
Figure 5.17	Impaction of cup into acetabular cavity using multiple 1.3 kg impactors	169
Figure 5.18	Boundary conditions applied in the sacral-iliac and pubic symphysis regions of the pelvis	170
Figure 5.19	Mesh density in convergence study varied between (a) 5,500 elements (b) and 720,000 elements	174
Figure 5.20	Mesh convergence achieved with approximately 180,000 elements to achieve accuracy of the (a) polar gap remaining and (b) deformation to within 1%.....	175
Figure 5.21	Cup abduction and version angles as determined by orthopaedic surgeons in young (Y1 – Y4) and old (O1 – O4) pelvis models, within the safe zone.....	177

Figure 5.22	Cup deformations observed after insertion in the optimum position in the four young (Y1 – Y4) and four old (O1 – O4) pelvis models.....	178
Figure 5.23	Maximum distortion as a result of pinching between iliac and ischeal columns. Deformed cup scaled by a factor of 25 on the right	178
Figure 5.24	Direction of pinch points modelled in foam modelled (grey regions) in the previous chapter	179
Figure 5.25	Greater amount of boney contact with cup rim in the pinch directions of (a) the Ischium (b) the Ilium	180
Figure 5.26	Deformation of the cup with position in (a) version and (b) abduction was varied from the ideal (marked as solid circles on curves)	182
Figure 5.27	Cup deformation for the heterogeneous and homogenous model with different angles of version in young pelvis 1.....	184
Figure 5.28	Change in the deformation of the cup, normalised to cup deformations in the optimum position, as its position was varied in version in (a) the young pelvis models and (b) the old pelvis models	185
Figure 5.29	Change in the deformation of the cup, normalised to cup deformations in the optimum position, as its position was varied in abduction in (a) the young pelvis models and (b) the old pelvis models	186
Figure 5.30	Cup impacted in the same orientation into (a) young pelvis 1 and (b) young pelvis 2. Differences in the support at the rim between the two models are clearly visible	188
Figure 5.31	Cross sectional schematic showing the presence of a gothic arch in the acetabulum of the right hemi-pelvis. The absence of the gothic arch is illustrated in the left hemi-pelvis	190
Figure 5.32	The position of the major and minor axis in the ellipsoidal cavity formed during hand reaming	191
Figure 5.33	Maximum cup deformations observed with increasing deviations from the spherical cavity during hand reaming	192
Figure 5.34	Normalised log-log (a) short-term and (b) long-term creep curve (Experimental is black dashed line).....	193
Figure 5.35	Relaxation of the deformation of the 56 mm Co-Cr cup after insertion into a young pelvis model	195
Figure 6.1	Cup diameter much larger than head diameter	201
Figure 6.2	Contact between cup rim and head possible due to excessive deformations.....	202
Figure 6.3	Femoral head contact within the polished region of the cup	203
Figure 6.4	Rim of acetabular cup in contact with the femoral head	203
Figure 6.5	Larger contact area with a low clearance increases risk of rim contact	205

List of Tables

Table 2.1	Material properties reported for cancellous and cortical bone	22
Table 2.2	Modern Metal-on-Metal Hip Replacement Systems	39
Table 2.3	Summary of experimental studies investigating the deformation of press-fit acetabular CoCrMo cups and titanium shells	55
Table 2.4	The measured dimensions of four commercially available 58 mm acetabular cup designs	60
Table 2.5	Summary of finite element studies investigating the deformation of press-fit acetabular CoCrMo cups and titanium shells	65
Table 3.1	SI units used in model development	71
Table 3.2	Mesh densities used to reach convergence	75
Table 3.3	Mechanical properties of the acetabular cup and foam cavity	79
Table 3.4	Deformations obtained for varying amounts of friction with 0.5mm interference	80
Table 3.5	Deformations obtained for varying amounts of interference and friction	81
Table 3.6	Polar gaps observed for varying amounts of interference and friction	82
Table 3.7	Mesh densities used to reach convergence	87
Table 3.8	Mechanical properties of the acetabular cup, foam cavity and impactor	89
Table 3.9	Viscoelastic parameters defined for foam cavity and examples of values used	90
Table 3.10	Different cup-foam parameters used in the study	92
Table 3.11	Number of impacts to fully seat Co-Cr cup after impaction using a free cap and at the pole, at 1.5 m/s with 1mm interference at various coefficients of friction	94
Table 3.12	Impactions required to fully seat the cup or after which any further impaction makes no difference to seating, with a coefficient of friction of 0.3. *Cup bounced out of cavity after first impact. <i>Italic</i> = percentage seated.....	95
Table 3.13	Polar gap remaining and cup deformation with and without yield after full seating of cup using a free cap, coefficient of friction of 0.3.....	101
Table 4.1	Parameters tested experimentally, indicating the test descriptors for each variable	111
Table 4.2	Polar gap remaining after each impact and the final experimental deformations. Bold value for the polar gap remaining indicates an additional impact that was performed to confirm seating	112
Table 4.3	Mean number of impacts (n = 3) until the change in polar gap remaining between subsequent impacts is less than 10 µm and the final polar gaps (Pa) and diametrical cup deformations ($\Delta\phi$) observed	113
Table 4.4	Mechanical properties of the acetabular cup, foam cavity and impactor. A Poisson's Ratio of 0.3 was assumed for all materials	126
Table 4.5	Cup deformation and insertion behaviour with varying cup orientation and uniform cup support	139

Table 4.6	The cup behaviour as a function of cup support with the cup orientated at 5° with respect to the cavity, resulting in the greatest deformations	140
Table 4.7	Cup parameters varied in Taguchi DOE	148
Table 4.8	Taguchi Orthogonal Array Selector, highlighting that 16 simulations were required in this instance	148
Table 4.9	Taguchi Orthogonal Array with 4 parameters and 4 levels	149
Table 4.10	The component deformations observed with varying dimensions	150
Table 4.11	The Signal / Noise (S/N) ratio obtained for the different cup parameters using the Taguchi DOE	151
Table 5.1	Material properties defined in each pelvis model based in the apparent density	168
Table 5.2	Definition of master and slave surfaces of the different structures in the model	171
Table 5.3	Cup and shell parameters used in the pelvis Taguchi DOE	197
Table 5.4	Showing the S/N ratio for the different cup parameters using the Taguchi DOE	198

Acknowledgements

I would like to express my gratitude to my supervisors Professor Julia Shelton and Dr James Busfield for their invaluable advice and guidance.

I would also like to thank the following people for all their help in this project:

Alister Hart, Johann Henckel, Mark Thompson, Graham Isaac, Cath Hardaker, Philip Wright and all the support staff at QMUL.

I acknowledge the sponsors of this project, DePuy International Ltd and the EPSRC

Finally, a big thank you to all my family!

Chapter 1

Introduction

The hip, often referred to as a ball and socket joint, is one of the largest joints in the human body and is essential for mobility, with the average person spending approximately 30% of their day performing movements such as running, walking and stair climbing [Morlock et al., 2001]. The hip can become damaged for a number of reasons such as the cartilage in the joint degrading or wearing away, resulting in bone contact or through a fracture suffered during a fall or impact. These conditions can result in a considerable amount of pain, severely limiting mobility. Some patients are able to use exercise, walking aids and medication to relieve pain but if this is no longer effective, the restoration of hip function is commonly achieved by replacing the damaged joint with an artificial one. The hip replacement procedure is one of the most successful operations performed by orthopaedic surgeons, normally reducing pain, increasing mobility and improving the quality of life for the patient.

The earliest attempts at replacing a damaged hip joint using a prosthetic implant dates back to 1890 when carved ivory was used to replace the femoral head [Ratner et al., 2004]. These initial efforts saw little success and it was not until the 1960s and 1970s that significant advancements in the hip replacement procedure were made. Much of these were due to the contributions by Charnley which have guided the design of recent implants and the surgical procedure itself. Charnley's early design comprised of a stainless steel femoral head on a stem and a cemented polytetrafluoroethylene (PTFE) acetabular cup. Whilst long term success was demonstrated using these designs in some patients, there were many reports of relatively early failure largely due to wear of the polyethylene cup, associated with osteolysis and loosening of the implant. Metal-on-metal (MoM) implants were introduced at the same time with the expectation that the wear rates would be reduced by using two 'hard' bearing surfaces [Callaghan et al., 2006]. These 1st generation MoM implants saw poor overall survivorship with great variability and were limited in their use. More recently, a greater understanding of some of the reasons for failure and improvements in

manufacturing methods resulted in an introduction of 2nd generation cementless MoM bearings which demonstrated better survival rates. Increasing life expectancies and the treatment of younger, physically active patients that have high expectations of regaining pain free movement placed a greater demand on implants with longer survival rates which can withstand greater levels of activity. This led to the introduction of the MoM resurfacing procedure which served to preserve the femoral head by placing a larger diameter, short stemmed metal cap over the bone, allowing for easier revision, whereas a traditional total hip replacement (THR) introduces a metal head with a substantial stem running into the femur. The use of large diameter MoM implants in THR and resurfacing procedures has a number of perceived advantages such as improving the range of motion, reducing the risk of dislocations and lowering wear rates [Haddad et al., 2011]. Whilst the short-to-mid-term clinical data has shown excellent results, the longer term performance of these large diameter cementless components has recently been shown to be disappointing with failure rates approximately twice as high as when non-metal-on-metal cementless cups have been used [National Joint Registry, 2010]. Whilst the wear rates of MoM bearings is considerably lower than those composed of polyethylene, there have been associations made between the type of wear debris and the occurrence of pseudotumours and tissue necrosis.

Factors such as misalignment of the components and orientating the cup at high abduction angles have been shown to contribute to failure and high wear rates [Hart et al., 2008; Langton et al., 2008]. However unexplained early failure and high wear rates are found to occur in some patients despite the implant being seemingly well positioned and correctly seated [Hart et al., 2012a]. One suggested contributing factor in these cases is that of the diametrical deformation of the acetabular cup following insertion into the acetabulum. Deformations may be high enough, when compared to clearances between the cup and femoral head, that normal articulation is disrupted and in extreme cases contact between the cup rim and femoral head may occur resulting in increased wear and possibly locking of the joint. Previous experimental and finite element studies that have investigated cup deformations have largely been limited in their approach. Whilst they have demonstrated that deformations may occur, they have neither investigated the many factors that may influence the extent of deformation nor if these factors are clinically relevant.

The work of this thesis sought to identify key clinical and design factors that influence cup deformations following insertion and determine if these may be large enough to potentially hamper the normal function of the hip bearing.

Chapter 2

Literature Review

2.1 Anatomical Reference Planes and Terms

The body is commonly referred to in three anatomical planes, namely the transverse, coronal and sagittal planes [Marieb and Hoehn, 2010], Figure 2.1.

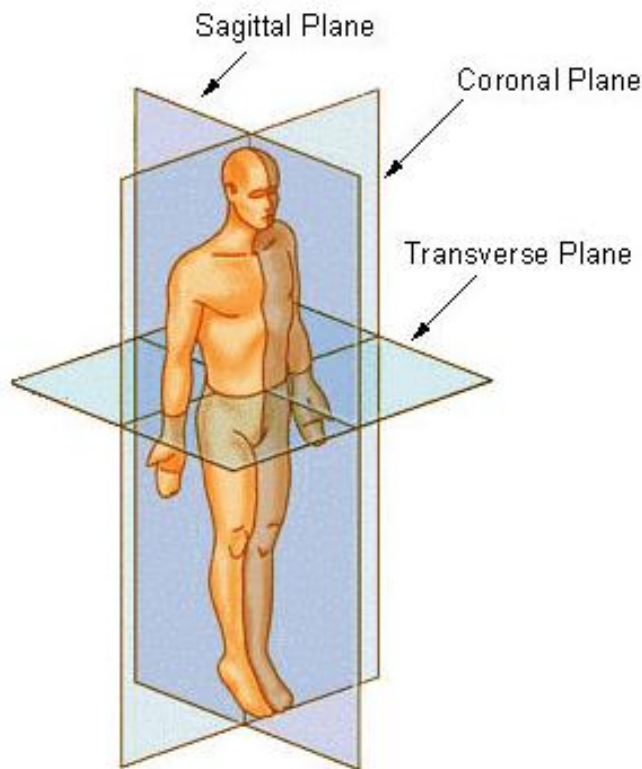


Figure 2.1: Reference planes used to describe the human anatomy [NCI, 2009]

The positions of the different areas of the body are usually described relative to the trunk of the body. Figure 2.2 illustrates the anterior, posterior, proximal, distal, medial and lateral terms that are often used. Also shown in an example of the movement of the hip joint which is often described as being in three degrees of freedom relative to the three reference planes [Levangie and Norkin, 2005]:

- Flexion and extension of the hip occurs in the sagittal plane.
- Abduction and adduction occurs in the coronal plane.
- Medial and lateral rotation of the hip joint occurs in the transverse plane.

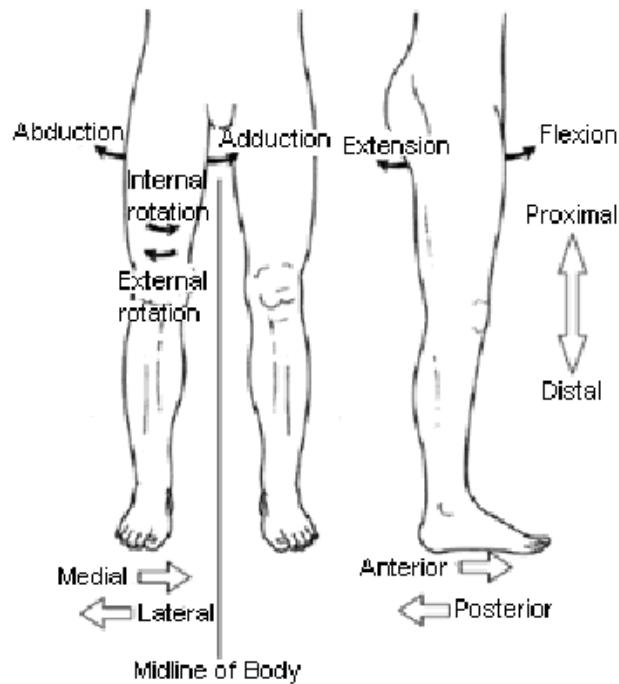


Figure 2.2: Terms used to describe different regions of the body [Martini and Bartholomew, 2000]

2.2 Anatomy of the Hip Joint

The focus of this work is on the behaviour of acetabular cups upon insertion into the acetabulum. As such the focus of this section will be on the pelvis rather than the femur.

2.2.1 Function of the Hip

The main function of the hip is for weight bearing; it must be able to support the load from the upper body in both static and dynamic situations, such as when standing and running. It has been reported that the compressive forces at the hip joint can be as much as the total body weight of an individual when in a normal standing position and can increase considerably during movement. The hip joint is highly suited to maintaining stability under these different conditions and through a large range of motion. It is composed of a deep socket known as the acetabulum and a spherical head attached to the femur which is known as the femoral head [Hall, 2011].

2.2.2 The Hip Joint

The hip joint is a synovial joint which consists of the femoral head articulating in the acetabular cavity. Both the femoral head and the acetabulum are lined with a layer of articular cartilage which allows for smooth articulation and sliding between the two surfaces [Tortora and Derrickson, 2006] Figure 2.3.

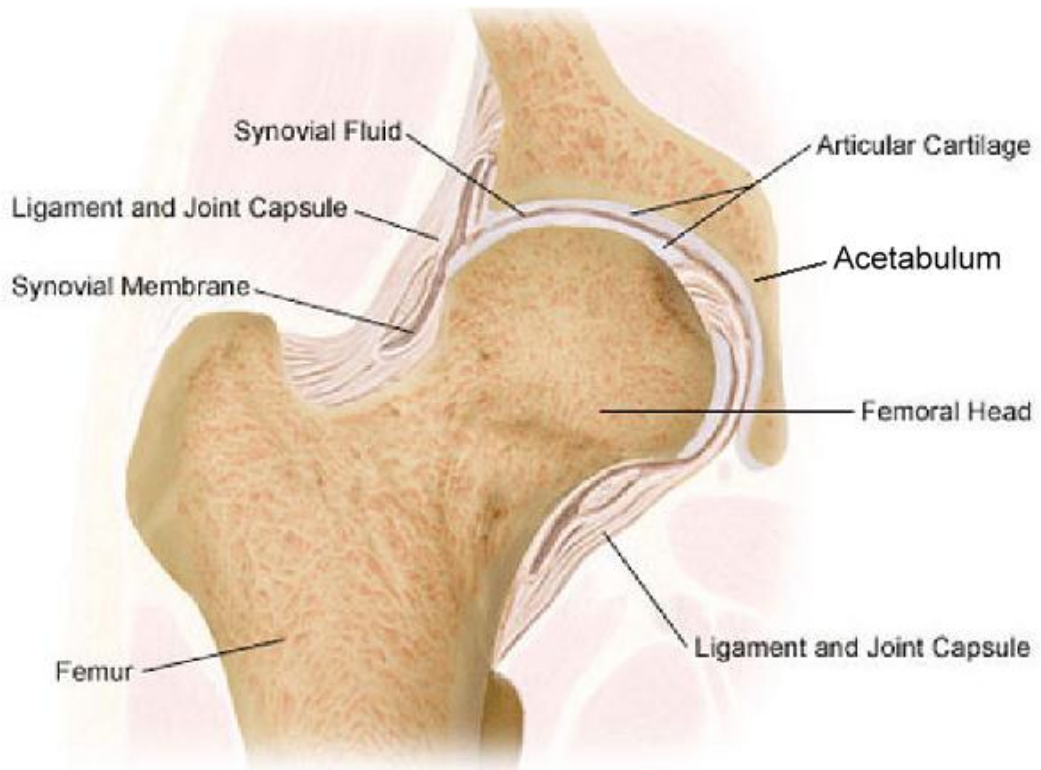


Figure 2.3: Key features of the hip joint [Adapted from CUMC, 2007]

Cartilage tissue is composed of a matrix embedded with cells and in the hip it helps to distribute the loads between the acetabular cavity and femoral head. It is lubricated by synovial fluid which serves to create a very low coefficient of friction, between approximately 0.001 and 0.03, between the two sliding surfaces [Green and Nokes, 1988; Poitout, 2004]. Synovial fluid is secreted by the synovial membrane which is lined by a strong fibrous capsule which surrounds the joint and also provides additional support. The edge of the acetabular cavity is surrounded by a ring of fibro cartilage known as the acetabular labrum. This serves to deepen the cavity, increasing the stability of the femoral head in the cavity and leading to a very low number of dislocations in a healthy joint [Tortora and Derrickson, 2006].

2.2.3 Structure of the Pelvis

The pelvis is composed of three distinct regions of bone connected together at three joints. The regions consist of two hemi-pelves that are symmetrical about the sagittal plane of the body and the sacrum which is located between the two hemi-pelves [Standring, 2004], Figure 2.4.

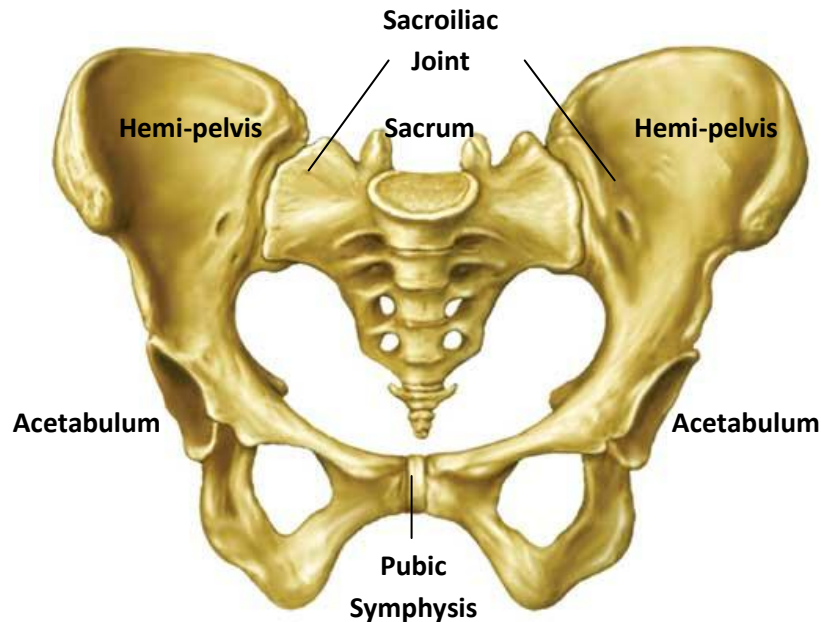


Figure 2.4: Structure of the pelvis viewed in coronal plane [Adapted from Medical Blog, 2009]

Each of the two hemi-pelves can be defined in terms of three regions of bone; the pubis, the ilium and the Ischium, Figure 2.5. Key features of each hemi-pelvis can be related to their position relative to the anterior and posterior columns.

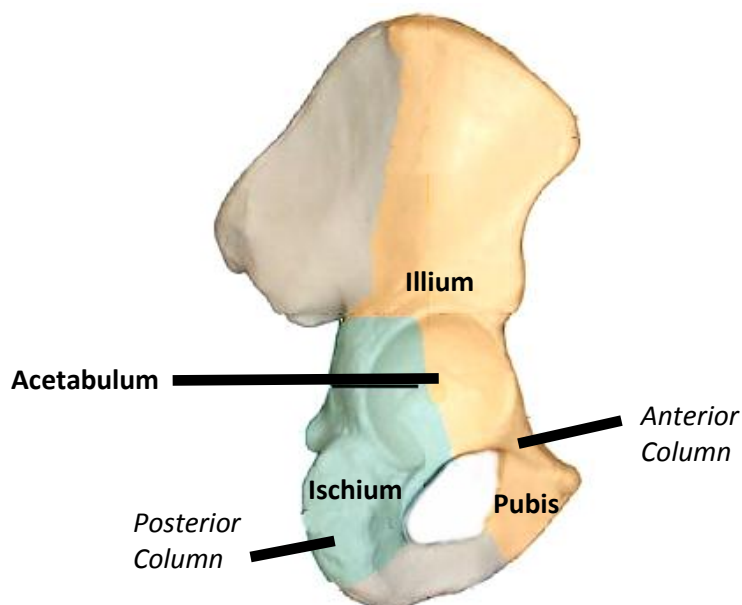


Figure 2.5: Key bony regions of the right hemi-pelvis, viewed in sagittal plane

The two hemi pelvises are connected posteriorly to the sacrum via the sacroiliac joints which have one section with fibrous connective tissue where movement is limited and another section where synovial fluid is present, allowing sliding to occur. Anteriorly the hemi-pelvises are connected by the pubic symphysis joint. This consists of a fibrocartilage disc together with four ligaments known as the pubic ligaments which all help to limit movement in this region [Standring, 2004].

2.2.4 Bone Structure in the Pelvis

The bones located in the pelvis are made from two different types of bone, namely cancellous and cortical bone. Cortical bone makes up the strong outer shell on the pelvis whilst cancellous bone, which has variable extents of porosity and is less stiff, forms the inner layer of the structure. The distribution of the density of the bone in the pelvis varies depending on its location; this therefore has a direct correlation with the stiffness of the bone in different regions [Standring, 2004].

Bone is viscoelastic in nature and this behaviour can be observed as creep, which is the increase in strain under a constant stress, or as stress relaxation, which is the decrease in stress of the material under a constant strain. Bone also demonstrates a load-rate dependence on its stiffness. Deligianni et al. [1994] reported that stress relaxation in cancellous bone reaches a steady state in approximately 24 hours whilst Pawlikowski et al. [2008] found that experimental creep curves reach a steady state after approximately 27 hours.

The reported values for the Young's modulus (E) and Poisson's ratio (ν) for cortical and cancellous bone vary considerably due to differences in the location of bone samples tested as well as the individual subject or bone type. Table 2.1 summarises a range of values for E and ν that have been reported for cancellous and cortical bone [Dalstra et al., 1993; Thompson et al., 2004; Turner et al., 1999]

Table 2.1: Material properties reported for cancellous and cortical bone

Bone Type	E / GPa	ν
Cancellous	0.001 - 1	0.01 – 0.50
Cortical	4.4 – 22.8	0.2 – 0.5

2.3 Common Indicators for a Hip Replacement

A hip replacement is often required when an individual experiences a great amount of pain and reduced mobility due to changes in the hip which cannot be treated non-operatively or where this is not a sustainable long term treatment option. Causes for the failure of the natural hip can be due to disease or accidents, which can be gender and age related. The main reasons that a hip replacement may be required have been previously described [Malchau et al., 2002; National Joint Registry, 2010] and are summarised as follows.

Osteoarthritis

Osteoarthritis is a degenerative disease of (but not limited to) the hip joint that is most often found to occur in elderly and middle aged women. Factors such as obesity can increase the chance of developing osteoarthritis. It occurs as a continued loss of the function and structure of the healthy articular cartilage at the interface between the femoral head and the acetabulum. This can result in the bones of the joint articulating directly with each other, leading to severe pain for the patient. Osteoarthritis is the most common reason for a hip replacement being carried out, with 94% of primary hip operations performed annually being due to this disease [National Joint Registry, 2010].

Fracture

Fractures of the hip that may require hip replacement are those that occur in the bone of the pelvis or the proximal femur. These hip fractures are most commonly found to occur in elderly patients that experience a fall, who may also have weakened joints due to osteoarthritis. If fractures of the femoral neck occur, hemiarthroplasty is commonly used in which the only the femoral head replaced [Nagle, 2011]. Approximately 75,000 hip fractures are reported to occur annually in the UK. The average age of a patient requiring treatment due to a hip fracture is 80 years and approximately 80% of fractures occur in women [NICE, 2011].

Inflammatory Arthritis

Inflammatory arthritis, also referred to as rheumatoid arthritis (RA), is a disease which results from the inflammation of the synovial joints. It can break down bone and the

articular cartilage surrounding the joint, limiting the amount of function and increasing considerably pain in this region. Osteoarthritis can develop as a secondary condition due to the loss of articular cartilage [Callaghan et al., 2006]. The use of anti-inflammatory drugs however has improved non-operative treatment techniques, resulting in fewer hip replacements being necessary as a result of RA.

Other Causes

Other reasons that may require hip replacements include disease of the femoral head due to a reduction or loss of the supply of blood to the region, diseases in childhood such as dysplasia and the occurrence of tumours [Malchau et al., 2002].

2.4 History of Hip Arthroplasty

A hip replacement involves replacing the hip joint with a mechanical bearing system which is comprised of a femoral component and an acetabular component. During a hip replacement the acetabulum is reamed and the acetabular component is fitted into the cavity and the femoral component can either be placed over a reamed femoral head, in a procedure referred to as hip resurfacing, or positioned inside the femoral shaft during a total hip replacement [Callaghan et al., 2006], Figure 2.6.

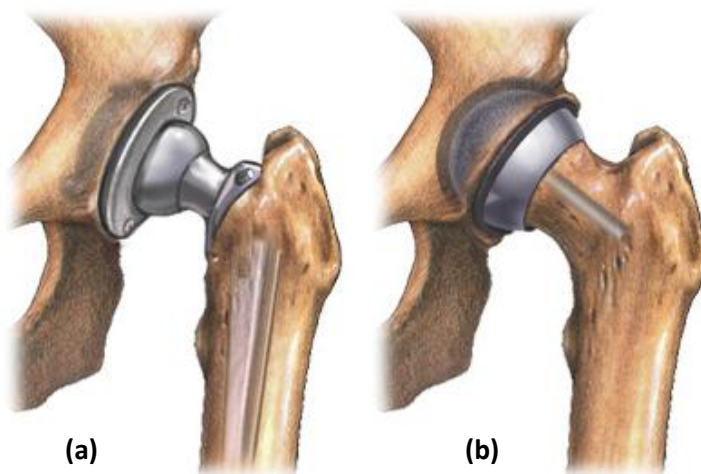


Figure 2.6: (a) Total hip replacement (THR) and (b) Hip resurfacing replacement [FDA, 2012]

The first recorded attempts at reducing pain and restoring mobility to the hip joints of patients are reported as being as early as the 1820s, in which the procedure involved simply removing the problematic acetabular or femoral bone. The period from the

1830s to the 1880s saw crude attempts at improving this procedure by positioning materials such as blocks made of wood or animal tissue between the acetabulum and the femoral head. The first use of a prosthetic hip replacement is reported to have been in 1890, in which a femoral head replacement made from carved ivory was implanted using plaster of Paris and pumice [Ratner et al., 2004].

The use of placing a membrane between the acetabulum and the femoral head continued into the 1920s, with the patient's own soft tissue being a popular material choice for the membrane. These early attempts at restoring normal hip joint function and reducing associated pain were found to be very unsuccessful and alternative techniques were strongly desired [Ratner et al., 2004].

1923 saw a significant step in the development of modern total hip replacements, with the introduction by Marius Smith-Peterson of the "mold" arthroplasty, as shown in Figure 2.7, which highlights the different total hip replacement designs that have evolved over the years. This cup design was made of glass and was intended to be positioned between the acetabulum and the femoral head, and being such that articulation occurred on both surfaces. Attempts at improving the fracture resistance of the glass mold were made by Smith-Peterson, by using early polymers such as Formica or improved glass, such as Pyrex. However it was not until 16 years later in 1939 when a metal cobalt alloy with high corrosion resistance was used, that enough biocompatibility and performance was observed for the total hip arthroplasty to be considered as having the potential for success [Ratner et al., 2004].

The first total hip arthroplasty is reported to have been performed by Philip Wiles in 1938, in which he used a bolt to attach a stainless steel ball to the femur and screws to attach a stainless steel acetabular liner into the acetabulum. The presence of high stress concentrations and the poor corrosion resistance of the stainless steel, yielded disappointing results [Ratner et al., 2004; Dollar, 2004]. An evolution of this design was introduced in 1951 by G.K. McKee and J. Watson-Farrar, which was found to be successful. They initially used a stainless steel acetabular cup with a long femoral stem, however poor corrosion resistance of the cup component led to a change in the design to use a cobalt-chromium alloy, which proved to be a lot more successful at reducing the failure rate [McKee and Watson-Farrar, 1966]. The McKee-Farrar design was soon adapted to include a fully spherical femoral head that allowed for greater mobility by

reducing the impingement of the head on the rim of the acetabular cup, as shown in Figure 2.8 [Ratner et al., 2004].

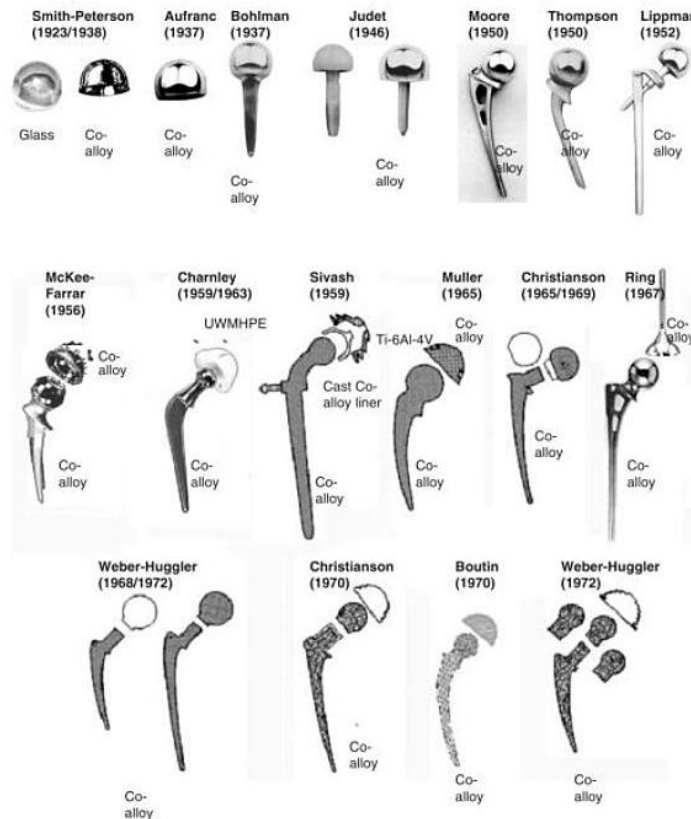


Figure 2.7: The evolution of Total Hip Replacement designs [Ratner et al., 2004]

The next major point in the development of total hip replacements was the introduction of acrylic dental bone cement, which was used first in 1950 by Sven Kiar in the fixation of a plastic prosthesis to bone [Charnley, 1964]. In the same year PMMA bone cement was used as a fixation method in total hip replacements and this was found to significantly reduce the rates of loosening of the hip replacement components [Charnley, 1960a]. As such, McKee and Watson-Farrar incorporated bone cement into their designs [Ratner et al., 2004].

2.4.1 Total Hip Replacement

Total hip replacement (THR) in elderly patients and those with severe arthritis has proved to be a successful procedure for alleviating pain and improving their quality of life. The Swedish Hip Registry reports that THR performed in older patients, with a mean age greater than 65 years, has a success rate of 90 percent at 20 years [Garellick

et al., 2010]. However for younger, more active patients, particularly men younger than 55 years of age, the survival rate of the THR drops to as low as 33 percent after 16 years [Grigoris et al., 2005]. The subsequent revision surgery that is required is often technically challenging for the surgeon, who is usually presented with less bone stock and weaker muscle tissue, thus leading to further risks of instability.

The high expectations and demands of young, active patients has led to the re-emergence of hip resurfacing, a method in which the femoral bone stock is left intact and the diameter of articulation is larger, thus reducing the risk of dislocation and increasing the range of motion of the hip. Large diameter metal-on-metal bearings surfaces have also been made available as modular heads in traditional THR.

2.4.2 Hip Resurfacing

Based on the original idea by Smith-Petersen, the first attempt at total hip resurfacing was carried out by John Charnley in the early 1950s, using two thin polytetrafluoroethylene (Teflon) cups pressed over the femoral head and into the acetabulum. Although early results were encouraging, offering substantial pain relief and very good range of motion, the high wear rates and high sliding distance due to a large articulation diameter meant that early failure and therefore the requirement of revision surgery was highly likely, and the procedure was quickly abandoned [Charnley, 1960b; Ebied and Journeaux, 2002].

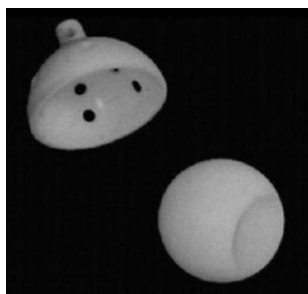


Figure 2.8: The Charnley press-fit Teflon-on-Teflon design [Grigoris et al., 2005]

The late 1960s and early 1970s saw a range of resurfacing designs utilised globally. In 1968 Maurice Muller introduced a cementless metal on metal articulating design with variable neck sizes and larger heads. However the need for revision surgery in half of the 18 cases utilising this method, caused him to abandon this technique [Callaghan et al., 2006]. In 1970 Gerard utilised two metal cups which were such that motion was

possible between the bone and the cups and also between the two cups themselves. 2 years later, Gerard altered his design to use a polyethylene acetabular cup and then in 1975, he changed this to a metal-backed polyethylene component [Gerard, 1978; Callaghan et al., 2006].

In 1971, clinical trials with cemented metal-on-polyethylene resurfacing designs were carried out in Italy by Paltrinieri and Trentani [Callaghan et al., 2006; Trentani and Vaccarino, 1978] and in Japan by Furuya, who subsequently changed the material of the femoral component to stainless steel [Callaghan et al., 2006; Furuya et al., 1978]. A year later in England, Freeman utilised high-density polyethylene femoral components articulating with metal acetabular components. Rapid polyethylene wear and high rates of loosening caused Freeman to reverse the materials in 1974, such that the acetabular component was composed of high-density polyethylene. In the same year, Tanaka in Japan described the use of the same materials in a cementless design, whilst Wagner started to use cemented metallic femoral components with cemented polyethylene cups [Callaghan et al., 2006].

A cemented metal-on-polyethylene resurfacing design was introduced in 1975 by Amstutz and a year later in Vienna, Salzar started to use an uncemented ceramic design utilising pegs to fixate the acetabular component.

2.4.3 Failure of Early Hip Resurfacing Designs

By the mid-1980s, the hip resurfacing procedure was used in a limited way due to numerous reports of high rates of failure with cemented surface replacements [Amstutz et al., 1986; Callaghan et al., 2006]. The expectation that revision surgery would be free from complications was not realised, mainly due to the substantial loss of acetabular bone [Callaghan et al., 2006]. This bone loss was in part due to the high reaming levels required to accommodate the oversized acetabular components and the cement mantle, but more due to the wear induced osteolysis [Callaghan et al., 2006].

The use of polyethylene cups with large articulating diameters often resulted in high wear rates and large volumes of wear debris, resulting in bone loss, leading to implant loosening. Wear debris, generated from liners with poor locking mechanisms and coatings, was also a contributing factor to the failure of cementless resurfacing designs [Callaghan et al., 2006].

Femoral head size was found to significantly affect implant survival rates, however the presence of polyethylene wear debris ultimately led to cup loosening and clinical failure of the implant [Callaghan et al., 2006].

An alternative to ultra-high-molecular-weight polyethylene (UHMWPE) was strongly desired and it was noticed that a number of the metal-on-metal articulations that had been abandoned by surgeons, had survived for at least 20 years, showing little signs of wear or osteolysis. The results of a 20 year study by Jacobsson et al. [1996] found that the survival rate of the total hip replacement Charnley design was 73% and that wear of metal-on-metal designs was heavily affected by the choice of materials, tribological design and surface finish. Furthermore the success rate of the metal-on-metal McKee-Farrar total hip arthroplasty was also found to have similar long term success rates of 77% [Jacobsson et al., 1996].

2.4.4 Re-Introduction of Metal-on-Metal Bearings

As well as producing disappointing long term results, another problem associated with earlier resurfacing designs was that a lot more of the acetabulum had to be reamed than was the case for standard total hip arthroplasty, due to the femoral head having a larger diameter. Wear tests have demonstrated that the wear resistance of highly cross-linked UHMWPE is significantly improved over earlier UHMWPE designs [Gordon et al., 2006]. However, cross-linked polyethylene and ceramics had the disadvantage of requiring comparatively thicker acetabular cup geometries, thus conserving less bone. Metallic components became the material choice that allowed a thin shell to be utilised which conserved a lot more bone than is possible for ceramic or cross-linked polyethylene cups [Amstutz and Le Duff, 2005].

A high carbon cobalt-chromium alloy bearing exhibiting excellent wear characteristics was developed by Weber in 1988. This was found to produce very encouraging early clinical results and became a popular choice in Europe [Weber, 1996]. In 1991, based on the success of this metal design, Heinz Wagner developed a hip resurfacing system consisting entirely of cementless metal components [Wagner and Wagner, 1996]. At the same time, a new cementless cobalt-chromium metal-on-metal hip resurfacing design was developed by McMinn. Due to problems of aseptic loosening and early failure, the design was modified and a hybrid system consisting of a cemented femoral component and a cementless acetabular cup with a hydroxyapatite coating was

introduced in 1994 [Grigoris et al., 2005]. Although this specific design was withdrawn shortly afterwards, the basis of the hybrid metal-on-metal design became key to the most recent series of designs [Grigoris et al., 2005].

2.5 Modern Hip Replacement Acetabular Components

The components used in modern hip replacements differ between manufacturers primarily in their geometry, the materials that they are made of and the methods that are used to ensure their long term fixation following insertion [Callaghan et al., 2006]. Whilst there are many different commercially available acetabular cup designs, they all fall in to one of two categories: cemented or press-fit (cementless).

Cemented Acetabular Cups

When cemented cup designs are used, a PolymethylMethacrylate (PMMA) bone cement is utilised to ensure full fixation of the cup to the bone in the reamed acetabular cavity. This cement, which is placed between the outer surface of the cup and the bone, is able to aid in the distribution of the surrounding loads [Bronzino, 2006]. Cement is most often used in conjunction with Ultra High Molecular Weight Polyethylene (UHMWPE) cups however metal cups with UHMWPE liners are also used. Due to the lower resistance to wear and the lower stiffness of UHMWPE cups, their wall thickness is made considerably larger than when metal cups are used, resulting in the use of small diameter femoral head components which are not representative of the femoral head in natural bone [Ranawat and Ranawat, 2006].

Press-Fit Acetabular Cups

Uncemented cups can be used in both THR and resurfacing procedures and do not use cement but rather rely on the growth of bone onto their outer porous surface for fixation [Callaghan et al., 2006]. Initial stability is achieved by reaming the acetabular cavity smaller in size than that of the cup. A larger femoral head component, closer in size to the natural bone can be selected as cement is not used, allowing for a larger range of motion [Peters and Miller, 2006].

2.5.1 Cup-Head Articulating Surfaces

The surfaces of the cup and head in the joint can be found in a number of combinations:

- Metal-on-Metal (MoM)
- Metal on UHMWPE
- Metal on ceramic
- Ceramic on UHMWPE
- Ceramic on ceramic

From a tribological perspective it is more desirable to use bearing surfaces that have a different hardness to each other and to replace the worn surface when required [Medley, 2008]. Practically however it is difficult to replace either component, and the associated wear particles have been reported to lead to component loosening and osteolysis [Howie et al., 2007]. As a consequence MoM components have been used with clearances between the two surfaces to allow fluid-film lubrication. These components have been reported to have lower wear rates than metal on UHMWPE surfaces [Williams et al., 2007] however recent studies and patient experiences have suggested that failure rates of MoM implants and the associated health risks from metal wear debris may be much more severe than expected [Hart et al., 2009; Hart et al., 2012b].

2.5.2 Orientation of Acetabular Cups

The orientation of the acetabular cup can be described with respect to the underlying bone. Clinically however it is common to refer to its position in the acetabulum using two angles, namely version and abduction (also known as inclination) [Wheless, 2011]. The version of the cup refers to the angle between its rim and the sagittal plane between the lateral and medial sections of the acetabulum. The abduction angle is measured between the rim of the cup and the transverse plane between the superior and inferior sections of the acetabulum, Figure 2.9.

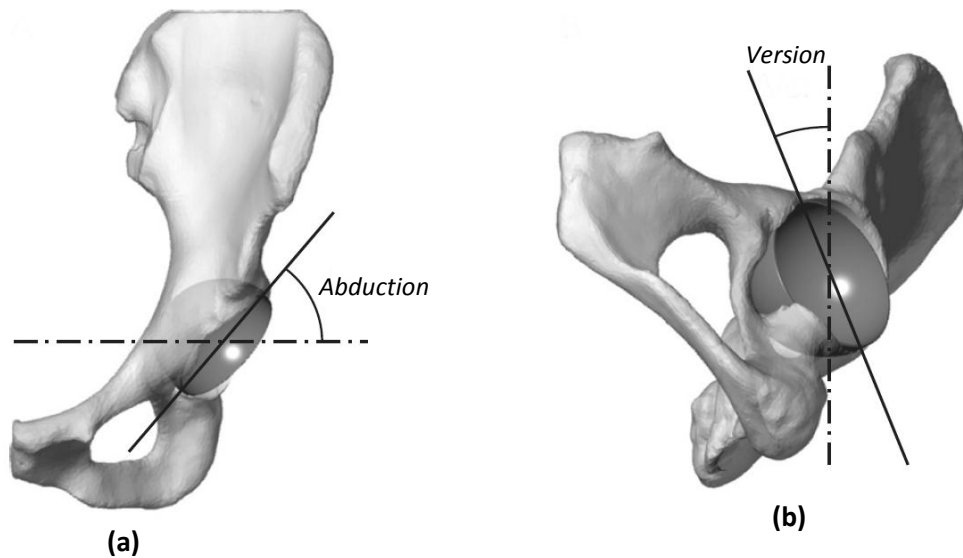


Figure 2.9: (a) Angle of cup abduction and (b) cup version [Adapted from Clarke et al, 2012]

The term *safe-zone* was created by Lewinnek et al. [1978] to describe cup orientations of between 5 and 25° in version and 30 and 50° in abduction which were observed to reduce the risk of the femoral head dislocating from the cup. The safe-zone is routinely used to guide the position of the inserted cups however the precise orientation can vary considerably due to a range of factors such as patient anatomy and the skill or experience of the surgeon, Figure 2.10

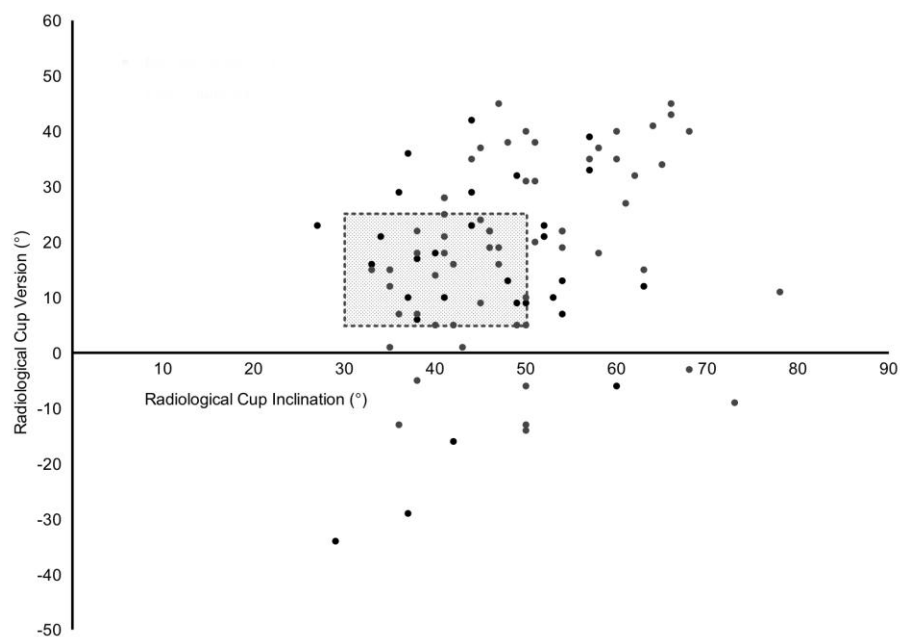


Figure 2.10: Distribution of acetabular cup orientations in 105 patients with metal-on-metal implants. Shaded region indicates safe-zone [Adapted from Matthies et al., 2012]

2.5.3 Current Cementless Designs

All the cementless acetabular cups that are currently used clinically, have a porous covering over a hemispherical shape, and are made of pure titanium, a titanium alloy or a chromium-cobalt alloy. The porous surface coatings most frequently used are plasma-sprayed titanium particles, sintered cobalt-chromium beads, cancellous structured titanium and titanium fibre metal. Generally cementless acetabular cups are available in sizes with an outer diameter ranging from 40 mm to 80 mm, in increments of 2 mm [Callaghan et al., 2006].

In a clinical situation, the most critical factor for ensuring that long term fixation is maintained by fully integrated bone ingrowth, is to ensure that immediate implant stability is achieved. In earlier designs this was achieved using supplementary fixation whereas later designs have utilised the concept of press-fit fixation, with the option of combining this with supplementary fixation.

2.5.4 Supplementary Fixation

Supplementary fixation can be achieved using spikes, pegs or screws [Peters and Miller, 2006]. There have been a number of studies carried out investigating the initial stability of acetabular fixation using these methods [Perona et al., 1992; Won et al., 1995; Cook et al., 1992]. A number of key points can be drawn from them, as follows:

- Achieving initial acetabular cup fixation using spikes, pegs or screws allows bone ingrowth into porous acetabular cup surfaces to occur [Cook et al., 1992].
- Although supplementary fixation appears to allow for acceptable initial stability for bone ingrowth to occur, there is no consensus regarding the extent of the initial stability achieved for the different methods, and how bone ingrowth is affected [Perona et al., 1992; Won et al., 1995].
- As small tolerances exist between machining a metallic acetabular cup and the acetabular bone into a matched shape, care is required to ensure that the acetabulum is reamed accurately for supplementary fixation to be most beneficial [Won et al., 1995].

Acetabular cups, such as the Harris-Galante porous cup, have shown to produce very good results when screw fixation is used. These cup designs are referred to as line-to-

line and are such that the outer diameter of the implanted acetabular cup is equal to the diameter of the acetabulum [Archibeck et al., 2001]. However despite these very encouraging medium to long term results, there are a range of risks associated with this method. These risks include the potential for neurovascular injury occurring, the risk of fretting between the metal cup and the screws, and the possibility of damage of the polyethylene liner by the screws heads. Additionally the use of supplementary fixation in the form of screws could also create a pathway for wear debris to migrate through and this could lead to osteolysis [Callaghan et al., 2006].

2.5.5 Press-Fit Fixation

In order to overcome the problems associated with supplementary fixation with screws, press-fit fixation has become more widely used in clinical practice, in which an oversized acetabular cup is inserted into an under-reamed acetabulum. With a press-fit fixation, a hemispherical acetabular cup with a porous outer surface coating, and with an outer diameter of 1 mm to 4 mm greater than that of the reamer used to prepare the acetabulum (referred to as the size of the interference fit), is forced into the acetabulum via impaction. The surrounding bone is able to deform to allow the cup to be inserted, then as a result of the elastic and viscoelastic properties the bone partially returns to its undeformed shape applying compressive forces to the surface of the cup, thereby generating a stable fixation [Curtis et al., 1992].

One advantage of press-fit fixation over using screws is that it eliminates that risk of corrosion and fretting between screw heads and polyethylene liners if they are used, and also eliminates the risk of wear debris passing through screw holes. The second clear advantage of press-fit fixation is that it serves to maximise the area of surface contact between cup and bone, thus encouraging greater bone ingrowth [Peters and Miller, 2006] (Figure 2.11). Bone ingrowth is also encouraged by:

- An osteoconductive porous coating such as Hydroxyapatite with a rough, uneven surface for bone to attach and grow onto and into.
- Osteoinduction, where primitive, undifferentiated and pluripotent cells are stimulated into the development of new bone tissue.

The geometry of the cup and an efficient surgical technique, in terms of the accuracy of acetabulum reaming, are two important factors influencing the stability of fixation

in the absence of any supplementary fixation [Adler et al., 1992]. A crucial factor influencing the stability of the fixation is the amount of peripheral cup/bone contact, dependent partly on the specific size and design of the cup.

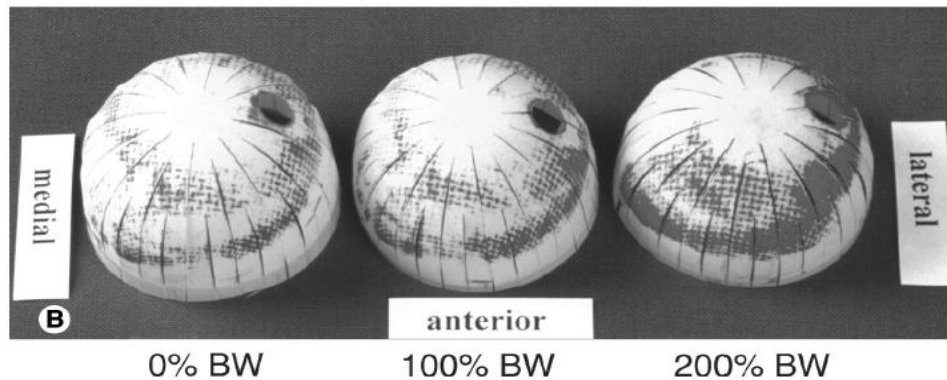


Figure 2.11: Large surface area contact between cup and bone shown by dark patches on reverse of cup lined by a pressure sensitive film after impaction into cadaveric models [MacKenzie et al., 1994]

2.5.5.1 Incidence of Polar Gaps

The incidence of gaps occurring between the dome of the cup and the acetabular bone in press-fit cups is more common than with other fixation techniques, such as using screws. Polar gaps have been reported to have occurred in the cups impacted into cadaveric models, Figure 2.11, due to the absence of dark patches indicating contact in this region. Gaps in the polar region will often be greater when larger interferences are employed [MacKenzie et al 1994]. In many cases these gaps are not visible when radiographs are taken after 2 years, suggesting that bone growth occurs across this gap (Figure 2.12). The maximum size of the gap is critical to ensure that bone growth occurs; it was found by Sandborn et al. [1988] that for gaps up to 2 mm in size, bone growth will occur into the porous surface coating on the cup, and for a gap size less than or equal to 0.5 mm, the rate of bone ingrowth was notable higher. Gaps larger than 2 mm need be avoided as bone growth is likely to be limited or very slow and there is a risk that wear debris could start to collect in this space.

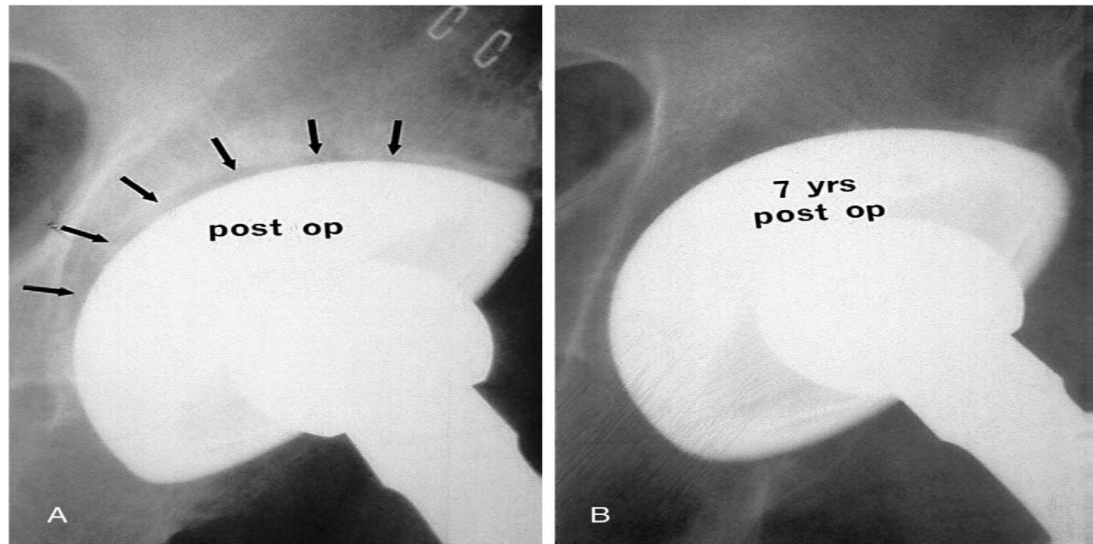


Figure 2.12: Incidence of polar gap at (a) insertion and (b) bone growth across gap after several years [Springer et al., 2008]

2.5.5.2 Influence of Interference Size on Fixation Stability

Interference provides a high degree of peripheral cup/bone contact that can seal and prevent the formation of spaces between the cup and bone [MacKenzie et al., 1994]. The optimal criteria to achieve superior fit and mechanical stability of press-fit acetabular cups with or without the addition of screws has been reported in cadaveric models [Kwong et al., 1994; Stiehl et al., 1992; Won et al., 1995]. A 1 mm interference with a press-fit cup, with or without the use of screws, was found to result in the optimum balance between the fit of the component and mechanical stability with satisfactory surface contact and minimal polar gaps between cup and bone. A 1 mm interference has also been shown to provide better stability at the rim of the cup than using either a cup with a larger 2 mm interference [MacKenzie et al., 1994] or a cup diameter that is the same as that of the cavity [Stiehl et al., 1992]. An interference of 2 mm is more likely to result in an improper fit of the cup into the reamed acetabulum, particularly in younger patients with greater bone density [Stiehl et al., 1992], which can increase the strains in the bone surrounding the cup thus leading to a higher risk of fracture. The use of screws with press-fit cups is not necessary as they do not result in a notable improvement in the stability of fixation [Won et al., 1995].

2.5.5.3 Effect of Press-Fit Fixation on Surrounding Bone

An increase in periacetabular strains have been reported whilst a cup is impacted into the pelvis and a further increase after the cup has been fully seated [Kroeber et al., 2002]. Acetabular strains produced when press-fit cups with a range of interferences are fitted into the acetabulum are greatest at the periphery of the cup (Figure 2.13), suggesting that fixation stability is increased by the compressive forces between the cup and the lateral pelvic bone. For the same interference, larger strains will develop in smaller acetabulum sockets than larger ones [Ries et al., 1997]. This leads to the conclusion that a greater interference is required when impacting press-fit cups into larger acetabulum sockets to achieve the same stability as when smaller sockets are impacted into.

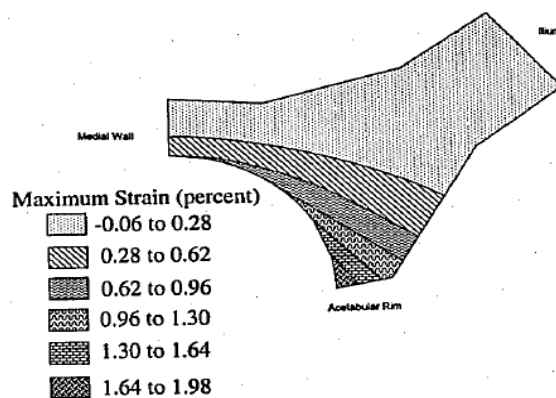


Figure 2.13: Highest strains visible at periphery of acetabular bone [Ries et al., 1997]

An issue that the surgeon is aware of during impaction of the press-fit cup is that of the risk of fracture of the acetabulum. The stability of the fixation is correlated to the stresses around the periphery of the cup, which can be increased by increasing the interference [Udofia et al., 2006]. However a balance must be obtained such that the stresses are below the ultimate strength of the pelvic bone, and therefore does not damage or fracture the acetabulum. It was found in a cadaveric study that in 18 out of 30 cases of press-fit cup insertion, fracture of the acetabulum occurred, and that this was more likely to occur when cups with an interference of 4 mm were used rather than 2 mm [Kim et al., 1995], highlighting the potential issues with using higher interferences.

2.6 Recent Metal-on-Metal Designs

A large number of hip implant systems that have been used in the past decade have involved a metal-on-metal articulation. There is however currently great concern surrounding their use; whilst this bearing surface was still used in up to 35% of patients in 2009 in the USA [Smith et al., 2012], its use has declined considerably in the UK since 2008, Figure 2.14.

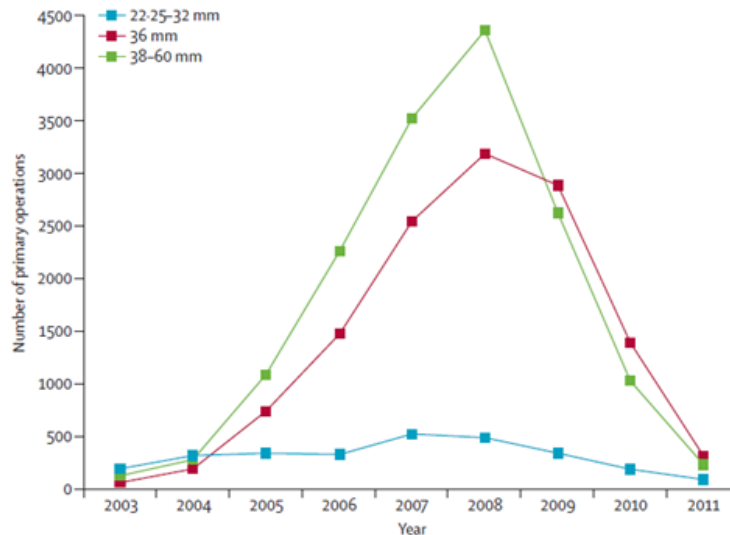


Figure 2.14: Number of MoM implanted by head size [Adapted from Smith et al., 2012]

Table 2.2, adapted from a review paper by Grigoris et al. [2005] highlights a number of metal-on-metal designs that have been used. The main differentiating factors between the different designs are geometry of the cup, method of fixation of the acetabular and femoral components and the processing methods of the metals, of which there is some debate as to the most effective method [Bowsher et al., 2003; Grigoris et al. 2005]. Considering the limited ways in which an acetabular cup may differ between manufacturers, recent designs have been fairly similar in their design. It is interesting therefore to observe the considerable differences in their individual success rates. For example, the Birmingham Hip Resurfacing (BHR) system has demonstrated high clinical success with a survival rate of 93.5% at 10 years [Treacy et al., 2011] whilst the ASR design (DePuy Orthopaedics) has fared much more poorly. The ASR was recalled by the manufacturer in 2010, five years after its introduction due to it experiencing a higher than normal early failure rate in that time period; one study [Langton et al., 2011] reported that approximately 25% and 48% of patients that had been implanted with an ASR resurfacing and THR cup respectively required revision surgery. Additionally the

Durom cup (Zimmer) experienced a high rate of loosening and the sale of this device was suspended [FDA, 2008].

Whilst the ASR design has more recently been highlighted due to its high rates of failure, it is the case that approximately 12% of hip operation procedures that are currently performed are done so as revision procedures [National Joint Registry, 2010]. This indicates that the issues relating to the incidence of failures may not be related to just one design but rather be a more widespread issue that requires attention. There is also now much concern about the issues surrounding wear of metal on metal implants. Whilst the wear rate of these components is low, there is apprehension over the metal ions being created in the body. There have been associations made between high levels of metal ions in blood and the occurrence of large cysts [Hart et al., 2009] and there have been calls by many to completely halt the use of MoM hip replacements.

Table 2.2: Modern Metal-on-Metal Hip Replacement Systems [Grigoris et al., 2005]

System	Bearing		Acetabular Cup		
	Process	Heat Treatment	Diameter Range / mm	Shape	Back Surface
Conserve plus, Wright Medical Technology	Cast	HIP and SHT	46 – 64	Truncated Hemisphere	Co-Cr beads, sintering \pm HA
BHR, Smith & Nephew	Cast	None	44 – 66	Hemisphere	Co-Cr beads, cast in \pm HA
Cormet resurfacing hip system, Corin Medical	Cast	HIP and SHT	46 – 64	Equatorial expansion	Ti, VPS + HA
DUROM Zimmer*	Wrought-forged	N/A	44 – 66	Truncated Hemisphere	Ti, VPS
ASR DePuy Orthopaedics*	Cast	HIP	44 – 70	Truncated Hemisphere	Co-Cr beads, sintering \pm HA
ReCap, Biomet	Cast	None	44 – 66	Hemisphere	Ti, VPS + HA
Icon Hip Resurfacing, International	Cast	None	44 – 66	Hemisphere	Co-Cr beads, cast in \pm HA
ADEPT hip system, Finsbury Orthopaedics	Cast	None	44 - 66	Hemisphere	Co-Cr beads, cast in \pm HA

HIP – Hot Isostatic Pressing; SHT – Solution Heat Treatment; HA – Hydroxyapatite

VPS – Vacuum Plasma Spraying;

**Recalled by manufacturer*

2.6.1 Causes of the Failure of Hip Replacements

There are a range of different causes that can lead to failure of the implant [Sundfeldt et al., 2006] and a number of specific causes have been proposed [Huiskes et al., 1993; Sundfeldt et al., 2006].

Damage Accumulation

Activities such as walking will lead to continuous dynamic loading to the implant which could lead to mechanical damage of the components. Similarly, cracks and localised damage in the surrounding bone could occur as a result of high stresses, possibly leading to micromotion and eventually loosening of the implant [Huiskes et al., 1993].

Particulate Reactions

The presence of metal wear debris in the tissue surrounding the implant may lead to tissue reactions. Macrophages phagocytose wear debris, leading to the release of mediators such as cytokines that stimulate the resorption of bone. The creation and destruction of bone is controlled by osteoblast and osteoclast cells respectively, which in turn controls the amount of bone remodelling that takes place. If the balance between the numbers of both cells present is disturbed then it is the case that either not enough bone will be created or too much bone will be destroyed [Sundfeldt et al., 2006]. It has been suggested that the occurrence of wear debris will lead to a greater number of osteoclasts [Van der Vis et al., 1998], resulting in the resorption of bone [Bauer and Schils, 1999]. The localised destruction of bone and inflammation can result in areas of weakened bone, increasing the chance of implant failure; loosening of the component is more likely as the interface between the component and bone is weakened. This bone resorption is often known as osteolysis however it has been suggested by some that this may also be caused by high fluid pressures [Aspenberg and Van der Vis, 1998].

It was reported [Sundfeldt et al., 2006] that implant loosening could not occur solely due to the presence of wear debris; other contributing factors including infection and motion at the interface had to be present as well. It is not possible to directly correlate the failure of an implant to the number of wear particles present, but rather the particle size, the specific patient, the implant material and the process involved in its manufacturing will all influence the inflammatory reactions due to wear debris

[Matthews et al., 2000; McEwen et al., 2005; Sundfeldt et al., 2006]. Further factors such as the gaps between bone and implant due to a lack of bone ingrowth or the presence of screw holes, all create pathways for wear debris to reach the interface between bone and the component.

Poor Bone Ingrowth

The long term stability of press-fit cups is achieved through bone growing directly onto the outer porous surface of the cup. Whilst the forces acting on the cup from bone due to the use of an interference fit aid with stability, poor ingrowth will substantially increase the likelihood of cup migration. The occurrence of migration, by approximately 0.85 mm, can often indicate that future implant failure is likely [Karrholm et al., 1994].

Bone ingrowth is unlikely to occur if micromotion at the interface between the component and the bone is more than 150 μm ; the component will instead be surrounded by a fibrous membrane [Pilliar et al., 1986]. A fibrous membrane relating to micromotion was reported in implants that have not achieved adequate ingrowth [Engh et al., 1992], whilst implants that had achieved satisfactory bone ingrowth, micromotion of the components was less than 40 μm . The distribution of loads in the implant has also been reported to influence the extent and regions of bone ingrowth [Engh et al., 1992]. Low loading, the presence of infection and wear debris can result in bone resorption even if initial ingrowth has been achieved.

Stress Shielding

When a component is implanted it can alter the way in which forces are transferred through the bone. This will result in a remodelling of the local bone, resulting in a change in the regions of stiffer and weaker bone surrounding the component. For example, if the implanted component has a considerably higher stiffness than that of the surrounding bone, then this bone will become progressively weaker as the large forces that it experienced previously are transferred away from it. The occurrence of stress shielding balances after approximately two years and few cases of implant failure have been reported as a direct result of stress shielding [Huiskes, 1993; Laursen et al., 2007; Shetty et al., 2006]. Metal press fit cups are higher in stiffness than cemented UHMWPE cups therefore are more likely to result in stress shielding in the

long term; a localised weakening of the bone may increase the risk of other causes of failure such as poor ingrowth or fractures [Callaghan et al., 2006].

Wear

All bearing surfaces will generate wear debris during their use [Bronzino, 2006]. There are a range of circumstances in which this can be accelerated, leading to early failure and other associated health problems. A number of ways in which wear of the components can take place are commonly described [Bauer and Schils, 1999]:

- The normal articulation between the surfaces of the acetabular cup and femoral head.
- When the femoral head is in contact with an unintended surface, such as the metal edge of the cup, due to poor component positioning or manufacturing design.
- When a third party particle is introduced between the two normal articulating surfaces. These could include fragments of cement or particles from the porous outer surface of a press-fit cup.
- When two surfaces interact with each other that are not intended to. For example contact between the rim of the cup and the femoral neck.

High Fluid Pressure

It has been reported that the presence of high fluid pressure between the component and the bone can result in resorption of the bone [Van der Vis et al., 1998]. However it has also been reported by others that the main issue with high fluid pressure is that it aids in the movement of wear particles to the interface between the bone and the component [Sundfeldt et al., 2006].

Surgeon Technique

Poor positioning of the component or inadequate seating of the cup resulting in large polar gaps could also contribute to early failure [Ong et al., 2009]; high abduction angles could result in edge loading and cup impingement [De Hann et al., 2008]. Inaccurate reaming of the acetabular cavity could additionally create issues such as a

change in the distribution of the loads in the implant, stress shielding and greater deformations of the component.

2.6.2 Indicators for Revision Surgery

There are a number of possible measurable indicators of revision surgery being necessary due to the reasons discussed previously.

Aseptic Loosening

This has previously been shown to be the most common reason for revision surgery and there is a similar rate of the occurrence of loosening of both the cup and the femoral stem [Havelin et al., 2000]. A good predictor of loosening can be the presence of micromotion due to poor initial bone ingrowth, however there is not a single contributing factor that leads to this mode of failure. Other issues such as the number and location of wear particles, stress shielding and high fluid pressure may also contribute to loosening.

Dislocations

Dislocation of the femoral head from the acetabular cavity may occur due to poor positioning of the acetabular cup, the design of the component and the anatomy of the specific patient [Kristiansen et al., 1985]. Large diameter femoral heads with large cups increase the range of motion of the implant before the occurrence of impingement and can reduce the risk of dislocations occurring due to an increase in the jump distance of the femoral head, which is the amount of lateral translation of the head that must occur before dislocation occurs [Conroy et al., 2008; Sariali et al., 2009].

Fracture of the Bone

Fractures may occur if a patient experiences a fall; the risk of damage occurring is increased in weaker bones and as such factors including the age and gender of the patient are associated with a greater change of fracture. Other factors such as implant loosening, stress shielding and diseases such as osteoporosis may also lead to fractures requiring revision of the implanted components.

Fracture of the Implanted Components

The occurrence of this is considerably rarer than that of the fracture of bone and is most likely to occur as a result of a high energy trauma or fatigue.

Wear of Components

Wear between the articulating surfaces can be accounted for in a component's design however other factors such as impingement of the component can result in higher wear rates. MoM hip replacements have been shown to have low wear rates. However recent studies have shown that the failure rate of these components is higher than was expected and the associated wear debris may be the reason for the presence of tissue necrosis and large masses in the region of the implant for some patients [Hart et al., 2009].

2.7 Implant Tribology

A wear rate of less than 1 mm^3 per million cycles has been defined in MoM articulations as being low wear [Fisher, 2011]. At these rates the metal particles that are created are small enough (nanometre in diameter) so that they are either relatively easily transferred away from peri-prosthetic tissue or that they corrode rapidly, ensuring that high levels of particles do not appear to accumulate around the implant [Fisher, 2011].

A key factor that will control the amount of wear generated is the type of lubrication between the two articulating surfaces [Flannery et al., 2008]. In ideal situations the lubricating film between the cup and the head will be thick enough so as to separate the two surfaces. The minimum film thickness (h_{\min}) is influenced by a number of factors including fluid viscosity, the sliding velocity of the two surfaces relative to each other, the bearing loads, the surface area of the two components and their elastic moduli. The amount of separation between the articulating surfaces will also be influenced by the roughness of each surface. The Ra value is defined as a mean of the peaks and valleys above and below the surface of the cup or head, Figure 2.15. The Ra value for a polyethylene surface can be as high as $1 \mu\text{m}$ whilst for metal components can be less than $0.015 \mu\text{m}$ [Dowson and Jin, 2006].

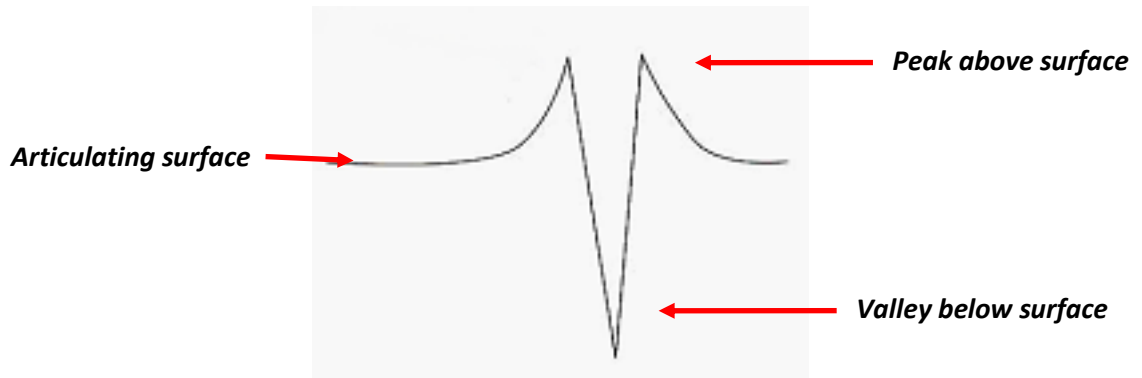


Figure 2.15: Schematic representing a peak above the articulating surface of a component, indicating roughness [Adapted from Khairy, 2005]

An estimation of the mean minimum fluid-film thickness in the dynamically loaded bearing can be obtained as [Hamrock and Dowson, 1978]:

$$\frac{h_{min}}{R} = 2.8 \left(\frac{\eta\mu}{E'R} \right)^{0.65} \left(\frac{w}{E'R^2} \right)^{-0.21} \quad (2.1)$$

where:

h_{min} = minimum film thickness

R = equivalent radius

E' = effective elastic modulus of the two bearing components

w = load

η = viscosity of the synovial fluid

μ = entraining velocity

The lambda ratio (λ) refers to the ratio of minimum fluid-film thickness (h_{min}) to the roughness of the two bearing surfaces (Ra_1 and Ra_2) [Flannery et al., 2008]:

$$\lambda = \frac{h_{min}}{\sqrt{(Ra_1)^2 + (Ra_2)^2}} \quad (2.2)$$

The lambda ratio can provide an indication of which of the three types of lubrication that will occur between the two surfaces [Khairy Flannery et al., 2008]. When lambda values are larger than 3, this suggests that the fluid-film thickness is larger than the height of the asperities of the rough articular surface and this signifies fluid-film lubrication, Figure 2.16a. When lambda values are between 1 and 3, this signifies

mixed film lubrication, Figure 2.16b, and when the lambda ratio is less than 1, boundary lubrication is represented, Figure 2.16c. It is clear that when the roughness of the surface is higher, such that the height of the asperities is larger, then a greater fluid-film thickness is required, than for a smoother surface in order for fluid-film lubrication to occur. For example, if the diametrical clearance between cup and head was kept constant a rougher acetabular cup surface could lead to poor lubrication, negatively affecting the performance of the bearing [Jacobs and Craig, 1998]. A larger diameter femoral head can increase the entraining velocity of the fluid in the bearing, potentially improving its lubrication properties [Dowson et al., 2003].

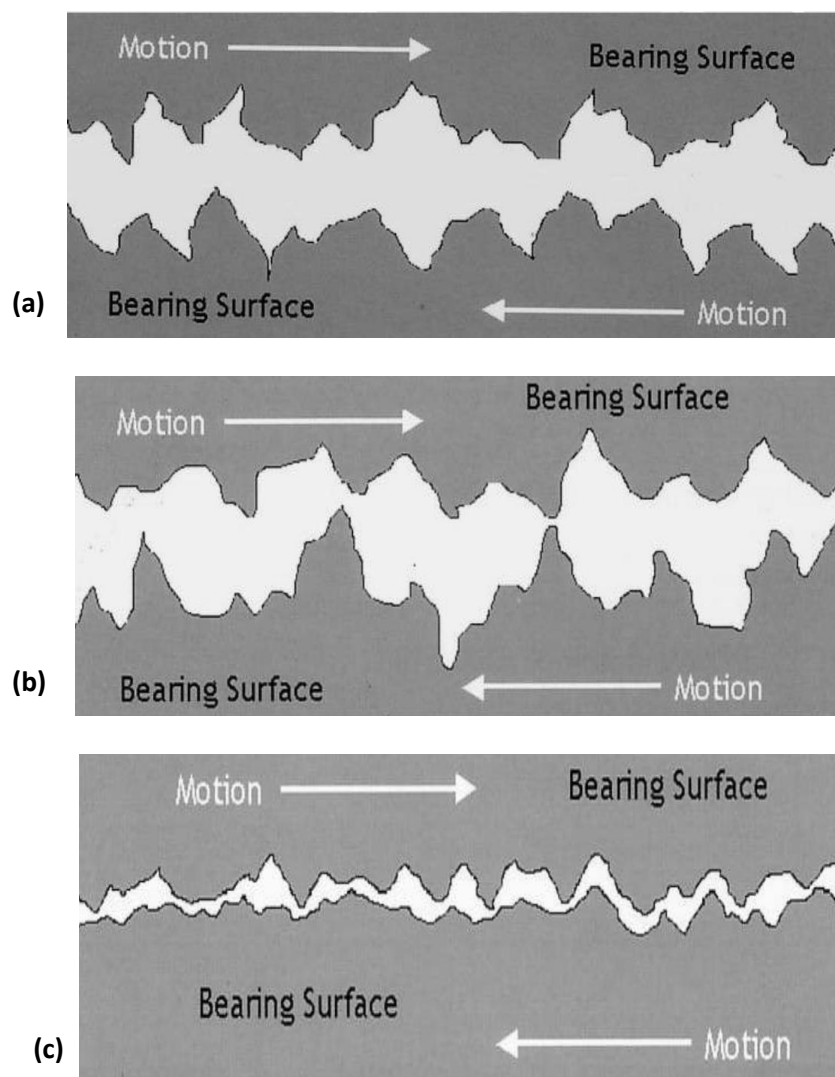


Figure 2.16: (a) Lambda value greater than 3, indicating full fluid-film lubrication, (b) lambda values between 1 and 3, indicating mixed lubrication and (c) lambda ratio less than 1 indicating boundary lubrication [adapted from Khairy, 2005]

In clinical situations however mixed lubrication ($1 < \lambda < 3$) is often present at the bearing surface [Dowson et al., 2000] with variations between clear separation of the surfaces and periods of MoM contact occurring. The coefficient of friction between the cup and head is approximately 0.008 to 0.02 and is a function of the type of lubrication present [Khairy, 2005]; it is clear, for example, that boundary lubrication will result in an increase in friction, whilst low friction will occur with low thickness full fluid film lubrication. The Stribeck curve (Figure 2.17) plots the change in friction in relation to increasing speed and viscosity or reducing load (horizontal axis), which are often related together by the Sommerfeld number as:

$$S = \left(\frac{r}{c}\right)^2 \frac{\mu N}{P}$$

Where r is radius, c is the radial clearance, μ is viscosity, N is speed and P is load [Dowson, 2006]. Also illustrated is the relationship between friction and film thickness.

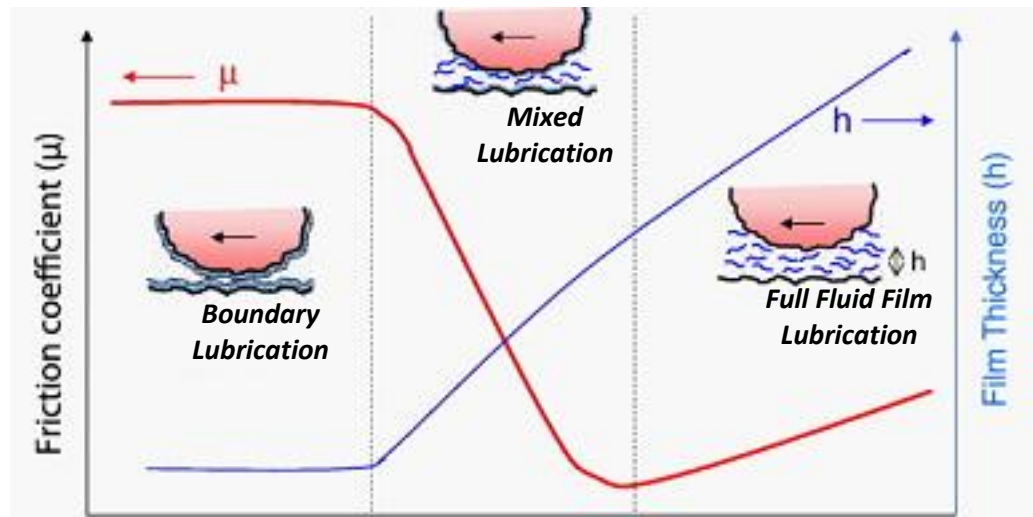


Figure 2.17: Stribeck curve illustrating the coefficient of friction as related to the film thickness and therefore the mode of lubrication. Increasing speed and viscosity or reducing load are on the horizontal axis [adapted from Coles et al., 2010]

Three key factors, related to the geometry and design of the components, are known to affect the mode of lubrication [Khairy, 2005; Liu, 2006;]:

- The diameter of the components.
- The sphericity of the components.
- The size of the clearance between the cup and head.

Simulator tests of the hip joint using MoM components have demonstrated that increasing the diameter of the bearing couple results in a clear change in the mode of lubrication from boundary to mixed [Smith et al., 2001; Dowson, 2003; Dowson et al., 2004]. For small head diameters between 16 and 22.225 mm, an increase in wear rates has been reported as the majority of load is supported by direct contact between the head and the cup. However for bearings with diameters greater than 28 mm, a considerable decrease in the wear rates is observed with increasing head size as more of the loads are carried by fluid film lubrication, Figure 2.18.

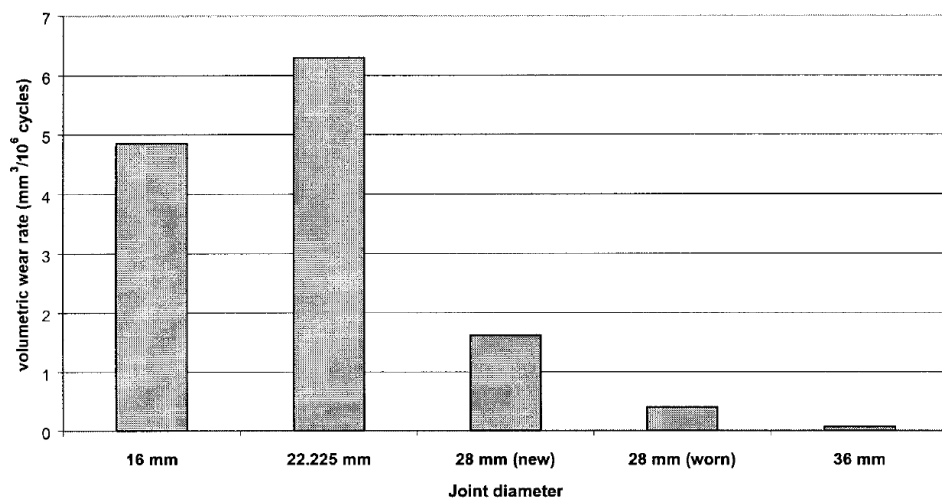


Figure 2.18: Influence of femoral head diameter on volumetric wear rates [Smith et al., 2001]

The protocol for measuring the sphericity of a metal acetabular cup has been defined [ASTM F2033]. Using a three-dimensional measuring machine a number of points should be measured about the circumference of three planes along the depth of the articulating surface, namely 8 points along each plane, AA, BB and CC and a single point at the pole, Figure 2.19. An average diameter is then determined from the data using the least squares method, and the coordinates of the centre of a sphere is determined from the average diameter of the cup. The sphericity of the cup is defined by the *departure from roundness* and is calculated by determining the difference between the maximum and minimum distances from the centre of the average diameter sphere and the measured points on the articulating surface. The maximum accepted out of roundness of a cup is stated as being 15 μm [ASTM F2033].

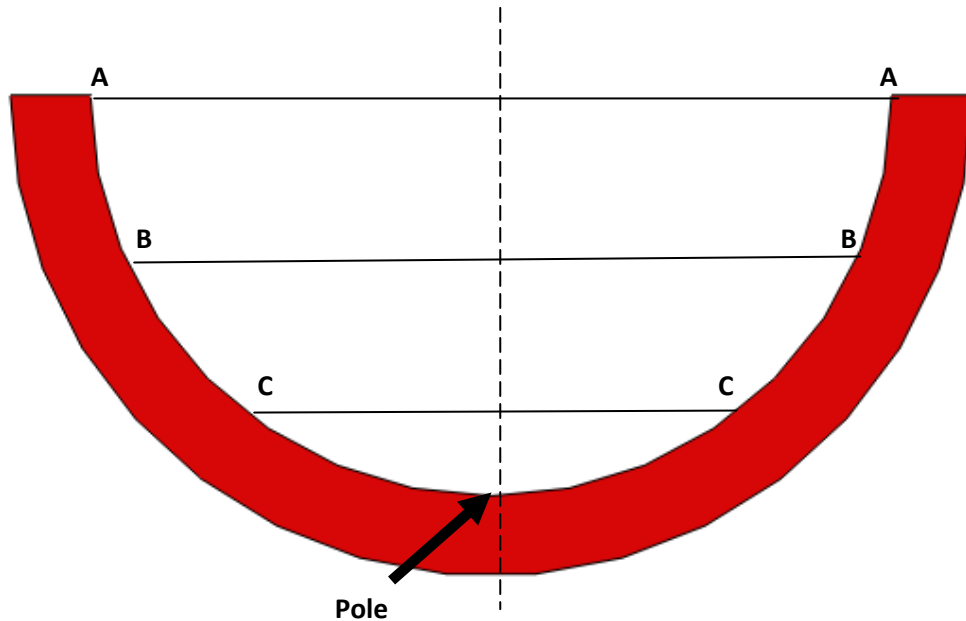


Figure 2.19: Measurement of points on articulating surface of cup to determine sphericity [ASTM F2033]

In a similar manner to measuring the sphericity, the clearance between a head and cup can be determined by calculating the difference between the outer radius of the head and the inner radius of the cup, Figure 2.20, measured using a coordinate measuring machine [Jedenmalm et al., 2010]. Clearance is reported as either as radial or diametrical (two times radial). Diametrical clearances of component pairs typically lie between 60 and 250 μm [Chang et al., 2007] and have been shown in simulator studies to influence wear rates.

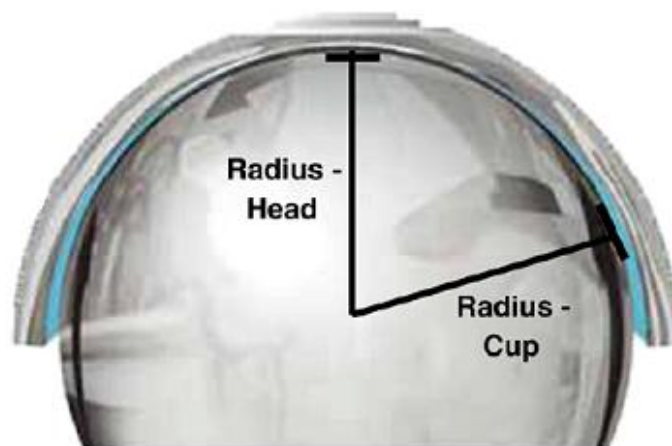


Figure 2.20: Radial Clearance determined by calculating the difference between the outer radius of the head and the inner radius of the cup [adapted from Springer et al., 2011]

2.8 Concerns surrounding the use of Metal-on-Metal Implants

Extensive simulator testing has demonstrated that MoM bearing surfaces have very low wear rates even with large femoral head sizes [Smith et al., 2001; Dowson, 2004; Medley et al., 1996; Firkins et al., 2001]. Larger head sizes allow for better fluid-film lubrication than smaller head sizes and also reduced the risk of dislocations, creating a larger range of motion of the hip joint [De Haan et al., 2008]. For these reasons, the use of large diameter MoM hip components had become popular amongst surgeons. However very recently the use of MoM implants has come under very strong scrutiny, although they do remain commercially available. There are two main concerns surrounding the use of these components; firstly that current evidence is suggesting that these implants have a notably higher (and earlier) failure rate than expected [Langton et al., 2010] and secondly that the metal wear ions released into the blood stream may have considerable toxic effects on the body [Haddad et al., 2011].

Analysis [Smith et al., 2012] of registry data from the National Joint Registry of England and Wales concluded that MoM stemmed hip implants have a higher rate of failure than other bearing options and should no longer be implanted in patients, particularly in younger women with large diameter heads. It reported that the five-year revision rate for 46 mm MoM implants (excluding the ASR) was 6.1% for younger women, and was significantly greater than a revision rate of 1.6% for metal on polyethylene implants with 28 mm head diameters. In contrast, a five-year revision rate of 3.3% was observed in men aged 60 years using a ceramic-on-ceramic bearing and this was improved with a larger diameter head of 40 mm, resulting in a revision rate of 2%. The most frequent reasons for revision surgeries were those of implant loosening and associated pain; it has been suggested that this may be due to poor lubrication or trunion wear leading to the release of metal wear debris and consequently soft-tissue reactions. It is difficult currently to identify the precise scenarios that led to this mode of failure.

The toxicology of metal ions generated by implants in the body is currently unclear. High levels of cobalt and chromium have been found in the blood and organs of patients implanted with MoM components and is commonly referred to as metallosis [Haddad et al., 2011]. Metallosis is often linked with soft-tissue reactions, necrosis, pain and tissue swelling however it is unclear to what extent metal ions from implants contribute to this in the body. Some studies have reported that cobalt concentrations

in the blood can reach levels up to 600 times greater than normal physiological levels of approximately 0.5 µg/L [Engh et al., 2009]. An increase in metal ion levels has also been observed when using larger diameter components from a range of manufacturers. A review was carried out by Haddad et al. [2011] which served to discuss the clinical literature data available about the effect of metal ions released when using MoM bearings. The following summarises the main points of this article:

Frequency of Reactions to Metal Ions

Overall there is a low occurrence of soft-tissue reactions following the implantation of MoM THR that result in adverse symptoms, however this does vary notably between manufacturers, ranging from 0 to 18%. Adverse reactions in hip resurfacing implants ranged from 0.3 to 3.4% after a 7.1 year follow up. Adverse reactions were often in the form of pseudotumours and revision surgery related to this was notably higher in women than in men.

The Importance of Implant Position

Positioning of the acetabular cup, the femoral head and the stem during a hip replacement procedure is known to influence the success of the prosthesis [Schnurr et al., 2009; De Hann et al., 2008]. Whilst surgeons have established methods to seat the femoral component [Najarian et al., 2009], there is still a degree of uncertainty about the optimum position to place an acetabular cup [Lewinnek et al., 1978; Hart et al., 2008; Wan et al., 2009; Babisch et al., 2008]. Cup placement within the safe-zone has been reported to minimise the risk of high wear, component loosening, impingement and dislocation [Hart et al., 2008; Hart et al., 2009; Langton et al., 2008; Ryan et al., 2010].

There is a strong positive correlation between high abduction angles (>50°) of the acetabular cup and the rate of revision. Edge loading at these orientations often results in accelerated wear rates, with greater particle release. The precise effects of cup version have been more difficult to report on, in part due to the difficulties in measuring this orientation from traditional X-rays. However of the studies to date, there has been little evidence relating cup version with elevated blood metal ion levels. Optimal positioning of the acetabular cup in hip resurfacing has been suggested as being 20° version and 45° abduction. The incidence of pseudotumours has been

found to be four times lower when cups are positioned within 10° of this recommended optimum. It should be noted however that this optimum will vary between different patients and it may be more appropriate to consider the safe zone proposed by Lewinnek et al. [1978] of a version between 5° and 25° and abduction between 30° and 50°.

Importance of Implant Size

There is much evidence that suggests that smaller MoM hip resurfacing components are more susceptible to generating greater amounts of wear debris due to comparatively poor fluid lubrication between the bearing surfaces [Smith et al., 2001; Dowson, 2003; Dowson et al., 2004]. However there have been reports of high wear and soft-tissue metal reactions in large diameter MoM THRs with suggestions that this may be due to a poor connection at the junction between the shortened taper of the stem and the femoral head [Cohen, 2012; Long, 2005].

Significance of Gender

A higher occurrence of pseudotumours has been reported in women following MoM resurfacing procedures. These may be due to the anatomical differences between men and women but may also be due to the differences in implant sizes between the genders [Latteier et al., 2011].

Effect of Differences in Implant Designs

The design of resurfacing components is thought to have a significant effect on the failure of the implant. For example, the ASR cup which had a low diametrical clearance may have resulted in increased edge loading and wear rates. Differences between the THR and resurfacing large diameter components are currently unclear, however it is suggested that wear at the junction of the head and the trunion in THR could result in higher metal ion levels [Haddad et al., 2011]

What are the accepted levels of Metal Ions in the Blood?

The presence of high levels of metals ions can be used as an indicator that the implant is not functioning properly; there is however no clearly defined cut-off level for the number of ions that signify poor implant behaviour. Higher levels of cobalt ions have

been reported in well functioning MoM components compared to pre-operative levels and to some extent may be regarded as a feature of the implant and not have any adverse effects. However it has also been shown that cobalt levels were doubled in patients that experienced pain following implantation [Hart et al., 2011].

2.8.1 Uncertainty of the Factors Causing MoM Problems

The behaviour of MoM implants is variable. There is strong evidence that large diameter components implanted in younger women lead to early failures. Conversely it has also been reported that hip resurfacing can be a successful procedure when performed in younger men with the appropriate anatomy [Treacy et al., 2011]. Whilst failures and elevated wear rates can be explained in part by factors such as poor cup positioning or implant design, it is sometimes the case that poorly seated cups do not present with any problematic symptoms that require revision. On the other hand component failures, high wear rates and soft-tissue reactions have been observed in implants that have been well positioned; the reasons for these are not fully understood. It is clear however that surgical technique and appropriate patient selection do have strong influences on the success of an implant [Hart et al., 2012b; Latteier et al., 2011; Bordini et al., 2007].

In ideal circumstances with well positioned components, wear in MoM implants is very low however a deviation from the ideal situations can increase wear rates by up to 100 times. It has been suggested that the occurrence of contact between the femoral head and the acetabular cup can be associated with the increased wear rates and ion levels in MoM bearings, which can lead to an increased rate of failure [De Haan et al., 2008]. It is known that excessive cup-head contact can occur during edge loading however it has been suggested [Jin et al., 2006] that contact between the two surfaces may also occur as a result of the acetabular cup deforming so that it experiences a reduction in its diameter. Cup deformations upon insertion into the acetabular cavity may be significant enough, when compared to the cup-head clearances, that equatorial contact occurs, changing fluid-film lubrication and therefore the wear properties, and in extreme cases a locking of the joint all together. There have been a limited number of experimental and finite element studies carried out that have investigated the extent of cup deformation. These studies have had a range of associated limitations in their design and have not reached a consensus about the true clinical relevance of the

deformation of acetabular cups when attempting to explain its significance towards component failure and elevated wear rates.

2.9 Deformation of Acetabular Cups

As MOM hip components are typically larger in diameter than those used in other bearing surfaces such as ceramic, the acetabular cups are also made thinner to ensure that bone conservation is kept to a maximum [Ebied et al., 2002]. Thinner cups are likely to deform more, which may be beneficial to distribute load around the cup [Ebied et al., 2002]. However, the greater deformation associated with these thinner oversized cups could create problems with the performance of the component and this requires full consideration. For example, the micromotion at the interface of the cup and bone has been found to increase due to excessive cup deformation, increasing wear and hampering bone in-growth [Ebied et al., 2002]. Diametrical clearances of between 60 and 250 μm are usually specified between the cup and femoral head [Chang et al., 2007] and high deformations could result in the reduction of these clearances and the deformations could ultimately have a negative effect on fluid-film lubrication, potentially causing equatorial contact. Where deformation is very large the joint could potentially seize [Jin et al., 2006].

There have been a number of studies that have previously attempted to investigate the extent of cup deformation and shell deformation, from a range of manufacturers, made of either cobalt-chromium or a titanium alloy, and with a range of diameters. Test methods have varied from finite element simulations, to experimental studies using foam or cadaveric models and mechanical rim loading of the component.

2.9.1 Experimental Methods

The deformation of metal acetabular cups has been investigated experimentally by impacting them into foam cavities representing the acetabulum [Jin et al., 2006; Schmidig et al., 2010; Ong et al., 2009; Fritsche et al., 2008], applying opposing loads to the rim of the cup [Squire et al., 2006; Everitt et al., 2010; Springer et al., 2011] and impacting the component into cadaveric models [Jin et al., 2006; Markel et al., 2010]. In all experimental studies, the deformation of the cups is reported as being the maximum change in its diameter following insertion into a cavity, Table 2.3. It is clear

that there is considerable variation in the deformations observed in the studies. This may be due the differences in the experimental design, for example rim loading mimics boney contact on two comparatively small localised regions of the cup whereas in a cadaveric model, considerably more contact between the cup and underlying bone would occur.

Table 2.3: Summary of experimental studies investigating the deformation of press-fit acetabular CoCrMo cups and titanium shells

Cup Design	Cup Material	Cup / Shell Diameter/ mm	Nature of Study	Diametrical Change/ μm	Study
DePuy ASR	CoCrMo	60	Foam	60 (thin cup) 30 – 50 (thick cup)	Jin et al. [2006]
Press-fit Metal Shell	CoCrMo	56	Foam	8 (max)	Fritsche et al. [2008]
Press-fit EP FIT PLUS	Titanium	56	Foam	4 (max)	Fritsche et al. [2008]
Stryker Trident	Titanium	42 – 58	Foam	320 - 830	Schmidig et al. [2010]
Stryker Trident	Titanium	50	Foam	450	Ong et al. [2009]
Press-fit Cup	CoCrMo	48 - 62	Rim Loading (3000 N)	310 - 530	Everitt et al. [2010]
Various Designs	CoCrMo	44 - 66	Rim loading (200 – 2800 N)	15 - 350	Springer et al. [2011]
DePuy Pinnacle	Titanium	48 – 66	Rim loading (200 – 2000 N)	340 \pm 210	Squire et al. [2006]
DePuy ASR	CoCrMo	56 - 60	Cadaveric	25 – 103 (thin cup) 21 – 22 (thick cup)	Jin et al. [2006]
Press-fit EP FIT PLUS	Titanium	46 - 50	Cadaveric	4 (max)	Fritsche et al. [2008]
Stryker Trident	Titanium	50 - 58	Cadaveric	150 - 600	Markel et al. [2010]
DePuy Pinnacle	Titanium	50 – 60	In Vivo	160 \pm 160	Squire et al. [2006]

The extent of deformation of the components has been determined by measuring the diameter of the cup or shell before and after impactation using callipers [Ong et al., 2009], or measuring the inner surfaces of the cups using a coordinate-measuring machine (CMM). The deformation of the cups have also been assessed using matching femoral heads with dye smeared on them, to visually determine the area of contact between head and cup after impactation [Jin et al., 2006]. Measurements of tangentially arranged strain gauges have also been used to determine the change in diameter of the cups [Fritsche et al. 2008], Figure 2.21.

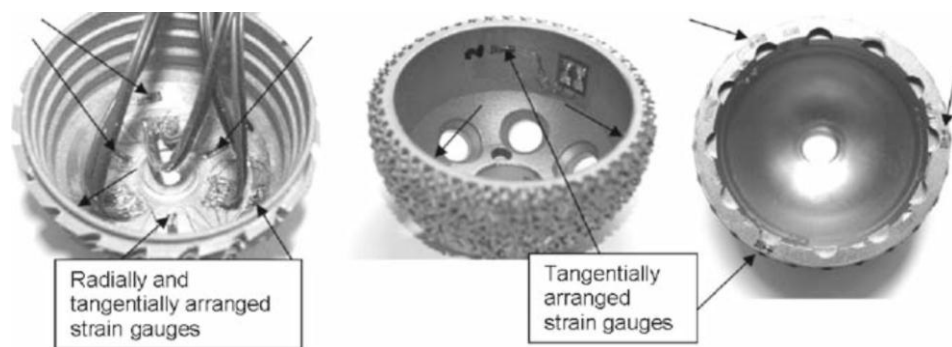


Figure 2.21: *Distribution of strain gauges within the various acetabular cups [Fritsche et al., 2008]*

A two point pinching load on an impacted cup has been found to be present in cadaveric models between the ilial and ischeal regions [Jin et al., 2006; Widmer et al., 2002]. In order to replicate the pinching of the ilial and ischeal regions, reamed spherical polyurethane foam models (Sawbones) have been used with the cavity typically relieved on opposite sides of the foam [Jin et al., 2006; Schmidig et al., 2010; Ong et al., 2009], Figure 2.22 . These foam cavities can approximate the diametrical deformations of CoCrMo cups that have been found to occur in cadaveric tests [Jin et al., 2006] however it is unclear how representative of the wider patient population they are in terms of variations in age, gender and bone health.

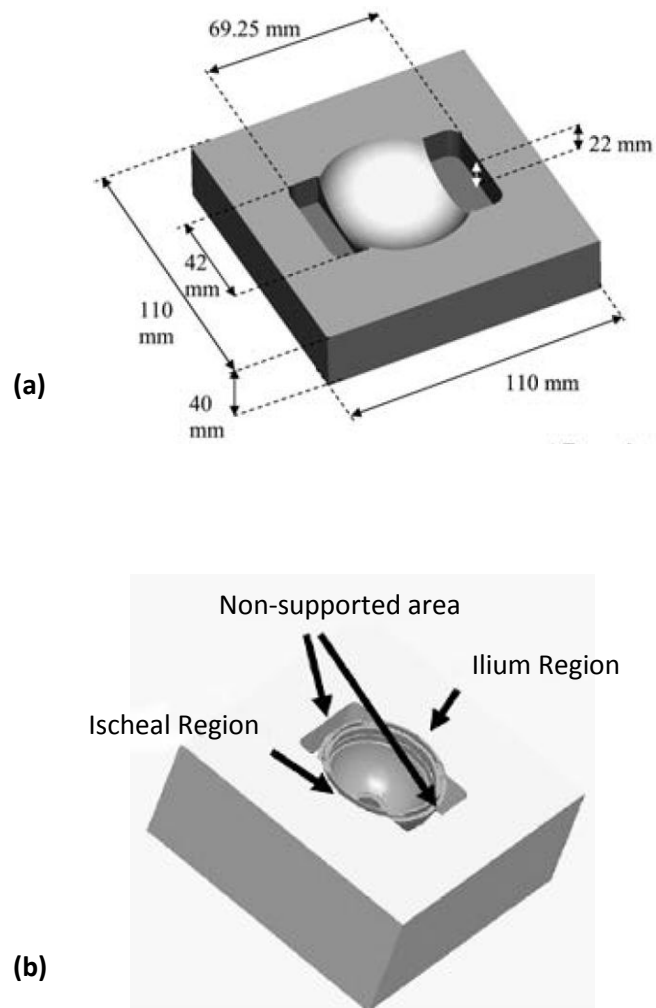


Figure 2.22: Pinching in the pelvis simulated in experimental foam models by **(a)** Jin et al. [2006] and **(b)** Schmidig et al. [2010]

The maximum cup deformations of 8 μm observed in the study by Fritsche et al. [2008], Table 2.3, are considerably lower than in other studies using foam cavities [Jin et al., 2006; Ong et al., 2009; Schmidig et al., 2010], despite the fact that the perceived force applied on the cups was found to be substantially greater than that found by Squire et al. [2006]. This may largely be due to that fact that no artificial pinch point was created in this study, in contrast to the other studies, highlighting the significance of the influence of cup pinching.

The comparatively larger values for deformation reported for titanium shells [Ong et al., 2009; Schmidig et al., 2010] compared to cobalt-chromium cups are to be expected due in part to their lower material stiffness and also because the shells tend to have

thinner profiles. It is of note however that the initial high shell deformations are likely to lessen following the insertion of the liner and seating of the femoral head as a result of the viscoelastic properties of the bone. It has been reported that the shell deformation immediately following impaction of 450 μm , was reduced to 380 μm and 280 μm when a liner and femoral head were seated respectively [Ong et al., 2009].

Diametrical clearances between the femoral head and the acetabular cup are generally specified as being between 60 and 250 μm , to allow for normal tribological performance and for fluid film lubrication. With the exception of the findings by Fritsche et al. [2008], the results from the foam studies suggest that the cup deformation experienced may be excessive, when compared to these clearances. It was observed [Jin et al., 2006] that using a thin cup design resulted in high deformations compared to clearances; it was suggested that cups be thickened and lower interferences be used to prevent high deformations from occurring. Cups deformed by 75 μm have been described as having unrestricted articulation with no dome contact [Jin et al., 2006]. When deformations increased to 103 μm , there was again no dome contact however in this situation articulation was reported to be poor. This suggests that the maximum allowable deformation for normal articulation to be maintained would be in the region of 75 μm and this correlates with the specifications of the ASTM [ASTM F2033] which state that clearances between the cup and head should be a minimum of 70 μm .

It has been suggested that the viscoelastic relaxation of bone would result in a reduction in the stresses on the inserted cup and in the long term result in a reduction in the deformations; this however has not been fully investigated in previous work. It has been reported [Jin et al., 2006] that neither the foam nor the cadaveric bone models presented any significant features of time dependency and therefore were not considered in their study. Squire et al. [2006] observed no change in the deformation of cups inserted into patients after measurements taken 20 minutes apart during surgery and Markel et al. [2010] also did not report any notable changes after approximately 30 minutes in their cadaveric model. The time periods considered by these studies however may be too short and further work is necessary to fully appreciate the significance of time dependency on cup and shell deformation. It was also reported that large errors were found to have occurred in the accuracy of hand reamed cavities, resulting in interference fits lower than intended [Jin et al., 2006].

This raises an interesting question about the influence of hand reaming errors during the preparation of the acetabular cavity, on the deformation of the component; it is reasonable to expect that a perfectly spherical cavity may not be achievable clinically and its consequences to cup deformation need investigation.

Another in vitro approach to simulating the pinching observed in cadaveric models has been to apply increasing loads to the rim of cup and shell from opposite ends along the diameter, Figure 2.23 [Squire et al., 2006; Everitt et al., 2010; Springer et al., 2011].

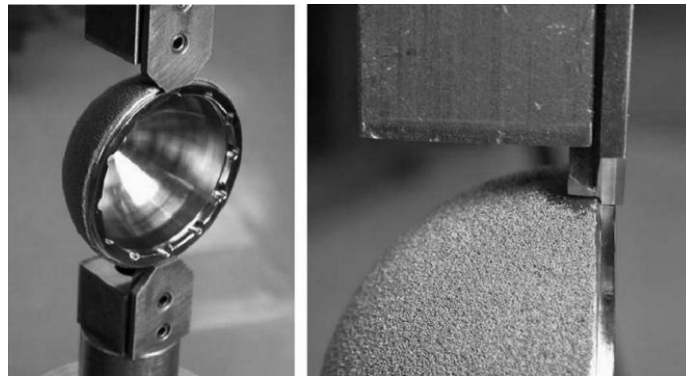


Figure 2.23: Compressive loads applied to cup along diameter using custom load platens
[Squire et al., 2006]

Whilst rim loading may be a poor representation of the bony cup support in vivo the results of these studies can provide an understanding of the behaviour of different cup designs. For example it has been reported that the stiffness of a particular titanium shell (DePuy Pinnacle) increases from approximately 2250 N/mm to 5000 N/mm as the diameter is increased from 54 mm to 66 mm [Squire et al., 2006]. This is in contrast to another report which observed a linear decrease in the stiffness of a CoCrMo cup with increasing diameter [Everitt et al., 2010].

Another experimental study using rim loading [Springer et al., 2011] has specifically investigated the influence of cup design on stiffness and deformation by considering cup designs from a range of manufacturers with varying diameter, thickness at the rim, thickness at the pole and the height. The results of this study provide an interesting understanding of the cups developed by different manufacturers, showing that there are notable differences in their designs. For each cup size, described by its diameter, there are variations in the wall thickness at the pole and rim. Table 2.4 presents five

particular designs and the dimensions that were reported for 58 mm components and a single 44 mm cup with very similar wall thicknesses to the larger diameter design by the same manufacturer.

Table 2.4: *The measured dimensions of four commercially available 58 mm acetabular cup designs and one 44 mm cup [Springer et al., 2012]*

Cup Design	Measured Diameter /mm	Depth /mm	Wall Thickness at Rim /mm	Wall Thickness at Pole /mm
Smith and Nephew Birmingham	58.34	21.18	6.53	4.53
Wright Medical Conserve Plus	59.23	23.42	4.82	3.88
Stryker Cormet	59.78	22.61	6.35	4.21
Biomet Magnum	58.02	23.46	5.80	3.26
Biomet Magnum	44.09	16.35	5.80	3.33

It appears that some manufacturers attempt to thin the entire profile of the cup to accommodate large head sizes whilst others vary the thickness of the rim and pole. It has been demonstrated [Yew et al., 2006] that larger sized cups will deform more and that wall thickness can strongly influence the deformation of the cup by stiffening the construct. This behaviour is observed in the deformations reported by Springer et al. [2011] when an opposing force of 1000 N was applied at the rim of each cup presented in Table 2.4, Figure 2.24. It can be seen that the Birmingham and Cormet cups, with similar dimensions for the wall thicknesses, experience similar deformations of approximately 60 μm . The Conserve cup however with its smaller wall thickness at both the pole and rim experiences larger deformations of over 120 μm . The 58 mm Biomet cup also deforms by approximately 120 μm but has a lower wall thickness than the Conserve cup but also a smaller measured diameter by over 1.2 mm. The 44 mm Biomet cup deforms considerably less than the 58 mm cup of the same design with very similar wall thicknesses.

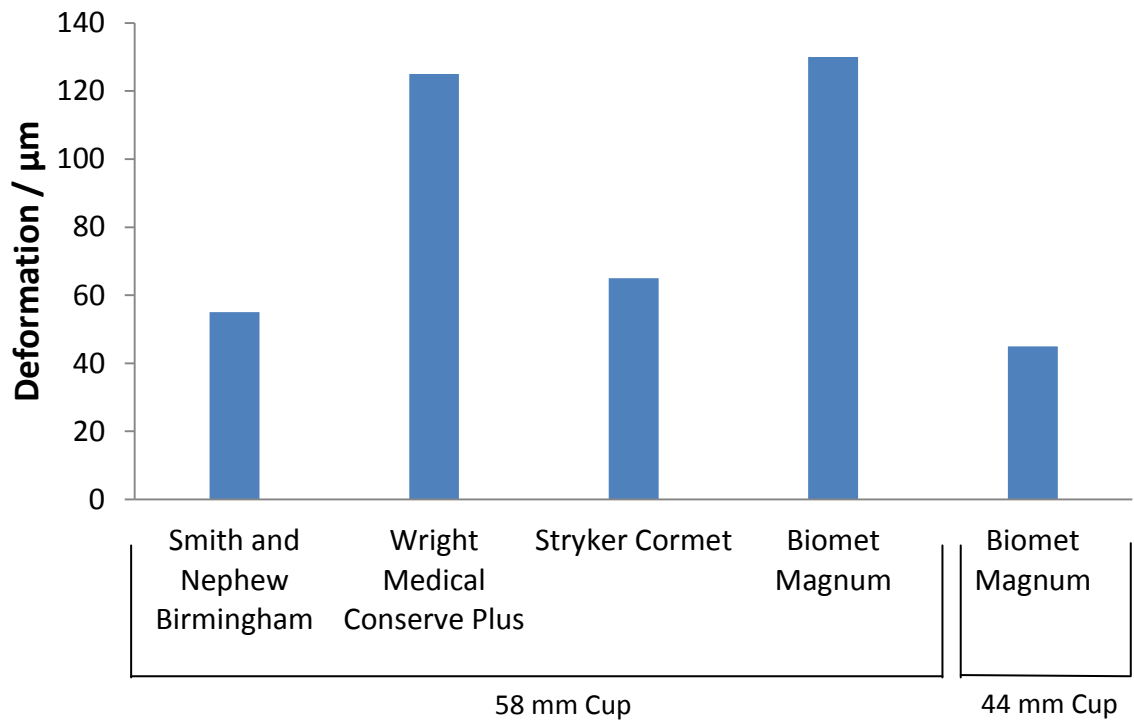


Figure 2.24: Radial deformation observed by Springer et al. [2012] for different cup designs following rim loading with a 1000 N load

It is logical that manufacturers should attempt to stiffen their designs as the diameter of the cup is increased. However this does not always appear to be the case, Figure 2.25 [Springer et al., 2011]. In the majority of designs the stiffness of the component actually decreases with increasing size, indicating that controlling this feature may not have been a design consideration by manufacturers. The deformation of large diameter cups which are comparatively lower in stiffness than smaller diameter designs may be sufficient to impact on the performance of the implant. The consequences of this may be important in understanding the high wear rates and unexplained failures in some patients, and may be due to poor cup design as some reports have eluded to.

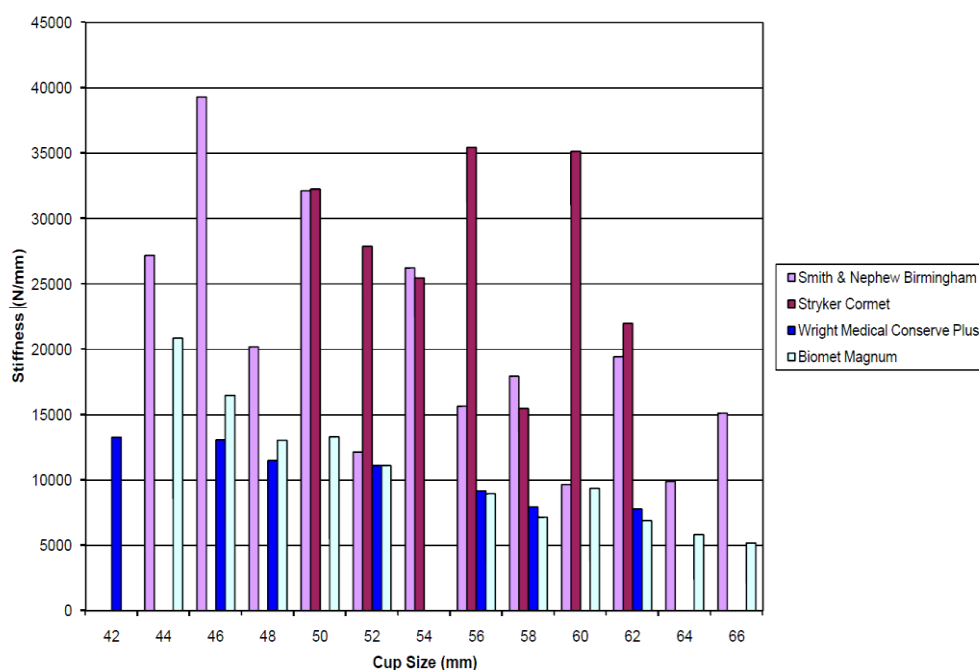


Figure 2.25: Calculated stiffness values for different cup sizes by various manufacturers [Springer et al., 2011]

Only one detailed cadaveric study has been carried out to investigate acetabular shell deformation [Markel et al., 2010], using pelvises from six donors. This concluded that bone mineral density could be used as a predictor for the cup deformations that could occur and is in agreement with the suggestion by Squire et al. [2006] that there may be a trend between bone quality and cup deformation. It was also suggested that factors such as surgical technique in reaming and component positioning may influence deformations and require further investigation.

In addition to experimental methods, acetabular cup deformation has also been investigated using finite element models [Yew et al., 2006; Hogg et al., 2009, Hogg et al., 2010; Everitt et al., 2010].

2.9.2 Finite Element Modelling

The following serves as an introduction to the finite element method based on the report by Felippa [2001]. Finite element (FE) modelling uses methods in which a domain is characterised in terms of a number of sub-domains referred to as elements. The behaviour of each element is readily defined and understood by numerical equations which together allow for the behaviour of the entire body to be analysed. Elements are connected together at nodes which have degrees of freedom that can be

controlled, Figure 2.26. The process of creating individual elements is known as meshing.

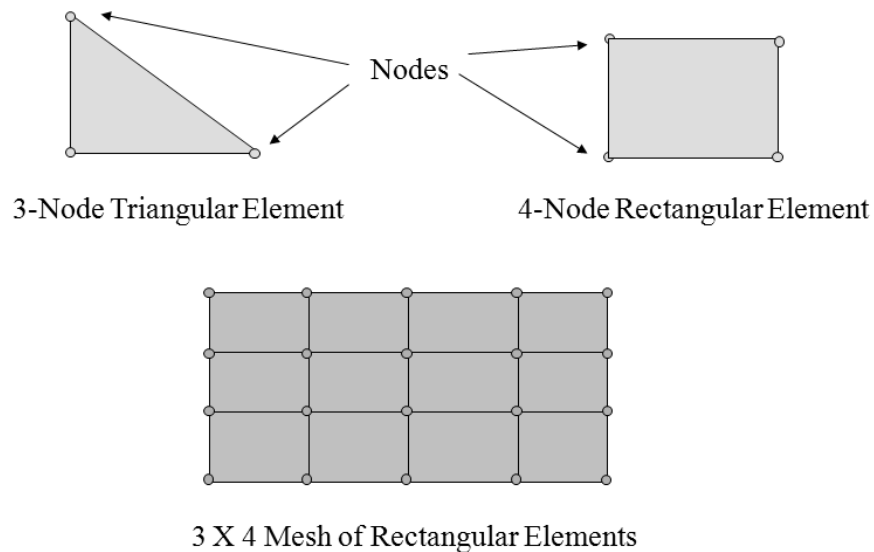


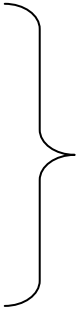
Figure 2.26: Elements are connected together at nodes to form a mesh [Felippa, 2001].

There are a range of elements that are available to be selected when creating a mesh. In their simplest form, these can be linear two dimensional triangular or rectangular elements and in three-dimensional models elements can be tetrahedral or hexahedral and may also be quadratic in nature, resulting in greater accuracy in complex shapes than using similarly sized linear elements.

As the computational power required for FE modelling increases, the use of this method has become accepted as a viable research tool to understand complex biomechanical behaviour which may not otherwise be feasible experimentally. For example it is an essential tool when understanding the behaviour of implants before they reach the stage of clinical testing, or if an understanding of the effect of variations of an existing clinical design is desired. Using the example of the acetabular cup, it is less expensive financially and in terms of time to carry out FE simulations with many different cup geometries than it is to manufacture and experimentally test different incremental cup designs. This allows for design optimisation to be performed before carrying out additional experimental and clinical tests. Another clear advantage is that FE models allow for perfectly reproducible results to be obtained which are not possible in cadaveric models.

There are a range of commercially available FE packages that are used by researchers, of which the most popular is Abaqus. This package uses a system or pre and post-processors to solve complex numerical problems generated in the models. There are two main types of FE analysis that exist, namely static implicit (steady state) and explicit dynamics (transient). A key difference between the two approaches is in the consideration of velocity. An implicit model does not consider displacements as a function of time therefore velocity is not modelled, whereas an explicit approach considers velocity, mass and therefore momentum. In a static approach a body is under equilibrium conditions from which displacements can be predicted as loads are applied. It is common practice to initially utilise a static model to understand the behaviour of a system before adopting a dynamic approach, if required. Dynamic analysis involves the application of a load as a function of time and is most often used when there is inertia in a system, for example a hammer blow during acetabular cup impaction.

The development and analysis of FE models can be broken up into a number of stages:

- Creation of the specific geometry of a body.
 - Definition of the static or dynamic analysis system.
 - Meshing of the body.
 - Definition of material properties.
 - Application of boundary conditions.
- 
- Pre-processing
- Processing: solving linear/non linear numerical equations related to each element.
 - Post-processing: obtaining results relating to deformations, stresses, etc.

An important process in the development of reliable models that can be trusted for analysis is that of validation. This can take the form of experimental tests specifically performed to represent the FE model or the FE model can be related to existing published experimental data. The processes of the development of finite element models are discussed in more detail in chapters 3-5.

2.9.3 Finite Element Models of Acetabular Cups and Shells

There have been a limited number of studies that have used finite element models to simulate the deformation of metal cups and shells following insertion, Table 2.5.

Table 2.5: Summary of finite element studies investigating the deformation of press-fit acetabular CoCrMo cups and titanium shells

Cup Design	Cup Material	Cup Diameter/mm	Nature of Study	Diametrical Change/ μm	Study
DePuy MOM	CoCrMo	46 - 70	FEA	110 (thin cup) 19-69 (intermediate cup) 17 (thick cup)	Yew et al. [2006]
Press-fit Shell	Titanium	54	FEA	>120	Hogg et al. [2009; 2010]
Press-fit Cup	CoCrMo	48 - 62	FEA	310 - 530	Everitt et al. [2010]

A rim loading design that was performed experimentally was also simulated in an FE model, Figure 2.27 [Everitt et al., 2010]. The models showed that increasing the cup diameter, whilst keeping the same wall thickness, resulted in a reduction in the stiffness of the cup, as expected. The FE model developed in this study is a considerable simplification of the loads that a cup would experience in the pelvis. It therefore may be most beneficial as a means of understanding the differences in stiffness between different cup designs and not a representation of deformations in vivo.

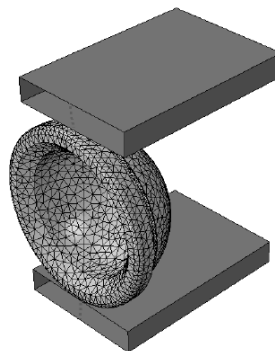


Figure 2.27: Finite element simulation of the rim loading used experimentally [Everitt et al., 2010]

Another FE study [Yew et al., 2006] served to simulate the experimental foam models performed previously [Jin et al., 2006]. The press-fit procedure was first simulated using a two dimensional axisymmetric finite element model, Figure 2.28.

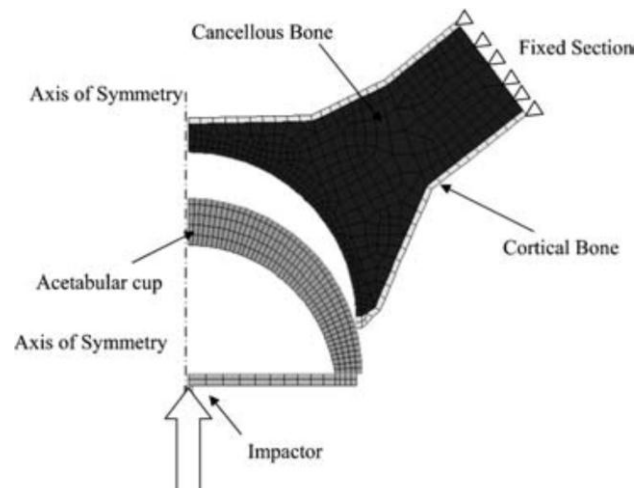


Figure 2.28: Two-dimensional finite element model of insertion of press-fit cup with interference [Yew et al., 2006]

This was followed by the development of a three-dimensional model in which the pinching of the cup could be included, to investigate deformation for the different cup sizes. It was demonstrated that for a consistent cup diameter, increasing the amount of interference led to an increase in the deformation of the cup. This is in agreement with the findings of a previous study [Ries et al., 1997] that increasing the interference led to an increase in the strains at the periphery of the cup. The results also showed that increasing the diameter of the cup leads to an increase in its diametrical deformation upon impaction. This was also found to be the case when the wall thickness was decreased. The FE results were in some cases found to be inconsistent when compared to the previous experimental study [Jin et al., 2006], for example the model appeared to overestimate the deformation of the thin cup by 65 μm . As in the experimental study, the complex anatomy of the pelvis was simplified by representing the acetabulum as a uniform foam cavity and the cups were simulated as being inserted perfectly aligned with the cavity. Whilst the foam model was reported to provide values of cup deformation similar to those observed in the earlier cadaveric studies, the definition of uniform material properties using a single value for the

Young's modulus cannot be an accurate representation of the behaviour of the pelvis clinically.

The method of insertion of the cup is also an important consideration. One FE study [Yew et al., 2006] has looked at simulating the hammer blows administered by a surgeon by using either a multiple-displacement or multiple-load method. The multiple-displacement method serves to move the cup by a predetermined amount in the cavity in a series of steps to replicate how far the each hammer impact would displace the cup. The first step of this method is performed by moving the cup into the cavity by far enough that the polar gap is eliminated. When the displacement control is removed, the cup bounces back by a certain amount and the displacement is reapplied in increments of 1 mm until it can no longer move any further into the cavity. With the multiple-load method, static loads are applied to the cup in a series of steps to drive it further into the cavity. Both of these methods of insertion can be likened to squeezing the cup into the cavity, similar to an approach used previously [Spears et al., 1999]. This however is not representative of the clinical situation and should be regarded as a limitation of the study. The authors elected to use the multiple-displacement method as it was said to be computationally less expensive. However this resulted in unrealistically high associated insertion load of 100 kN. This may have been due to the displacements in each step being too high however this was not investigated by the authors. It is clear that to accurately model the insertion process, implicit dynamics FE models must be developed that mimic the multiple mallet blows a surgeon administers clinically.

Only one study [Hogg et al., 2009; Hogg et al., 2010] has attempted to address the issue of the over simplification of the cup impaction process, by creating a model of the pelvis into which a Co-Cr cup was impacted into a cavity using a number of impacts with a momentum of 2.7 kgms^{-1} , Figure 2.29. Cup deformations of approximately $66 \mu\text{m}$ were observed however the authors have not since used their model to investigate any parameters further.

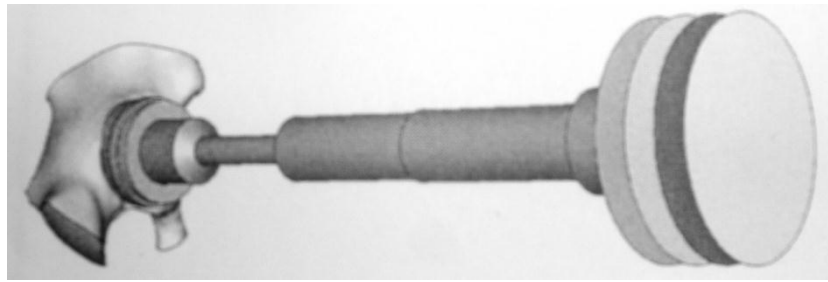


Figure 2.29: *Finite element model created of pelvis and hammer [Hogg et al., 2009]*

The simulation of rim loading [Everitt et al., 2010] which is the least representative of the clinical situation results in deformations considerably larger than in the foam and pelvis models, Table 2.5. As expected, the titanium shell with a lower stiffness [Hogg et al., 2010] deforms more than the CoCrMo cup [Yew et al., 2006].

Whilst 2D and 3D foam models, such as those developed by Yew et al [2006], are also a simplification of the clinical situation, they are a valuable tool for understanding cup deformation before developing more detailed models of the pelvis. These allow for the number of variables that could influence deformation to be minimised and the individual effect of specific parameters to be investigated. It is important to consider that the deformations observed in these foam models may not be replicated in the pelvis however they will allow researchers to clearly identify key factors, such as in cup design that would increase or decrease the changes in diameter of the cup. Good finite element practice calls for the initial development of simplified models which are then modified and expanded as a better understanding of the subject under investigation is obtained. For example the use of dynamic impaction could first be modelled in 2D and 3D foam models to truly understand the importance of parameters such as the number and velocity of impacts required to fully seat a cup and the influence of different methods of impaction. The use of anatomically correct models will help to provide a more realistic representation of the amount of deformation observed in a clinical situation, allowing factors such as the yielding of bone to be better modelled. These should only be developed however when the key factors influencing deformation have been identified in preliminary models.

2.10 Aims and Objectives

The aim of this thesis was to gain an understanding of the diametrical deformation behaviour of acetabular cups and shells following impaction into the reamed acetabulum. The influence of a range of factors on deformation was investigated to ascertain if cup and shell deformation may be high enough to potentially contribute to early failure and high wear rates in metal-on-metal implants.

A number of objectives were defined in the thesis:

- Develop finite element models using explicit dynamics to mimic mallet blows during cup/shell insertion, initially using simplified experimentally validated foam models to represent the acetabulum.
- Investigate the number, velocity and position of impacts needed to insert a cup.
- Determine the relationship between the size of interference between the cup and cavity and deformation for different cup types.
- Investigate the influence of non-uniform cup support and varying the orientation of the component in the cavity on deformation.
- Examine the influence of errors during reaming of the acetabulum which introduce ovality to the cavity.
- Determine the relationship between changes in the geometry of the component and deformation for different cup designs.
- Develop three dimensional pelvis models with non-uniform bone material properties from a range of patients with varying bone quality.
- Use the key parameters that influence deformation, as identified in the foam models to determine the range of deformations that may occur clinically using the anatomic models and if these deformations are clinically significant.

Chapter 3

2D Foam Model Development and Methods

3.1 Introduction

The thickness of MoM cups are kept to a minimum to ensure that bone conservation is maximised, and as a result they are likely to deform more, which may be beneficial to distributing load around the cup but may also disrupt fluid-film lubrication [Jin et al., 2006].

The greater amount of deformation associated with the larger, thinner metal cups during and after impaction could create problems with the performance of the component and this must be given proper consideration. Clearances of between 60 and 250 μm are usually specified between the cup and femoral head [Chang et al., 2007] and high deformations could result in the reduction of these clearances, potentially causing equatorial contact which could have a negative effect on fluid-film lubrication. Micromotion at the interface of the cup and bone has been found to increase due to excessive cup deformation, increasing wear and hampering bone in-growth [Ebied et al., 2002] and under the largest deformations the joint could potentially seize [Jin et al., 2006].

In this chapter two-dimensional axisymmetric static implicit models, similar to previous studies [Yew et al., 2006; Spears et al., 1999], were developed to simulate the insertion of press fit metallic acetabular components into a foam cavity representing the human acetabulum. This was followed by the development of a more realistic impaction method using explicit dynamics models in which impact momentums were defined, allowing for a better approximation of the cups position and deformation in the cavity after impaction clinically. The effect of changing interference, cup-foam friction, impact velocity, cup material and impact method on cup seating and deformation were all investigated.

3.2 Static Implicit 2D Model Development

A two-dimensional static implicit axisymmetric model was developed to simulate an acetabular cup being inserted into a polyurethane foam cavity, used to replicate the human acetabulum. The model was developed based on cup and foam characteristics used in the two part experimental and finite element study by Jin et al. [2006] and Yew et al. [2006]. The grade 30 (pounds per cubic feet) foam [Sawbones, 2011] used was found to be the most suitable alternative to using cadaver specimens in experimental studies [Jin et al., 2006]. Two separate ‘parts’ of the acetabular cup and foam cavity were created in the CAE interface, and SI units were used as summarised in Table 3.1

Table 3.1: SI units used in model development

Length	Force	Mass	Time	Stress	Density
mm	N	tonne (10 ³ kg)	s	MPa	tonne/mm ³

Figure 3.1 shows the construction the cup ‘part’ in the CAE interface. The vertical construction line was added to position the axis of symmetry for the model.

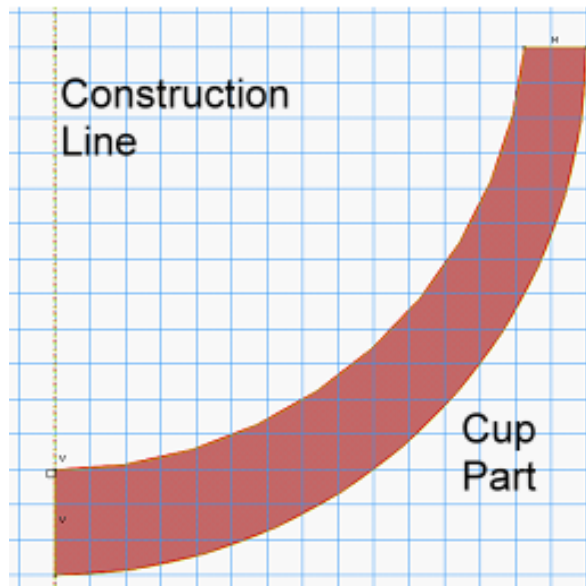


Figure 3.1: Construction of cup ‘part’ in Abaqus CAE

A single cup geometry was considered in this study as defined in Figure 3.2.

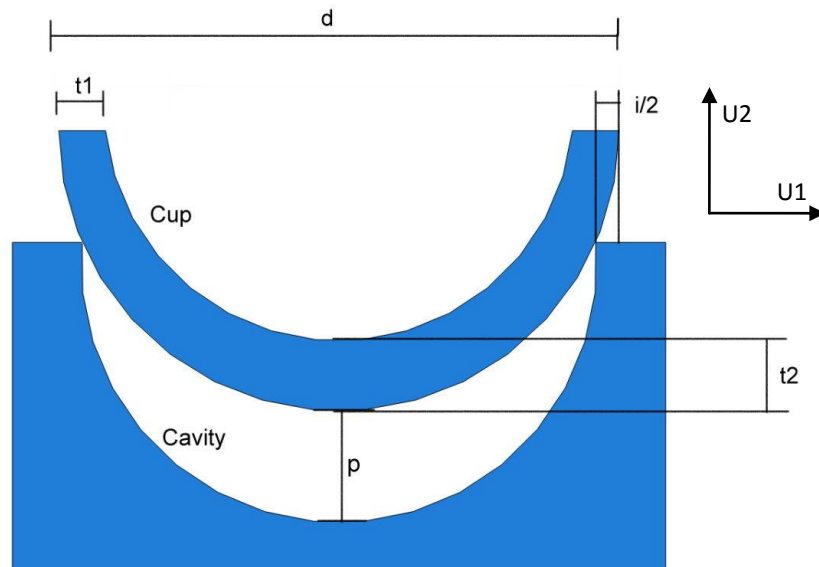


Figure 3.2: Cross-sectional dimensions of acetabular cup in foam cavity

An outer diameter (d) of 60 mm was used and the cup thicknesses t_1 and t_2 were defined as 3.5 and 6 mm respectively, as used by Yew et al. [2006], whilst the interference between the cup and cavity (i) was varied from 0.25 to 2 mm. The polar gap (p) was defined as the distance between the outer pole of the cup and the inner pole of the cavity. The initial polar gap depended on the interference used, such that the smallest interference produced the smallest initial polar gap, before impaction. In this study, cup seating was determined by observing the reduction in the polar gap and this was achieved by monitoring the vertical displacement between two nodes on the outer pole of the cup and the inner pole of the foam cavity. Cup deformation was defined as the reduction in the diameter of the cup which was monitored using the horizontal displacement of the node on the inner equatorial edge of the cup. A single set was created, containing all the nodes required to monitor cup seating and deformation. A history output request was used to record the displacement in the U_1 (x) and U_2 (y) directions at regular intervals.

3.2.1 Meshing of Static Implicit 2D Model

The following details the methods that were used to mesh the static axisymmetric model. The selection of appropriate elements was determined based on the required contact interaction properties of the cup and cavity, the geometry of the two parts and the need to minimise the computational run time whilst maintaining the required accuracy of the results. The process of mesh refinement was carried out to ensure the efficiency of the model, whereby the mesh density was continually increased until the differences in the monitored outputs reached a steady state solution. Multiple mesh verification tests were utilised to ensure that excessive distortion of the elements did not occur. Element failure criteria used in the checks were if that the face corner angle was less than 10° , the aspect ratio was greater than 10 and the edge length shorter than 0.01 mm. Any distorted elements that were identified were removed by remeshing the model. These element quality checks ensured that the simulations were able to run without convergence issues.

In a similar approach to that used by Spears et al. [1999], it was assumed that the comparatively high stresses at the point of contact between the cup and the edge of the cavity (Figure 3.3a) would cause this edge to experience a degree of wear and be smoothed. This area was modified to introduce a curved profile rather than a sharp right angled edge; this change eliminated the risk of the cup 'locking' with the foam edge at this point during the modelling of insertion (Figure 3.3b).

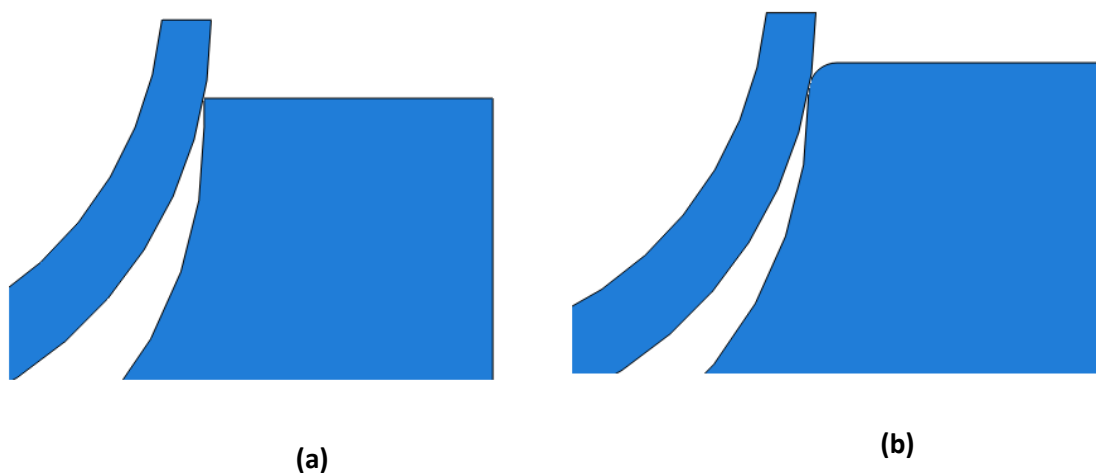


Figure 3.3: (a) the sharp corner at the point of contact between cup and cavity and (b) the introduction of a radius to allow cup to move smoothly into the cavity

All the axisymmetric models were developed in Abaqus/CAE 6.7 using four noded linear axisymmetric elements (CAX4R) to mesh the acetabular cup and foam cavity. The use of quadrilateral elements was justified as they have been shown to have accurate simulation efficacy when contact between two objects is modelled (Simulia, 2010). Conversely triangular elements generally have poor contact capabilities and as such were avoided.

Mesh refinement studies were performed to ensure the accuracy of the models. Comparison of relevant results between incremental increases in the mesh density was carried out. In this study the diametrical deformation of the inserted cup was used to monitor the convergence of the model. This was defined by the change in displacement of the node on the inner corner of the cup (B), relative to the horizontally positioned node on the axis of symmetry (A), Figure 3.4. The final polar gap, defined as the displacement between the outer node of the cup (C) and the inner node of the cavity (D) was also used to ensure that a good convergence to the accurate solution was achieved.

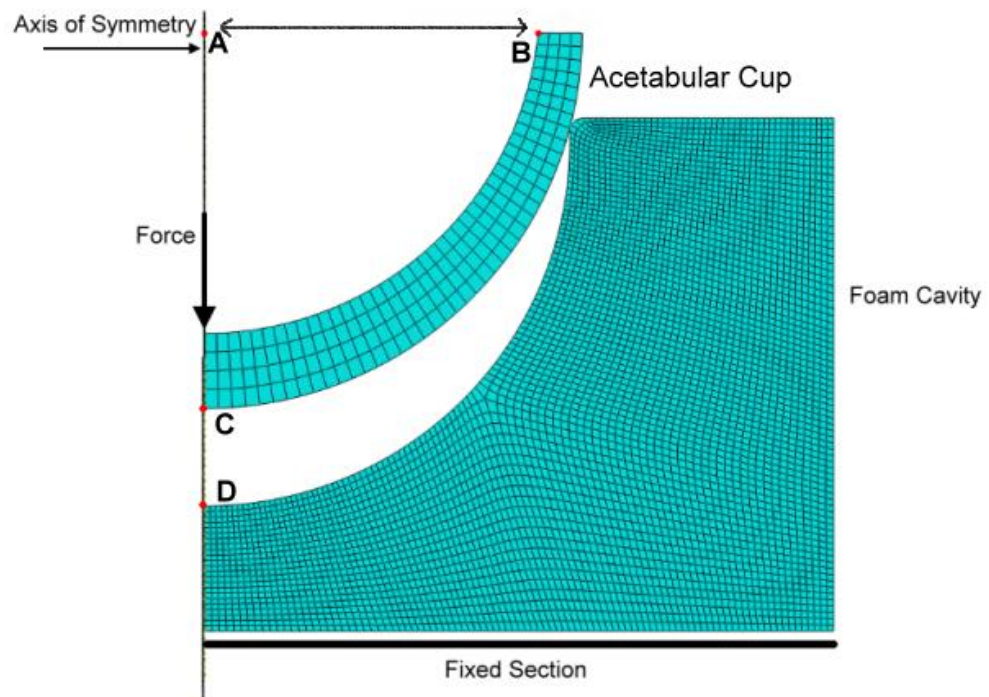


Figure 3.4: Axisymmetric finite element model of the acetabular cup and the foam cavity

The model was determined to have reached a point of convergence when the differences in the diametrical deformation (ΔD) and polar gap (ΔP) were within 1% of these values when an initial high mesh density was used with a total of 6014 elements. The percentages differences in displacement were calculated using the following equations:

$$\Delta D = \frac{D_E - D_H}{D_H} \times 100 \quad (3.1)$$

$$\Delta P = \frac{P_E - P_H}{P_H} \times 100 \quad (3.2)$$

Where D_E and P_E are the deformation and polar gap values of the current simulation and D_H and P_H are the deformation and polar gap values when the maximum mesh density was modelled. The models were meshed using the built-in meshing algorithms in ABAQUS. The mesh density in each case was increased by reducing the global node edge seed size which decreases the edge length for each element. Due to the relative simplicity of this initial 2D model, mesh verification tests did not identify any problematic regions within the foam cavity or cup. Table 3.2 details the mesh densities that were used in the cavity and the cup to reach convergence.

Table 3.2: Mesh densities used to reach convergence

Simulation	Global Seed Size / mm		Number of Elements			ΔD / %	ΔP / %
	Cup	Cavity	Cup	Cavity	Total		
1	0.50	0.5	774	5240	6014	-	-
2	0.75	1	285	1315	1600	0.1	0.1
3	1.00	2	172	352	524	0.8	0.8
4	1.25	3	102	158	260	2.9	2.8
5	1.5	4	56	85	141	5.8	5.8

It can be seen that in this model convergence was reached when a total of 524 elements were used, resulting in a difference of 0.8% from the previous simulation. It was observed during the mesh refinement stage that the simulation run time for this static 2D model was very quick for all the models. With a maximum total of approximately 6000 elements, the simulation was completed in a period of less than 8

minutes. As such it was justified, from the prospective of computational run time, to utilise approximately 6000 elements in the cavity and cup model. This ensured that a good accuracy of the results was obtained whilst still maintaining a reasonable time for completion of the simulations.

3.2.2 Boundary Conditions and Interaction Properties in Static Implicit 2D Model

Boundary conditions were applied to the model such that the base of the foam cavity was constrained; this was achieved by applying an encastre condition to the base region such that translational and rotational movement was not permitted:

$$\mathbf{U1} = \mathbf{U2} = (\mathbf{U3}) = \mathbf{UR1} = \mathbf{UR2} = (\mathbf{UR3}) = \mathbf{0} \quad (3.3)$$

Where U and UR refer to translational and rotational movement and 1, 2 and 3 refer to the x, y and z directions. As this was a 2D model movements in the z direction were automatically restricted by the software.

The movement of the nodes on the axis of symmetry was restricted to the vertical direction only:

$$\mathbf{U1} = (\mathbf{U3}) = \mathbf{UR2} = \mathbf{0} \quad (3.4)$$

The definition of the contact interaction behaviour was based on the appropriate identification of the *master* and *slave* surfaces used in ABAQUS, the selection of relevant contact discretisation approaches and the correct use of friction models.

ABAQUS requires that surfaces that are to interact with each other during the simulation must be defined as contact pairs. In this initial static model the outer surface of the cup and the inner surface of the foam cavity were defined as contact pairs. To ensure effective contact is simulated between the two surfaces, the cup and foam is assigned either a *master* or *slave* role. The stiffer component in the contact pair (the cup) was assigned the master role [Simulia, 2010]. Two discretisation methods were available to the contact pair of the cup and foam, namely node-to-surface and surface to surface discretisation. When node-to-surface discretisation is utilised the nodes on the slave surface are projected onto the master surface. As the simulation progresses the master surface is able to penetrate the slave surface however the slave nodes are not able to penetrate the master surface. Surface-to-

surface discretisation differs in that the contact between the master and slaves surfaces is averaged and this is able to produce a better representation of the distribution of stresses in the components. It is recommended [Simulia, 2010] that when a comparatively low number of nodes are in contact, such as in 2D models, that node-to-surface discretisation be used to reach convergence. Surface-to-surface discretisation tends to result in unreasonably high over-closure of the surfaces in contact when the number of nodes in the interaction is low. As such the contact pair of the cup and foam in this initial model was defined with node-to-surface discretisation. ABAQUS requires that the method of sliding between the surfaces of a contact pair be defined as either finite sliding or small sliding. In the same approach used by Yew et al. [2006], finite sliding was defined between the cup and the cavity; this selection was applicable for surfaces that experience non-linear movement and changes in the contact separation during the analysis.

A penalty contact was used to model the Coulomb friction between the contact pair of the cup and cavity. This contact method ensured that movement between two surfaces was always possible to the point of convergence, allowing for elastic slip. The coefficient of friction was varied from 0.1 to 0.6, with the increasing values representing a rougher outer porous coating on the cups surface. These values were similar to those used in previous studies [Spears et al., 1999; Yew et al., 2006].

A similar approach was used by Spears et al. [1999] and Yew et al. [2006], where the actual porous coating was not modelled as it was considered to have a negligible effect on the deformation behaviour of the cup. This assumption was also made in this study with the effect of the coating being represented by a change to the friction coefficient. In order to vary the interference of the cup, the diameter of the foam cavity was altered to produce interferences of 0.25, 0.5, 1 and 2 mm.

3.3 Application of Load in Static 2D Model

The clinical approach for inserting a press-fitted cup is to repeatedly hammer the cup via an impactor using a mallet. This procedure was initially simulated by applying six load pulses to the cup, with each pulse consisting of a static load increased from zero to a maximum force and then reduced back to zero. The load was applied to a single node on the inner surface of the cup which was positioned in line with the plane of the

rim of the cavity. Due to the restrictions of using an axisymmetric model, it was not straightforward to alter the cup's orientation at this stage.

The load pulses were created by defining twelve steps each for a 'time period' of one second. Each step was coupled with an amplitude definition which ramped the force from zero at time *zero* to a maximum at time *one*. On the following step the force was ramped back down from a maximum at time *zero* to a zero at time *one*. This was repeated to produce six pulses using twelve steps. For interferences of 0.25 to 1 mm, the maximum force was increased for each pulse such that the first pulse was 500N, followed by 1000, 2000, 4000, 6000 and 8000 N, as used previously [Spears et al., 1999] (Figure 3.5).

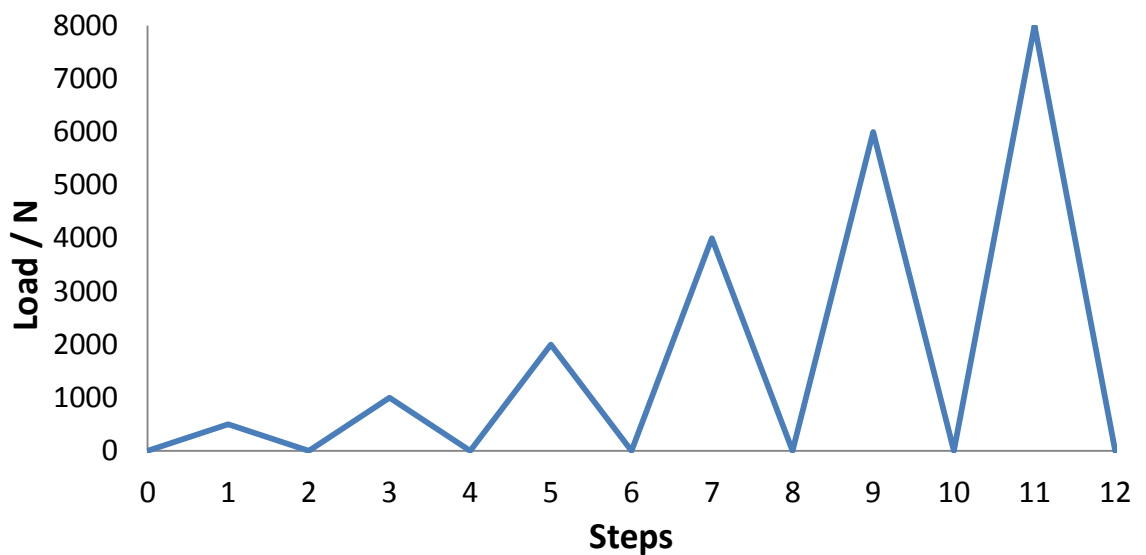


Figure 3.5: A schematic representation of the load impulses applied to the acetabular cup

When an interference of 2 mm was used, the maximum pulse forces ranged from 1000N to 20,000N, to ensure that each impulse resulted in the cup moving further into the cavity. It should be noted that these values are significantly greater than those experienced clinically. In a similar manner to Spears et al. [1999], loads were applied to the central node on the inner polar surface of the cup and as no time dependent material properties were considered, the time for each load pulse was not important. Both the cup and the foam cavity were assumed to be linear elastic and their relevant material properties are summarised in Table 3.3. The Young's modulus of 0.553 GPa of the foam cavity was reported by Jin et al. [2006] to produce similar cup deformations

to a cadaveric model. Table 3.3 also presents the typical range of values for the material properties of cortical and cancellous bone for comparison.

Table 3.3: Mechanical properties of the acetabular cup and foam cavity

Material	Young's Modulus (GPa)	Poisson's Ratio	Density (Tonne/mm ³)	Source
Co-Cr	210	0.3	8.3×10^{-9}	Ratner et al [2005]
Grade 30 Foam	0.553	0.3	4.8×10^{-9}	Sawbones [2011]
Cancellous Bone	0.001 – 1	0.01 -0.5	$0 - 1 \times 10^{-9}$	Dalstra et al [1993]; Thompson et al [2004];
Cortical Bone	4.4 – 22.8	0.2 – 0.5	$1 \times 10^{-9} - 2 \times 10^{-9}$	Helgason et al [2008]

As well as investigating the deformation behaviour of the acetabular cup, the gap between the polar nodes of the cup and foam cavity were monitored, as well as the percentage contact area between the two surfaces. The von Mises stresses were also monitored to observe its distribution within the component and the cavity following insertion.

3.3.1 Results

Figure 3.6 shows the amount of diametrical deformation of the acetabular cup when inserted in to the foam cavity with an interference of 0.5 mm. It can be seen that increasing the coefficient of friction between cup and foam leads to an increase in diametrical deformation when a peak load is applied. However upon removal of the load, the deformations appear to be similar. The maximum deformations occur when the last (and highest) load is applied. Table 3.4 shows the maximum cup deformation obtained for the different coefficients of friction with 0.5 mm interference. Also shown are the final deformations obtained when the load is removed at the end of the last pulse.

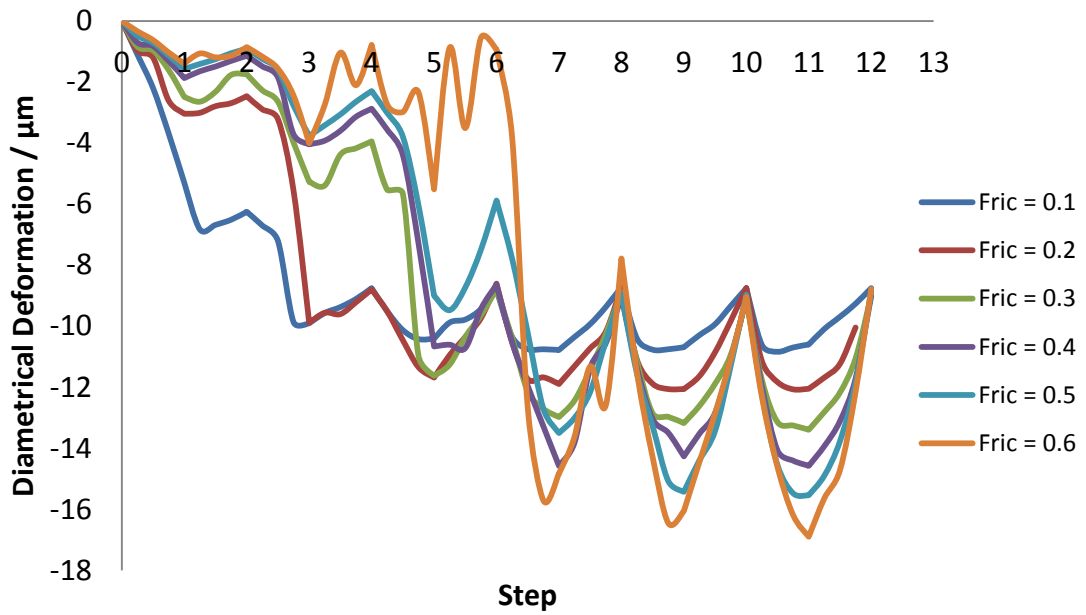


Figure 3.6: Deformation of 60 mm cup with 0.5 mm Interference when inserted into grade 30 foam

Table 3.4 Deformations obtained for varying amounts of friction with 0.5 mm interference

Coefficient of Friction	Maximum Deformation (μm)	Residual Deformation after last pulse (μm)
0.1	10.6	8.7
0.2	12.1	8.7
0.3	13.4	9.0
0.4	14.6	9.0
0.5	15.3	8.9
0.6	16.9	8.8

The deformation behaviour observed for varying coefficients of friction for 0.5 mm interference was found to be similar for the other interferences tested.

Figure 3.7 shows that increasing the cup interference caused a notable increase in diametrical deformation with a coefficient of friction of 0.3. Similar deformation behaviour was observed with the other degrees of friction tested. Table 3.5 shows the maximum cup deformations obtained for the different interferences at values of

coefficients of friction of 0.1, 0.3 and 0.6. Also shown are the final deformations obtained when the load was removed at the end of the last pulse.

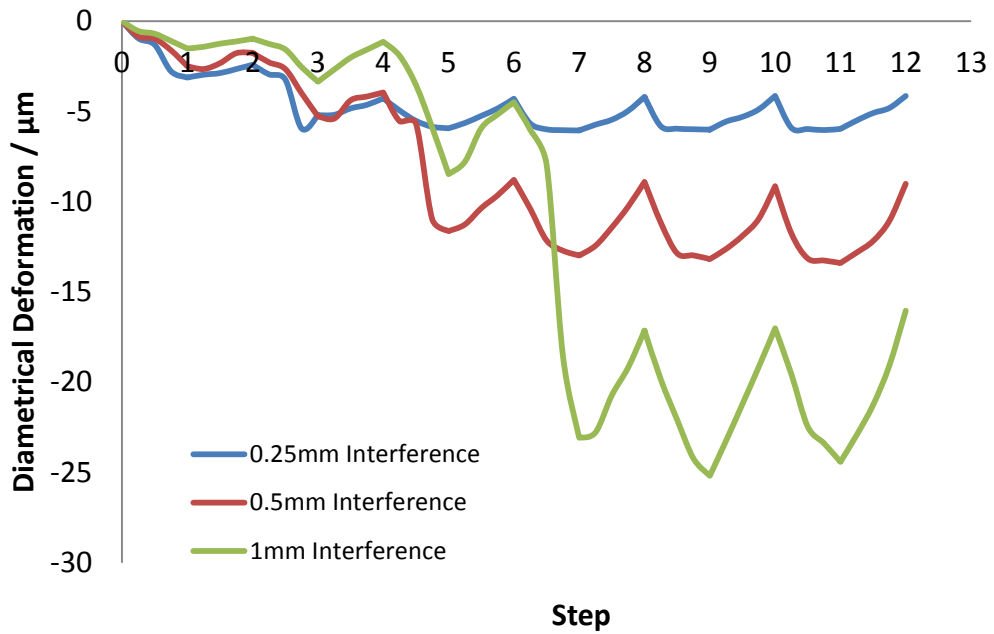


Figure 3.7: Deformation of 60 mm cup at different interferences (Friction = 0.3)

Table 3.5: Deformations obtained for varying amounts of interference and friction

Interference (mm)	Coefficient of Friction	Maximum Deformation (µm)	Deformation after last pulse (µm)
0.25	0.1	5.0	3.2
	0.3	6.0	4.1
	0.6	7.2	3.9
0.5	0.1	10.8	8.7
	0.3	13.4	9.0
	0.6	17.0	8.8
1	0.1	21.2	17.0
	0.3	24.4	16.0
	0.6	31.7	17.8
2	0.1	41.7	32.0
	0.3	46.2	31.0
	0.6	58.1	28.5

Table 3.6: Polar gaps observed for varying amounts of interference and friction

Interference (mm)	Coefficient of Friction	Minimum Polar Gap During Insertion (mm)	Polar Gap after Last Impulse (mm)
0.25	0.1	0	0.05
	0.3	0	0.08
	0.6	0	0.07
0.5	0.1	0	0.25
	0.3	0	0.30
	0.6	0	0.28
1	0.1	0.06	0.50
	0.3	0.12	0.40
	0.6	0.23	0.58
2	0.1	0.04	1.08
	0.3	0.09	0.75
	0.6	0.28	0.97

Table 3.6 shows the minimum polar gaps obtained for the different interferences at values of coefficients of friction of 0.1, 0.3 and 0.6. Also shown are the final polar gaps observed when the load was removed at the end of the last pulse. All non-zero values for the minimum gap were found after the last pulse was removed.

Figure 3.8 shows the polar gap remaining with 1 mm Interference at different coefficients of friction. It can be seen that as the impulses are applied, the polar gap progressively decreases. However at the end of each pulse, when the load is removed, elastic spring back of the cup can be seen for each case. It is observed that although increasing the force causes the cup to be driven further into the cavity, the model eventually reaches a stage where further loading does not appear to decrease the polar gap after the removal of the load.

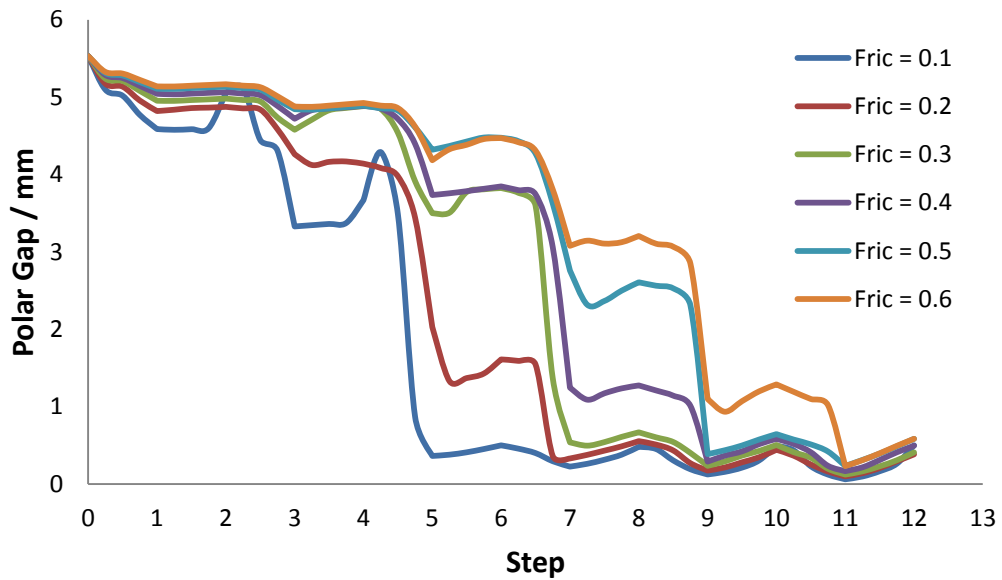


Figure 3.8: Polar gap remaining with 1 mm Interference at different coefficients of friction

Figure 3.9 shows that reducing the cup interference causes the polar gap to reduce by a higher amount at a lower load. It also shows that after the last pulse is applied, a lower interference leads to the smallest polar gap and at peak points of the load application, the gap closes completely.

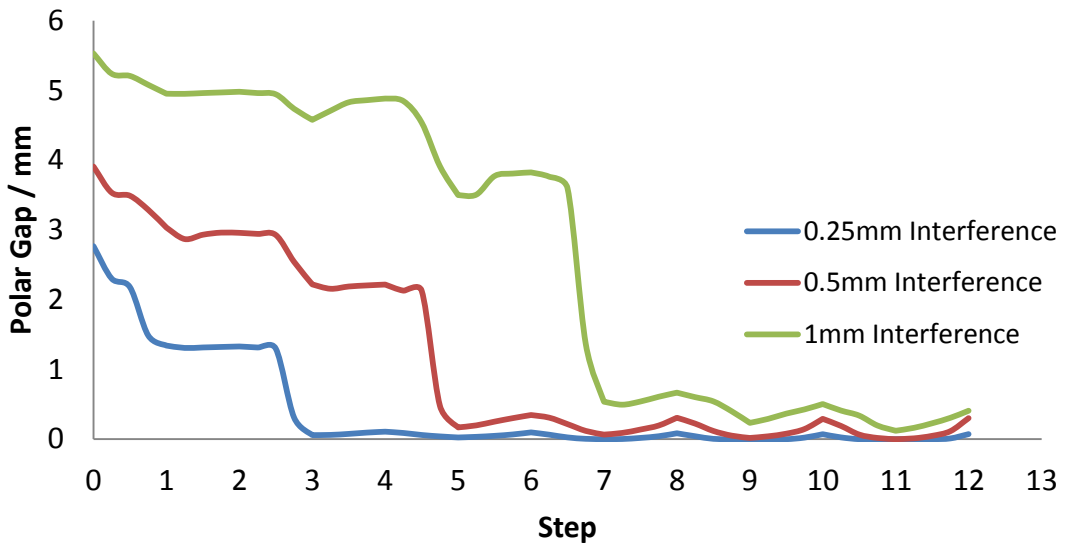


Figure 3.9: Polar Gap Remaining with different interferences (Friction = 0.3)

Figure 3.10 shows the percentage contact area between the cup and the foam cavity for different coefficients of friction. It clearly shows that a lower friction coefficient resulted in a higher maximum contact area, with a coefficient of 0.1 resulting in a

maximum contact area of 95% and a coefficient of 0.6 resulting in a maximum contact area of 59%. It must be noted that these maximum contact areas were achieved at the peak of the last (and greatest) impulse. Upon removal of the final load, the percentage contact area reduced notably to 40% for a friction coefficient of 0.1 and 32% for a coefficient of 0.6. The greatest contact stresses were found to occur at the rim of the cup after insertion and were greater for higher interference fits.

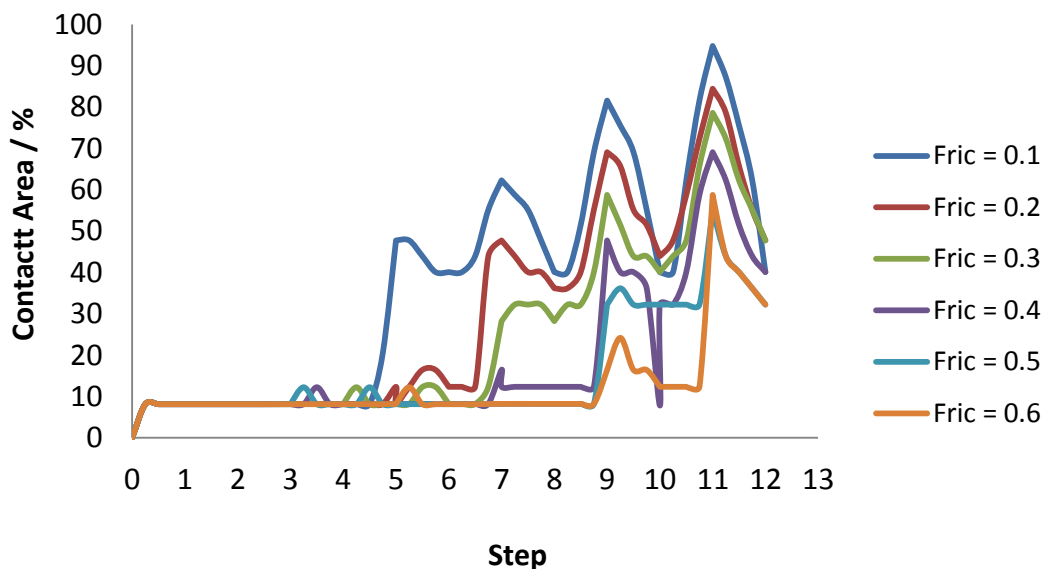


Figure 3.10: Contact Area (%) - 1 mm Interference

3.3.2 Discussion

The procedure of press-fitting an acetabular cup into a foam cavity mimicking the human acetabulum was successfully simulated using two dimensional axisymmetric models. Initially a progressively increasing impulse force was applied to the cup to simulate clinical impactions with a mallet, and the cup interference and cup-foam friction was varied. The impulse forces considered were similar to those used in a previous finite element study [Spears et al., 1999] however the maximum forces used in the final impulses were notably larger when an interference of 2 mm was modelled. An unrealistically high peak impulse force of 20,000N was required to achieve adequate cup seating. Forces of over 3500N have been estimated [Mackenzie et al., 1994] to increase the possibility of damaging or fracturing the pelvis and therefore the peak forces reached in this model are not clinically relevant. The study by Yew et al. [2006] also found that an unreasonably high load of over 100 kN was required to initiate cup seating in their axisymmetric model. The cup deformations and incidence

of polar gaps in the current study were found to be in keeping with the behaviour observed by earlier studies [Yew et al., 2006; Spears et al., 1999].

It was observed that with each increasing impulse force on the cup, the percentage area of contact between the cup and the foam cavity increased and the polar gap decreased as the cup was driven further into the cavity. It has been reported [Sandborn et al., 1988] that for polar gaps up to 2 mm in size, bone growth will occur into the porous surface coating on the cup, and for a gap size less than or equal to 0.5 mm, the rate of bone ingrowth is notably higher. In this study it was found that the final polar gap was less than 2 mm for all interference and friction combinations examined and that for interferences of 0.25 and 0.5 mm, the polar gap was less than 0.5 mm, meaning that optimum bone ingrowth would be possible. This was also the case when an interference of 1 mm was considered with a coefficient of friction of less than or equal to 0.3. Rebounding of the cup occurred when the load was removed at the end of each impulse. The degree of friction was seen to influence the amount of spring back and this was especially evident when comparing the effect of the extreme values of friction of 0.1 and 0.6 on the polar gap and percentage contact area; a lower friction between the cup and foam resulted in notably higher levels of rebounding upon load removal, particularly during the earlier impulses. This spring back behaviour was also reported in a previous experimental study [Jin et al., 2006] and in previous finite element studies by [Yew et al., 2006; Spears et al., 1999].

Commonly manufacturers of press-fit cups do not consider the porous surface coating when detailing the diameter of the cups [Sharkey et al., 1999] and that this omission could undersize the diameter by more than 1 mm. Therefore in experimental and clinical situations, there is a risk that the interference will be underestimated.

3.4 Development of Explicit Dynamics 2D Axisymmetric Model

Whilst the initial static implicit models provided information about the deformation behaviour of a cup during insertion, they were not able to represent the mallet impacts used clinically to seat the component. It is difficult therefore to estimate the position of the seated cup clinically and the corresponding deformations when only static loads are used, which also may not be realistic when compared to those generated by impact momentums. Therefore, before considering complex three-dimensional models, it was important to develop a simple 2D model that incorporated dynamic loading and more detailed cancellous bone properties. This ensured that appropriate modelling techniques were developed and any problems overcome before transferring the cup impaction simulation into three-dimensions, which is more complex and more demanding computationally.

3.4.1 Single Cup Impact

The clinical approach for inserting a press-fitted cup is to repeatedly hammer the cup into the acetabulum via an impactor using a mallet. The static implicit two-dimensional axisymmetric model that was previously developed was altered to include a third independent 'part' representing the mallet in the current explicit dynamics model. Initially, the impaction process was simplified such that only one impact on the inner polar surface of the cup was simulated with a constant velocity. This was achieved by defining the impactor with a predefined velocity to begin in the initial step, using the predefined field function. The velocity of the impactor was determined so that it was high enough to force the cup into the cavity, such that the polar gap was as small as possible for each cup-foam interaction. A single impact approach was used initially to minimise the computational run time of the simulation and to determine the optimum model parameters to use in order to maximise the efficiency of the model whilst maintaining the accuracy of the results obtained. One such parameter that was investigated was the mesh size used in the model; it was determined that mesh density in the initial static 2D model was unnecessarily high but as the computational run time was reasonably short, its use was justified. When an impactor with a defined velocity was introduced, the run time increased significantly to several hours when using the previous mesh density of 6000 elements. Mesh refinement studies were

therefore repeated with the addition of the impactor component and are summarised in Table 3.7.

Table 3.7: Mesh densities used to reach convergence

Simulation	Global Seed Size / mm			Number of Elements				$\Delta D /$ %	$\Delta P /$ %
	Cup	Cavity	Impactor	Cup	Cavity	Impactor	Total		
1	0.50	0.5	1	774	5240	589	6603	-	-
2	0.75	1	2	285	1315	159	1759	0.2	0.2
3	1.00	2	4	172	352	24	548	0.7	0.7
4	1.25	3	6	102	158	14	274	2.7	2.6
5	1.5	4	8	56	85	8	149	4.6	4.6

Mesh convergence to within 1% was found to occur when a total of 548 elements were used with only elastic properties defined in the foam cavity (Figure 3.11).

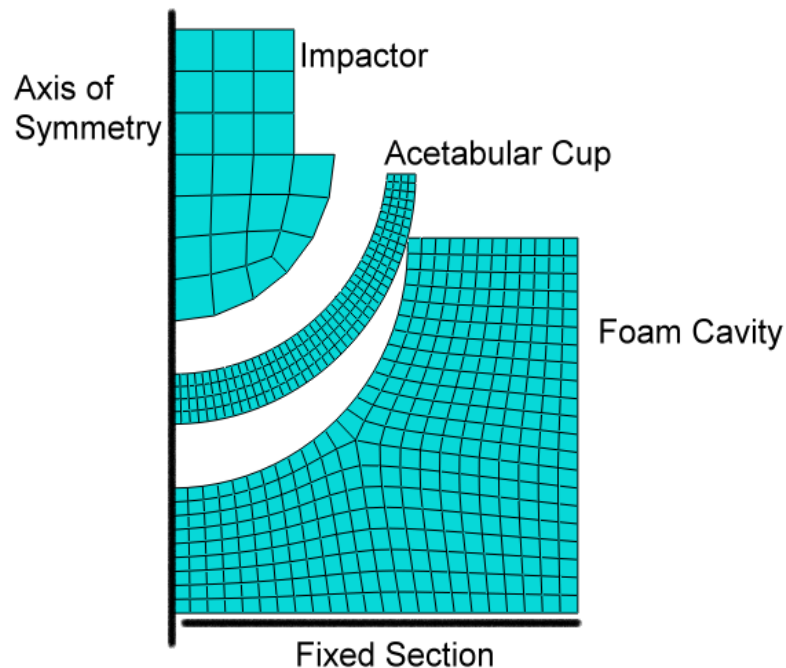


Figure 3.11: Axisymmetric finite element model of the acetabular cup, foam cavity and impactor

When time dependent properties were later introduced into the foam, further convergence studies found that the mesh size in the cavity was now too coarse and had to be refined by a considerable amount to ensure the values of the displacements observed were accurate; this finer mesh was therefore used in subsequent models

(Figure 3.13). As a consequence of increasing the number of elements used in the model, the computational run time increased notably to approximately 3 hours. In an effort to reduce the run time, a mass scaling factor of 2 was introduced to selected elements in the foam cavity that were at a distance from the interaction point between the acetabular cup and foam.

3.4.2 Multiple Cup Impacts

In order to mimic the multiple mallet blows administered by a surgeon in a clinical setting, a number of simple impactors were modelled with the same initial velocity and were positioned such that they were equally spaced away from the acetabular cup. This allowed for the cup to be impacted with the same momentum at regular time intervals. The multiple impactors were assembled as instances dependent on a single constructed impactor 'part'. This allowed all impactor instances to be meshed and be given property definitions quickly by applying these definitions to the single impactor 'part'.

Each impactor was modelled with a diameter of 40 mm and its mass was set to be 1.3 kg, as used experimentally by Fritsche et al. [2008].

All the solid models were developed in Abaqus/CAE 6.8 and a total of approximately 3000 four noded linear quadrilateral elements were used. The model, with 4 of the impactors that were used, is shown in Figure 3.12.

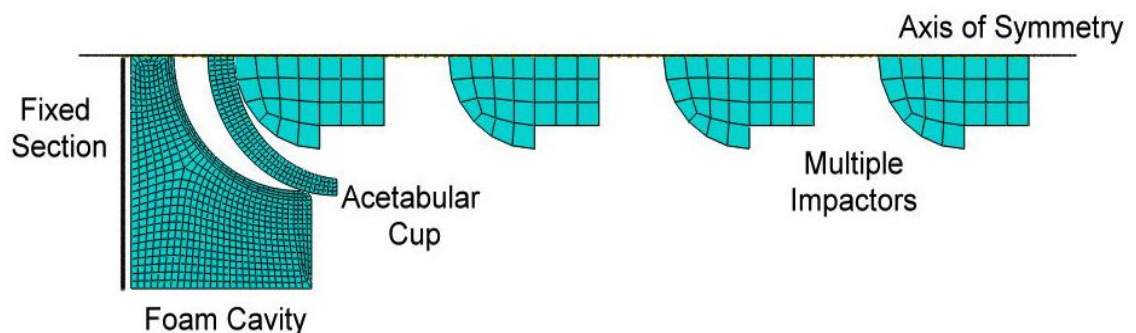


Figure 3.12: Axisymmetric finite element model of the acetabular cup, foam cavity and impactors

In a similar manner to the static 2D model, boundary conditions were applied such that the base of the foam cavity was constrained and the movement of the nodes on the axis of symmetry was restricted to along the direction of the axis only. In these models only one explicit dynamics step was defined.

Surface-to-surface explicit contact was defined between the impactors and cup and the cup and the foam. Initially kinematic contact was defined for the interaction between the cup and the foam however this resulted in large levels of noise in the results of the nodal displacements. A penalty contact method was therefore used with finite sliding for the interaction between the cup and the cavity.

Frictionless contact was assumed between the impactors and the cup and small finite sliding was defined in this contact pair as the two components experience low relative motion during their time in contact. As no contact definitions were defined between one impactor and another, they were able to effectively pass through each other as they moved towards the cup and when they rebounded away from the cup after impaction.

3.4.3 Definition of Material Properties

Linear elastic properties for the impactor, cup and foam were defined and are summarised in Table 3.8. In subsequent simulations, a rigid cap was modelled between the cup and impactor and the cup material was changed to Titanium to represent a typical metal shell that may be used with a ceramic or polyethylene cup.

Table 3.8: Mechanical properties of the acetabular cup, foam cavity and impactor

Material	Young's Modulus (GPa)	Poisson's Ratio	Density (kg/m ³)	Source
Co-Cr Cup	210	0.3	8300	Ratner et al., 2004
Grade 30 Foam	0.553	0.3	480	Sawbones, 2011
Impactor	210	0.3	47000	Fritsche et al., 2008
Ti-6Al-4V Cup	113	0.3	4430	Ratner et al., 2004
Rigid Cap	2000	0.3	100	-

Short term viscoelastic properties were also defined in this model and were determined using values of the loss tangent ($\tan\delta$) and the storage modulus (E') of cancellous bone for frequencies between 0.01 Hz and 100 Hz [Guedes et al., 2006]. The loss tangent and storage modulus for 1000 Hz were estimated from the data whilst the values of the long-term shear modulus (G_{∞}) and the long-term bulk

modulus (K_{∞}) were taken as being 204.22 MPa and 442.48 MPa respectively [Bandak et al., 2001].

Using the relationships shown in equations 3.5 to 3.8, between the Complex Young's Modulus (E^*), Complex Shear Modulus (G^*), Complex Bulk Modulus (K^*), loss tangent ($\tan\delta$), storage modulus (E'), loss modulus (E'') and poisson's ratio (ν), the parameters summarised in Table 3.9, were determined and defined in Abaqus for frequency values between 0.01 and 1000 Hz; ν was assumed to be 0.3.

$$E' = E^* \cos\delta \quad (3.5)$$

$$E'' = E^* \sin\delta \quad (3.6)$$

$$K^* = E^*/3(1 - 2\nu) \quad (3.7)$$

$$E^* = 2G^*(1 + \nu) \quad (3.8)$$

Table 3.9: Viscoelastic parameters defined in Abaqus for foam cavity and examples of values used

G^*/G_{∞} (Real)	G^*/G_{∞} (Imag)	K^*/K_{∞} (Real)	K^*/K_{∞} (Imag)	Frequency (Hz)
The real part of the complex shear modulus	The imaginary part of the complex shear modulus	The real part of the complex bulk modulus	The imaginary part of the complex bulk modulus	Loading frequency
0.104	0.036	0.104	0.357	0.01
0.069	-0.130	0.069	-0.130	1

3.4.4 Addition of Rigid Cap between Cup and Impactor

Following the simulation of the simple model of impaction on the polar surface of the cup, the model was modified to include a frictionless loading cap between the cup and impactor to simulate impaction devices used commercially which are designed to impact the cup rim and avoid any contact with the articulating surface, thus preventing damage to this area (Figure 3.13).

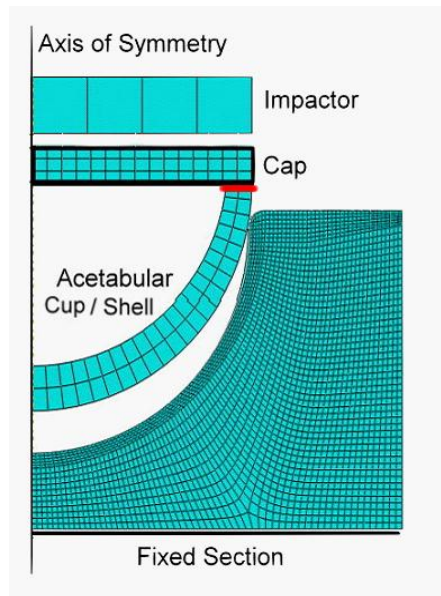


Figure 3.13: Axisymmetric finite element model of cup impaction with rigid cap

The effect of changing various model parameters on cup seating and deformation were investigated and compared with the cup behaviour observed when impacting directly on its polar surface.

In order to prevent the cap from rebounding away from the cup after each impact, a multi-point constraint was defined such that the distance along the axis of symmetry between a node from the cap and a node from the cup rim remained constant throughout the simulation, Figure 3.14.

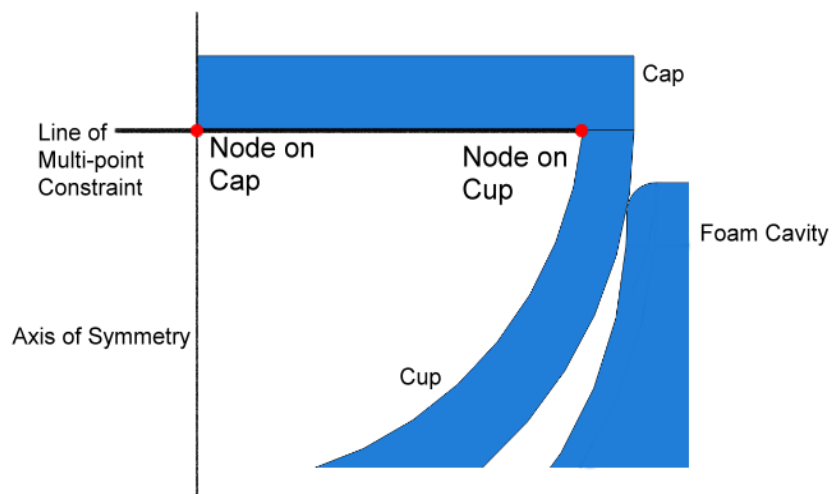


Figure 3.14: Definition of Multi-point constraint between cup and cap

3.5 Simulation Parameters

Upon developing a more realistic cup impaction model, a study was carried out in which a number of parameters were varied and their effect on cup seating and deformation investigated, as described in the following sections.

3.5.1 Method

Table 3.10 shows the parameters that were varied in the study, using a frictionless cap (*free cap*) and impacting directly on the inner surface of the cup (*polar impact*). Purely elastic properties were used in each of these simulations.

Table 3.10: Different cup-foam parameters used in the study

	Parameters		
Simulation	Interference (mm)	Friction	Impact Speed (m/s)
A	1	0.3	0.5
B	1	0.3	1
C	1	0.3	1.5
D	1	0.1	1.5
E	1	0.2	1.5
F	1	0.4	1.5
G	1	0.5	1.5
H	0.25	0.3	0.5 / 1 / 1.5
I	0.5	0.3	0.5 / 1 / 1.5
J	2	0.3	0.5 / 1 / 1.5

Simulation B was repeated with contact defined between the cap and cup rim such that no separation or sliding between the two surfaces was possible. This was performed in order to simulate a cap being locked onto a cup during impaction (*locked cap*). Once the cup was fully seated, the cap was separated from the cup and removed, and the effect of using a locked cap on cup seating and deformation was investigated. The simulation was presumed to have completed when subsequent impactions had no additional effect on the seating of the cup or if the cup bounced out of the cavity. If the

polar gap at the end of the simulation was less than or equal to 0.5 mm, which has been shown to be the maximum gap for optimum bone in-growth to occur, then the cup would be regarded as being fully seated in the cavity.

In an additional model, the Cobalt-Chromium properties of the cup were replaced with the elastic properties of Titanium Alloy Ti-6Al-4V (Table 3.8) and the differences between the two different cup materials with a purely elastic foam cavity were investigated by repeating simulation B, using a free cap, locked cap and polar impact.

Initially the cup, cap, impactors and foam were all assumed to be linear elastic and the properties defined for these components are summarised in Table 3. The mass density of the impactor was deemed to be much larger than the other components because its volume was smaller than in clinical situations, and the mass of 1.3 kg [Fritsche et al., 2008] needed to be maintained. A small mass density was defined for the cap so that its mass did not influence the seating of the cup.

3.5.2 Results

As expected, increasing the impact velocity resulted in fewer impacts being required to seat the cups. Using simulations A to C with a free cap, velocities of 1 and 1.5 m/s appeared to fully seat the cup, resulting in a diametrical deformation of 17 μm , however at 0.5 m/s the cup could not be fully seated and a substantial polar gap still remained at the end of the simulation, producing a lower diametrical deformation of 9 μm .

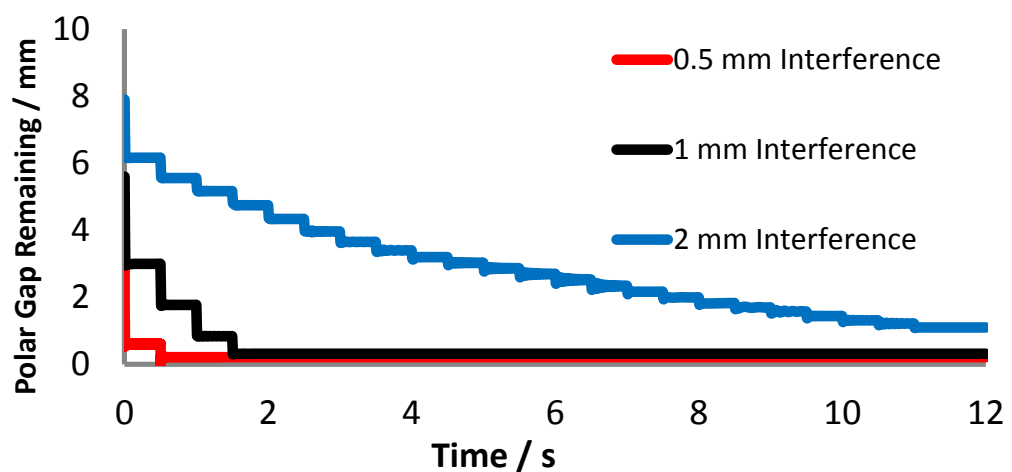


Figure 3.15: Polar gap observed after impaction at 1.5 m/s at different interferences with a coefficient of friction of 0.3

Figure 3.15 shows the polar gap remaining after impaction for Co-Cr cups with different interferences using a free cap with a velocity of 1.5 m/s, with a constant friction coefficient of 0.3. The data for 0.25 mm interference has not been included as the cup bounced out after the first impact. An increase in interference results in more impacts being required to insert the cup and also in higher cup deformation occurring. It was found that although the cup with 0.5 mm interference was fully seated, it had only experienced a diametrical deformation of 9 μm , whereas the cup with 2 mm interference still had a polar gap of about 1.5 mm remaining when it reached a steady state, whilst still experiencing a larger diametrical deformation of 28 μm .

Table 3.11: Number of impacts to fully seat Co-Cr cup after impaction using a free cap and at the pole, at 1.5 m/s with 1 mm interference at various coefficients of friction

	Coefficient of Friction between Cup and Foam				
	0.1	0.2	0.3	0.4	0.5
Free Cap Impact	2	3	4	6	10
Polar Impact	3	4	7	9	13

Table 3.11 shows the influence of the coefficient of friction between the Co-Cr cup and the foam on the number of impacts required to fully seat the cup at a constant velocity of 1.5 m/s with 1 mm interference using both the free cap and polar impaction methods. Increasing the coefficient of friction led to a greater number of impacts being required to fully seat the cup, to get to the same final diametrical deformation of 17 μm . Using a free cap between the cup and impactor resulted in slightly fewer impactions being required, with the largest differences occurring at the highest coefficient of friction.

Table 3.12 compares the number of impactions that were needed when using either a free cap or impacting on the inner polar surface of the cup, to either fully seat the cup or after which further impactions made no change to the cup position, at different impact velocities and interference values, with a constant coefficient of friction of 0.3. Using a free cap, as used in commercial devices to prevent damage to the articulating surface, resulted in fewer impactions being required than when impacting at the pole to fully seat the cup, particularly for interferences greater than 0.5 mm. For interferences of 0.5 and 1 mm increasing the impact velocity also meant that fewer

impactions were required to seat the cup with a free cap. For the smallest interference of 0.25 mm, the higher impact velocities resulted in the cup displaying significant elastic spring back after the first blow. With the largest interference of 2 mm, it was observed that as the impact velocity was increased, more impacts were possible before they no longer affected cup position, and the cup could be driven further into the cavity using the free cap. However with both impaction methods, full seating could only be achieved when the velocity was increased to 2 m/s.

Table 3.12: *Impactions required to fully seat the cup or after which any further impaction makes no difference to seating, with a coefficient of friction of 0.3. *Cup bounced out of cavity after first impact. Italic = percentage seated.*

			Impactor Velocity (m/s)								
			0.5		1			1.5		2	
			Free Cap	Polar Impact	Free Cap	Polar Impact	Locked Cap	Free Cap	Polar Impact	Free Cap	Polar Impact
Initial Interference (mm)	Co-Cr Cup	0.25	3	3	*	*	-	*	*	*	*
		0.5	9	10	3	3	-	2	2	*	*
		1	17 <i>(64 %)</i>	14 <i>(50%)</i>	10	14	5	4	7	1	3
		2	7 <i>(24%)</i>	4 <i>(12%)</i>	11 <i>(56%)</i>	8 <i>(30%)</i>	-	23 <i>(86%)</i>	20 <i>(67%)</i>	9	12
	Ti Cup	1	-	-	10	9	5	-	-	-	-

When a Co-Cr cup with a higher Young's Modulus is considered, insertion using a free cap as opposed to impacting at the polar surface of the cup required fewer impacts to insert the cup; each impaction using a free cap moved the cup further into the cavity than when the cup was hit at the pole. Locking the cap to the cup around the rim significantly further reduced the number of impacts required to seat the cup. The diametrical cup deformations observed during insertion were considerably lower than the other two methods due to the rim being locked to the cap, however when the cap was separated from the cup, the final deformation increased as expected to similar levels for all three impaction methods (Figure 3.16).

The use of a free cap compared to the polar impact did not make a difference to the number of impacts needed when a titanium alloy cup was considered, however 5

fewer polar impacts were required compared to the Co-Cr cup. Higher deformations of 34 μm were observed for the titanium alloy cup compared with 17.6 μm for the Co-Cr cup during polar and free cap impaction. With a locked cap, the deformations observed during impaction are the same for both cup materials as the locked cap drives the overall performance, however once the cup was fully seated and the cap was released from the cups (* on Figure 3.16) the final deformations increased to the same level as that observed for the two materials using the other two impaction methods.

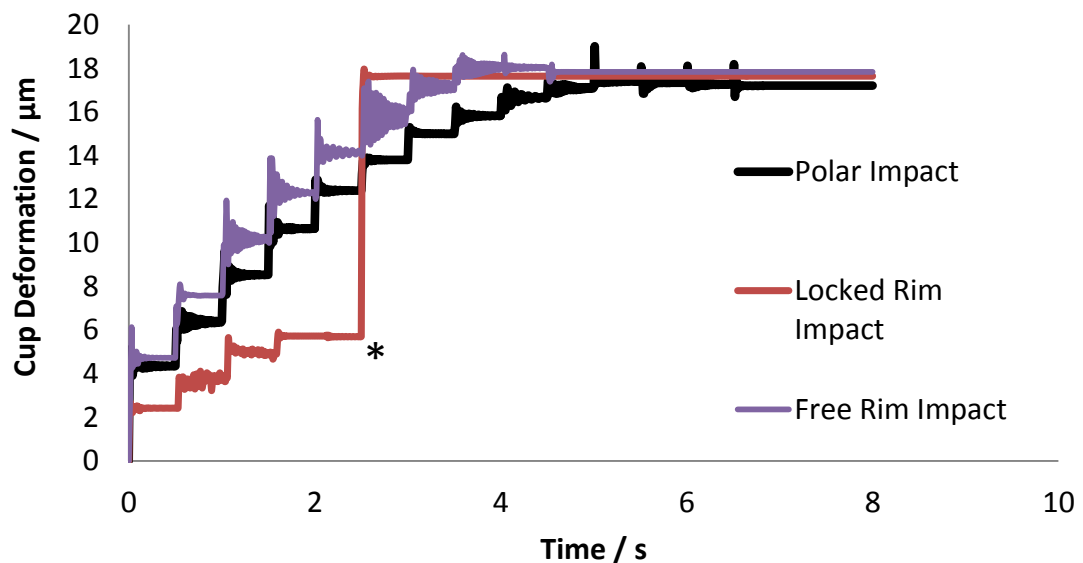


Figure 3.16: Cup Deformation observed after impaction of Co-Cr cup at 1 m/s with an interference of 1 mm and a friction coefficient of 0.3 *Cup fully seated at this point and locked cap released from cup and removed

3.5.3 Discussion

Following the development of the initial static cup insertion model, an explicit dynamics model was created to simulate the multiple mallet impacts administered by an orthopaedic surgeon to seat a metallic press fit acetabular cup into the acetabulum. As previously indicated by the static impulse model, increasing the interference and cup-bone friction resulted in more impacts at a higher velocity being required to seat the cup. Of significance to the design of insertion tools, the use of a cap locked on the cup rim made insertion considerably easier than impacting directly on the polar surface for cups made from Co-Cr and Titanium alloy. When the modulus of the cup

was lower, polar impaction became slightly easier than impacting around the rim using a cap that was free relative to the cup rim.

Dynamic loading is clearly a more realistic approach to simulating the insertion of press fit cups, as presented in the current study when compared to previously reported studies [Yew et al., 2006; Spears et al., 1999] which have used static implicit finite element solvers to seat the components, effectively squeezing them into the acetabula cavity. The impact velocities that were defined in this study were estimated based on observations of the clinical procedure where it was noted that on average a surgeon will impact the acetabular cup once every 0.5 seconds [West et al., 2008].

The momentum of impaction was changed by altering the impactor velocity, keeping the impactor mass constant. Simulations were ended if further impactions made no difference to its position or if the polar gap was less than or equal to 0.5 mm, at which optimum bone ingrowth begins to occur. As would be expected, higher velocities were shown to result in fewer impactions being required to seat the cups. Although the current study allowed impactions to be repeated until cup seating was observed, it is unlikely for a surgeon to completely replicate this behaviour. However the simulation provided useful information, for example indicating that with a 2 mm interference, the cups would probably not be fully seated unless hit with considerable force on many occasions. It is important to consider the influence of increasing the impactor velocity on the precision of hitting that can be performed by the surgeon during insertion. At higher velocities, there is likely to be a higher risk of the surgeon mis-hitting the cup causing it to be inserted incorrectly, or damaging the cup or surrounding bone. The higher forces associated with the higher velocities would also likely increase the risk of damage to the cup or surrounding acetabula bone.

The effect of changing interference on cup deformation is in agreement with the findings by a previous finite element study [Yew et al., 2006] in that increasing the interference caused an increase in the amount of diametrical deformation observed. Deformations were found to correspond to the position of the cup within the foam cavity; the further the cup was within the cavity, that is the smaller the polar gap, the larger the observed diametrical deformations. Whilst higher interferences made insertion more difficult with a constant velocity, using too high an impact velocity with too low an interference, resulted in the cup bouncing out of the cavity; these

observations are similar to those reported in a previous experimental study [Jin et al., 2006].

When Co-Cr cups are inserted clinically, two different methods can be used. If they are used as a backing shell to a polyethylene or ceramic cup, as can be the case in THRs, then they may be hit at the pole [Smith & Nephew, 2010]. However if the component is a monoblock and has a polished bearing surface, as is the case in MoM hip resurfacing components, this articulating surface is protected and a 'cap' is commonly used which transmits the insertion impacts through the cup rim [Zimmer, 2008]. When this free cap was modelled in the current study, fewer impactions were necessary to seat the cup than when it was impacted directly on its polar surface; this difference was more pronounced for higher interferences. Titanium shells are used exclusively with ceramic or polyethylene cups rather than independently [Which Medical Device, 2011] and it was interesting to discover that it was slightly easier to impact a titanium alloy shell at the pole than it was to insert either the titanium shell or Co-Cr cup by impacting on the rim. This may be explained by considering that the stiffness of the titanium shell is significantly less than that of the Co-Cr cup. For the titanium shell, the diameter of the shell reduces more during the insertion procedure, and therefore is able to move into the cavity somewhat more easily than for higher stiffness shells, or when a free cap is used. It is clear that the modulus of the metal acetabular components and the method of impaction are important factors in determining the ease of insertion and should therefore be given careful consideration during the design of cups and impaction devices.

Hitting the cups at the rim with the free cap resulted in the cup position oscillating considerably more than hitting directly at the pole, as can be seen in the oscillations of the cup deformations in Figure 3.16. Whilst the oscillations after polar impact did not affect the final cup position, the larger oscillations that occurred after rim impact were found to cause micro-motion of the cup, resulting in it moving about 0.01 mm further into the cavity in the 0.5 s between each impact. Although this movement is comparatively small, this outcome suggests that intentionally increasing the amount of high frequency oscillations generated might aid cup insertion. These findings are contrary to the suggestion made by Spears et al. [1999] who stated, following their static analysis, that the position of the applied load is inconsequential.

Of greatest significance, it was established that substantially fewer impacts were required to seat both the titanium and Co-Cr cups when the rigid cap was locked to the cup, effectively stiffening the whole cup construct. This may be explained by considering that when polar and free cap impaction is modelled, much of the impact energy is transferred directly to the cup. However when the cap, which has a very high stiffness, is locked to the cup, less energy from each impaction is transferred to the cup and substantially more is transferred to the foam cavity. This results in the diameter of the cavity increasing more readily, allowing the cup to be inserted more easily. Once the cup is fully seated, the cap is removed and the high strain energy from the foam is immediately transferred to the cup, resulting in the sudden increase in cup deformation, as shown in Figure 3.16. These findings are significant to the design of impaction devices, showing that securing a cap to the cup in a manner that stiffens the whole construct during insertion could make impaction easier than simply using a free cap, as is the case with many commercial impaction devices currently used.

A notable limitation of the model in this study was the simplification of a three-dimensional foam cavity structure to a two-dimensional axisymmetric model. This was evident when comparing the deformations observed in this study with the deformation observed in the three-dimensional model of the cup and foam cavity by Yew et al. [2006]. Maximum deformations were found to be notably smaller in the current study and this can be reasoned by considering that the study by Yew et al. [2006] was able to create “pinching points” acting on two diametrically opposed ends of the cups, thus being able to simulate the non-uniform deformation behaviour of the cup in the human pelvis. The significance of adding pinching is highlighted in a study by Ong et al. [2009] who, using pinch points, found cup deformations to be 50 times greater than a study by Fritsche et al. [2008] who used uniform support in a circular cavity, with similar cups. It is clear therefore that the experimental conditions created in investigating cup deformation, particularly that of non-uniform support to the cup, can have a significant effect on the results. Despite this limitation in the initial models, it was observed that maximum contact stresses occurred at the periphery of the cup and in the corresponding contact region at the rim of the foam cavity and is in agreement with previous experimental and finite element reports [Jin et al., 2006; Yew et al., 2006]. It has also been reported [Ries et al., 1997] that acetabular strains in the bone were greatest at the periphery of the cup.

The deformations generated in the cup using elastic foam in the current study are still high enough to be a cause for concern. A cup with a 2 mm interference fit has been shown to result in diametrical deformations of 35 μm . The typical diametrical clearances for these components are typically between 80 and 120 μm specified for a 60 mm cup [Yew et al., 2006], so it is clear that these deformations could hamper the tribological performance at the bearing surface interface. For the backing shells the diametrical changes could influence the behaviour of the proper seating of the ceramic or polyethylene cups. Decreasing the shell or cup thickness or increasing its diameter can result in higher deformations [Yew et al., 2006], therefore this appears to be a factor that must be given careful consideration during the design and use of press fit cups.

3.6 Introduction of Plasticity into Foam Model

Earlier studies that have modelled foam cavities have assumed the material as being purely elastic. The influence of the plastic yielding of the foam model on the behaviour of the cup was simulated in the current study.

3.6.1 Method

Plasticity was introduced into the material model for the foam cavity using a perfectly elastic plastic model with a yield stress of 20 MPa [Sawbones, 2011] and its effect on cup seating and deformation was compared with that of elastic foam, during and after impaction with a free cap using a coefficient of friction of 0.3.

3.6.2 Results

The influence of elastic-plastic foam properties on the remaining polar gap and the final diametrical cup deformations observed after full seating of the Co-Cr cup using a free cap are shown in Table 3.13. As the interference increased, the minimum possible polar gap increased, as did the cup deformation. Introducing a yield stress into the foam resulted in lower final deformations than for a purely elastic foam, with the greatest differences being observed for the highest interferences. No differences were noted in the cup position during and after impaction.

Table 3.13: Polar gap remaining and cup deformation with and without yield after full seating of cup using a free cap, coefficient of friction of 0.3.

		Polar Gap Remaining / mm	Final Co-Cr Cup Deformation / μm	Final Cup Deformation with Yield / μm
Interference (mm)	0.25	0.16	4.68	4.44
	0.5	0.18	9.39	8.89
	1	0.37	17.6	15.59
	2	0.48	35.2	30.8

3.6.3 Discussion

The limited modelling studies to date that have examined press fit cup deformation behaviour, have not considered the consequences of the plastic yielding and micro-damage of bone; rather they have all assumed bone as being linearly elastic. Plasticity was introduced in this study through a yield stress and this was found to create lower cup deformations than using purely elastic foam. The results suggest that using higher interferences may result in more cancellous bone micro-damage occurring during insertion. However it is of note that the differences in the deformations are comparatively small; overall, the long term effect of bone remodelling will be of significance as it is due to this that bone in-growth can occur over time between the porous outer surface of the cup and the damaged surrounding bone. It is expected that the surface interactions with weaker bone, such as osteoporotic bone, could be more accurately modelled by using lower yield stresses in the cavity, in conjunction with lower values for the coefficient of friction.

3.7 Introduction of Viscoelastic Properties into Foam Model

Viscoelastic properties were defined for the foam in addition to its linear elastic definitions, and simulation C was repeated by impacting on the cups inner polar surface. This simulation was run for a time period of 100 seconds and the effect of viscoelasticity on cup seating and deformation in this time period was observed.

3.7.1 Results

It was found that cup seating was largely unaffected by the addition of viscoelasticity however differences are observed between the cup deformations during polar impaction; after 93 seconds the deformation with viscoelastic foam reduces to approximately $0.07 \mu\text{m}$ less than that observed when using purely elastic foam, Figure 3.17.

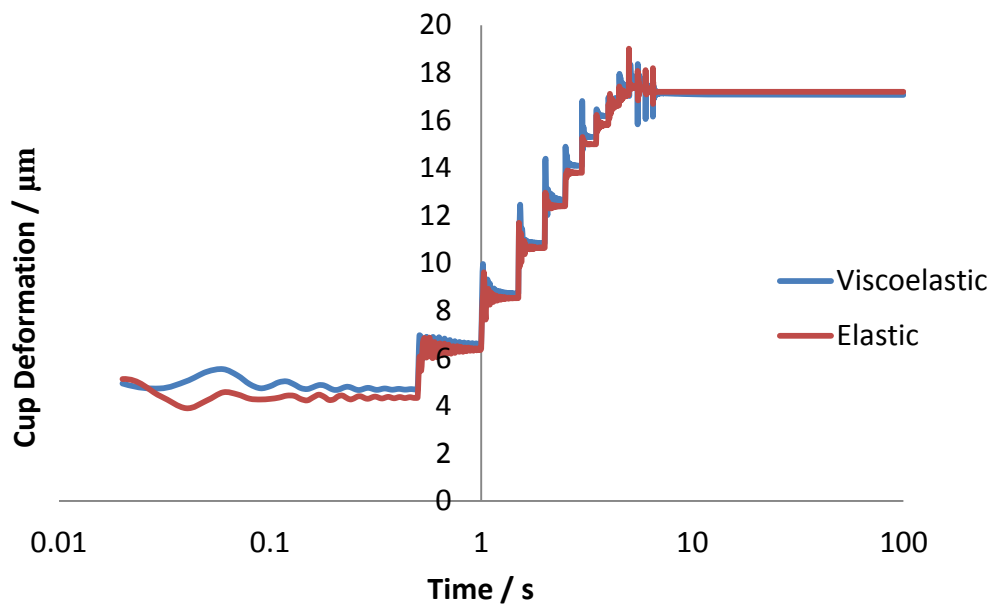


Figure 3.17: Diametrical cup deformation after impaction at 1m/s with 1mm interference and coefficient of friction of 0.3 - comparison of viscoelastic and elastic foam after polar impaction.

3.7.2 Discussion

When comparing the results obtained between using purely elastic foam and foam with time dependent properties, it was found that the difference in cup position during and after impaction was negligible. However, differences in cup deformation were observed in the simulation time of 100 seconds; during impaction, the viscoelastic foam resulted in the peak deformation being consistently higher by up to $1 \mu\text{m}$ after

each impact. After the last impact was applied, the simulation ran for approximately a further 90 seconds and in this time the final deformation reduced by about 0.07 μm for the viscoelastic model, more than that observed for the elastic model, which did not experience a change in deformation. Although this decrease is not substantial, it is clear that the addition of viscoelasticity to the model resulted in the deformation relaxing, which supports the argument that the lack of clinical problems due to cup deformation may be also be attributed, in part, to the stress relaxation occurring in the acetabulum, allowing the cup to partially return closer to its undeformed state, such that optimal diametrical clearances are maintained. It should be noted that the time dependant properties calculated for this model are more accurately described as being rate dependant. Future model developments include the long term time dependent creep properties of bone, providing a more accurate representation of the static cup-bone interaction behaviour over a period of 24 hours.

3.8 Conclusions

The use of a dynamic model to simulate the impaction of an acetabular cup with a range of parameters has allowed a number of interesting observations to be made. Increasing cup interference results in higher impact velocities being required to seat the cup. Of great significance, locking a rigid cap to the cup rim during impaction for insertion was found to result in fewer impactions being required than using a free cap or impacting directly on to the polar surface. This is important to impactor design and would make cup insertion easier possibly and reduce acetabulum damage. The stiffness of the cup material used was also found to influence the ease of cup seating and slight micromotion of the cup into the cavity was found to occur between impacts when using a free cap. The addition of plastic yielding and time dependency to the foam cavity resulted in a slight decrease in cup deformation.

The concepts and understanding of the two-dimensional foam model was used to guide the development of a three-dimensional foam model which was used to carry out a more detailed analysis of key parameters.

Chapter 4

Experimental Validation and 3D Cup-Foam Model Development

4.1 Introduction

The previous chapter established that the method of impaction influenced the seating of the acetabular component and specifically that rim impaction resulted in a smaller final polar gap than polar impaction.

The effect of cup orientation, in relation to the underlying bony support of the acetabulum, on the deformation of the cup itself has not been widely investigated. Cadaveric testing [Widmer et al., 2002] has established three dominant regions within the acetabular cavity that transfer load to the acetabular cup, namely the ischeal, iliac and pubic bone. These three regions provide stability to the implanted cups, however the greatest contact forces are generated along the axis between the iliac and ischeal regions, resulting in a pinching of the component. Cup deformations due to variations in this pinching effect require better understanding. Whilst the two-dimensional axisymmetric models developed in the previous chapter are valuable in understanding the impaction behaviour, a three-dimensional foam model is necessary in order to simulate the implantation of cups at different orientations and the non-uniform support provided to the cup.

The current chapter describes the development of a 3D finite element cup impaction model based on an experimental design using foam cavities. This model can be used to investigate the influence of a range of parameters on cup deformation following impaction, including:

- the method of impaction,
- the variations in support provided to the seated cup by the underlying cavity
- the orientation of the cup with respect to the cavity
- variations in the geometry of the cup

4.2 Experimental Cup Impaction Study

The methods used and results obtained in the experimental study in which metal press-fit acetabular cups were impacted into foam cavities representing the human acetabulum are described in this chapter. The parameters of the size of the interference fit, the impact velocity and impaction method were varied and their influence on the seating and deformation of the cups established.

4.2.1 Experimental Methods

Three CoCrMo cups consisting of a single geometry with an outer diameter (ϕ) of 60 mm and depth (d) of approximately 22 mm were considered in this study with wall thickness of 3.5 mm at the rim (Tr) and 6 mm at the pole (Tp), similar to previous studies [Hothi et al. 2011; Jin et al. 2006; Yew et al. 2006]. The porous coating used on the outer surface of the cups tested was hydroxyapatite coated over a 200 μ m layer of Porocoat [Isaac et al., 2005]. The polyurethane foam [Grade 30, Sawbones] used in the current experimental study (Figure 4.1) was cut to sizes of 100 x 100 x 40 mm to allow for gripping in clamps; the foam has previously been reported to be a suitable alternative to using cadaver specimens [Jin et al., 2006]. The polar gap (Pb) was defined as the distance between the outer pole of the cup and the inner pole of the cavity (Figure 4.2), which was estimated by measuring the distance of the cup rim above the surface of the cavity (Pa) using a Vernier Height Gauge (Figure 4.3). Cup seating was determined by observing the reduction in Pa after each impaction.

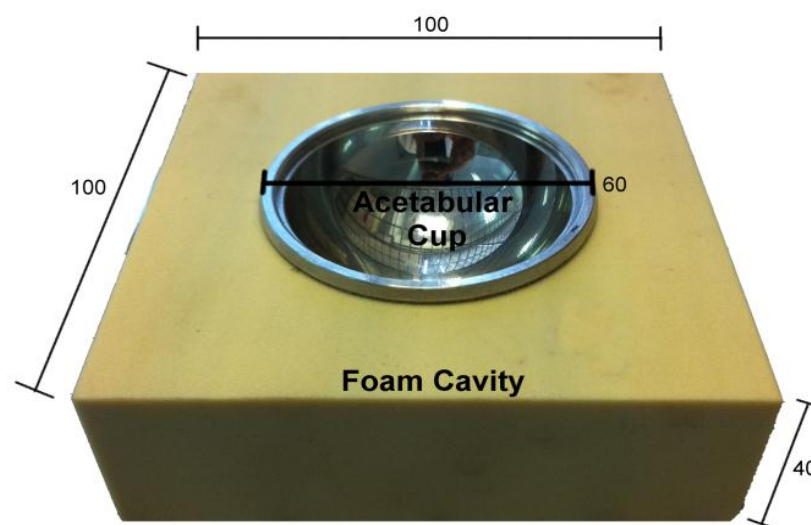


Figure 4.1: CoCrMo Cup impacted into foam cavity representing the human acetabulum

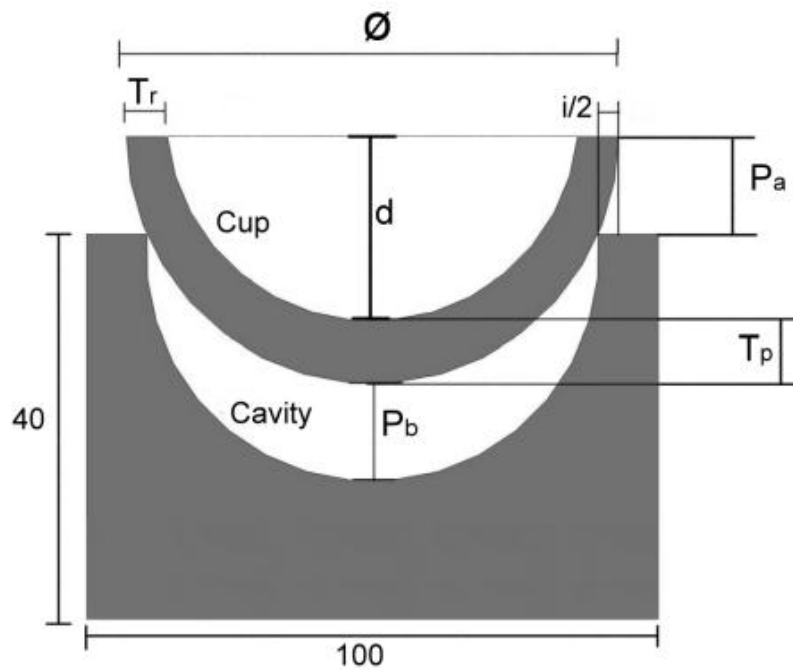


Figure 4.2: Cross-sectional dimensions, in mm, of the acetabular cup and foam cavity.

The cavities were under-reamed such that a diametrical interference (i) of 0.25, 1 and 2 mm was created between the cup and cavity, similar to interferences that have reported to have been used clinically [Adler et al., 1992; Spears et al., 1999]. The depth of the cavity was reamed such that it was approximately 1 mm less than the height of the cup, to ensure that the cup rim remained proud of cavity surface even after a full insertion.

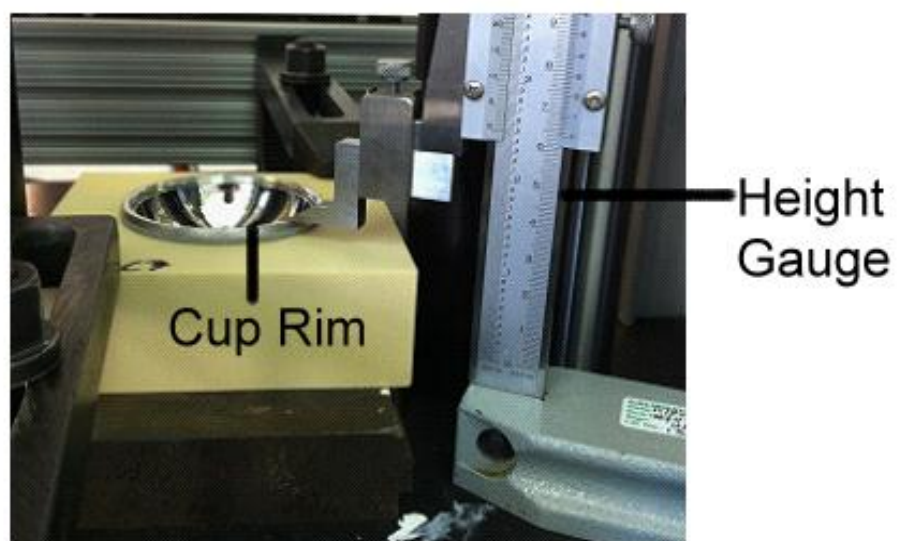


Figure 4.3: Height of cup rim above cavity surface measured after each impact to determine polar gap

In addition to using polyurethane cavities, three cavities made from foam with reported viscoelastic behaviour (Airex, Impag, UK) were impaction tested. This foam has been previously used as a bone substitute in experimental testing and has found to display creep [Palissery et al., 2004]. Three blocks used were cut to a width and length of 100 mm and were 50 mm in height for this foam. The cavities were reamed to produce an interference fit of 1 mm with a 60 mm diameter cup, with a depth approximately 1 mm shallower than the height of the cups.

In all foams a hole with a diameter of approximately 10 mm was drilled at the pole of each cavity to allow the cups to be easily removed after testing, Figure 4.4.

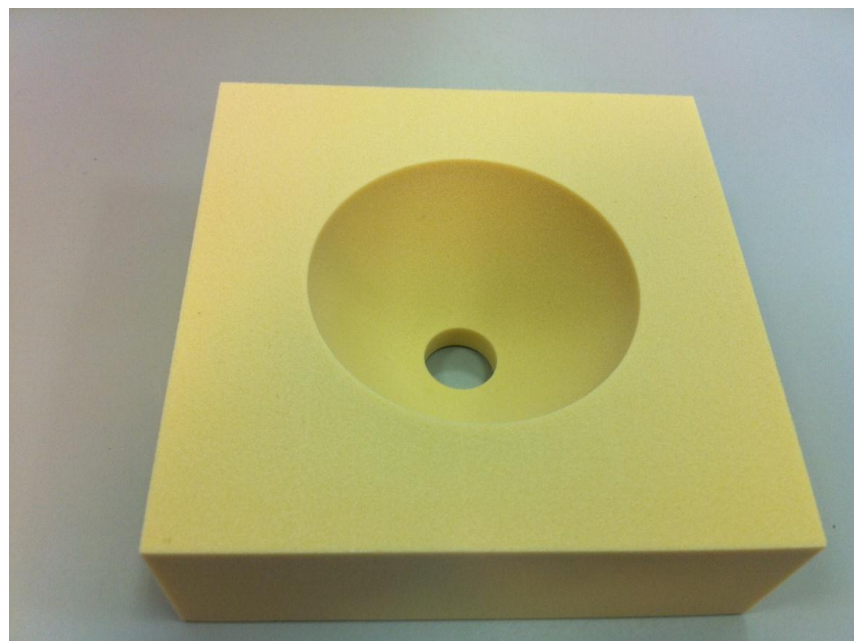


Figure 4.4: Foam block with a reamed cavity and a hole at the base to allow for removal of the cup

4.2.2 Impaction of the Cup

Before impaction the cup was carefully placed horizontally in the cavity and the height of the cup rim above the foam surface was measured at two diametrically opposite points to ensure that the cup was level and this was confirmed using a spirit level. The impaction process was performed using an Impact Testing System (Dynatup, Instron, UK), Figure 4.5. The foam cavity was clamped to the surface of the testing system. An impactor mass of 1.3 kg was dropped from heights ranging from 13 mm to 204 mm, generating final impact velocities of 0.5, 1, 1.5 and 2 ms⁻¹; the reaction forces between

the impactor and cup were recorded. A series of four experiments were performed as described in the following sections.

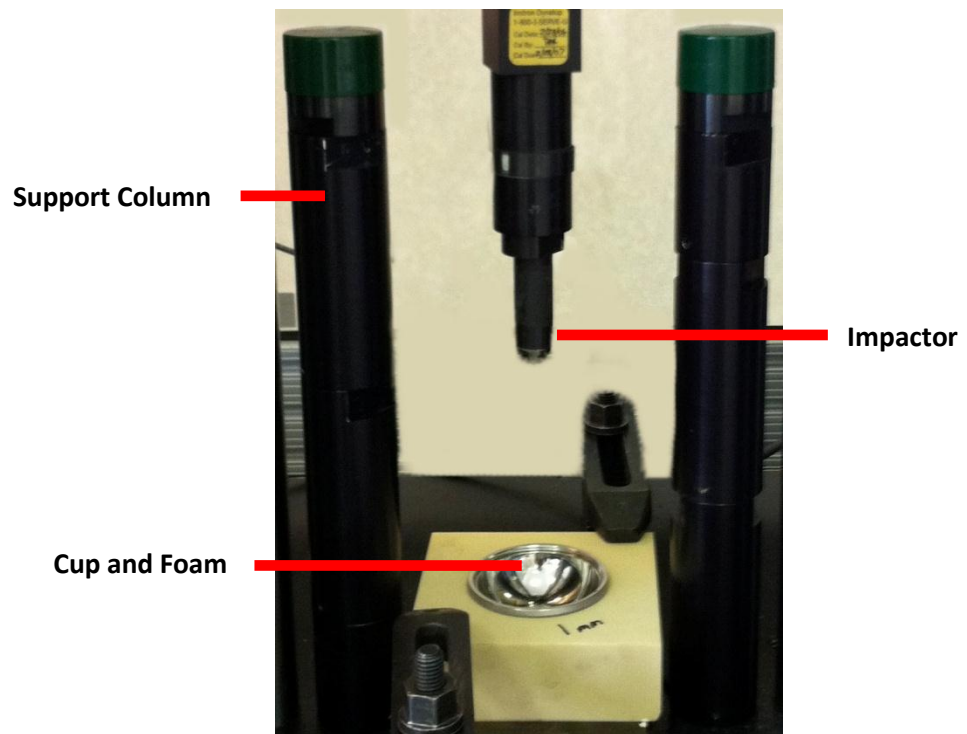


Figure 4.5: Impact Testing System used to perform impaction of cups into foam cavities clamped to rigid surface

Using three cups of the same design and size, each test configuration was repeated three times and the subsequent analysis of these results was based on the mean values from these three tests. The impaction process was continued until further impacts resulted in a change in the polar gap, P_a , of less than $10\ \mu\text{m}$ between consecutive cycles.

The inner diameter of each cup at a position 7.5 mm below the cup rim was measured before impaction using a coordinate-measuring machine (CMM) (Carl Zeiss Ltd), Figure 4.6. Following full impaction the inner diameter of each cup was remeasured immediately and the mean change in diameter determined.

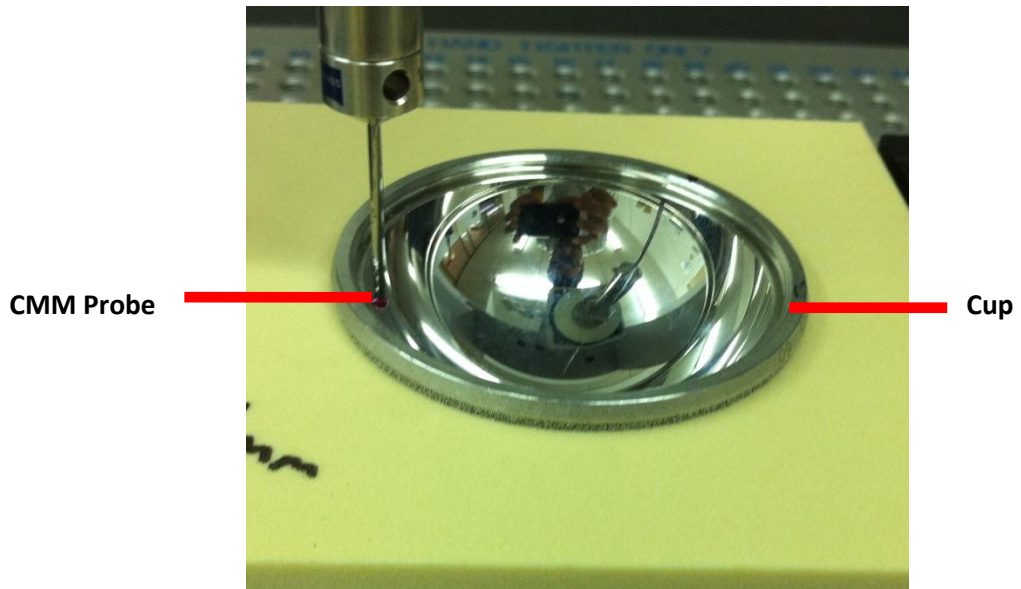


Figure 4.6: CMM used to measure inner diameter of cups before and after insertion

Part 1

The cup was impacted on its rim by placing a rigid circular steel cap between the cup rim and the impactor (*Free Rim Impact*), Figure 4.7. The cap was not constrained relative to the cup and it was repositioned centrally over the cup after each impact. The interference fit of the cup in the cavity and was varied from 0.25 to 2 mm using an impact velocity of 0.5 to 2 ms^{-1} , as shown in Table 4.1.

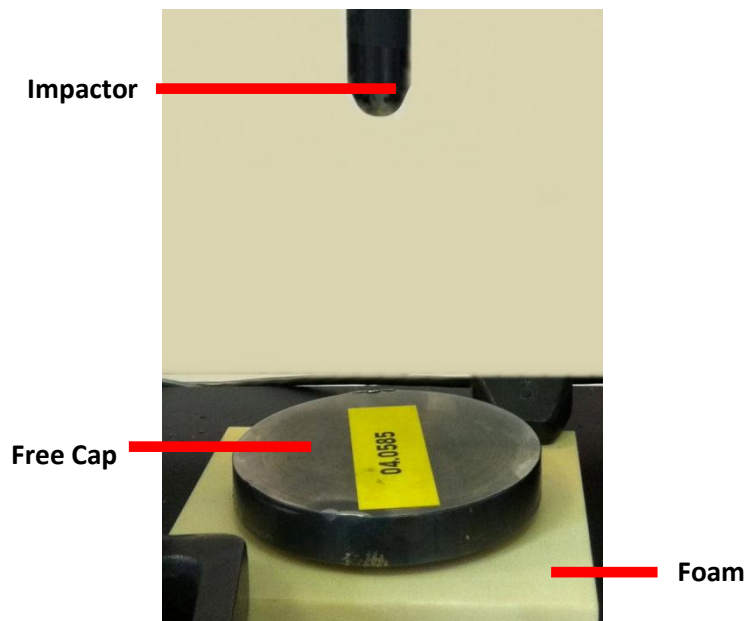


Figure 4.7: Cup inserted into foam cavities by impacting on its rim using a free cap

Part 2

The cup was inserted into the cavity by impacting on its inner polar surface (*Polar Impact*), Figure 4.8. With this test configuration, the impact velocity was maintained at 1 ms^{-1} , whilst the interference was varied between 0.25 and 2 mm.

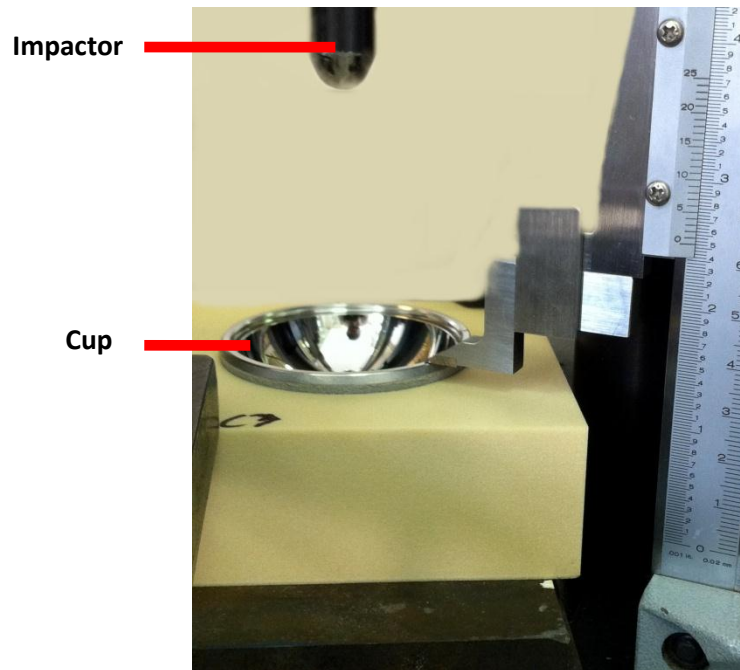


Figure 4.8: Cup inserted into foam cavities by impacting on the cups inner polar surface

Part 3

A rigid steel cap was locked to the cup by creating an interference fit between the cap and the inner surface of the cup rim, creating one rigid construct (*Locked Rim Impact*). A single impact velocity of 1.5 ms^{-1} was used with an interference of 1 mm between the cup and the foam cavity. Table 4.1 summarises all parameters that were tested, for the three parts of the study.

Table 4.1: Parameters tested experimentally, indicating the test descriptors for each variable

Initial Interference (mm)	Impactor Velocity (ms^{-1})					
	0.5	1			1.5	2
	Free Rim Impact	Free Rim Impact	Polar Impact	Locked Rim Impact	Free Rim Impact	Free Rim Impact
0.25	A	B	C	-	-	-
1	D	E	F	G	H	-
2	-	I	J	-	-	K

Part 4

A single cup was impacted into the viscoelastic foam cavity with an interference of 1 mm using a velocity of 1.5 ms^{-1} until further impacts had no effect on cup position. The inner diameter of the cup was measured before and immediately after insertion using the CMM machine. Subsequently, measurements of the diameter were taken at approximately 30 minute intervals for a period of 7 hours, with a final measurement taken 24 hours post impactation. This procedure was repeated once using the same cup inserted into a new reamed foam cavity.

4.2.3 Results of Experimental Study

Increasing the interference made insertion of the cup into the cavity more difficult, whilst increasing the impact velocity resulted in the cup seating further into the cavity. The polar gap remaining and final deformations after each impact for all the tests performed using the three cups are shown in Table 4.2. The same values for the polar gap observed from the last two impacts indicate that full seating with the test parameter had been achieved to within $10 \mu\text{m}$.

A high level of repeatability between the three cups for both the polar gap remaining and the final deformations following insertion were found for each test parameter.

Table 4.2: Polar gap remaining after each impact and the final experimental deformations ($\Delta\phi$). Bold value for the polar gap remaining indicates an additional impact that was performed to confirm seating.

Test	Polar Gap Remaining after each Impact / mm												$\Delta\phi$ / μm
	0	1	2	3	4	5	6	7	8	9	10	11	
A1	1.65	1.10	0.68	0.55	0.46	0.46							0.6
A2	1.62	1.00	0.67	0.54	0.44	0.44							0.6
A3	1.63	1.00	0.67	0.55	0.47	0.47							0.5
B1	1.63	0.32	0.32										0.5
B2	1.64	0.31	0.31										1.2
B3	1.64	0.30	0.30										1.2
C1	1.61	0.43	0.43										1.2
C2	1.61	0.44	0.44										0.7
C3	1.60	0.44	0.44										0.7
D1	4.35	3.60	3.40	3.11	2.96	2.89	2.85	2.82	2.78	2.75	2.70	2.70	0.8
D2	4.35	3.60	3.39	3.10	2.96	2.89	2.86	2.81	2.77	2.75	2.70	2.70	1.9
D3	4.30	3.59	3.39	3.12	2.97	2.89	2.85	2.82	2.77	2.76	2.71	2.71	1.9
E1	4.31	3.23	2.81	2.11	1.88	1.67	1.49	1.32	1.32				1.9
E2	4.33	3.21	2.79	2.10	1.88	1.68	1.50	1.33	1.33				3.3
E3	4.32	3.23	2.82	2.12	1.90	1.68	1.51	1.34	1.34				3.3
F1	4.37	3.10	2.75	2.55	2.35	2.16	2.00	1.90	1.82	1.76	1.65	1.65	3.2
F2	4.35	3.11	2.78	2.58	2.39	2.20	2.05	1.91	1.82	1.78	1.67	1.67	2.5
F3	4.31	3.09	2.75	2.54	2.34	2.45	1.99	1.89	1.80	1.74	1.64	1.64	2.5
G1	4.46	3.01	2.57	1.99	1.52	1.19	0.96	0.96					2.5
G2	4.5	2.99	2.52	1.93	1.49	1.17	0.94	0.94					5.8
G3	4.45	2.98	2.51	1.91	1.48	1.16	0.93	0.93					5.8
H1	4.31	2.70	2.10	1.60	1.30	0.89	0.89						5.8
H2	4.30	2.68	2.08	1.59	1.29	0.88	0.88						5.9
H3	4.32	2.69	2.09	1.59	1.28	0.88	0.88						5.9
I1	6.70	5.50	5.15	4.85	4.75	4.70	4.66	4.66					6
I2	6.68	5.48	5.13	4.84	4.73	4.69	4.65	4.65					3.3
I3	6.69	5.50	5.14	4.85	4.73	4.69	4.66	4.66					3.3
J1	6.41	6.10	5.95	5.82	5.68	5.45	5.45						3.4
J2	6.40	6.12	5.96	5.83	5.68	5.46	5.46						2.4
J3	6.42	6.11	5.97	5.83	5.69	5.47	5.47						2.4
K1	6.68	4.30	2.95	2.20	1.50	1.09	1.09						2.4
K2	6.69	4.31	2.94	2.22	1.51	1.08	1.08						12.7
K3	6.69	4.29	2.95	2.21	1.50	1.08	1.08						12.8

Table 4.3 presents the mean results for each of the test parameters, showing that increasing the impact velocity results in better seating of the cup with a consistent interference fit due to a smaller final polar gap; this in turn results in greater

deformation of the component. Similarly, increasing the size of the interference results in greater deformations. A polar gap of smaller than 0.5 mm was only achievable in these experiments when the smallest interference of 0.25 mm was used. This indicates that optimum bone ingrowth would only occur with this interference and that greater impact velocities may required when using higher interference fits to ensure that cup stability following insertion is achieved. Figure 4.9 shows the influence of varying the method of impactation on cup seating. As predicted in the 2D FE model in the previous chapter, locking a rigid cap to the cup rim makes insertion notably easier, requiring fewer impacts to seat the cup further into the cavity. Polar impactation was shown to be the least efficient method when impact Co-Cr cups.

Table 4.3: Mean number of impacts ($n = 3$), polar gaps (Pa) and diametrical cup deformations ($\Delta\phi$) observed at the point when the change in polar gap remaining between subsequent impacts was less than $10 \mu\text{m}$

Initial Interference / mm		Impactor Velocity / ms^{-1}					
		0.5	1			1.5	2
		Free Rim Impact	Free Rim Impact	Polar Impact	Locked Rim Impact	Free Rim Impact	Free Rim Impact
0.25	Number of Impacts	4	1	1	-	-	-
	Pa / mm	0.46	0.31	0.44			
	$\Delta\phi / \mu\text{m}$	0.53	1.20	0.73			
1	Number of Impacts	10	7	10	6	5	-
	Pa / mm	2.70	1.33	1.65	0.94	0.88	
	$\Delta\phi / \mu\text{m}$	1.90	3.27	2.50	5.80	5.90	
2	Number of Impacts	-	6	5	-	-	5
	Pa / mm		4.66	5.46			1.08
	$\Delta\phi / \mu\text{m}$		3.33	2.40			12.77

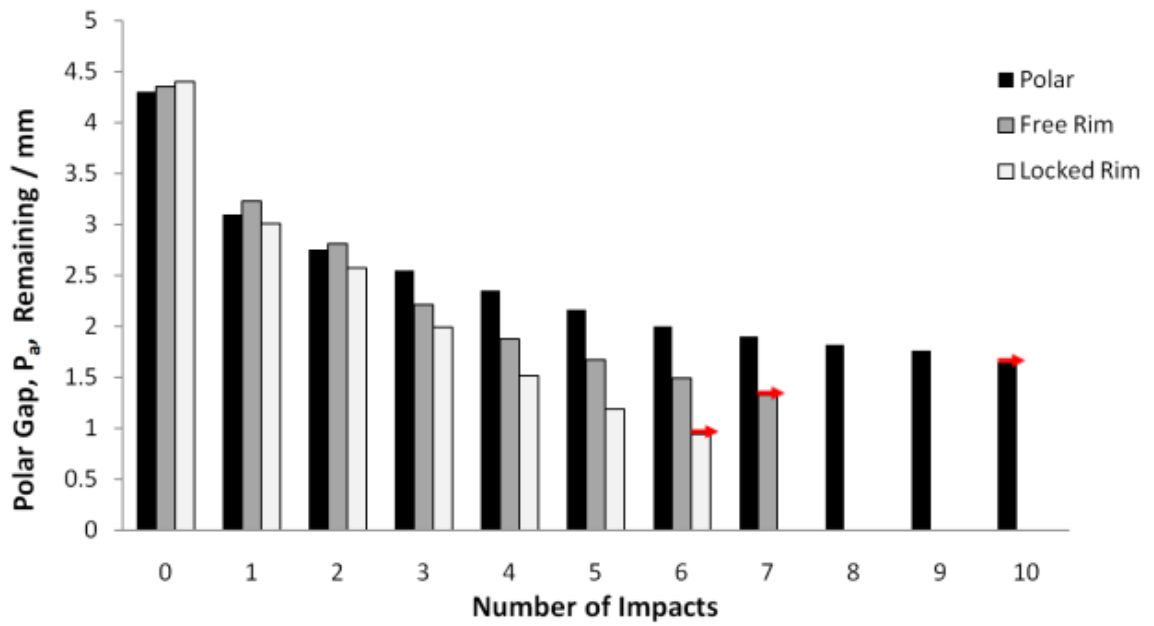
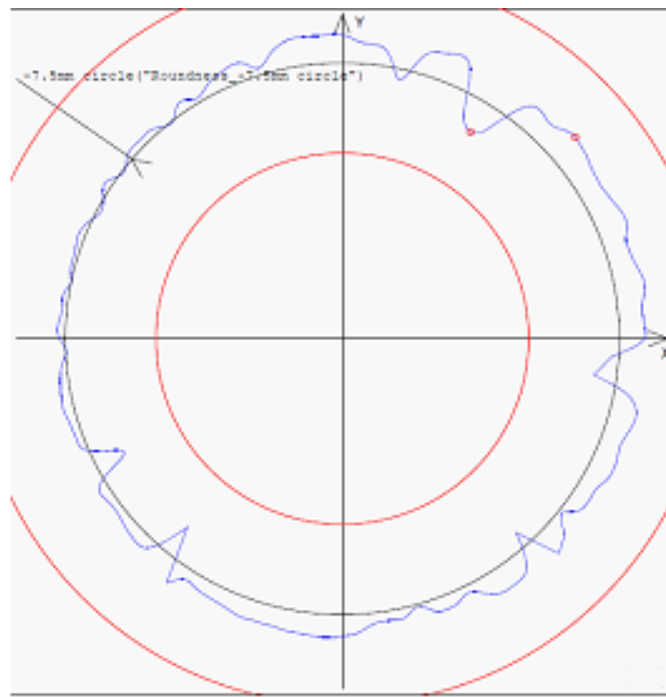
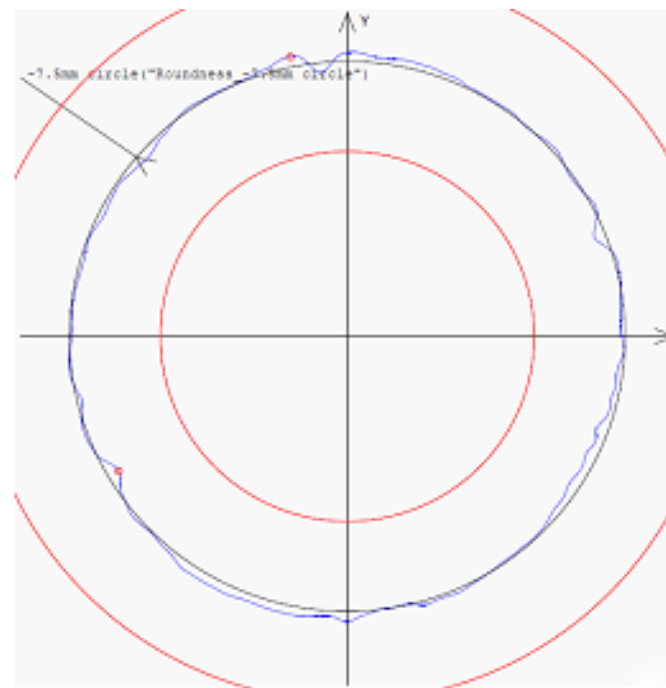


Figure 4.9: Mean polar gap remaining following impacts required to insert cups using impaction at the pole, around the rim (free rim) and on to a locked rim, with an impact velocity of 1 ms^{-1} and an interference of 1 mm . Arrows indicate that subsequent impacts reduce the polar gap remaining by less than $10 \text{ }\mu\text{m}$

Figure 4.10a presents the out of roundness of a cup immediately following impaction into the Airex foam cavity. It can be seen in the CMM measurement taken after approximately 24 hours (Figure 4.10b) that there was a relaxation in the deformation of the cup. It is clear from Figure 4.11 that there were considerable fluctuations in the recorded values for deformation during the first 7 hours when measurements of the maximum deformation were taken every 30 minutes. It can however be seen that there appears to be a relaxation of the deformation observed after 24 hours for both tests from a maximum of approximately $4 \text{ }\mu\text{m}$ to between 0.5 and $1.5 \text{ }\mu\text{m}$.



(a)



(b)

Figure 4.10: Out of Roundness plots determined using a CMM for a cup measured **(a)** immediately after impact and **(b)** 24 hours after impact. Cup deformations were recorded as the maximum reduction in diameter in each measurement

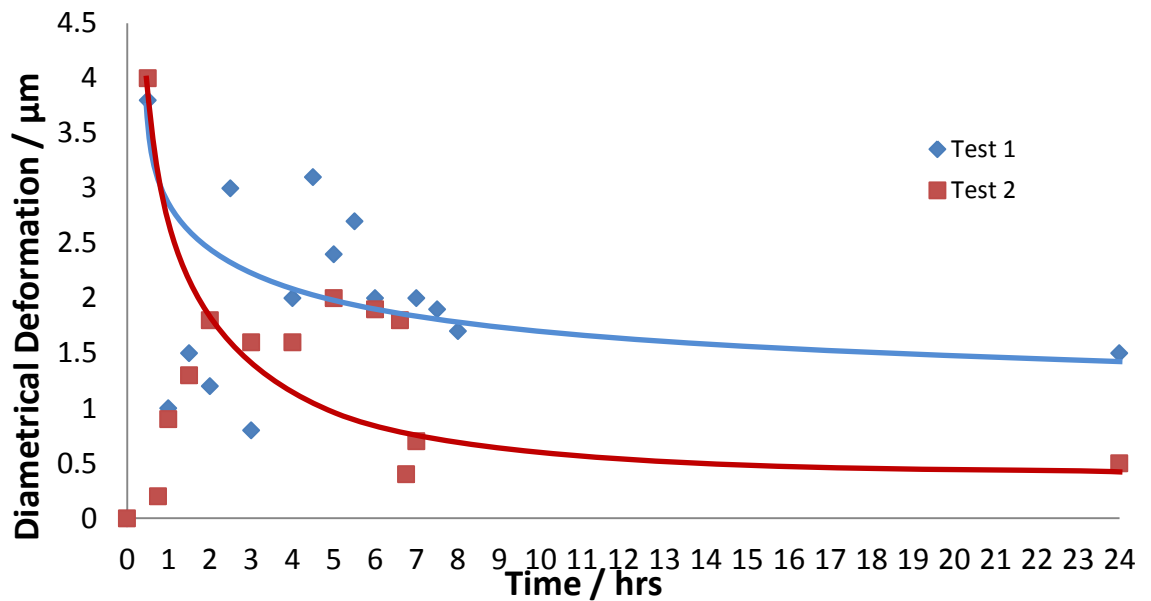


Figure 4.11: Change in cup deformation of a period of 24 hours following impaction in Airex foam

4.2.4 Discussion

The mean number of impacts that were required to seat the cups experimentally and their final diametrical deformations confirmed that insertion of the cup into the cavity was more difficult with increased interference, whilst increasing the impact velocity resulted in the cup being seated further into the cavity, Table 4.3. For a high initial interference (2 mm) the cup could not be fully seated, and further low velocity (1 ms^{-1}) impacts with momentums of 1.3 kgms^{-1} did not make any difference greater than $10 \mu\text{m}$ in its position; the remaining polar gap was substantial, at approximately 5 mm, when compared to the maximum gap of less than or equal to 0.5 mm for optimum bone ingrowth to occur [Sandborn et al., 1988].

In the current experimental study, as with the FE model developed in the previous chapter, the three different impaction methods were tested using an interference of 1 mm and impact velocity of 1 ms^{-1} . Whilst none of the methods resulted in full seating of the cup, due to the polar gap being significantly larger than 0.5 mm in all cases, there were clear differences in the seating behaviour between the different methods. Polar impaction was found to require the most number of impacts whilst still resulting in a polar gap of over approximately 1.65 mm remaining. When a rigid cap was used to lock onto the cup using an interference fit and this was found to require four less impacts than polar impaction to seat the cup approximately 0.71 mm further into the cavity. This is in accordance with the findings of the 2D FE model in the previous

chapter and could be significant in considering impactor design, especially if larger interferences are needed for full stability; locking a cap to the cup rim may mean lower impact forces are necessary to seat a cup than using free rim or polar impaction, therefore reducing the risk of bone damage or poor cup seating. West et al. [2008] observed that mean impact forces of approximately 18 kN were required to seat uncemented acetabular cups using an interference of 1 or 2 mm. In the current experimental study a maximum impact force of approximately 12 kN was observed when an impact velocity of 2 ms^{-1} was used. If the component was oversized, the current study suggests that it may not fully seat even with continued high momentum impaction. This highlights an important surgical issue and demonstrates the value of a dynamic FE model to simulate cup insertion as this behaviour cannot be predicted when static forces are applied. Interferences in the region of 0.25 to 1 mm might be preferable to allow the cup to be safely inserted, however initial cup stability is regarded as of primary importance for the longevity of the component [Spears et al., 2009]; the surgeon uses feedback from the ease of reaming to determine the size of a suitable interference, particularly for the apparently 'softer' osteoporotic bone to ensure that sufficient fixation is achieved [Valle et al., 2005].

Due to the way in which the CMM was set up, the change in diameter experimentally could only be measured at a depth 7.5 mm below the rim rather than at the equator itself. Inserting the cup into the viscoelastic Airex foam cavities resulted in lower deformations by up to $2 \text{ }\mu\text{m}$ being recorded than using polyurethane foam. The changes in deformations observed from the two tests performed with this cup showed a high level of variability, with the recorded deformation fluctuating considerably at each measured point. There was however a reduction in deformation by as much as $3.5 \text{ }\mu\text{m}$ in a period of 24 hours and the roundness plots did show a reduction in the change of shape in that time period. Whilst this does suggest that the foam used exhibits time dependent properties, there is presently insufficient test data from these pilot tests to comment on how well this behaviour correlates with that of bone. In future work it would be important to fully characterise the properties of the foam independently using static and long term compressive creep tests. The lower initial deformations observed however do suggest that a stiffer grade of Airex foam may be required to more accurately represent cancellous bone.

4.3 Preliminary Finite Element Simulations using a 3D Cup Design

Prior to developing 3D models to simulate the cup impaction processes that had been performed experimentally, a preliminary model was developed to simulate a simple acetabular component rim loading experiment performed by Squire et al. [2006]. The purpose of these preliminary simulations was to demonstrate the suitability of using finite element methods to simulate experimental results. Figure 4.12 shows the experimental set-up [Squire et al., 2006] where ten DePuy Pinnacle titanium acetabular shells measuring between 48 and 66 mm in diameter were subjected to compressive loads at the rim that were increased in increments of 200 N from 200 to 2000 N. The diametrical deformation of the component after each load was applied was measured and stiffness values were determined for the resulting load-deformation graphs.

This experimental procedure was simulated in the current study by developing a finite element model of the titanium cup within Abaqus/CAE, Figure 4.13.

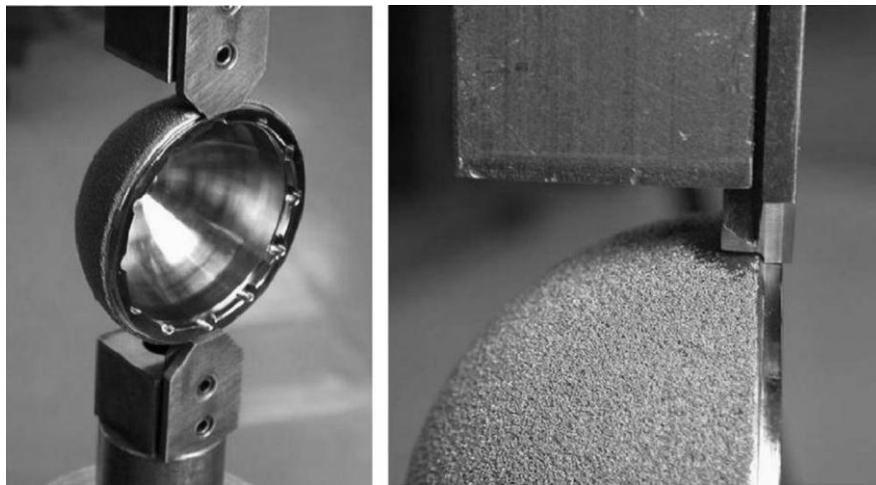


Figure 4.12: Titanium acetabular shells subjected to rim loading [Squire et al., 2006]

4.3.1 Preliminary FE Model Development

A single 60 mm cup design with a known uniform wall thickness of 3.5 mm and a Young's modulus of 113 GPa was considered. An encastre boundary condition was applied to the outer pole of the component to maintain its position in 3D space, whilst still allowing deformation of the component to freely occur.

Initially two opposing static point loads of 2000 N were applied to the rim of the component, Figure 4.13a. The results of this initial simulation highlighted that although the stiffness of the cup was high, the method of applying a point load to a single node resulted in a concentration of stresses at the node, leading to unrealistic modes of deformation in highly localised regions of the cup (Figure 4.13b).

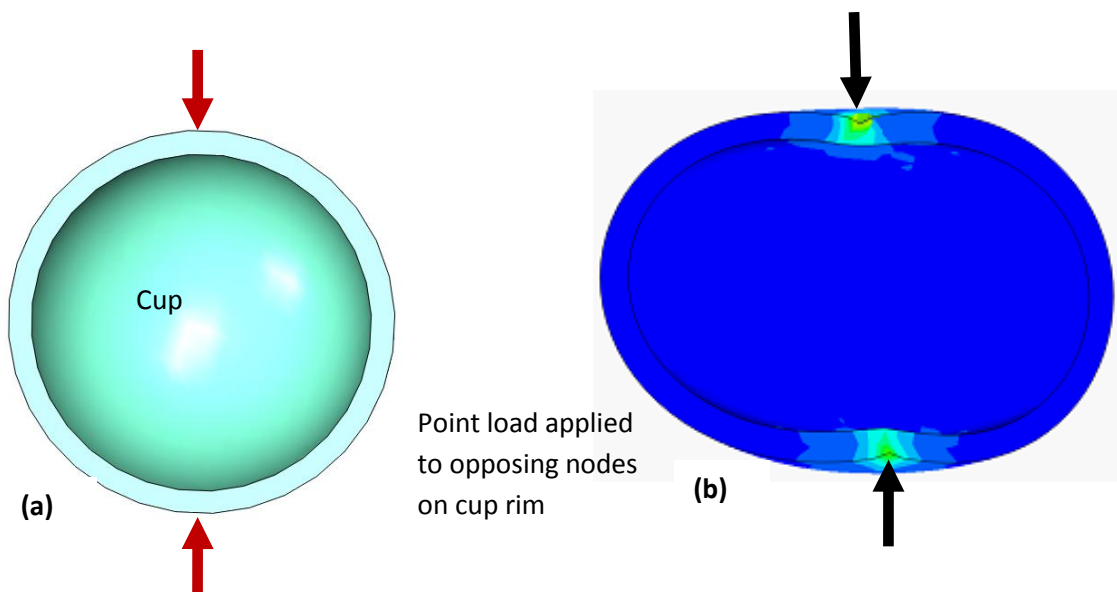


Figure 4.13: Showing (a) the direction of the point loads applied at the cup rim and (b) the resulting unrealistic mode of deformation from the FE model (scaled by a factor of 20)

An applied pressure was therefore modelled within Abaqus on opposing sides of the rim to simulate the application of the appropriate values of the force over an area of 10x5 mm (Figure 4.14), similar in size to that considered by Squire et al. [2006]. The total pressure applied was increased from 4 MPa to 40 MPa to simulate loads of 200 to 2000 N.

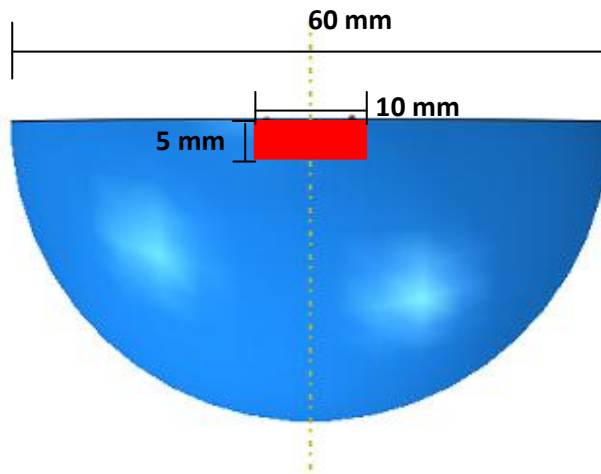


Figure 4.14: Showing the area on the rim where the opposing pressure was applied (in red)

A mesh convergence study was carried out in which an opposing rim load of 1000 N was applied to the cup and the number of elements in the model increased until there was no difference between the observed value for the deformation (mm), accurate to three decimal places. Figure 4.15 demonstrates the mesh convergence process that was utilised to determine the deformation

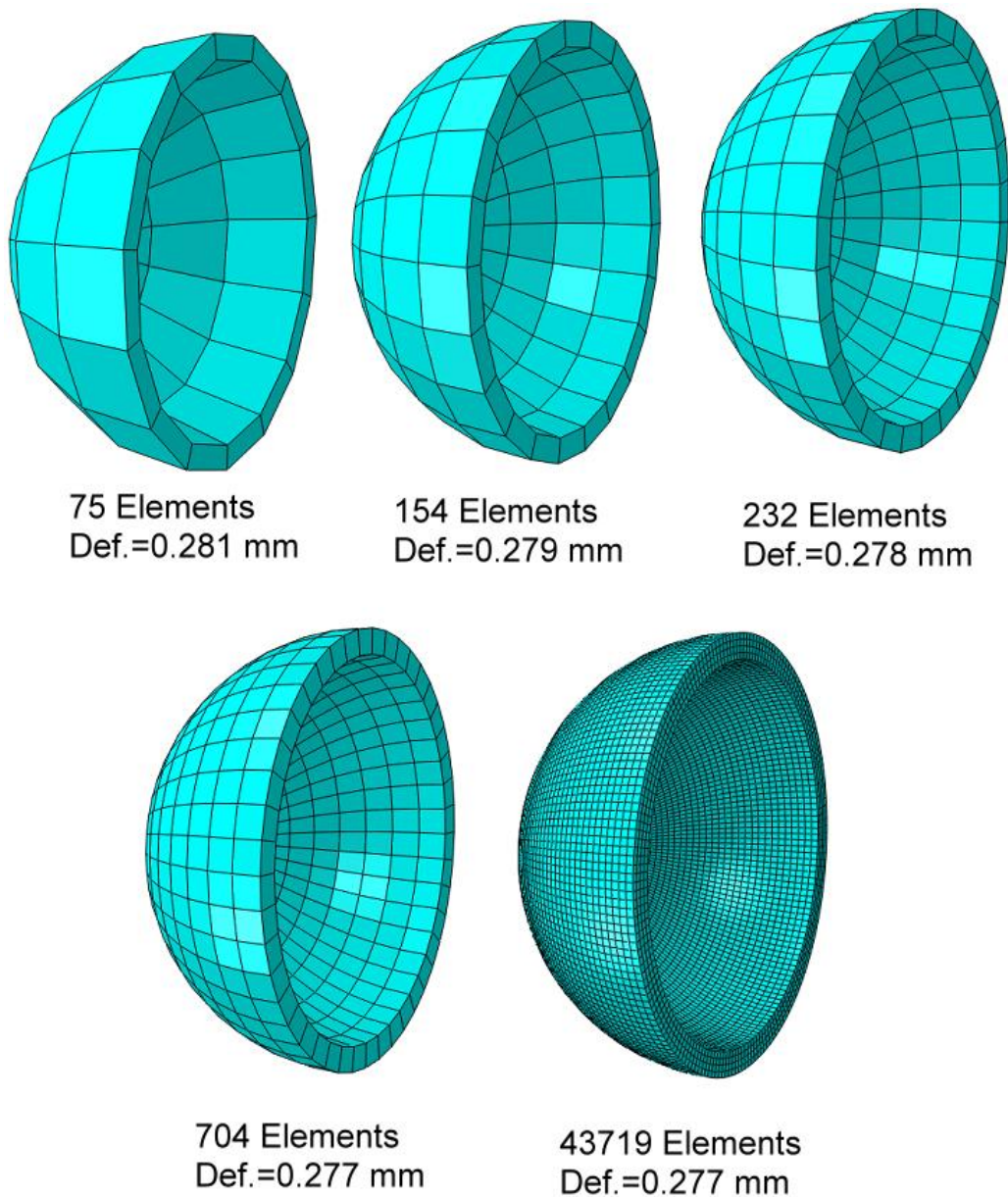


Figure 4.15: Mesh convergence achieved by increasing the number of elements in model

It can be seen that increasing the number of elements in the model to 704 resulted in convergence with respect to the deformation of the component and consequently this was used to mesh the component. Figure 4.16 displays the reduction in the cups diameter that was observed as the load on the rim was increased.

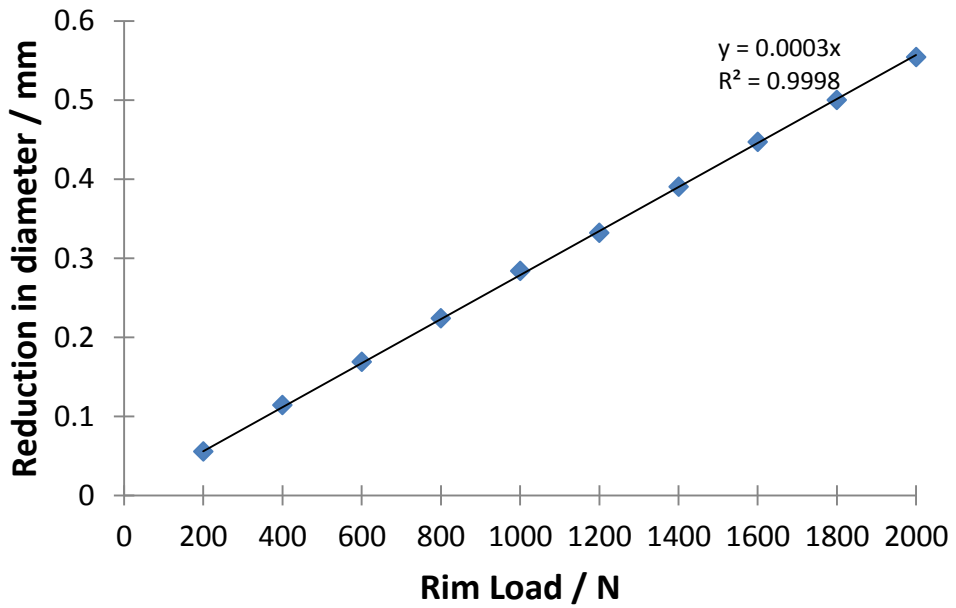


Figure 4.16: Graph showing the cup deformations observed as the rim load was increased

It can be seen that the correlation between increasing load and deformation is linear ($R^2 = 0.9998$) and is in agreement with the observations by Squire et al. [2006]. The stiffness of the component in the FE model was calculated as being approximately 3300 N/mm from the load/deformation graph and is comparable to the mean stiffness value of 3500 N/mm reported experimentally by Squire et al. [2006]. The results of this preliminary study demonstrated that the finite element method was appropriate to mimic the results of experimental studies.

4.4 Development and Validation of a 3D FE Cup Impaction Model

4.4.1 Preliminary Model Development using Static Cup Insertion Loads

A limitation of previous studies that have modelled the insertion of acetabular components, is that they have all used static point loads to seat the cups [Ong et al., 2009; Yew et al., 2006]. It was shown in the preliminary 3D cup model development that point loads on a single node can lead to localised concentrations of stress and unrealistic deformation behaviour. The use of a static load to insert a cup to a prescribed position as has previously been suggested can result in very high insertion forces of approximately 100 kN [Yew et al., 2006]. A model was developed in the current part of the study to demonstrate that the use of static loads was a poor representation of the clinical behaviour. A 3D foam model was developed consisting of a 60 mm Co-Cr cup and a foam cavity, reamed to create an interference fit of 1 mm, similar to the set up used experimentally. A static displacement control was applied to the node on the inner polar surface of the cup such that the component was translated 1 mm into the cavity (Figure 4.17). The corresponding insertion force that was required to achieve this displacement was observed.

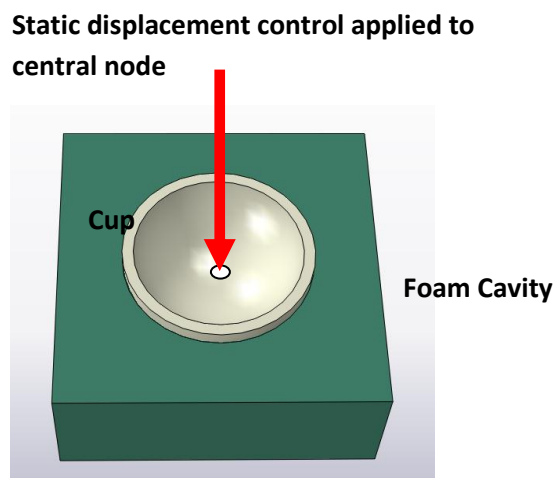


Figure 4.17: Displacement control applied to the central node of the cup

An insertion force of 128 kN when inserting the cup under displacement control was established in this preliminary static simulation in the current study. This means of insertion is clearly not a clinically realistic approach; modelling cup insertion in this manner does not allow an estimation of how far into the cavity a component will be seated as it places the cup at a final predefined position. As a result an estimation of the deformation after insertion cannot be made reliably.

4.4.2 Development of a 3D Cup Impaction Model

A previous study has suggested that peak impact forces of approximately 18 kN [West et al., 2008] are required to insert cups into the acetabulum; this magnitude of force may be generated when an impactor with a momentum in excess of 5.5kgms^{-1} is used [Hogg et al., 2009]. In clinical practice the cup is impacted on numerous occasions before it is fully seated.

A three dimensional explicit dynamics finite element model was therefore developed which defined an impactor with a momentum which simulated the impaction of the acetabular cup into the foam cavity (Figure 4.18). The current explicit dynamics study is a more realistic model that reflects the impaction velocities and impaction methods used by a surgeon to insert the component during surgery. It allows for a representation of the position of the cup in the cavity after multiple hits to reach an equilibrium position during insertion and hence provides a prediction of the diametrical deformation after insertion. A dynamic model can also provide an indication of the stresses generated in the component and surrounding cavity, which is important when identifying the limits of surgical impaction momentum to prevent damage to either the component or to the underlying bone. This will become critical in future studies that utilise this dynamic approach in 3D models of the pelvis, in which appropriate material properties such as the material yield and time dependency of bone are defined. The same dimensions were used to create the 3D finite element model as were used experimentally (Figure 4.2) and the model parameters were defined as described previously in the 2D explicit dynamics model.

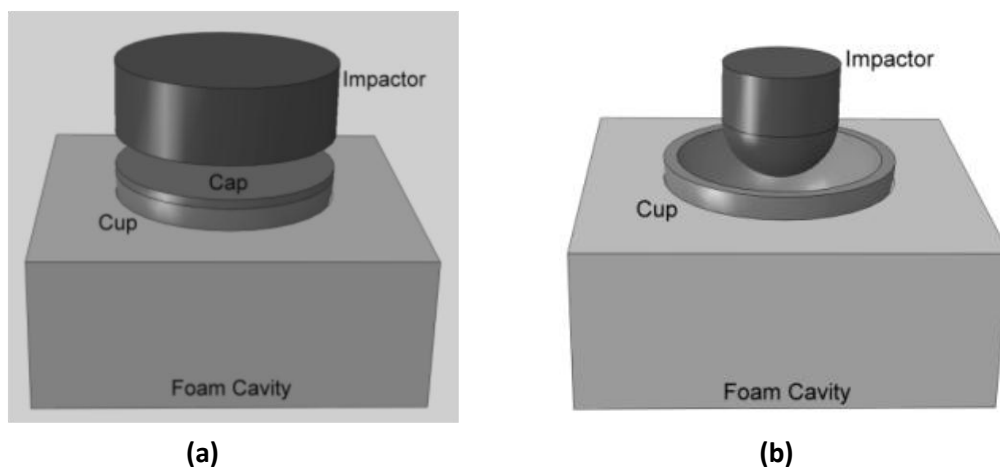


Figure 4.18: (a) Rim impaction using rigid cap and (b) Polar impaction

Fully constrained encastre boundary conditions were applied to the base of the foam with surface-to-surface contact defined between all the components. Penalty contact with finite sliding was modelled between the cup and foam. Explicit dynamic steps were defined for all the simulations to ensure that the effect of the impactor momentum was accurately modelled in the simulation.

A frictionless rigid cap was modelled between the impactor and cup (Figure 4.18a) to simulate the free rim impaction to reflect the earlier experimental investigation. A multi-point constraint (MPC) was defined to ensure that the cap remained centrally aligned with the cup rim after each impact. The impaction of the cup was simulated by modelling a number of independent 1.3 kg impactors that were positioned at above the cup (Figure 4.19). They were all defined with a single velocity and were modelled to begin moving at the same time so that an impact occurred every 0.5 seconds. Each impactor was disregarded after it had collided with the cup rim and therefore completed an impaction. No contact interaction properties were defined between one impactor and another, meaning that they were free to move through each other and this prevented the possibility of any of the impactors colliding.

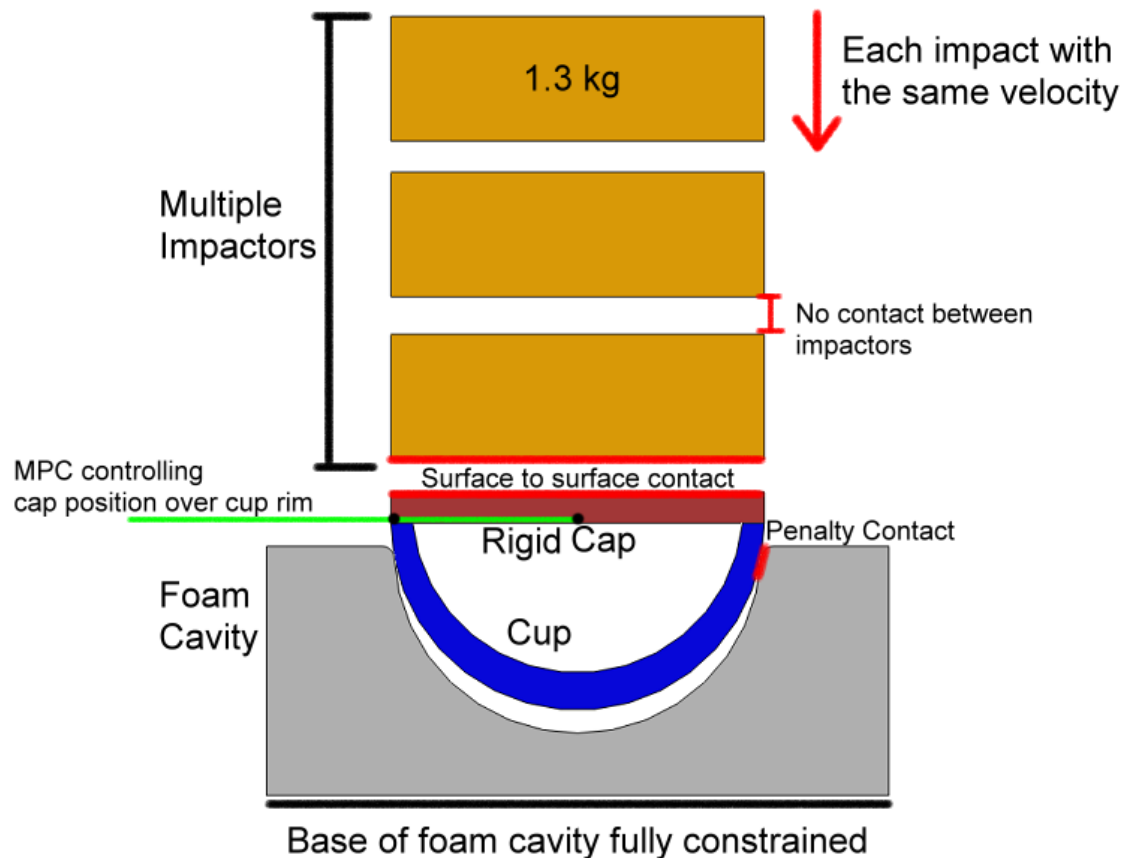


Figure 4.19: Cross-section of the 3D cup impaction process

4.4.3 Meshing and Material Property Definition of 3D FE Cup Impaction Model

The solid models were developed in Abaqus/CAE 6.9 and linear elastic material properties were defined in the foam cavity, Table 4.4. Plasticity was ignored in this instance to reduce complexity in the model as a previous experimental study [Yew et al., 2006] and the finite element model in the previous chapter found minimal differences in cup deformation (approximately 2 μm with a typical interference of 1 mm) when a yield stress was introduced in the foam's material properties.

Table 4.4: Mechanical properties of the acetabular cup, foam cavity and impactor. A Poisson's Ratio of 0.3 was assumed for all materials

Material	Young's Modulus / GPa	Density / kgm^{-3}	Source
Co-Cr Cup	210	8300	Yew et al. [2006]
Grade 30 Foam	0.553	480	Sawbones [2009]
Rim Impactor	210	23000	Fritsche et al. [2008]
Polar Impactor	210	73000	Fritsche et al. [2008]

The element failure criteria used in the mesh development for the cup and cavity models were set as a face corner angle of less than 10° , aspect ratio greater than 10 and an edge length shorter than 0.01 mm. In a similar approach to previous studies [Spears et al., 1999] it was assumed that that the comparatively high stresses at the point of contact between the cup and the edge of the cavity would cause this edge practically to experience a degree of wear and be smoothed. This area was therefore modified so that it had a curved profile rather than a sharp edge; this eliminated the risk of the cup 'locking' with the foam edge at this point during insertion.

Mesh convergence studies were performed considering the polar gap and deformation. A single impact with a momentum of 3.25 kgms^{-1} was used to seat the component and the number of elements in the model was increased until convergence was achieved for the values of the parameters accurate to 1%, Figure 4.20.

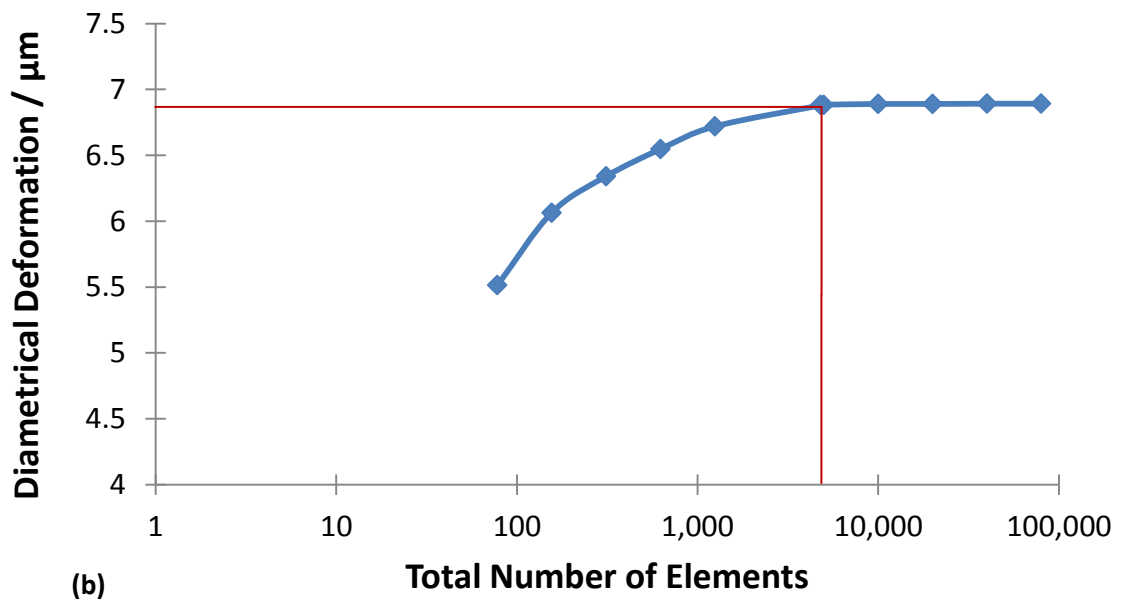
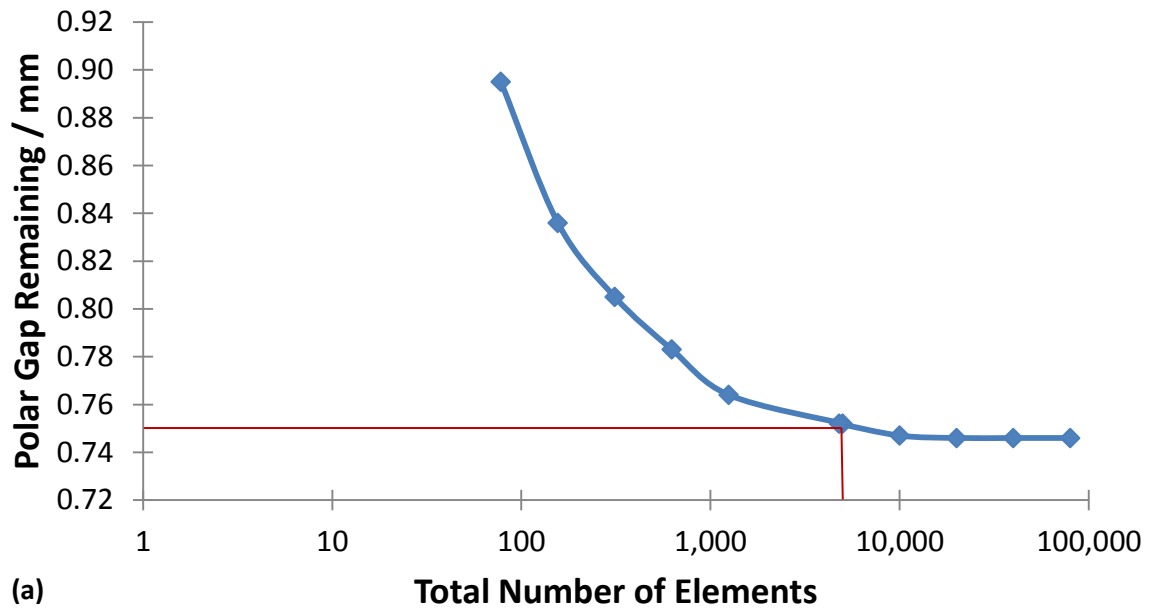


Figure 4.20: Mesh convergence achieved using (a) the polar gap remaining and (b) the diametrical deformation. Red line indicates the minimum number of elements for accuracy to within 1%

In order to minimise the computational run time, the mesh density was minimised whilst ensuring that the differences in the diametrical deformation (ΔD) and polar gap (ΔP) were within 1% of the values observed when convergence was achieved, as in the previous chapter.

$$\Delta D = \frac{D_E - D_H}{D_H} \times 100 \quad (4.1)$$

$$\Delta P = \frac{P_E - P_H}{P_H} \times 100 \quad (4.2)$$

where D_E and P_E are the deformation and polar gap values of the current simulation and D_H and P_H are the deformation and polar gap values when a maximum of approximately 80,000 elements were used.

A total of approximately 5000 linear brick elements (Figure 4.20) with reduced integration (C3D8R) was found to result in values accurate to 1%, whilst reducing the simulation run time from a maximum of approximately 4 days to approximately 3 hours, and was therefore used to mesh all the components. The mesh density in the model was such that it was greatest on the contact surfaces of each component and the number of elements in regions with lower strain gradient or away from the regions in contact were reduced. Due to the relative simplicity of the geometry of the components in the 3D model, mesh verification tests did not identify any significant regions where element distortion was a source of error.

Hourglass control may be required when C3D8R elements are used to ensure that artificial stresses are not introduced into the model [Rao, 2010; Simulia, 2010]. Hourglassing refers to circumstances in which an element locks and is unable to deform, becoming unrealistically stiff and therefore resulting in additional stresses which can skew the results of the simulation. Conversely, hourglassing may also refer to situations in which an element deforms but due to the manner in which this deformation occurs (a change to a trapezoid), no strains are present in the element. It was observed that enhanced hourglass control was necessary in the current model. Figure 4.21a shows the stresses that were observed in a cup that was inserted into a cavity with the poles aligned and uniformly supported. In this scenario it would be expected that the stress distribution within the cup after insertion would be uniform, however it is clear that there is an uneven distribution of stresses, suggesting that there is element locking. The inclusion of hourglass control (Figure 4.21b) results in lower stresses in the cup and an elimination of unexpected localised peak stresses.

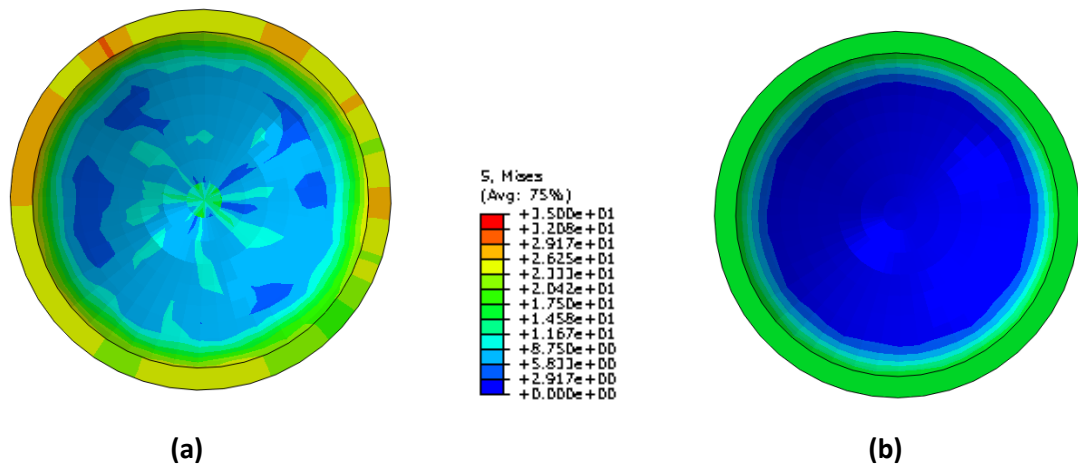


Figure 4.21: Von Mises stresses in cup with **(a)** no hourglass control and **(b)** enhanced hourglass control following impactation with the poles aligned and uniform cup support

4.4.4 Validation of Model using the Coefficient of Friction

Modelling of the behaviour at the cup-cavity interface has varied widely between the different studies, with the coefficient of friction between the two surfaces ranging between 0.3 and 1.2 [Dimaano et al., 2010; Grant et al., 2007; Isaac et al., 2005; Hogg et al., 2009, Hogg et al., 2010; Yew et al., 2006; Spears et al., 1999]. An appropriate coefficient of friction at this interface is required to allow relevant impact momentums to seat the cups to be defined.

Having established an impactation model in the current work, it was validated by identifying an appropriate coefficient of friction based on the results of the experimental data. Initial models used an impact velocity of 1 ms^{-1} and an interference of 1 mm. The coefficient of friction at the cup-cavity interface was varied between 0.3 and 1.0. These values were independently defined in the model and the impactation process was simulated until subsequent impacts reduced the polar gap by less than 10 μm . The number of impacts that were required to seat the cups and the corresponding remaining polar gaps for a range of friction coefficients were modelled until the result obtained experimentally was matched.

Having derived a suitable coefficient of friction, further simulations were performed using all the remaining parameters and impact methods tested experimentally (Table 2). This included polar impactation (Figure 4.18b) as well as using an impactor on the cup rim, modelled with both no friction between the impactor and cup, and also by locking

the rigid cap to the cup rim. The results from each simulation were compared with those obtained from the comparable experiment to validate the defined coefficient of friction under all test conditions.

4.4.5 Results

In order to optimise the FE model to represent the observed experimental behaviour, the coefficient of friction used in the FE model was adjusted between the cup and the foam. An optimised coefficient of friction was established when the difference in the polar gap remaining at the end of impactation, between the experimental and FE model was minimised, using rim impactation, an interference of 1 mm and an impact velocity of 1 ms^{-1} . The FE and experimental models were optimised using the polar gap as this parameter was recorded after each impact experimentally; it was only possible to record the deformation of the component after the impactation process had been completed. The coefficient of friction was varied between 0.3 and 1.0 as has been previously reported in the literature. A value of 0.8 in the FE model produced similar values for the polar gap after each impact as those observed experimentally, Figure 4.22.

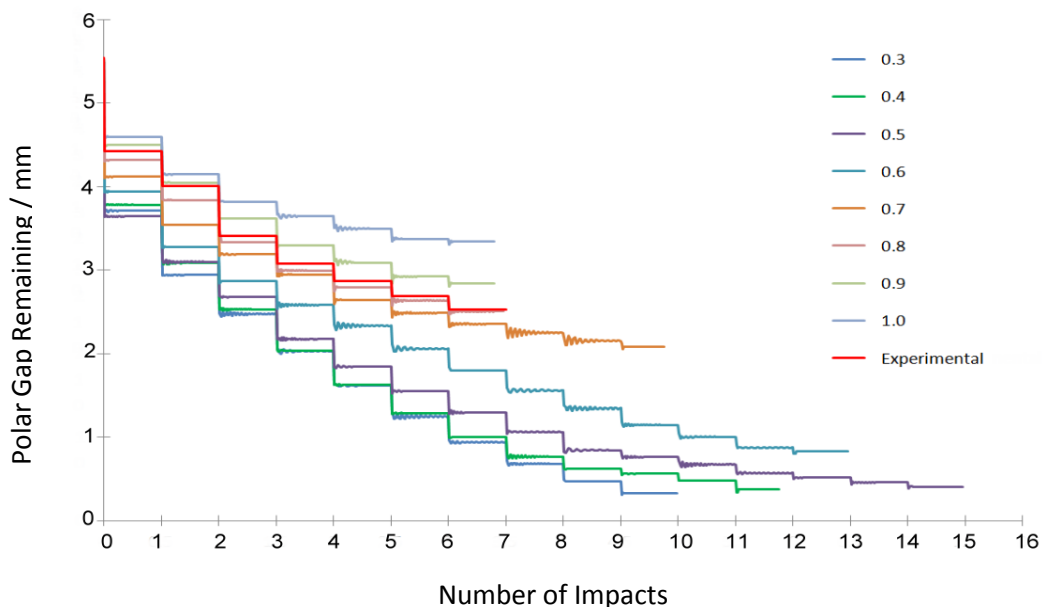


Figure 4.22: Comparison of experimental polar gap remaining with that observed in the FE model with varying coefficients of friction under free rim conditions

The friction value of 0.8 was identified as producing the smallest difference between the polar gap remaining experimentally and the polar gap observed when the

coefficient of friction was varied between 0.3 and 1.0, Figure 4.23a. The value of the coefficient of friction was refined by calculating the difference in the polar gap between the experimental results and when the value was varied in the FE model between 0.8 and 0.9. It was found that a coefficient of friction of 0.835 in the FE model produced polar gaps that most closely matched those observed experimentally (Figure 4.23b). The differences between the experimental and FE polar gaps with this value were consistently the smallest and produced results which predicted a polar gap remaining to be within 20 μm of those recorded experimentally after the 7th impact, after which further impacts had no effect on cup position.

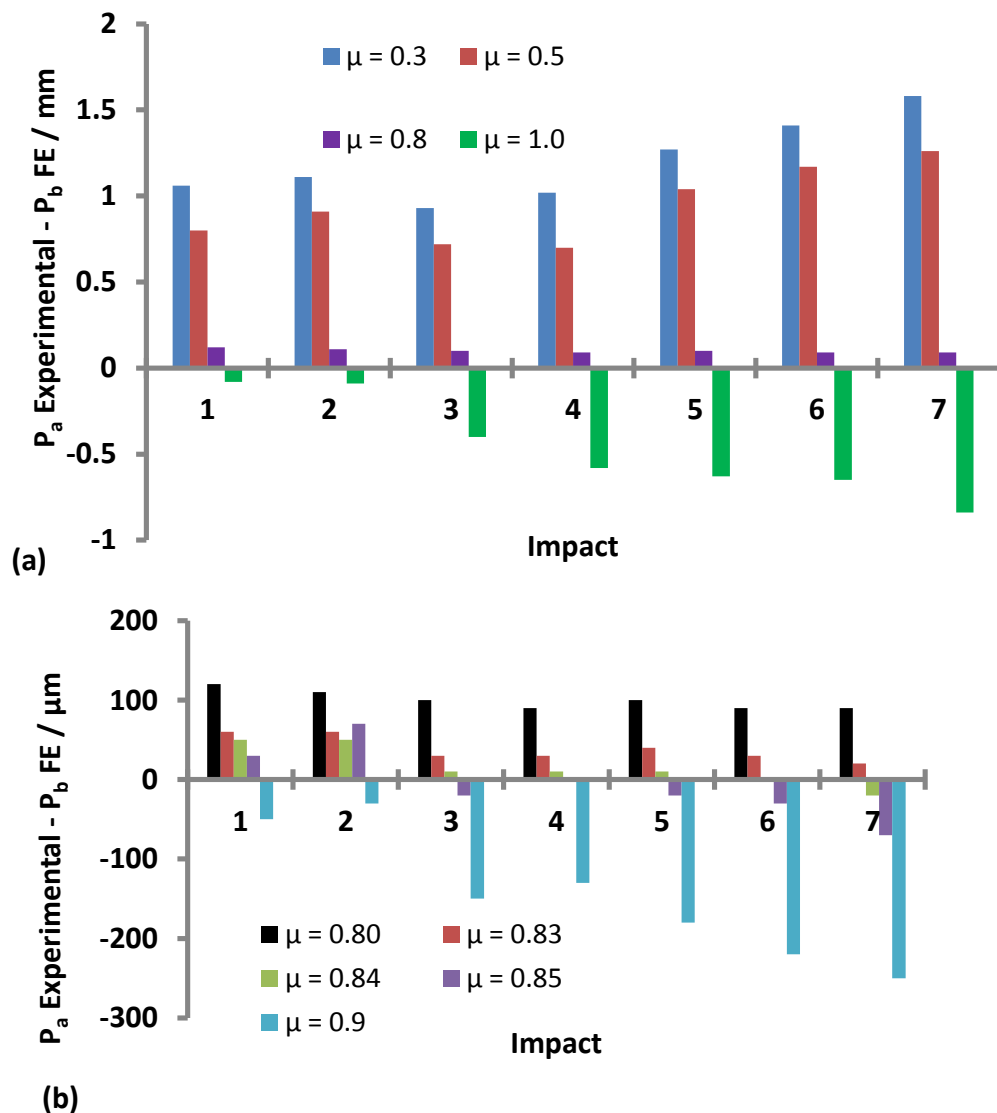


Figure 4.23: Difference in the polar gap remaining between the experimental and FE model ($P_a - P_b$) using coefficients of friction between (a) 0.3 and 0.1 and (b) 0.8 and 0.9, for each successive impact, using an interference of 1 mm and impact velocity of 1 ms^{-1}

Using the established coefficient of friction of 0.835 from one set of FE and experimental variables, comparisons were made for the remaining tests, Figure 4.24.

The polar gap remaining following each impact for each of the tests performed showed a very good agreement between experimental and modelled data. Although the determination of an optimised coefficient of friction was derived from a single test parameter, its validity was confirmed through the comparisons shown in Figure 4.24, with a significant correlation. A high level of agreement was also found to exist between the final deformation, following the last impact, between the experimental and FE data, with a difference of less than 2 μm (Figure 4.25).

The results from this optimisation of the coefficient of friction show that the initial value of 0.3 defined between cup and foam in the 2D model as suggested in previous studies [Hogg et al., 2009; Hogg et al., 2010; Yew et al., 2006; Spears et al., 1999] may have been too low. The value suggested in the current study is similar to the range of values suggested by Dimaano et al. [2010] when describing the interaction between porous outer surfaces and bone, but much higher than other authors have suggested and utilised [Hogg et al., 2009; Hogg et al., 2010; Yew et al., 2006; Spears et al., 1999]. The porous coating used on the outer surface of the cups tested is made from Duofix, which is composed of a thin layer (30 μm) of hydroxyapatite over a 200 μm thick layer of a porous coating with the commercial name Porocoat [Isaac et al., 2005]. This surface has previously been reported to have a coefficient of friction of 0.82 against bone [Grant et al., 2007], determined by creating contact using a normal force between 30 mm diameter discs of the porous surface and rectangular human trabecular bone cube samples.

The current model did not simulate compaction of the foam at the interface; for the deformations generated in this experiment, the local compaction of the foam did not appear to greatly alter the performance as shown by the high correlation for all data at each stage of the impaction process.

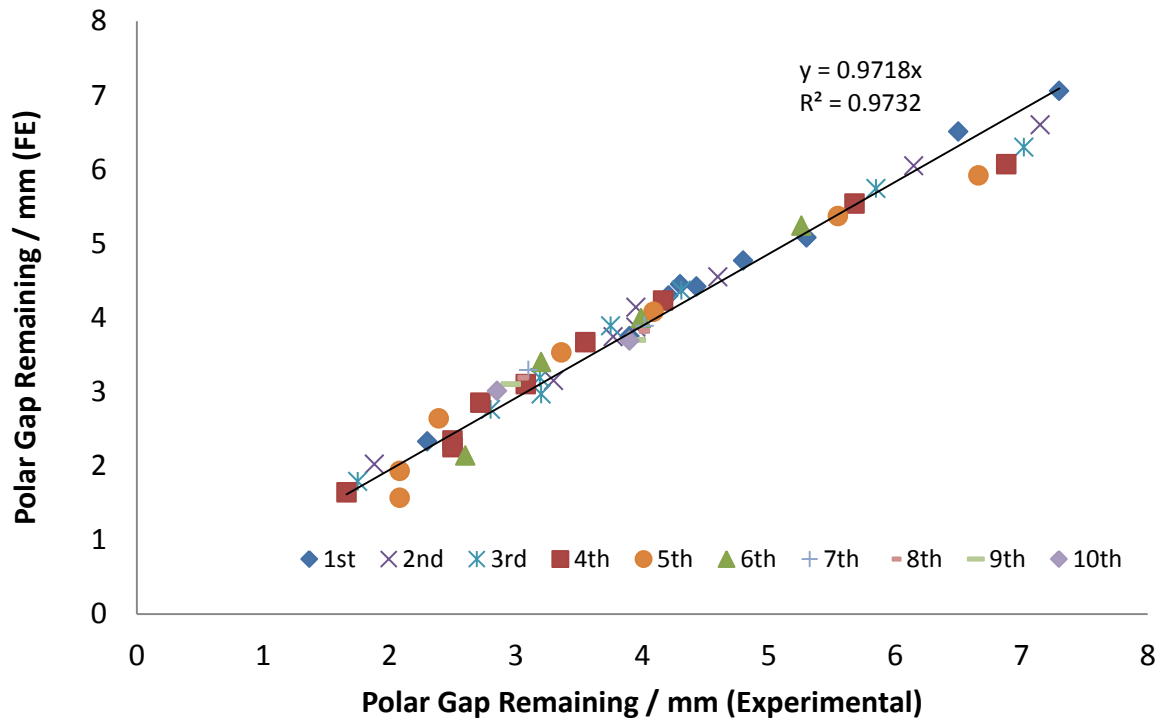


Figure 4.24: The relationship between the mean polar gap remaining after each impact (1 – 10), as measured experimentally compared with that observed in the FE model, under all test parameters.

The FE model was optimised through experimental tests simulating the multiple impacts required to insert a cup into a foam cavity representing the reamed acetabulum. The foam has a Young’s Modulus of 553 MPa, a value in the mid-range found for cancellous (80 to 1200 MPa) [Wirtz et al., 2000]. It is likely therefore that cup deformations observed clinically in patients with lower bone density and stiffness, will be lower than those reported in the current study. The bone quality is an important consideration for a surgeon to ensure the longevity of the implanted component. Higher interference fits may be required in older patients with lower quality bone stock, to ensure long-term stability. Conversely a lower interference may be desirable in younger patients with stiffer acetabular cavities to ensure that the cups can be fully seated and also to minimise cup deformations.

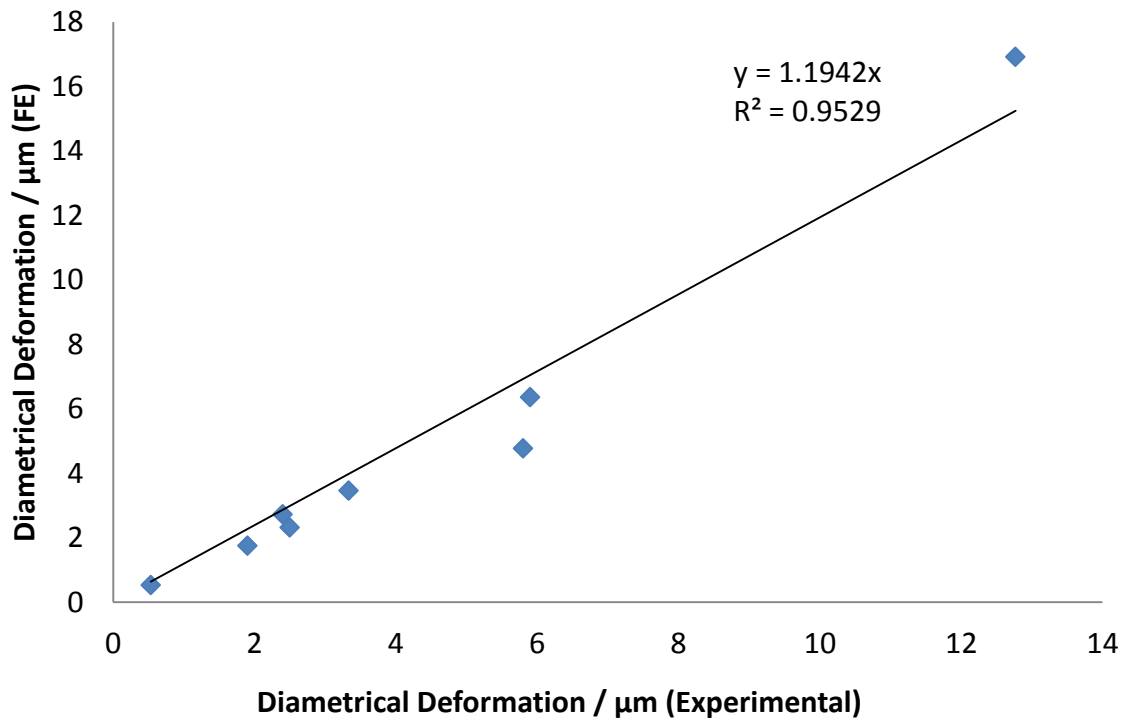


Figure 4.25: Final diametrical deformations after the final impact for each test parameter, measured experimentally compared with that estimated in the FE model

The polyurethane foam does not exhibit the same viscoelastic properties as has been reported for bone and the effect of the time dependent behaviour of bone was not considered in the current study. It is expected that the cup deformations observed immediately following insertion would reduce over time; it has been reported that stress relaxation and creep behaviour in cancellous bone reaches a steady state after approximately 24 hours [Deligianni et al., 1994; Pawlikowski et al., 2008]. This is likely to be the period of patient recovery post operatively, over which period it would be unlikely that the patient would walk many steps [Rao et al., 1998]. It was important therefore that the influence of the time dependency of bone was considered in later models which involved simulating the structure of the pelvis.

4.5 Influence of Cup Support and Misalignment on Deformation

It has been suggested [Ong et al., 2009] that the orientation of the cup could influence the stress distribution within it, and the position of the cup may influence the deformation observed [Markel et al., 2010], however previous studies have not demonstrated these effects and it remains unclear how the precise location of the cup in variable support conditions may alter the cup's behaviour. A previous cadaveric

study [Fritsche et al., 2008] observed that orientating the cup at 15° to the cavity during insertion had no effect on cup deformation when compared to aligning the poles of the cup and cavity. It has been suggested that inexperienced surgeons may align the acetabular cup with the acetabulum rim without fully considering the safe zone [Birbeck et al., 2010]; however the effects of misaligning the cup, relative to the bony support, in these situations has not been previously reported.

The variable support in the surrounding acetabulum may influence the deformation in the cup following impaction as well as the ease of cup insertion [Ong et al., 2009; Markel et al., 2010; Jin et al., 2006; Yew et al., 2006]. In addition to the accuracy of the reaming of the acetabulum and subsequent cup placement, cup support will be influenced by the location, volume and density of the cortical and cancellous bone [Ong et al., 2009; Markel et al., 2010]. Jin et al. [2006] described how the pinching on the cup between the ilial and ischeal regions in the pelvis, which are typically positioned at approximately 150° to each other [Krebs et al., 2009], cause diametrical deformation in the cups. This effect has been simplified previously in both experimental and finite element studies [Jin et al., 2006; Yew et al., 2006; Ong et al., 2009] by simulating the pinching effect by using foam models representing the dominant regions in the acetabular bone, and removing areas of the foam on opposite sides of the reamed cavity, generating cup deformations of up to 100 µm. This approach has been described as *the worst-case scenario* in terms of the resulting deformation, however clinically the extent of pinching would be governed by the differences in location and stiffness observed between the ischeal and ilial columns and the remaining regions in the acetabulum [Widmer et al., 2002]. This will vary between patients, depending on a range of factors including age, gender, size and general health [Brinkmann et al., 1981; Tauge, 1989].

In the current work, the support provided to the cup by the underlying foam cavity was varied and the orientation of the component with respect to the cavity was varied. The influence of these two parameters on the deformation of the component following insertion was investigated.

4.5.1 Methods

The foam cavity was partitioned into three segments (Figure 4.26a) and initially all the segments were defined with the same properties, Table 4.4, thereby providing uniform support to the cup. A coefficient of friction of 0.835 was defined and an impact velocity to insert the cup into the cavity was set to 4.5ms^{-1} in order to generate a peak contact force between the impactor and cap of approximately 18 kN, similar to those observed in a cadaveric study [West et al., 2008]. The effect of changing the angle of orientation between the cup and cavity, assuming uniform support, on the final cup deformation was investigated for angles between 0 and 15° using an interference of 1 mm. In the subsequent simulations the properties in the central segment for the Young's modulus and density were maintained at 0.553 GPa and 480kgm^{-3} respectively whilst in the outer segments these were reduced to 75%, 50% and 25% (0.75E, 0.5E and 0.25E) to simulate the pinching effect resulting from the greater bone density and stiffness in the direction of the ischeal and ilial regions. These simulations were repeated with the regions of increased stiffness positioned 150° to each other (Figure 4.26b) over a 30 mm band, simulating the clinical situation more closely; the pubic bone, which was shown to be less significant to cup deformation, was disregarded. Varying the position of the cup relative to the pinch points of the ischeal and ilial regions, located at 150° to each other, simulated changes in the version of the cup. The simulations were repeated with a maximum degree of pinching (0.25E) and the cup rotated between 0 and 15° in the plane of abduction.

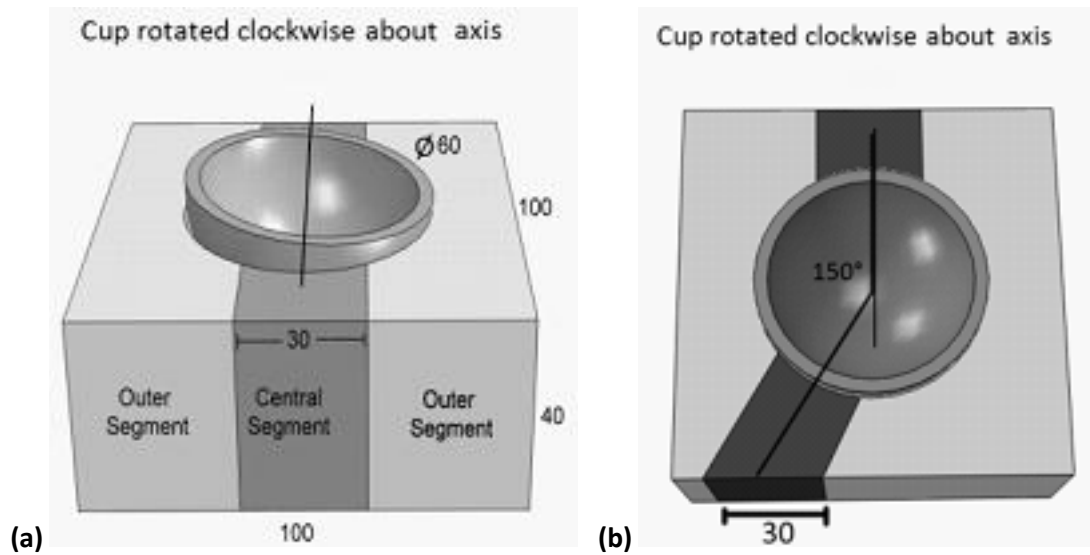


Figure 4.26: Foam cavity partitioned into three segments to model non-uniform support and orientation of cup with respect to cavity varied during impaction, with **(a)** opposing pinch points and **(b)** pinch points at 150° to each other

The influence of changing both the cup support and its orientation with respect to the cavity, on the deformation was evaluated by determining the maximum reduction in diameter (Figure 4.27).

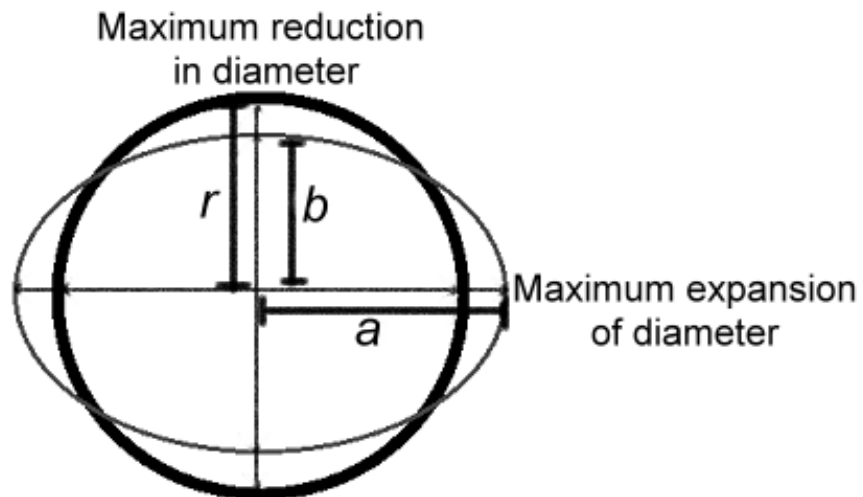


Figure 4.27: Maximum reduction and expansion of diameter recorded after a change in shape of the cup

The maximum reduction in diameter, $\Delta\phi$, was defined as being the difference between the diameter ($2r$) of the un-deformed cup and the minimum dimension ($2b$) of the deformed cup:

$$\text{Maximum Reduction in Diameter, } \Delta\phi = 2(r - b) \quad (4.3)$$

The eccentricity (e) of the ellipse was established as:

$$e = \sqrt{1 - \left(\frac{b}{a}\right)^2} \quad (4.4)$$

4.5.2 Results

When the FE model was simulated with the cup positioned with its pole aligned with the cavity providing uniform support, uniform diametrical deformations occurred and a uniform distribution of stresses within the cup was observed. Changing the orientation of the cup, with respect to the cavity, from a tilt of 0 to 15°, resulted in an ovality in the cup and a non-uniform distribution of stresses

It was observed experimentally by Fritsche et al. [2008] that there was little difference in deformation when the cup was aligned at 15° compared to when the cup was uniformly aligned with the cavity. In the current study it was also observed that the maximum deformations at 0° and 15° were similar however the deformed shape of the component was different at the two orientations, with an ovality present at 15°.

Between 7 and 9 impacts at 4.5 ms⁻¹ were possible before the change in polar gap remaining between subsequent impacts was less than 10 μm. Table 4.5 summarises the cup behaviour that was observed as the orientation of the component with respect to the cavity was varied with uniform support.

Table 4.5: Cup deformation and insertion behaviour with varying cup orientation and uniform cup support

Cup orientation with respect to cavity / °	Maximum Expansion of Diameter/ μm	Maximum Reduction in Diameter/ μm	Eccentricity (e) of the ellipse	Polar Gap Remaining / mm
0	-11	11	0	0.69
1	4	13	0.024	0.70
2	8	15	0.028	0.70
3	11	22	0.033	0.71
4	16	26	0.037	0.72
5	19	33	0.042	0.72
6	17	31	0.040	0.72
10	5	13	0.024	0.74
15	5	12	0.024	0.74

It was found that increasing the orientation of the cup with respect to the cavity from 0 to 5° resulted in the cup deforming into an increasingly oval shape, with peak deformations and the greatest change in shape being observed at 5°. Beyond this deformation, the diametrical deformations decreased and at 10° were closer to those observed when the poles of the cup and cavity were aligned.

Decreasing the stiffness of the outer segments of the foam cavity also resulted in the cup deforming into an oval shape due to the pinching effect created by the stiffer central segment. In all cases the final polar gap was between 0.66 and 0.74 mm and was found to decrease slightly when the stiffness of the outer segments was decreased and the poles of the cup and cavity were aligned.

Figure 4.28 shows the cup deformation ratios obtained by varying the orientation and support of the cup ($\Delta\phi_{EG}$) relative to the uniformly supported and aligned cup ($\Delta\phi_o$). It can be seen that tilting the cup, with uniform support, by as little as 1° resulted in a notable change in shape. It is of note that whilst increasing the degree of pinching results in greater cup deformations, the relationship between varying the orientation and deformation (with peaks at 5°) stays very similar for all levels of support. When the pinch points are altered to an orientation of 150°, this relationship is maintained however deformations were slightly lower. Table 4.6 summaries the maximum deformations that were observed with varying cup support with the cup orientated at

5° with respect to the cavity. The maximum reduction in diameter ranged from 33 to 82 μm, close in magnitude to typical clearances between the cup and femoral head.

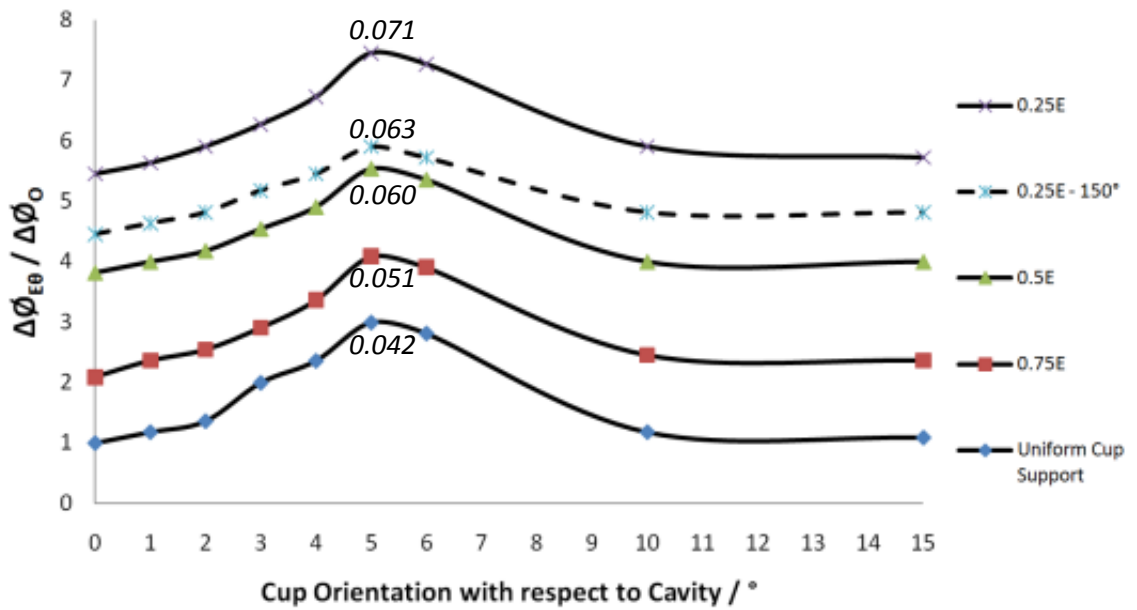


Figure 4.28: The ratio of cup deformation with variable cup support ($\Delta\phi_{E\theta}$) compared to the uniformly supported and aligned cup ($\Delta\phi_0$) as a function of cup orientation. The greatest eccentricity of the deformed cup with varying support is displayed in italics.

Table 4.6: The cup behaviour as a function of cup support with the cup orientated at 5° with respect to the cavity, resulting in the greatest deformations

Stiffness of Outer Foam Segments	Maximum Expansion of Diameter/ μm	Maximum Reduction in Diameter/ μm	Eccentricity (e) of the ellipse	Polar Gap Remaining / mm
Uniform cup support	19	33	0.042	0.72
0.75 of central segment	25	32	0.043	0.70
0.5 of central segment	49	61	0.060	0.69
0.25 of central segment	71	82	0.071	0.67

4.5.3 Discussion

Whilst there have been many studies that have reported on the consequences of poor acetabular cup alignment in terms of the *safe zone* [De Haan et al., 2008; Hart et al., 2009; Angadji et al., 2009], the effect of the cup's position relative to the underlying bony support, has not been widely investigated. The study in the current chapter developed an FE model to determine the effect of varying the support on an uncemented cup along with altering the angle of cup orientation with respect to the cavity, on its deformation. It was found that although these two factors alone did not result in significant deformations, the combination of non-uniform support and cup misalignment by 5° led to high deformations of up to 82 µm when compared to the clearances between the femoral head and cup.

In the experimental impaction process a considerable polar gap remained at the end of each experiment when using a wide range of parameters. Sandborn et al. [1988] estimated that the maximum polar gap for bone in-growth to occur is 2 mm but that bone in-growth is more rapid below 0.5 mm. It has been reported previously [Morlock et al 2008] that prosthesis failure due to acetabular problems was in part due to poor cup anchorage, stemming from difficulties in fully seating cups; this was supported by the experimental work. The impact velocity was increased to 4.5 ms⁻¹ during the impaction investigations of cup orientation and support; as expected this resulted in 'better' seating of the components with polar gaps less than 0.8 mm.

In a clinical situation the velocity and precise point of impact would be likely to vary due to the skill and technique of the surgeon [Bordini et al., 2007]. Large interferences would require high impact momentums to fully seat the cups, leading to an increased risk of the surgeon losing accuracy with the mallet [Campbell et al., 2006], and potentially causing damage to surrounding bone. Interferences in the region of 0.25 to 1 mm might be preferable to allow the cup to be safely inserted, however poor initial cup stability, particularly for osteoporotic bone [Springer et al., 2008], may be problematic and requires further investigation.

The FE model was validated when positioning the cup such that its pole was aligned with that of the cavity, providing uniform support; this resulted in uniform diametrical deformations. However introducing an angle between the two poles before insertion resulted in the cup deforming into an oval shape. Figure 4.28 shows that misaligning the cup, with uniform support, by as little as 1° resulted in a notable change in shape

and that the deformations and out of roundness of the cup was greatest at 5°. Increasing the angle of the cup to 15° resulted in a smaller change in shape with the maximum reduction in diameter closer to that observed when the cup was misaligned by 1°; this is in agreement with the experimental findings by Fritsche et al. [2008].

The reason for the differences in deformation may be explained when considering the variations in cup support at the rim as the component is tilted, Figure 4.29. The polar gap increases slightly as the tilt is increased and the percentage area of the cup's outer surface in contact with the foam cavity decreases from 68% when the poles are aligned to 61% when the component is positioned at 15° to the cavity. When the cup is uniformly supported and aligned with the cavity, there is no pinching of the component therefore deformations are comparatively low. When the cup is tilted at 15° the rim is no longer uniformly supported, resulting in a pinching effect deforming the cup into an oval shape. At 15° foam contact on the exposed half of the cup occurs in an area notably below the rim; it has been reported that the greatest deformations occur when there is contact in the region of the cup rim [Jin et al., 2006]. As such the observed deformations are low, similar to those that occur when the cup is aligned. It is of note however that whilst the deformations at 0° and 15° are similar, they occur in different manners; pinching of the cup at 15° results in it deforming into an ellipse with a maximum reduction in diameter that is similar to the uniform deformation that occurs when the poles of the cup and cavity are aligned. At a tilt of 5° the cup is in a position in which it is non-uniformly supported, allowing pinching to occur but is at an orientation where foam contact is much closer to the exposed half of the components rim, meaning that deformations are maximised.

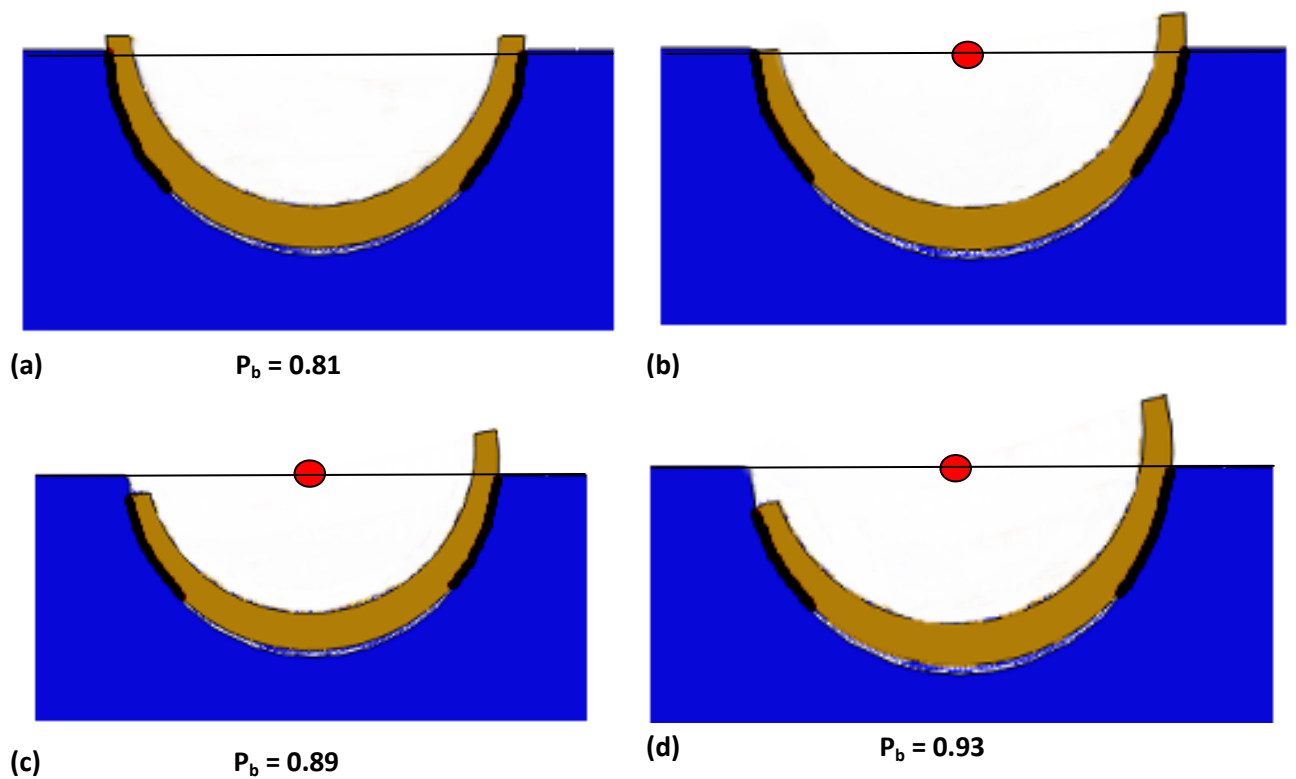


Figure 4.29: Cross-section showing the position of the seated component at 0° (a) 5° (b) 10° (c) and 15° (d) relative to the cavity after impaction. Pinching of the cup in the simulations occurred in a direction perpendicular to the red mark when a tilt was introduced. The contact area between the two surfaces in each model is highlighted.

The maximum deformations observed by varying the position of the cup alone were considerably smaller than clearances in the region of 80-120 μm for typical acetabular cups. Introducing non-uniform support to the cup, with its pole aligned with that of the cavity, resulted in a pinch effect which was heightened as the difference in stiffness between the outer and central segments of the cavity was increased. This resulted in a notably greater change to ovality by up to 2.2 times larger than that observed when misaligning the cup to 5° with uniform support. Figure 4.28 shows that the eccentricity of the deformed ellipse increased as the cup was misaligned from 0 to 5° with all levels of support and that most significant cup deformations were found to occur when misalignment of the cup was coupled with increasing the simulated pinching effect of the iliac and ischeal columns. These results highlighted that variations in the cup support are very significant to deformation and whilst it is a factor that cannot be controlled by a surgeon, it could be considered during operative procedures, for example selecting a component with a greater stiffness or reducing the interference size if appropriate.

Conversely a surgeon can control the angle of the cup in the acetabulum, mindful that high cup deformations can occur when misalignment of the cup, specifically at 5° to the cavity, is coupled with significant non-uniform support due to pinching between the iliac and ischeal columns. The greatest deformations were in the region of typical clearances.

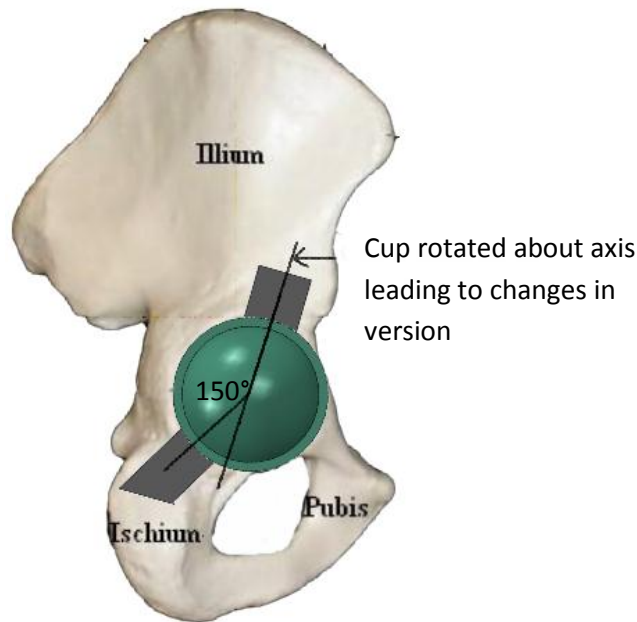


Figure 4.30: Schematic of the right hemi-pelvis, indicating the position of the pinch points more likely to be observed anatomically [Adapted from Tortora et al., 2006]. Rotations of the cup about the axis indicated simulated changes in the version of the cup

It was shown in Figure 4.28 that when the pinch points were positioned at 150° to each other, as is more likely to be the case anatomically [Krebs et al., 2009], the maximum reduction in diameter was lower. It has been shown however that higher interferences result in even greater deformations [Hothi et al., 2011], therefore the risk of articulation problems occurring could increase if greater interferences or thinner cup designs are used. Figure 4.30 shows that when the position of the pinch points in the model were at 150° to each other in relation to the right pelvis, the angle of the cup with respect to the cavity was varied such that it was misaligned in a similar axis to version, creating changes in the version angle. Misaligning the cup in this anatomical orientation resulted in the greatest deformations when coupled with the pinching of the stiffer ischeal and iliac columns, rather than varying the orientation of the abduction angle, suggesting that cup deformation may be more sensitive to its position in version than abduction.

The optimum cup angle stated in the literature is related to an inclination and version that minimises wear and maximises the range of motion [Angadji., et al 2009], however it is important that in addition to this, a surgeon is aware of the consequences of cup position in the cavity itself on diametrical deformation, and in particular that this may be increased in patients where the pinching effect in the acetabulum is more prominent.

4.6 Influence of Impaction Method on Deformation

The method of impaction was shown in the previous chapter to influence the seating of the component in the 2D insertion model. In the current 3D model, three different impaction methods were simulated.

4.6.1 Methods

The impaction methods were as summarised below (Figure 4.31):

Test A impact on rim using frictionless rigid cap and impactor perpendicular to cup

Test B impact on inner polar surface with impactor perpendicular to cup

Test C impact on inner polar surface with impactor perpendicular to the cavity

A single interference of 1 mm was maintained with uniform cup support and the effect of changing the angle of orientation between the cup and cavity and changing the impaction method on the final cup deformation was investigated.

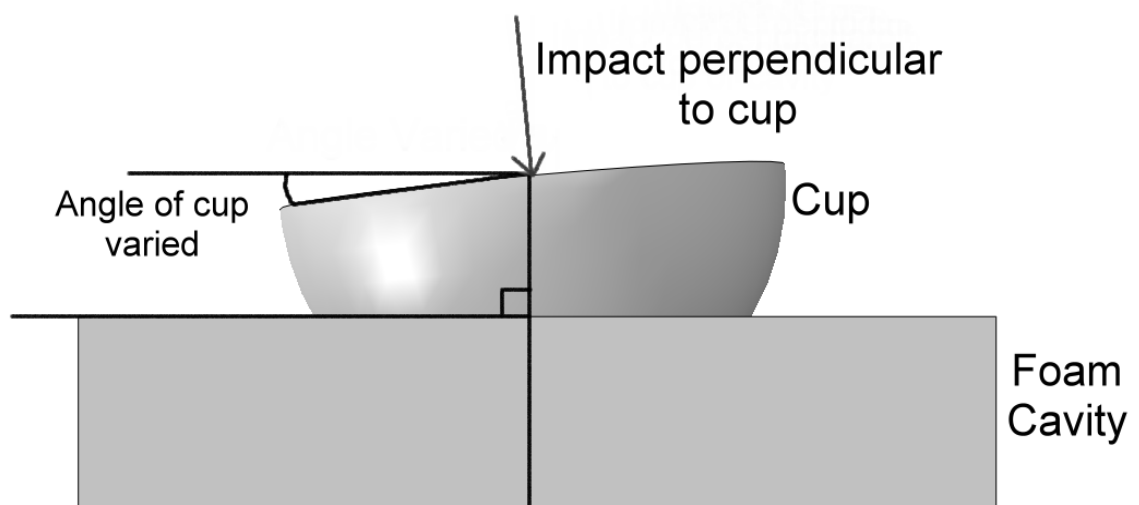


Figure 4.31: Orientation of cup with respect to cavity varied during impaction

4.6.2 Results

Figure 4.32 shows the maximum cup compressions that were observed at the different angles using the three different impaction methods from tests A, B and C. The angle of the cup with respect to the cavity remained largely unchanged before and after impaction when the impactor was position perpendicular to the cup for both rim and polar impaction. However aligning the impactor perpendicular to the cavity when impacting on the cups inner polar surface resulted in the cup rotating by up to an additional 2° after insertion. This resulted in greater deformations than polar impaction with the impactor perpendicular to the cup, however rim impaction resulted in the greatest change to ovality after insertion, although the effects were not substantial.

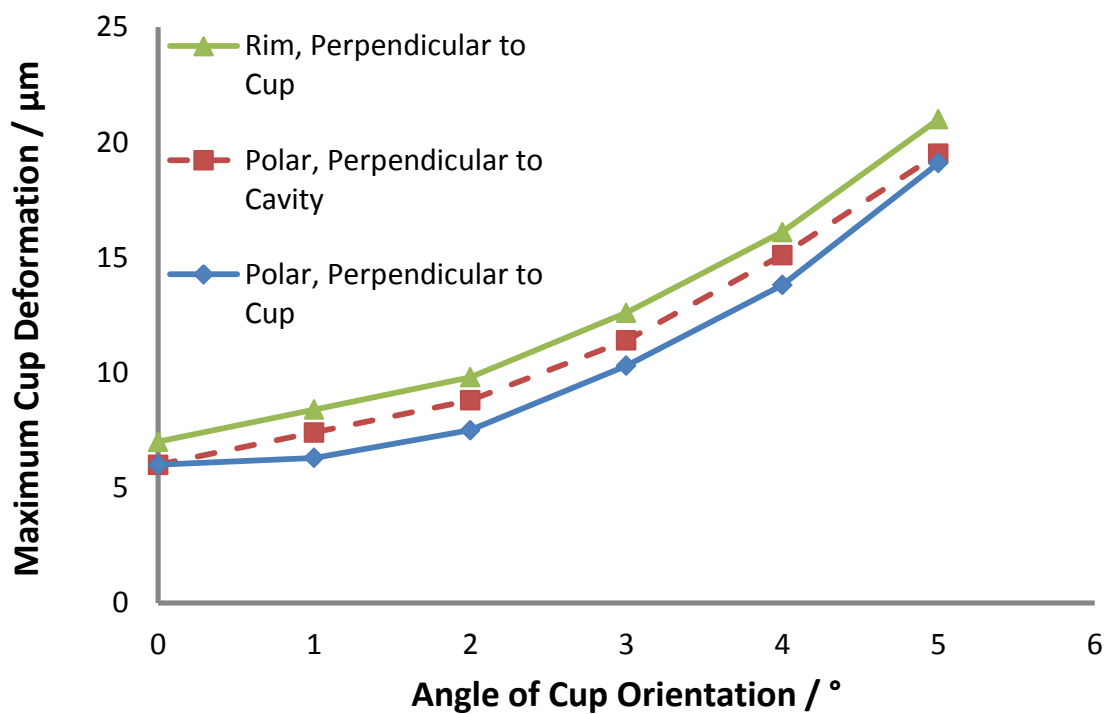


Figure 4.32: Maximum cup deformations observed with increasing cup orientation

4.7 Influence of the Geometry of the Cup on Deformation

It has been demonstrated [Yew et al., 2006] that independently reducing the thickness of an acetabular cup or increasing its diameter will result in it deforming by a greater amount upon insertion into the acetabulum. The dimensions of a number of commercially available acetabular cup designs have previously been reported [Springer et al., 2012]. It was shown that the diameter and wall thickness of a cup design was

important to influencing the stiffness of the component and therefore its deformation following rim loading. The consequences of simultaneously altering a range of parameters relating to cup geometry however have not been widely reported. The effect of varying the cup thickness at the pole and rim, the cup diameter and depth on deformation requires better understanding in order to fully optimise the design of metal cups. A Taguchi Design of Experiment (DOE) was therefore used to investigate the effect of varying the dimensions of the cup on the deformation of the component following impaction

4.7.1 Taguchi Design of Experiment to investigate the influence of cup geometry

The typical processes involved in a Taguchi DOE investigation are detailed in Figure 4.33.

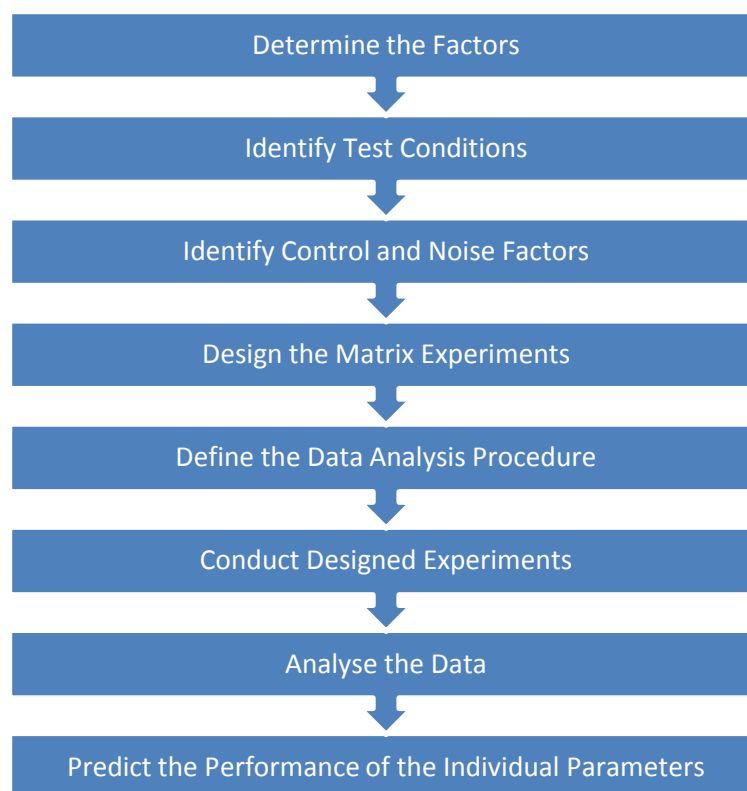


Figure 4.33: Development of a Taguchi Design of Experiment [Roy, 2001]

In the current study, the factors to be investigated were the depth, diameter and thickness at the pole and rim. The test conditions were such that the diametrical interference was maintained at 1 mm and initially the cup was uniformly supported

and aligned. The 4 control factors were varied between 4 levels of increasing size (Table 4.7).

The Taguchi Orthogonal Array system (Table 4.8) was used to identify 16 combinations of the parameters (Table 4.9), out of a total of 4^4 , that could be simulated, thus significantly reducing the time required for modelling and analysis. The resulting cup deformations from each of the 16 simulations were used to calculate the signal-to-noise ratio (S/N ratio) for each of the 4 control parameters as:

$$S/N \text{ Ratio} = 10 \text{ Log}_{10} [\text{Mean of sum of squares of \{measured deformation - ideal deformation\}}] \quad (4.5)$$

Table 4.7: Cup parameters varied in Taguchi DOE

Parameter	Level			
	1	2	3	4
Thickness at Rim (Tr) / mm	3	5	7	9
Thickness at Pole (Tp) / mm	3	5	7	9
Depth (d) / mm	21	23	25	27
Cup Diameter (ϕ) / mm	40	50	60	70

Table 4.8: Taguchi Orthogonal Array Selector, highlighting that 16 simulations were required in this instance

		Number of Parameters				
		2	3	4	5	6
Number Of Levels	2	L4	L4	L8	L8	L8
	3	L9	L9	L9	L18	L18
	4	L16	L16	L16	L16	L32
	5	L25	L25	L25	L25	L25

In the analysis of the data, the ideal deformation was defined as being 0 μm and the S/N ratio was defined such that the higher its value for each parameter, the greater the influence that parameter has on cup deformation.

In subsequent simulations the cup geometry, cup support and orientation were all varied such that the greatest and least deformation scenarios were simulated.

Table 4.9: Taguchi Orthogonal Array with 4 parameters and 4 levels

Experiment	Thickness at Rim (Tr) / mm	Thickness at Pole (Tp) / mm	Depth (d) / mm	Cup Diameter (ϕ) / mm
1	3	3	21	40
2	3	5	23	50
3	3	7	25	60
4	3	9	27	70
5	5	3	23	70
6	5	5	21	60
7	5	7	27	50
8	5	9	25	40
9	7	3	25	50
10	7	5	27	40
11	7	7	21	70
12	7	9	23	60
13	9	3	27	60
14	9	5	25	70
15	9	7	23	40
16	9	9	21	50

4.7.2 Results

Table 4.10 presents the cup deformations that were observed as the geometry of the component was varied. The dimensions of the cup clearly have a considerable influence on the stiffness of the cup, with the deformations varying between 11 and 43 μm .

Table 4.10: The component deformations observed with varying dimensions

Experiment	Control Parameters					SN Values
	Thickness at Rim (Tr) / mm	Thickness at Pole (Tp) / mm	Depth (d) / mm	Cup Diameter (ϕ) / mm	Maximum reduction in diameter / μm	
1	3	3	21	40	31	35.71
2	3	5	23	50	26	34.96
3	3	7	25	60	16	33.26
4	3	9	27	70	10	31.83
5	5	3	23	70	43	39.37
6	5	5	21	60	29	35.42
7	5	7	27	50	20	33.98
8	5	9	25	40	12	32.46
9	7	3	25	50	28	35.27
10	7	5	27	40	22	34.32
11	7	7	21	70	11	31.85
12	7	9	23	60	12	32.46
13	9	3	27	60	33	35.99
14	9	5	25	70	35	36.26
15	9	7	23	40	17	33.44
16	9	9	21	50	15	33.06

The depth of the cup and its rim thickness were the least influential on observed deformation, as indicated by the comparatively lower values for the Taguchi Signal/Noise (S/N) ratio obtained (Table 4.11), and variations of these parameters to accommodate the articulation of the femoral head, would not be expected to significantly affect the diametrical deformation of the cup. It was also established that the maximum pinching continued to occur when the cup was orientated at 5° to the cavity, regardless of the component geometry modelled.

Table 4.11: The Signal / Noise (S/N) ratio obtained for the different cup parameters using the Taguchi DOE

	Parameter			
	Thickness at Pole	Cup Diameter	Depth	Thickness at Rim
S/N Ratio	3.05	2.01	0.18	0.04

The highest deformation scenario was simulated whereby the cup depth and diameter were maximised and the thickness at the pole and rim minimised, and the cup misaligned by 5° and impacted under the greatest pinching support at 180°. This resulted in a maximum deformation 19 times greater than when the cup was stiffened by minimising the diameter and depth and maximising the thickness at the pole and rim, whilst being uniformly supported and aligned (*best case scenario*).

4.7.3 Discussion

In the current study, the DOE demonstrated that varying the geometry of the component can significantly alter its deformation following insertion (Table 4.11) and established that it is specifically the wall thickness in the polar region of the cup, in addition to changing its overall diameter, which most significantly influences the extent of the diametrical deformation observed. It has been reported that low clearances are beneficial to improved joint tribology and minimising wear [Harper, 2008; Isaac, 2006]. Furthermore, it has been shown [Dowson et al., 2004] that there is a strong correlation under ideal conditions between reducing the size of the clearance and lower wear rates. Consequently typical minimum clearances between the cup and the femoral head are low, in the region of 80 to 120 µm. The results of the current study suggest that when large diameter cups are used they will likely deform by a greater amount, significantly reducing localised clearances. This could create problems such as reduced fluid-film lubrication, increased wear and even locking of the joint. The DOE suggests that to minimise the deformation of larger diameter cups, the component should be stiffened by increasing its polar thickness. It is interesting to note therefore the results of the study by Springer et al. [2012] which showed that the majority of the manufacturers of different cups did not appear to fully consider the influence of increasing their cup diameter on the stiffness of the component. Indeed 3 out of the 4 cup designs tested [Springer et al., 2012] became less stiff as their diameter increased. As a particular example, the diameter of the Biomet Magnum cup varies between 44

and 66 mm, yet its thickness at the pole at these two diameters is almost the same at 5.80 and 5.83 mm respectively. This reflects clearly on the stiffness of the component, which was reported [Springer et al., 2012] as being 20,000 N/mm for the 44 mm cup and considerably less for the 64 mm design at 5,000 N/mm. Consequently, the deformations that were reported for the smaller and larger diameter cup with the same applied force of 1800 N at the rim were approximately 80 and 350 μm . This agrees with the results of the current study, suggesting that these larger commercially available designs may deform excessively, particularly when coupled with other contributing factors such as high interferences and stiffer bone stock in younger patients. Increasing the thickness of the wall at the pole would reduce the amount of deformation observed, therefore reducing the risk of adverse problems. The importance of wall thickness is further highlighted when observing that a 60 mm Stryker Cormet design with a wall thickness of 7.68 mm at the pole has a substantially higher stiffness of 35,000 N/mm than the 60 mm cups manufactured by Smith & Nephew and Biomet with polar wall thicknesses of 5.58 and 5.86 mm respectively, each with an approximate stiffness of 10,000 N/mm [Springer et al., 2012].

It has been reported [Dowson et al., 2004] that the largest head with the lowest clearance should be used to ensure optimal MoM tribology. This raises the issue of a conflict that exists in the design stage of a hip replacement, where the requirement of maximising the head size must be balanced with the need to ensure that the wall thickness of the cup is not reduced by too much, to accommodate the larger head, that high deformations occur. Indeed, some manufacturers do choose to 'thin' the cup design to allow for a larger head to be properly seated [Springer et al., 2012], which inevitably will result in greater deformations.

The large difference in deformation observed between the *best* and *worst case scenarios* highlights the sensitivities to variations of these parameters which should be considered during both the design and use of this component.

4.8 Conclusions

This study has developed 3D explicit dynamics finite element models to investigate the deformation of press-fit metal cups following insertion in the acetabular cavity. The cup deformation following insertion is clearly influenced by the forces encountered during insertion, the initial position of the cup in the cavity, the support provided by the underlying bone and the geometry of the cup itself.

Explicit dynamics finite element models were used to allow a physiologically relevant simulation of the impaction of cups, which is encountered in clinical practice, in comparison to previous studies that have used unrealistically high static forces to simulate a static press fit insertion. Experimental tests were performed to validate the modelling results, establishing that an appropriate coefficient of friction between the cup and a polyurethane cavity in the FE model was 0.835.

Whilst there have been many clinical studies that have reported on the consequences of poor acetabular cup alignment in terms of the *safe zone*, the effect of the cups position relative to the underlying bony support, has not been widely investigated. The current study showed that diametrical cup deformations were twice as large when the cup was tilted at 5° with respect to the cavity compared to when the poles of the cup and the cavity were aligned. The introduction of a non-uniform support to the cup increased deformations further by a factor of approximately 2.5. It was found that although these two factors alone did not result in significantly different deformations, the combination of non-uniform support and cup misalignment, relative to the bone support, by 5° led to high deformations when compared to the clearances between the femoral head and cup. The greatest deformations established in the model were between 80 and 120 µm similar to typical cup-femoral head clearances. Increasing the thickness at the pole of the cup and reducing the cup diameter resulted in significantly smaller deformations being generated.

These results suggest that small cup misalignments, which may not be noticeable in a clinical situation, may produce significant deformations after insertion especially when coupled with the non-uniform support found in the pelvis. Variations in cup geometry, specifically the polar thickness and diameter, and also the degree of cup support will notably influence this deformation.

Chapter 5

Development of Anatomic FE Models of the Pelvis

5.1 Introduction

Cadaveric testing has demonstrated that the acetabulum transfers loads to impacted cups primarily between the iliac and ischeal regions, which are often referred to relative to the anterior and posterior columns of the pelvis respectively [Widmer et al., 2002; Jin et al., 2006]. The non-uniform support results in a pinching effect on the cup which can alter the diametrical deformation of the component, the extent of which may be influenced by a range of factors including the age, gender, size and general health of the patient [Ong et al., 2009]. The previous chapter demonstrated that cup orientation and the underlying support influence its deformation. The current work involved using anatomically correct FE models to investigate a better estimation of the true clinical effect of these parameters, the results of which may be used to inform surgeon's decisions during hip replacement procedures.

5.2 Development of FE Pelvis Model

The FE models of the pelvis that were used in this study were developed using the image processing and design package Mimics 14.01 (Materialise, Belgium) and 3-Matic 5.1 (Materialise, Belgium). The main stages in the model development were to create 3D models from CT scans of the pelvis, convert the models to volumetric meshes, assign material properties and define boundary conditions.

A flowchart, Figure 5.1, summarises an overview of the methods used in convert the CT scans to FE models and the subsequent simulations that were modelled with varying cup and pelvis parameters.

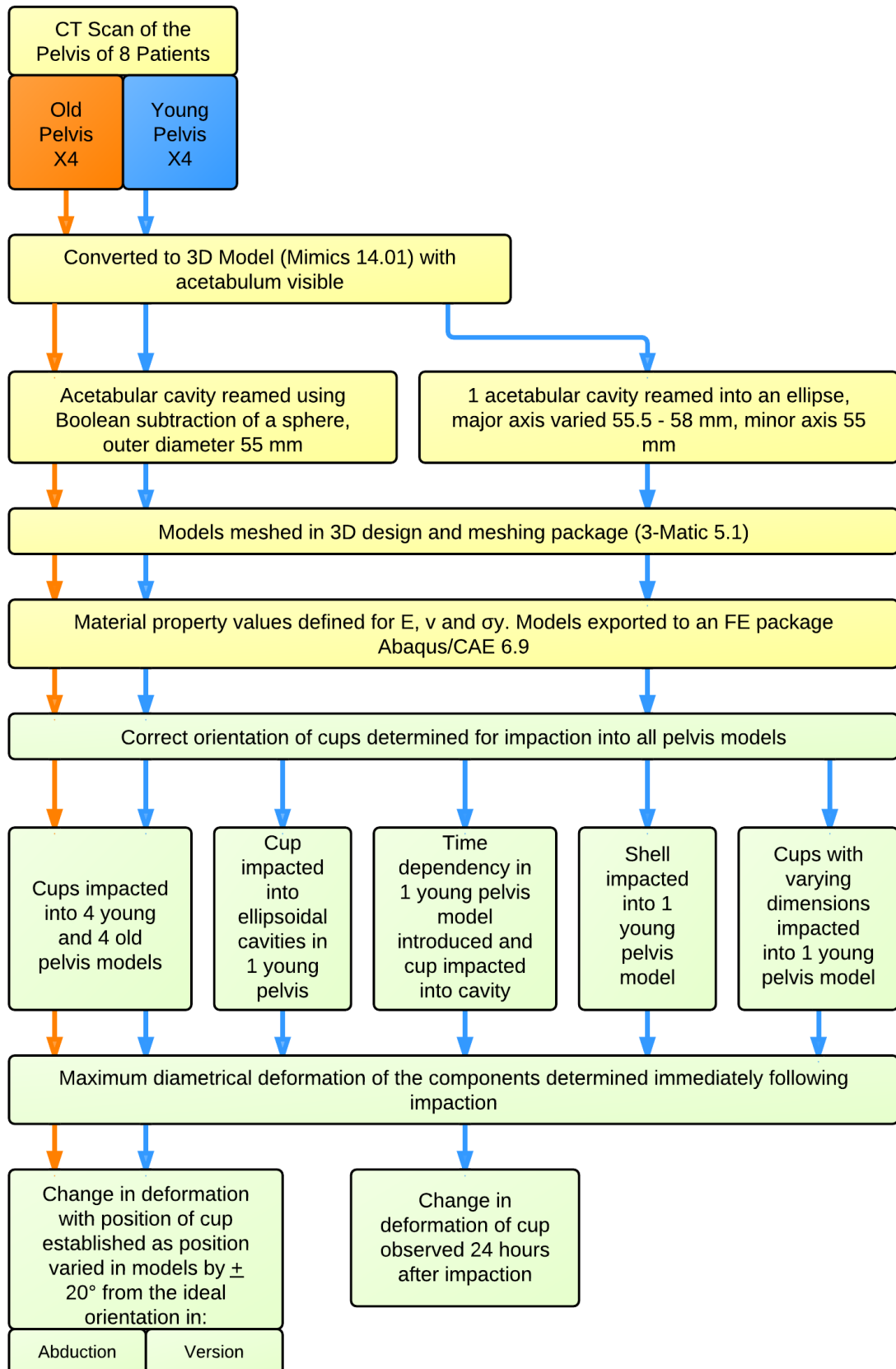


Figure 5.1: Flowchart summarising the steps involved in the development and simulation of the 3D pelvis models

5.2.1 Selection of Patient CT Data

Anonymised CT scans of unreamed pelvises of four female patients aged 43, 44, 46 and 52 years were obtained and subsequent models developed from these were defined as the *young pelvis*. A further four CT scans were obtained of female patients aged 68, 70, 72 and 77 years and models from this group were referred to as the *old pelvis*. Variations in bone stock and density of the pelvis are known to be influenced by the age and sex of a patient [Brinckmann et al., 1981; Tauge, 1989]. As such it was ensured that all CT scans were from only from female patients, and additionally were of a similar size in order to minimise the influence of these factors on the differences between patients of a similar age. Two discrete age populations were considered in order to compare the extent of the influence of age related changes in bone density on cup deformation.

The CT scans were obtained as a series of approximately 240 DICOM (Digital Imaging and Communications in Medicine) images, each slice with a thickness of 1mm, Figure 5.2.

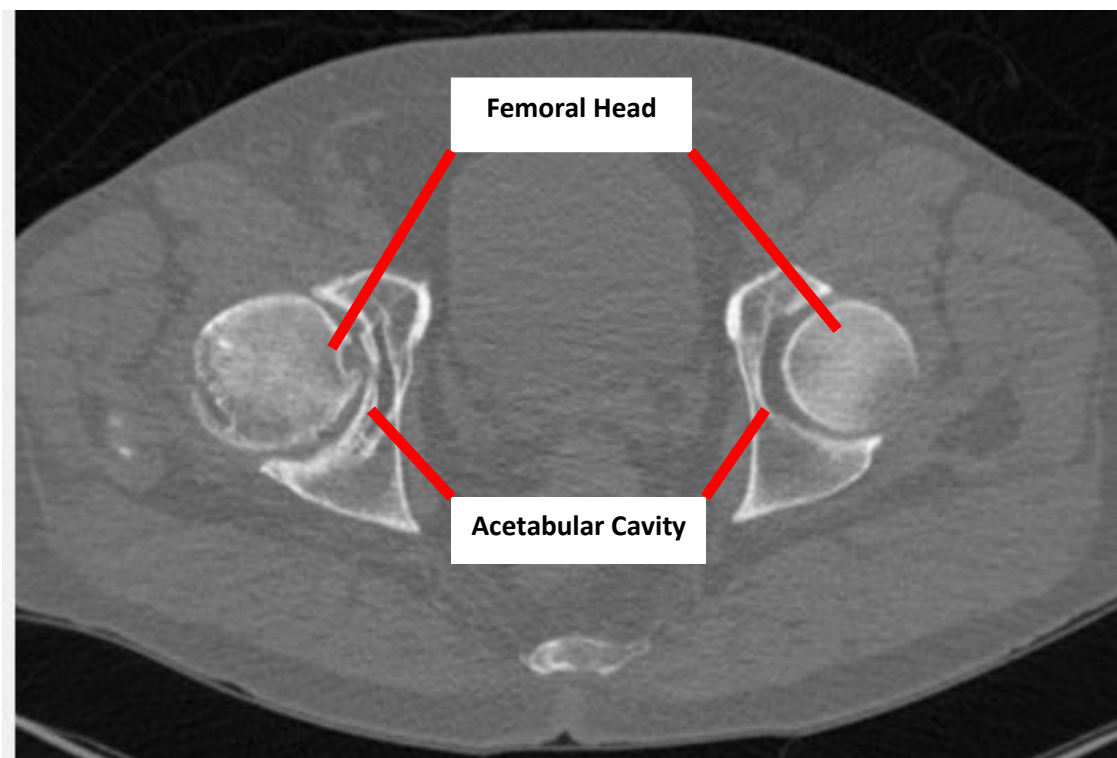


Figure 5.2: Typical DICOM image of the pelvis

5.2.2 Creation of 3D Model

The CT scans were imported into the image processing package Mimics 14.01. Figure 5.3 shows the unmodified scans in Mimics in three different planes: coronal, transverse and sagittal. It can be seen that in the coronal plane, the geometry of the pelvis, femoral head and shaft were clearly visible. For this reason, this plane was isolated and used to develop the 3D model from the images.

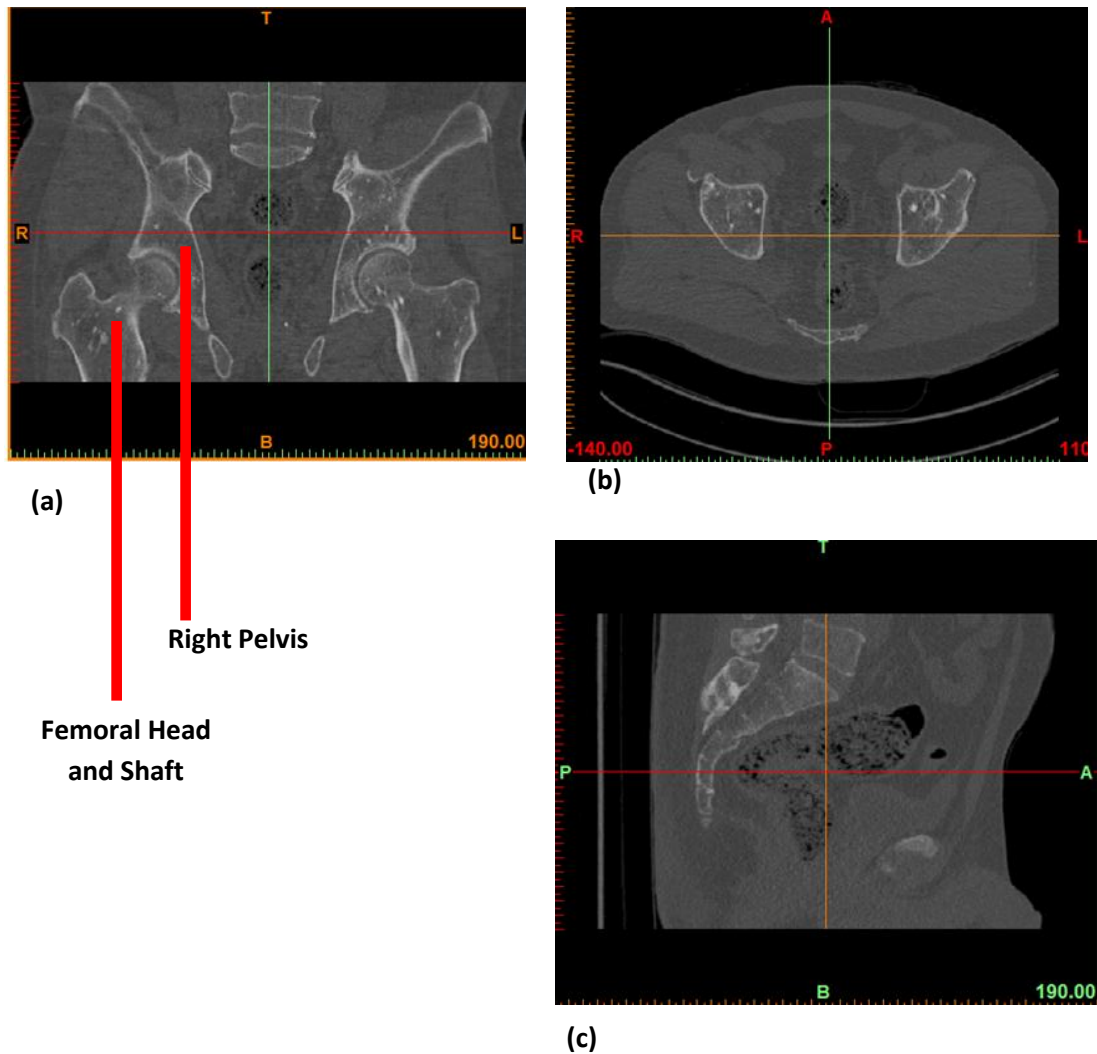


Figure 5.3: DICOM images imported into Mimics 14.01. Unmodified scans are visible in the **(a)** coronal, **(b)** transverse and **(c)** sagittal planes

As a first step, the bone in the CT scans was segmented to separate it from the surrounding soft tissue, Figure 5.4. This was achieved by using the built in *thresholding* in Mimics which served to identify grey scale regions in the images with values between 220 and 1613, as predefined for bone.

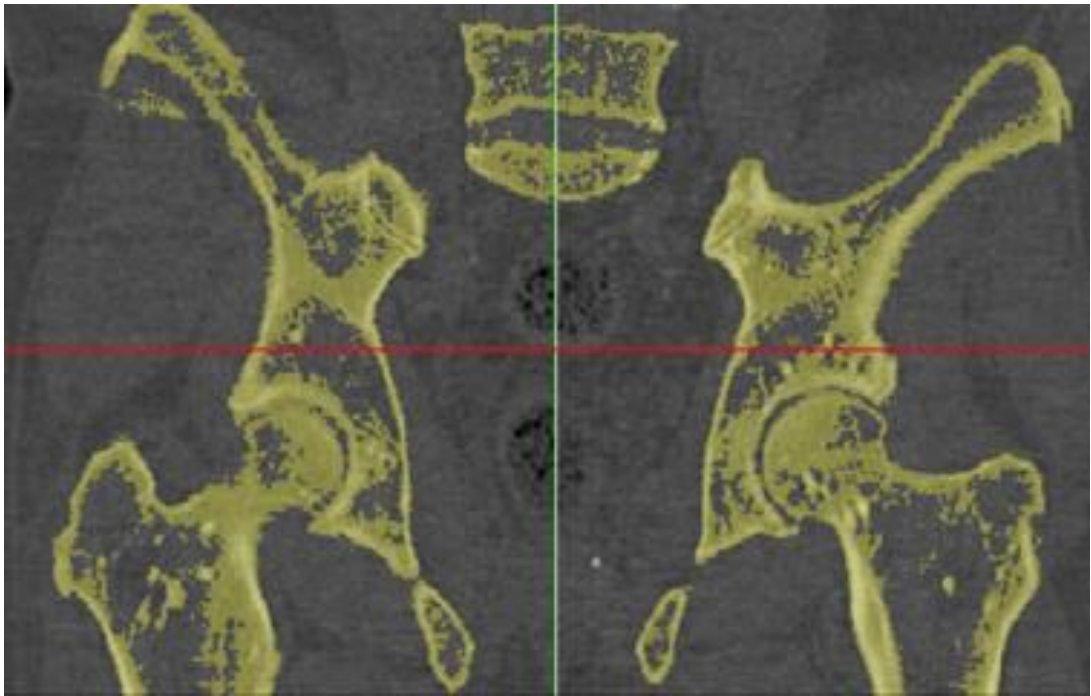


Figure 5.4: Segmentation of bone (yellow) from surrounding soft tissue

An initial 3D model consisting of the segmented bone was created for inspection, Figure 5.5.

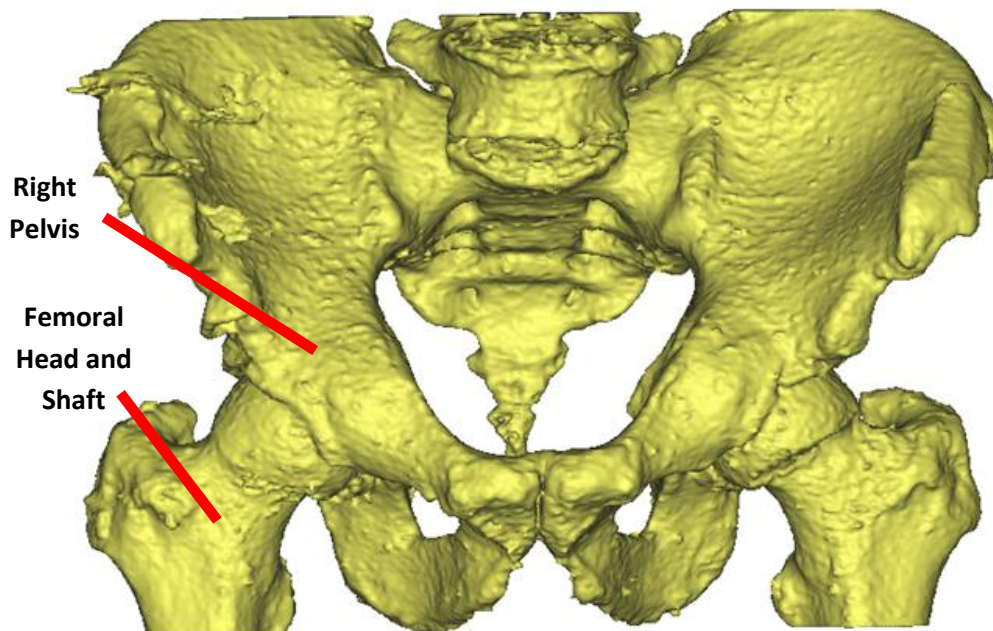


Figure 5.5: Initial 3D model created from segmented bone in CT scans

It can be seen that the initial segmentation served to isolate the bone in the CT scans. The next step in the model development was to remove the femoral head and shaft from the model to leave the acetabular cavity fully exposed. This was achieved by

manually deleting the segmented femoral head selection from each individual slice, thereby disconnecting the pelvis from the femoral bone, Figure 5.6. Additionally, the images were cropped to include only the right pelvis to reduce the final size of the 3D model.

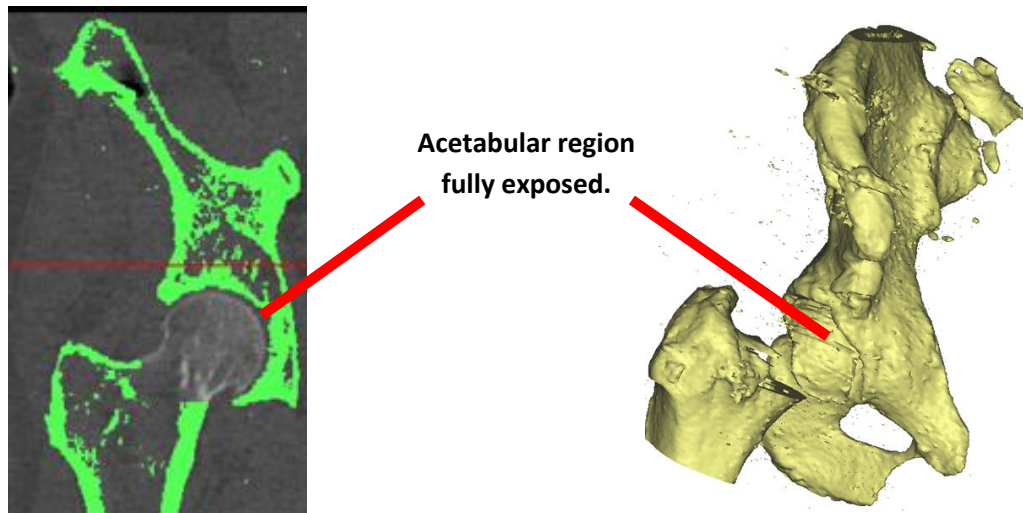


Figure 5.6: Femoral head and shaft removed from model to leave the acetabular region fully exposed.

The 3D model was redeveloped and the disconnected femoral bone and surrounding smaller fragments of bone were removed in the 3D environment. A *wrap* function was applied to the outer surface of the geometry in order to minimise difficulties in meshing due to irregularly shaped artefacts on the surface, Figure 6.7.

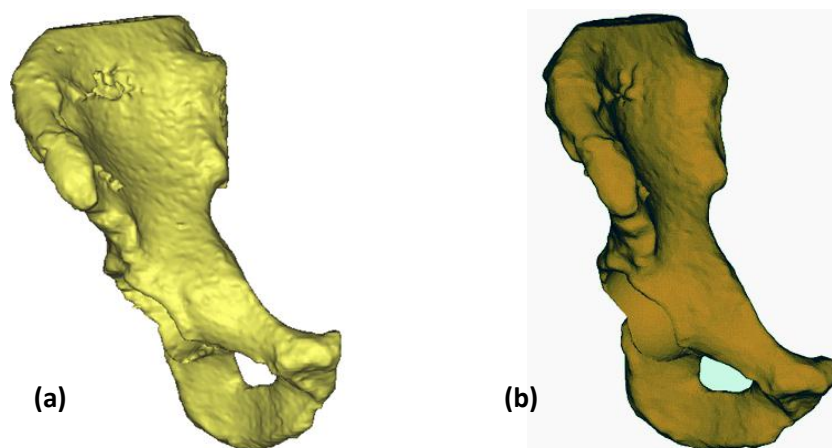


Figure 5.7: Cropped 3D model of the right pelvis with acetabular region visible with **(a)** artefacts present and **(b)** wrap function applied to smooth the outer surface

5.2.3 Cup Size Selection and Reaming of Acetabulum

Following the development of the 3D computer model, a physical rapid prototype model of the right pelvis was created, Figure 5.8.

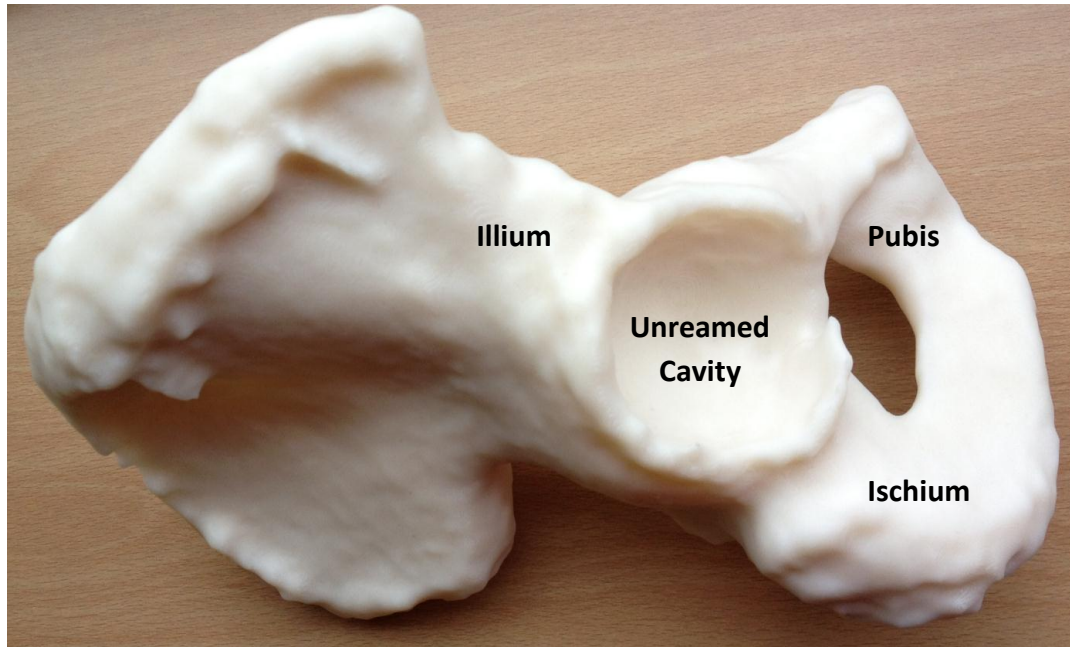


Figure 5.8: Rapid prototype model created of the cropped right pelvis.

This physical model was shown to two orthopaedic surgeons to discuss the most appropriate method of identifying the correct cup size for each model and how much of the acetabular cavity to ream. One option was to develop rapid prototype models for each of the eight patients, which could then be physically reamed by the surgeon and a correct cup size selected and positioned in the cavity. It was identified however that there would be difficulties in precisely relaying the physical information relating to the position of the reamer and the orientation of the cup to the finite element model. It was decided therefore that the surgeons would make all decisions relating to the insertion of the cup into the pelvis through the computational software.

It was noted by the surgeons that the pelvises were of a similar unusually large size for female patients. Cup sizes ranging between 52 and 60 mm were considered in the initial selection of the appropriate diameter to use. A single CoCrMo cup geometry was agreed to be suitable for all eight of the pelvis models, with an outer diameter (\varnothing) of 56 mm and depth (d) of 22 mm, a wall thickness of 3.5 mm at the rim (Tr) and 6 mm at the pole (Tp), similar to previous studies [Jin et al., 2006; Yew et al., 2006; Hothi et al.,

2011], Figure 5.9 and slightly smaller in diameter than that used in the previous chapters.

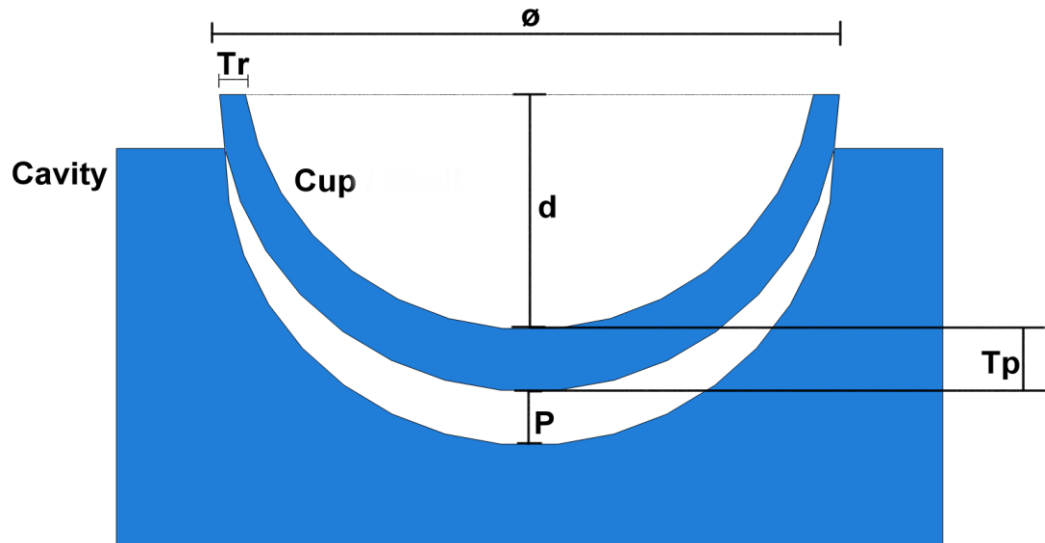


Figure 5.9: Cross-sectional geometry of the CoCrMo cup selected by the orthopaedic surgeons

As in the previous 2D and 3D foam model development, the cup considered in this model had a porous outer coating and clinically is impacted into acetabular cavities that have been reamed slightly smaller in diameter than that of the component, creating interference fits of between 0.25 and 2 mm [Kroeber et al., 2002], leading to stability after impaction. It was agreed by both surgeons that it would be appropriate to ream each cavity to a diameter of 55 mm, thereby creating an interference fit of 1 mm for the seated cup.

In order to simulate the reaming of the acetabulum, the 3D model was exported into the design and meshing package 3-Matic 5.1. The region of the acetabular cavity that was to be reamed was identified, Figure 5.10, and the centre of the cavity was determined by 3-Matic 5.1 based on the selected region.

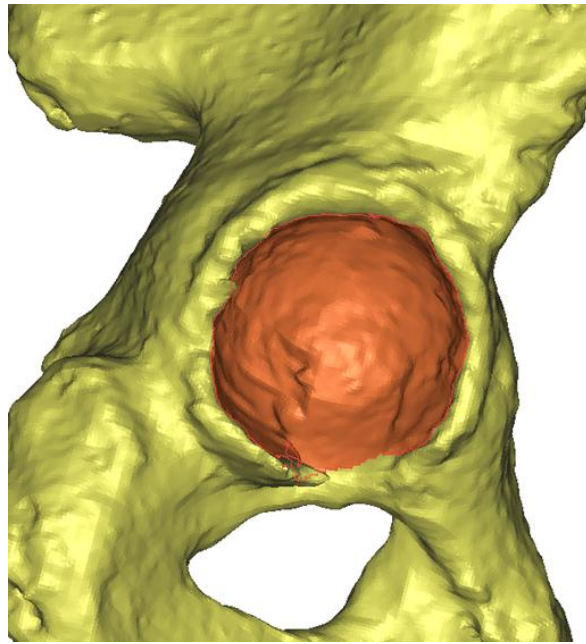


Figure 5.10: Region of acetabular cavity to be reamed was identified within 3-Matic 5.1

A sphere with a diameter of 55 mm was created and positioned within the centre of the cavity (Figure 5.11a); the outer surface of the sphere in this stage overlapped with the inner surface of the cavity. Boolean subtraction of the sphere was performed, which served to uniformly remove the regions of the bone overlapping with the sphere, thereby creating a hemispherical reamed cavity, Figure 5.11b.

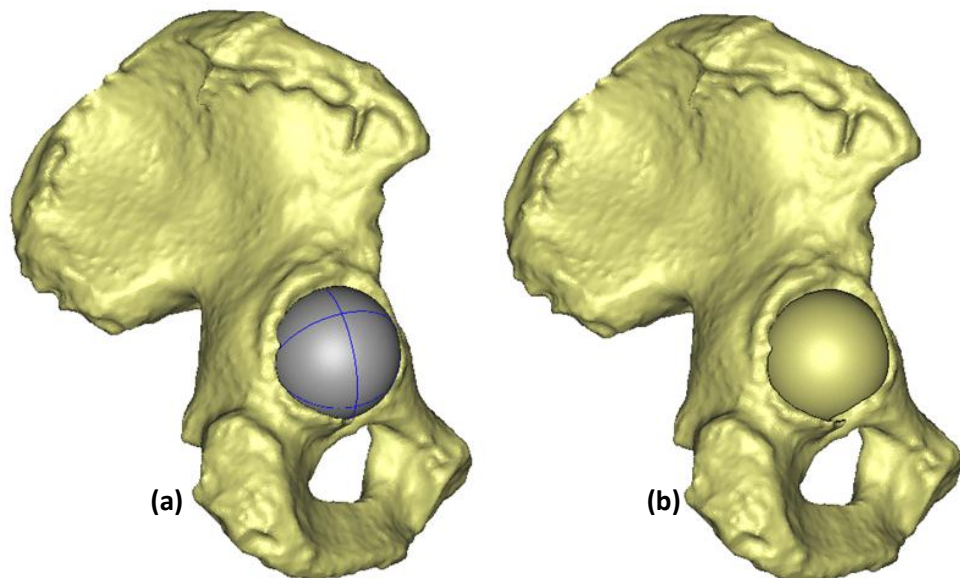


Figure 5.11: (a) Boolean subtraction of a 55 mm diameter sphere used to create (b) a hemispherical reamed cavity

5.2.4 Initial Meshing of Pelvis Models

Meshing of the models was carried out within 3-Matic. Eight noded brick elements are desirable when constructing a mesh, largely due to their uniformity [Felippa, 2001]. However these are more suited to simple models and in complex shapes such as the current pelvises, it is often more appropriate to utilise tetrahedral elements to more accurately map the contours of the shape [Rao, 2010].

As discussed in the previous chapters, the shape and size of an element will have a large influence on the accuracy of the results obtained. A mesh that has a low density, made up of larger elements will improve the simulation run time of a model however some detail can be wrongly reported or not at all. In the current model, where the cup deformations observed are comparatively very small, it is important to ensure that 'reasonable' accuracy is maintained. This will inevitably require smaller elements, finer mesh densities and therefore longer run times.

In addition to the size and shape of the element, the number of nodes that are present can also control accuracy. In a linear tetrahedral element, nodes will only be present at its corners, meaning that the element can only move between these points. However in a non-linear element, nodes are also located between corners, allowing a greater freedom of movement [Rao, 2010]. This places further demands on the simulation run time and in the current study it was decided that linear elements would initially be used in the model development stage and adapted through a mesh refinement study. Figure 5.12 shows an example of the typical initial volume mesh that was created by the software with approximately 5,500 tetrahedral elements and is used in this section to illustrate the mesh development process.

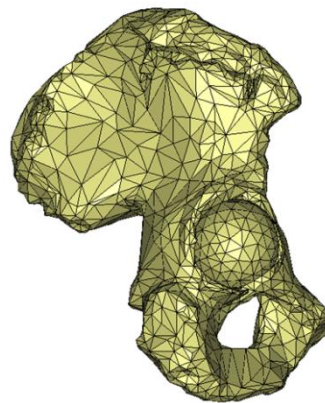


Figure 5.12: Typical element distribution mesh generated by 3-Matic

An inevitability of meshing a complex structure is that there will often be poorly shaped elements within the mesh that can lead to simulation problems such as

hourglassing or excessive distortion. In the current study poorly shaped elements were identified. Element failure criteria were set as a face corner angle of less than 10° , an edge length shorter than 0.01 mm and a height-base ratio of each element of less than 0.4. Figure 5.13 highlights the poor elements that were identified in the surface of this mesh.

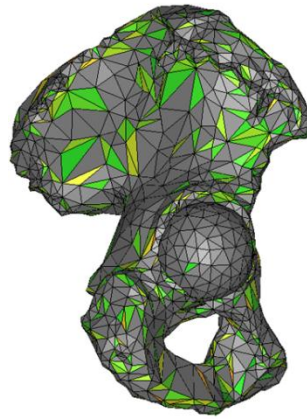


Figure 5.13: Elements that fail the defined criteria are highlighted

The presence of poorly shaped elements was largely due to them having a low height-base ratio and required that the model be remeshed with a greater density. Figures 5.14a and 5.14b demonstrate that increasing the number of elements within the model served to reduce these poor elements. Further refinement resulted in these elements being removed completely.

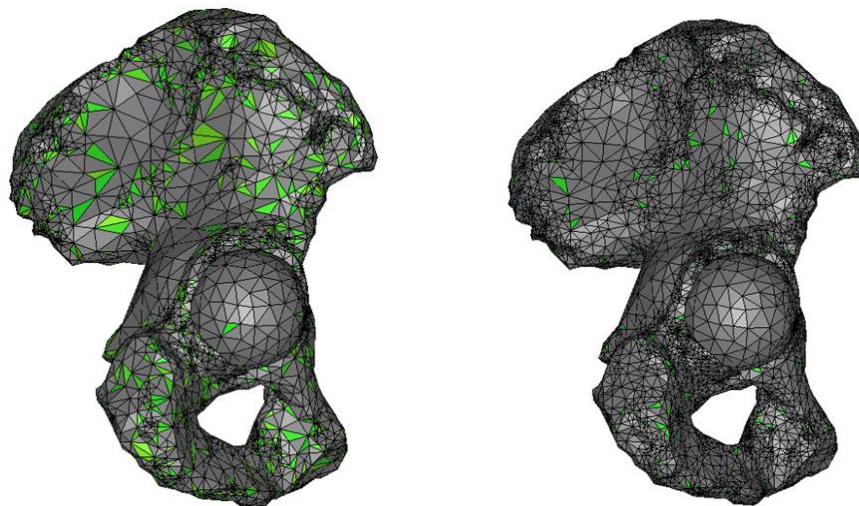


Figure 5.14: (a) Mesh density increased to 10,000 elements and (b) further increased to 15,000 elements, thereby reducing the number of poorly shaped elements

Before a mesh refinement study was carried out to optimise the number of elements in the model, the initial volume mesh was exported back into Mimics 14.01 and

material properties where defined within the cavity and the impaction process modelled, as discussed in the following sections.

5.2.5 Definition of Pelvis Material Properties

Material properties can be defined to the bone in the pelvis as either a homogenous or a heterogeneous material. Previous studies that have used homogenous material property definitions have usually maintained a distinction between cancellous and cortical bone [Spears et al., 2001; Hsu et al., 2006; Phillips et al., 2007]. When heterogeneous material properties have been defined, often using CT data, some studies have not actively differentiated between cancellous and cortical bone [Schileo et al., 2007]. Conversely other studies have sought to create a defined layer of cortical bone which has homogenous properties, placed over the cancellous bone [Anderson et al., 2005]. This approach of using two layers is however unnecessary if the apparent density range of all the bone lies between the values of 0.22 and 1.89 gcm⁻³ suggested by Keller [1994]. It has been shown that bone in the pelvis is anisotropic [Dalstra, 1993] however it is computationally very expensive to model directionality in the material properties of bone in FE models. Previous studies [Kowalczyk, 2003; Kadir, 2010] have modelled the micro structural behaviour of cancellous bone however it is not practical to include this detail on a larger scale such as in the pelvis model in the current study. Hounsfield units are defined as a *unit of measure that represents the different density levels of tissues* [Hoffer, 2000]. Typical values for the Hounsfield unit (HU) range from -1000 for air, 0 for water and greater than 1000 for bone. The values for the Hounsfield unit can be obtained from the greyscale data present in CT scans; this is performed automatically in Mimics 14.01. It has been demonstrated in previous studies that there is a strong correlation between the Hounsfield units and the material properties of bone [Les et al., 2005]. The most accurate method in converting the Hounsfield data to apparent density is to scan a phantom object at the same time as the CT scan of the patient to enable calibration of the data. When a phantom has not been scanned, it is appropriate to utilise the conversion system within Mimics 14.01 [Perez, 2011]. This can relate the Hounsfield unit to values of the apparent density [Jia, 2008] as:

$$\rho_a = 0.009HU + 0.105, HU \leq 816 \quad (5.1)$$

$$\rho_a = 0.000769HU + 1.028, HU > 816 \quad (5.2)$$

It was observed by Helgason et al. [2008] that whilst a number of relationships have been reported between density and material stiffness, there is variability between them. This is somewhat to be expected as these relationships have been defined in different regions of the body. There have been limited studies that have focussed on the bone in the pelvis and the work by Carter and Hayes [1977] appears to be the most appropriate, particularly when considering cortical bone in the same density-stiffness relationship as cancellous bone. It can be seen from Figure 5.15 that the majority of studies that have examined the relationship between apparent density and stiffness, have not considered densities greater than 1 gcm^{-3} , i.e. that of cortical bone.

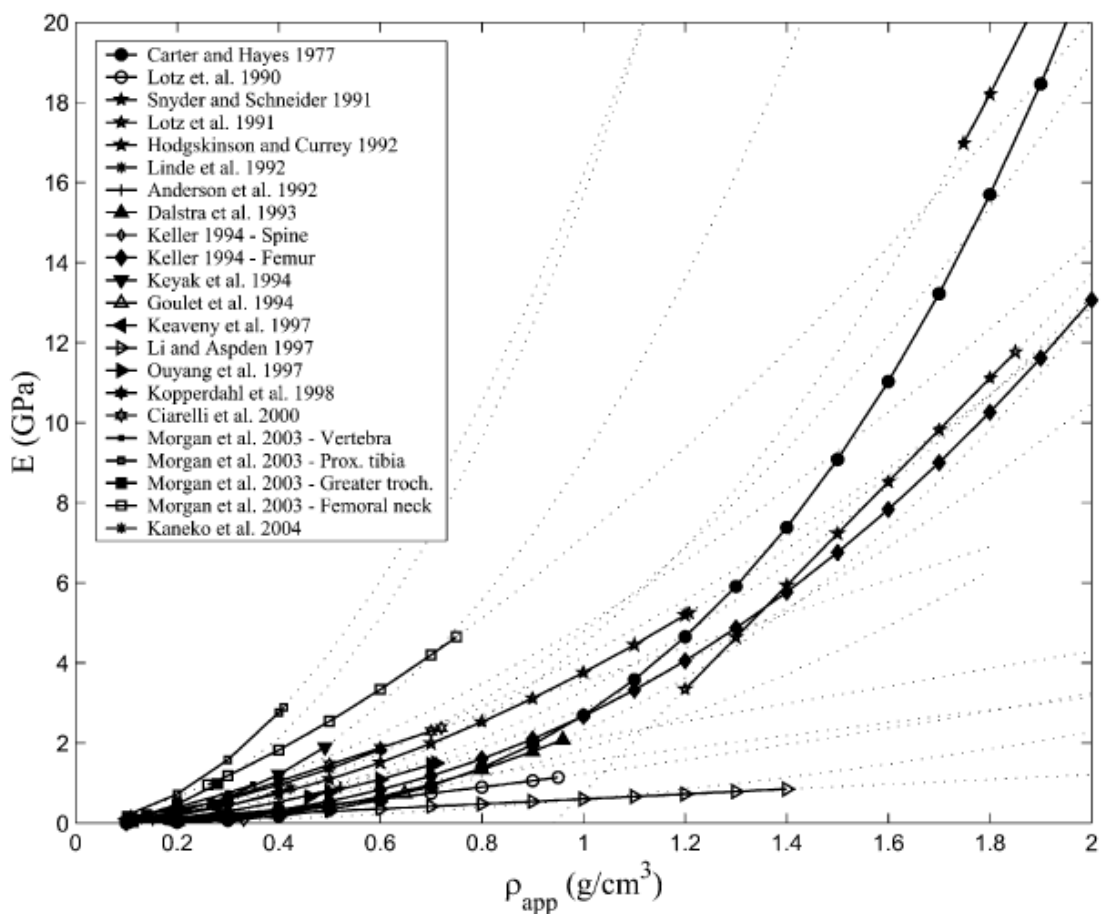


Figure 5.15: Relationships established from previous studies between apparent density and stiffness, adapted from Helgason et al. [2008]

The apparent density (ρ) of the bone in each element of the volume mesh was established in Mimics 14.01. Figure 5.16 shows a cross-sectional example of the variation in bone in density in one of the young pelvis models following reaming.

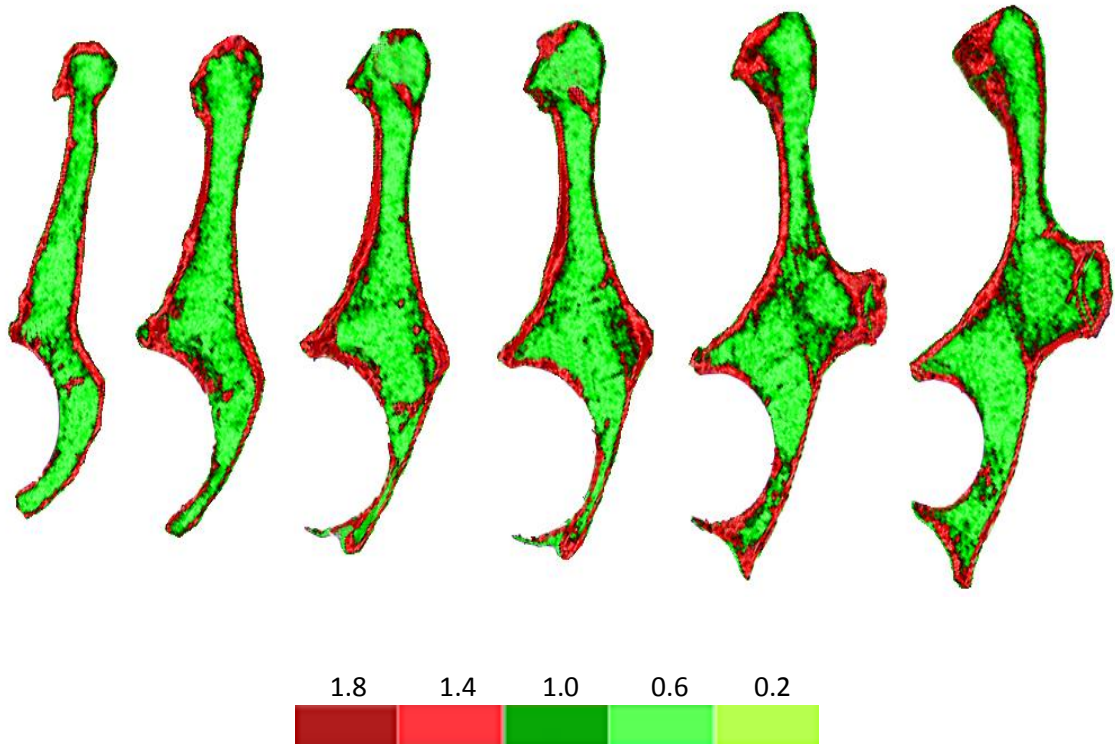


Figure 5.16: Variation in the apparent bone density, gcm^{-3} determined from the CT data in a young pelvis model

It was observed that the range of values of the apparent density for both cancellous and cortical bone were between those suggested by Keller [1994] as being suitable to use in heterogeneous density-stiffness relationships. Material properties were therefore assigned to each element based on relationships between the apparent density established from the Hounsfield scale, and the Young's modulus (E) [Carter and Hayes, 1977]. Additionally, a value for a yield stress (σ_y) was defined to each element based on its relationship with apparent density, as defined by Carter and Hayes [1977], Table 5.1.

$$E = 10 + 2875\rho^3 \quad (5.3)$$

$$\sigma_y = 52\rho^2 \quad (5.4)$$

In another set of models, the yield stress was removed so that only elastic material properties of bone defined from the CT data was modelled. This was carried out to understand the significance of the inclusion of the yield stresses on the final deformation.

Table 5.1: Material properties defined in each pelvis model based on the apparent density

Pelvis		Young's Modulus / GPa		Yield Stress / MPa	
		Minimum	Maximum	Minimum	Maximum
Young	1	0.180	14.325	7.89	151.63
	2	0.073	14.128	4.07	150.23
	3	0.124	14.639	6.05	153.83
	4	0.097	13.642	5.05	146.76
Old	1	0.041	11.566	2.54	131.47
	2	0.036	12.138	2.26	135.76
	3	0.060	12.691	3.49	139.86
	4	0.024	11.978	1.49	134.56

The CoCrMo cup was defined with a Young's modulus of 210 GPa and density of 8300 kgm⁻³ [Yew et al., 2006] and a Poisson's ratio (ν) of 0.3 was defined in all materials.

In order to understand how influential the use of heterogeneous material properties was on the deformation behaviour of the components, an additional model of young pelvis 1 was created and defined with homogenous material properties. A comparatively low Young's modulus of 553 MPa was defined throughout and was the same as that used in the polyurethane foam models developed in the previous chapters.

5.2.6 Development of Impaction Model

The models were exported to Abaqus/CAE 6.9 to define the impaction components and properties of the model. As in the previous chapter, a 1.3 kg rigid impactor was used to simulate the impaction of the components in the dynamic explicit models. A rigid cap was modelled between the impactor and cup to ensure that impaction occurred on the component's rim (Figure 5.17), in a similar manner to the technique used clinically and as developed in earlier chapters.

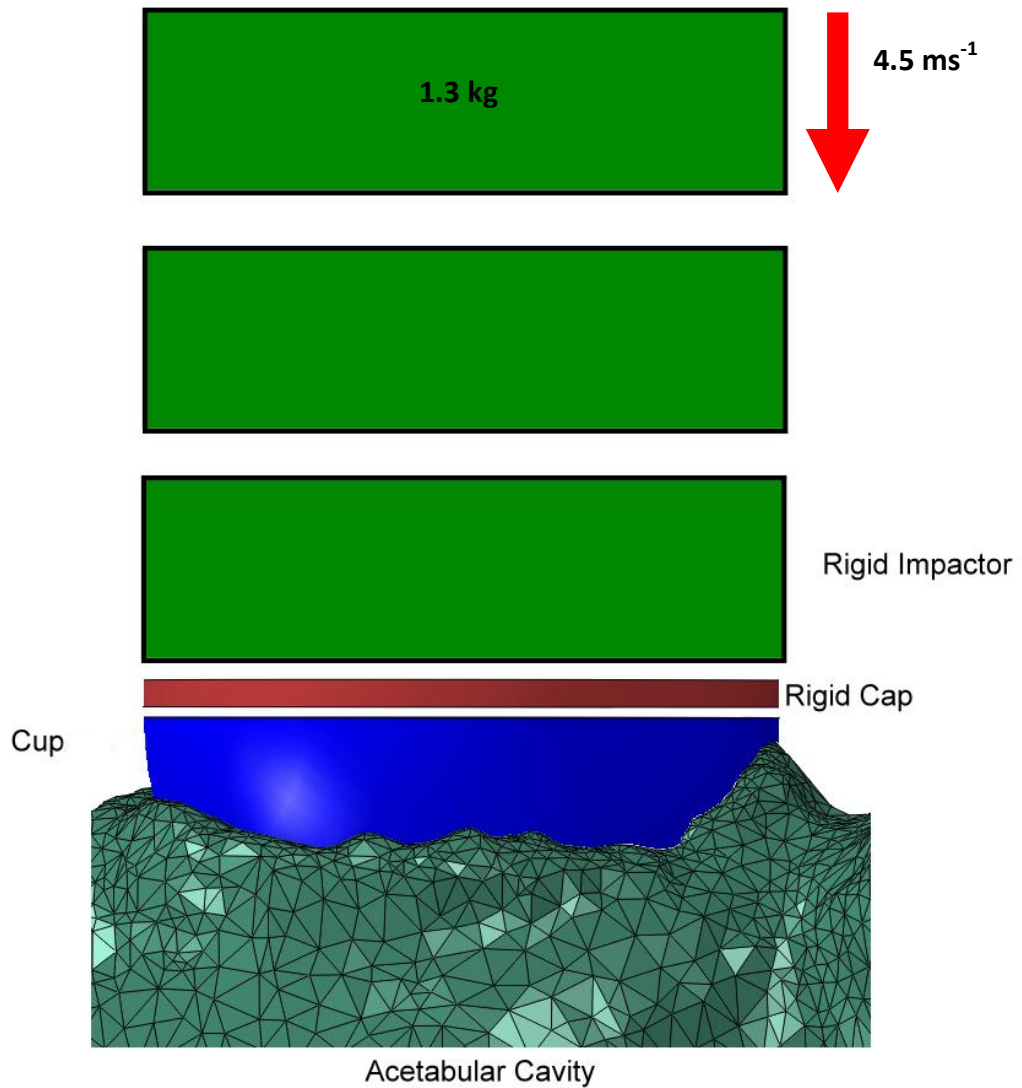


Figure 5.17: Impaction of cup into acetabular cavity using multiple 1.3 kg impactors

The simulation of the multiple impacts required for insertion was modelled using a series of impactors with a velocity of 4.5 ms^{-1} that was established in the previous chapter using 3D foam models, providing a momentum that might be applied during surgery. Multi-point constraints (MPC) were defined to ensure that the cap remained centrally aligned with the cup rim after each impact and that the predefined cup orientation was unchanged during insertion. The impaction process was allowed to run until subsequent impacts reduced the polar gap by less than $10 \text{ }\mu\text{m}$ and the cup was regarded as being fully seated when the final polar gap was less than or equal to 0.5 mm [Sandborn et al., 1988].

5.2.7 Definition of Boundary Conditions

The nodes on each element in a mesh can be such that they are free to move in any of the six degrees of freedom, are fixed rigidly in all directions or limited to moving in certain directions or by a certain amount. Previous studies have used a number of different locations to apply fixed boundaries to the pelvis to constrain it in 3D space [Dalstra, 1993; Siggelkow et al., 2004; Phillips et al., 2007]. There is of course no region in the body that is fixed rigidly in 3D space, therefore the application of boundary conditions will always be associated with assumptions and related to the specific region that is being investigated. For example when the interaction of muscle forces with the pelvis is of interest, such as when walking, previous studies have developed models free of fixed regions, supported instead using a number of non-linear springs. It has been reported [Phillips, 2005] that the distribution of strains and stress within the acetabular cavity do not change as the location of boundary conditions are altered. In the current study boundary conditions were applied in the regions of the pelvis in a similar manner to previous finite element studies [Udofia, 2007; Dalstra, 1993; Levenston et al., 1993] to constrain the movement of the pelvis, Figure 5.18. These locations are commonly used when the specific region being investigated is the acetabulum. Fixed boundaries have previously been applied closer than this [Mantell et al., 1998; Janseen et al., 2006] however generally it is accepted that as much distance as possible should be kept from the region of interest [Speirs et al., 2006; Phillips et al., 2007].

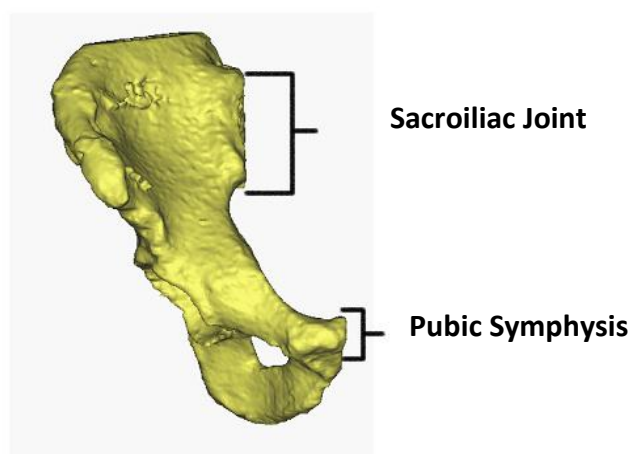


Figure 5.18: Boundary conditions applied in the sacral-iliac and pubic symphysis regions of the pelvis

5.2.8 Definition of Contact Behaviour

The mechanical interaction behaviour between two surfaces that come into contact can be defined in terms of its tangential and normal conditions. The tangential condition controls the amount of slip that can occur between the two surfaces and is adjusted by the definition of a sliding formulation and the coefficient of friction between the two contact surfaces. The normal condition controls the extent to which one surface can penetrate into the other. In the current work, the master and slave surfaces in the model were defined as in Table 5.2.

Table 5.2: Definition of master and slave surfaces of the different structures in the model

Interaction	Master Surface	Slave Surface
Impactor-Cap	Impactor	Top of Cap
Cap-Cup	Bottom of Cap	Cup Rim
Cup-Bone	Outer surface of Cup	Acetabulum

5.2.8.1 Tangential Condition: Sliding Formulation

When the interaction between two surfaces is defined, all of the nodes on the slave surface will interact with a corresponding node on the master surface using one of two sliding formulations. A *small sliding* formulation is considered the most basic of the interaction properties and limits the behaviour to allowing a node on one surface to interact with only a single node on the other surface, that is considered its *nearest neighbour*. As such a small sliding formulation is only appropriate when the degree of movement between two surfaces is small enough that the nearest neighbour nodes remain the same. The amount of allowable movement between two surfaces will be largely governed by the size of the elements at the point of contact; larger elements will have a greater spacing between nearest neighbour nodes, whilst a dense mesh will reduce the amount of small sliding that is possible.

If the amount of slip between the two surfaces is large, it is appropriate to utilise a *finite sliding* formulation. This permits a node on the slave surface to interact with different nodes on the master surface as the nearest neighbour node changes during a simulation. From the point of view of computational demands, it is more efficient to define small sliding formulations between surfaces. In the current work, a sliding formulation is only required to model the interaction between the porous outer

surface of the cup and the acetabular cavity. In this instance it is known that a considerable amount of sliding will occur between the two surfaces to seat the cup, therefore it was appropriate to use a finite sliding formulation.

5.2.8.2 Tangential Condition: Coefficient of Friction

The definition of the coefficient of friction between two surfaces can be made independent or it can be influenced by the change in contact pressure between surfaces. In the current work, the contact between the impactor and cap, and the cap and cup rim, was assumed as being frictionless. When modelling the interaction between the cup and the cavity, it is expected that, as well as the influence of contact pressure, the coefficient of friction may change as a result of damage to the local bone during impaction. This damage can be simulated in simpler models by including a damage model in which elements that yield beyond a certain defined stress, are removed from the model during the analysis. This approach however is very sensitive to the size of the elements used at the point of contact. To accurately model the damage and ‘crumbling’ of bone in the acetabular cavity a very dense mesh would be required, which in a complex FE model such as the current pelvis, would result in unreasonable computational run times. It is accepted therefore that in finite element models of the pelvis, that a single independent value of the coefficient of friction be used [Spears, 2000; Janssen, 2006; Kluess, 2009]. In the current model a value of 0.835 was used, as determined from the experimental and FE foam model in the previous chapter. This value was similar to that observed experimentally by Grant et al. [2007] when interacting bone with a hydroxyapatite coating similar to that used on the outer surface of the cup in this study.

5.2.8.3 Normal Condition

The interaction between two surfaces in terms of its normal contact behaviour is controlled by extent of “pressure-overclosure” which determines how easily and by how much one surface (typically the master surface) can overlap or penetrate another surface (typically the slave surface) [Simulia 2010]. *Soft normal contact* can be defined in which some penetration of the two surfaces is permissible but the depth of penetration is limited, such that if this limit is exceeded the simulation does not complete. The extent of the depth of penetration can be controlled by the number of

elements at the point of contact; a higher mesh density will reduce the amount of penetration that can occur. Soft contact is often used when there is difficulty reaching convergence in the model. In the current work however, where a specific interference of 1 mm was defined between the cup and cavity, the penetration or overlapping of the cup surface (master surface) into the surface of the cavity (slave surface) was undesirable as this would have underestimated the influence of the defined interference on the deformation of the cup. In this instance, a hard contact was defined in which penetration was not permitted. As a consequence the mesh density was required to be increased in the contact regions, which ultimately resulted in a longer simulation run time.

5.2.9 Mesh Refinement

Following the definition of material properties in the pelvis and the creation of an impaction model in Abaqus, a mesh convergence study was carried out to ensure efficiency of the model. Using the data from the previous chapter, the combined mesh density of the cup, cap and impactors was maintained at approximately 2,000 hexahedral elements. Whilst initially linear tetrahedral elements were defined in the pelvis model during the development of the impaction model, the mesh was modified to include non-linear ten noded tetrahedral elements which have been reported as being appropriate for use in hard contact problems [Simulia, 2010], such as the interaction between cup and bone in the current model. It is of note however that it has been reported [Ramos, 2006] that the type of element used in a model may be inconsequential if a proper mesh convergence study is performed.

In the current study, eight models of the pelvis were created with different mesh densities varying between approximately 5,500 and 720,000 tetrahedral elements, Figure 5.19.

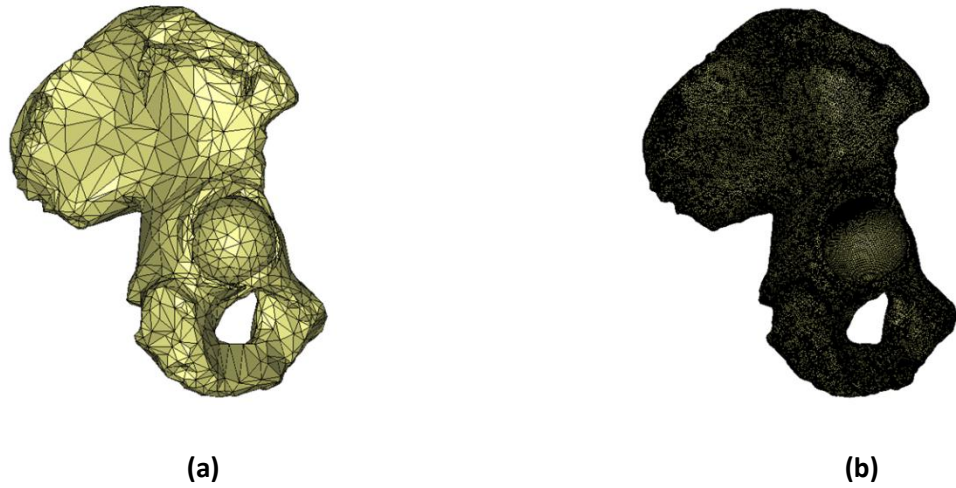


Figure 5.19: Mesh density in convergence study varied between **(a)** 5,500 elements **(b)** and 720,000 elements.

In each case, the mesh was refined to remove poorly shaped elements using the methods described earlier.

In a similar manner to the previous chapter the change in the polar gap and the deformation were used to evaluate the point of convergence. Initially a single impact with a high momentum of 9 kgms^{-1} was used to seat the cup into the acetabular cavity using the highest number of elements of 720,000 in the mesh. In subsequent simulations, a lower mesh density was used and the single impact repeated in a new model. Convergence was said to be achieved when differences in the diametrical deformation (ΔD) and polar gap (ΔP) were within 1% of the values observed when the maximum number of elements were used:

$$\Delta D = \frac{D_E - D_H}{D_H} \times 100 \quad (5.5)$$

$$\Delta P = \frac{P_E - P_H}{P_H} \times 100 \quad (5.6)$$

where D_E and P_E are the deformation and polar gap values of the current simulation and D_H and P_H are the deformation and polar gap values when 720,000 elements were used.

It was found that approximately 180,000 elements in each pelvis were necessary to minimise the run time of the simulation to approximately four days whilst maintaining

the accuracy of the cup deformation and polar gap to 1%. Figure 5.20 shows an example of the mesh convergence that was achieved using the polar gap and deformation for a single pelvis. Hourglass control was maintained in the current model to ensure that element locking did not occur, as was the case in the previous 3D foam model.

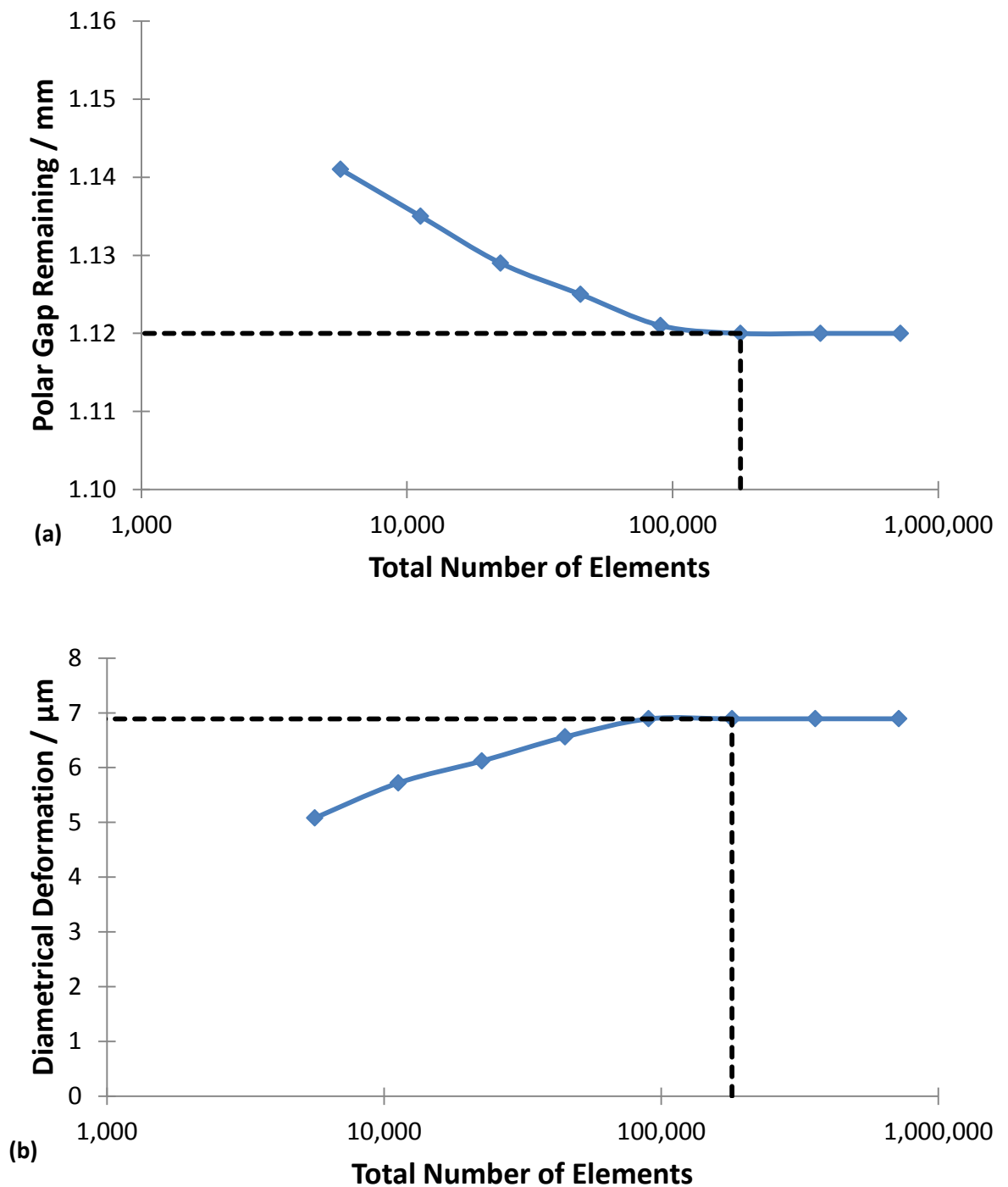


Figure 5.20: Mesh convergence achieved with approximately 180,000 elements to achieve accuracy of the **(a)** polar gap remaining and **(b)** deformation to within 1%

5.3 Influence of Cup Orientation

The orientation of the acetabular cup, relative to the anterior pelvic reference plane, by a surgeon is known to influence the longevity of the prosthesis [Schnurr et al., 2009; De Hann et al., 2008]. As discussed in the literature review, the orientation of the cup is described both in terms of its version and abduction angles. The importance of abduction and version angles that the cup should be positioned as has been highlighted and consensus on the *safe zone* has been accepted as being approximately 30-50° and 5-25° respectively [Lewinnek et al., 1978]. This range of positions in patients appears to minimise the risk of high wear, component loosening, impingement and dislocation [Hart et al., 2008; Hart et al., 2009; Langton et al., 2008; Ryan et al., 2010], as a result of reducing negative geometrical factors such as edge loading, although it does not guarantee long-term clinical success. Naturally, it is likely that there will be variations in the precise positioning of the cup between different surgeons [Birbeck et al., 2010]. It was demonstrated in the previous chapter using the FE foam model that a small deviation in the position of the cup by 5° with respect to the cavity led to peak deformations when compared to either aligning the poles of the cup and cavity or increasing the angle of insertion beyond 5°. It is important here to be clear that the description of the orientation of the cup will be different depending on if it is described with respect to the underlying bone or with respect to the pelvic reference plane. In clinical literature, the orientation is usually referred to with respect to the pelvic plane (i.e. abduction and version) and this definition will be used in the current model.

The clinically correct position for the 56 mm CoCrMo cup to be inserted into the acetabular cavity of each pelvis model was identified within the model (Abaqus/CAE) environment by two experienced orthopaedic surgeons. The abduction and version angles in the correct positions are referred to as the *optimum position* in the following sections.

5.3.1 Simulation of the Cup Impaction in Surgeon Defined Orientations

Figure 5.21 summarises the abduction and version angles that were determined for the optimum position of the cup in each pelvis model by the orthopaedic surgeons. The limits of the axis of for abduction and version have been set as the limits of the safe zones as defined by Lewinnek et al. [1978]. It can be seen that the optimum position for the cup in all the pelvis models falls within the safe zone and the mean

version of 15.25° and 16.5° for the young and old pelvis models respectively is very close to the middle of the safe zone. Similarly, the mean abduction angles of 39.75° and 42.75° for the young and old models respectively also lie in the middle of the safe zone. The very small range of the abduction and version values of 5° and 7° for the young pelvis and 9° and 5° for the old pelvis indicate that all the patients in this study had similar bony landmarks which informed the surgeon's decisions as to the final cup orientation in each model. Of note however is the angle of abduction of old pelvis 2 (O2) which was only 3° lower than the defined safe zone limit of 50°.

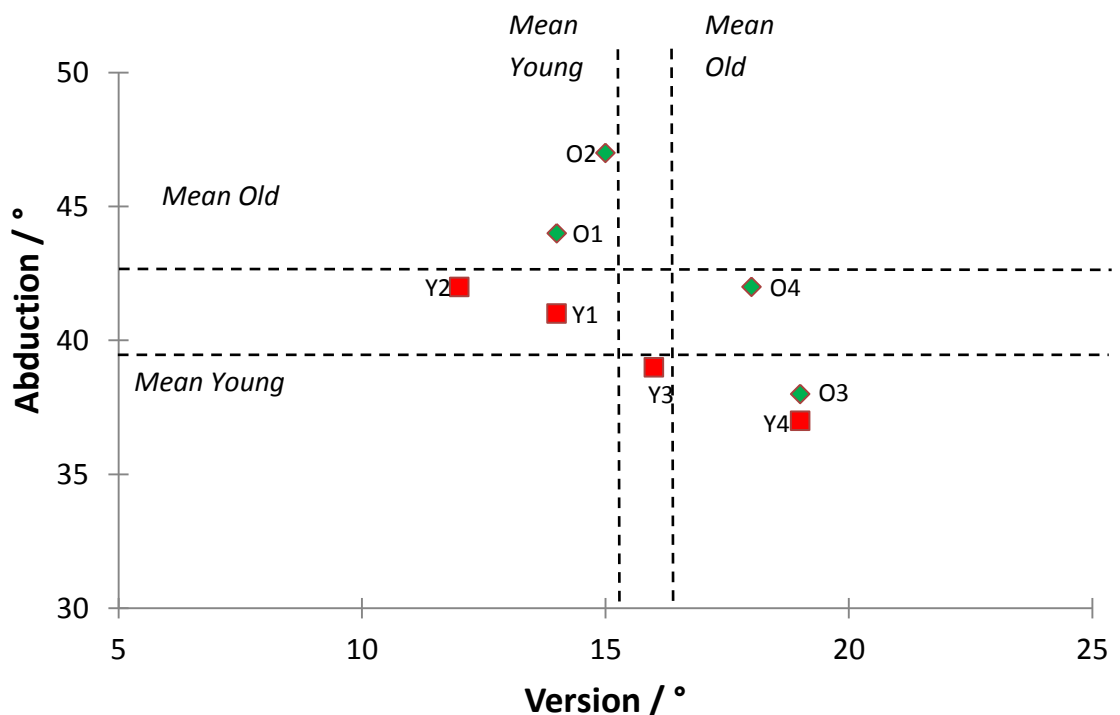


Figure 5.21: Cup abduction and version angles as determined by orthopaedic surgeons in young (Y1 – Y4) and old (O1 – O4) pelvis models, located within the safe zone

Between 6 and 10 impacts were necessary before further impacts had no change in the polar gap to within 10 µm. In all cases the final polar gap was reduced to below 1 mm however a gap below 0.5 mm could not be achieved.

Figure 5.22 shows that the deformations of the cup following optimum positioning are considerable greater, by approximately 50%, in the young pelvis models (mean 44 µm) than those observed in the old pelvis models (mean 21 µm) and are significantly so, $p < 0.005$ (Student's *t*-test).

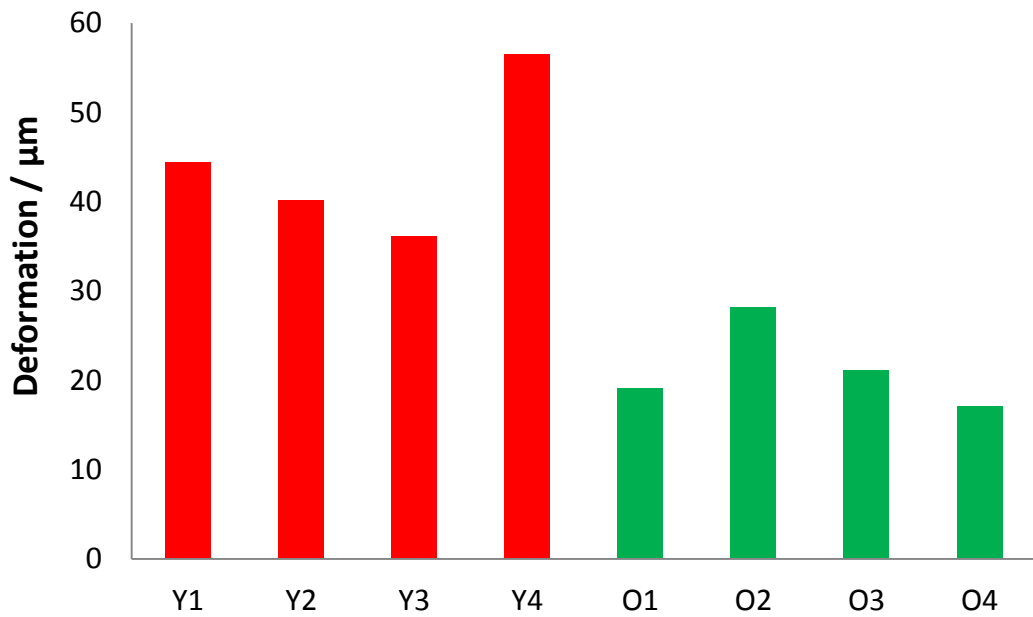


Figure 5.22: Cup deformations observed after insertion in the optimum position in the four young (Y1 – Y4) and four old (O1 – O4) pelvis models

In all models the maximum deformations were as a result of a pinching effect between the iliac and ischeal columns, Figure 5.23. This is in agreement with the direction of pinching that was modelled in the previous chapter with the pinch points at approximately 150° to each other, Figure 5.24.

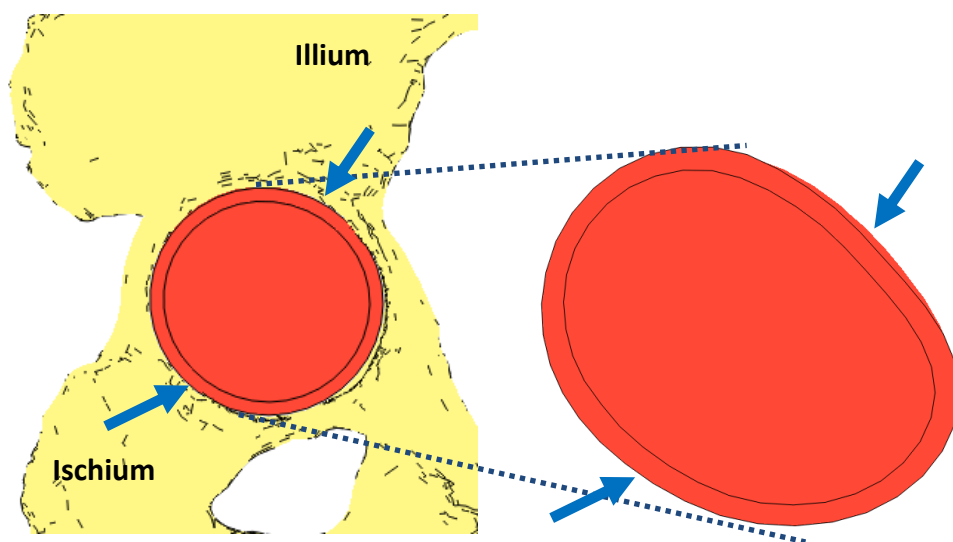


Figure 5.23: Maximum distortion as a result of pinching between iliac and ischeal columns. Deformed cup scaled by a factor of 25 on the right.

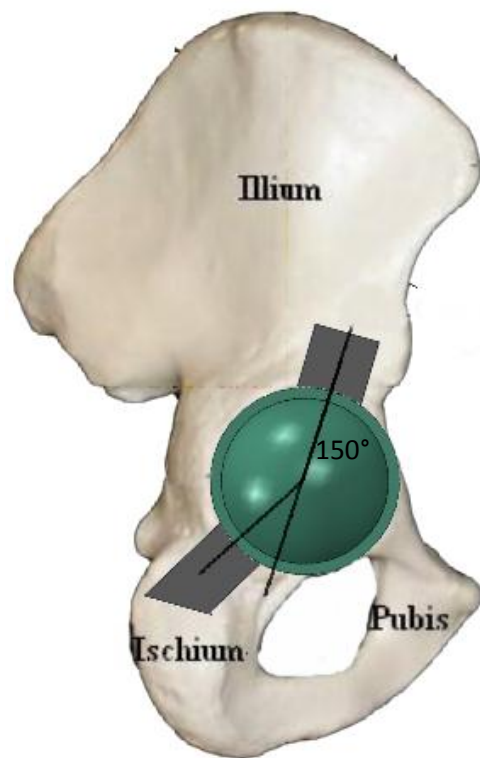
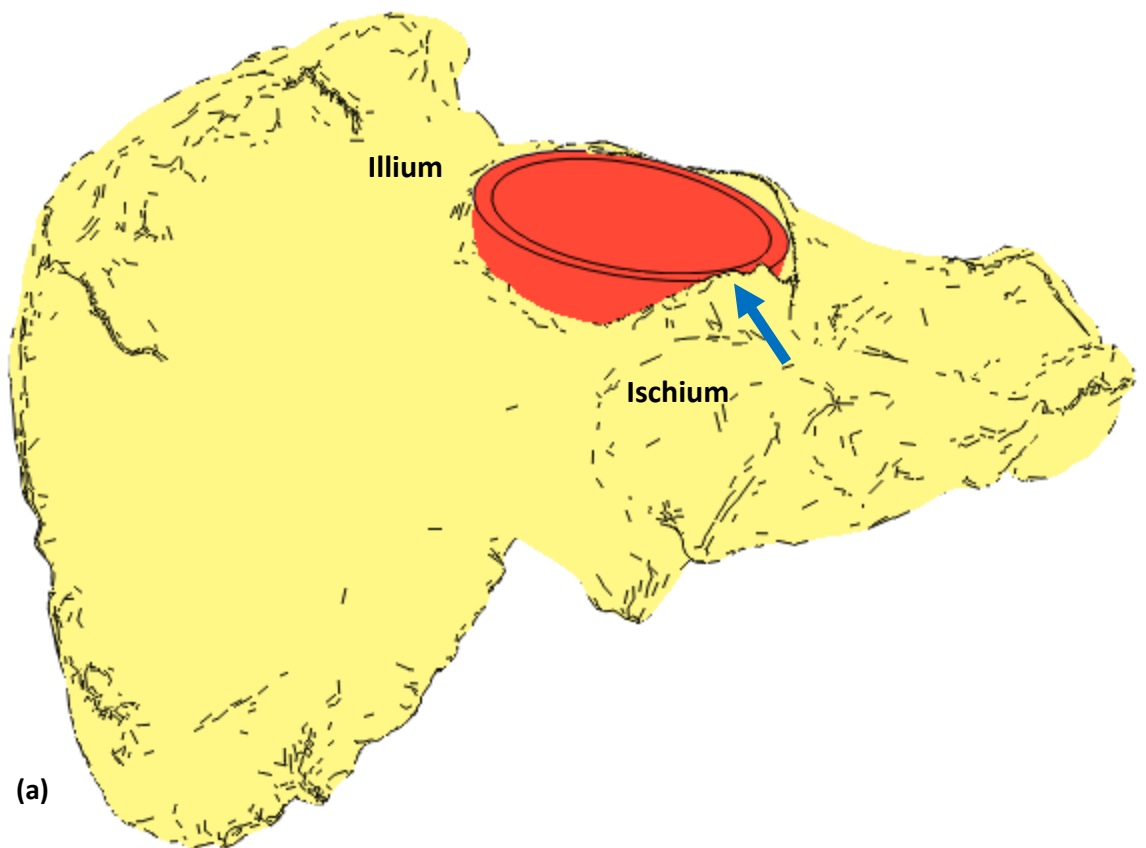
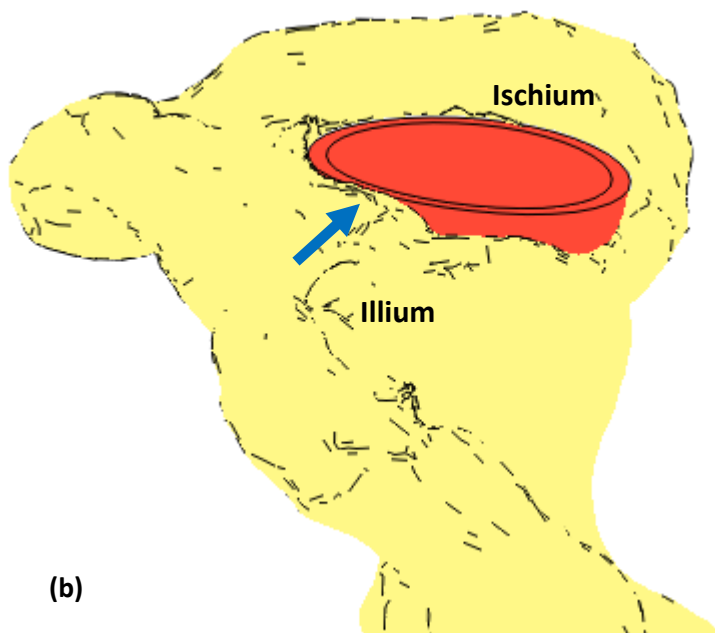


Figure 5.24: Direction of pinch points modelled in foam modelled (grey regions) in the previous chapter

When homogenous material properties were defined in young pelvis 1, the deformation of the cup reduced considerably to 8 μm , compared to 44 μm when heterogeneous properties based on the CT data were used. The lower deformations are to be expected as the homogenous Young's modulus of 0.553 GPa is considerably lower than the peak values of approximately 14 GPa in the heterogeneous material model. Interestingly however, the observation that the maximum deformation in the homogenous material model also occurred as a result of a pinching between the iliac and ischeal columns. This observation suggests that the pinch effect experienced by inserted cups may not be entirely due to variations in the distribution of bone density in the surrounding bone. Figure 5.25 shows that there is clearly a greater amount of contact between the cup rim and bone in the regions of the pinch points. This feature was present in all of the young and old pelvis models and is a major contributing factor to component deformation.



(a)



(b)

Figure 5.25: Greater amount of boney contact with cup rim in the pinch directions of **(a)** the Ischium **(b)** the Ilium

The FE model in the previous chapter modelled the pinching in the acetabulum using foam cavities and demonstrated that this contributes significantly to component deformation and that increasing the degree of pinching on a cup will increase its

deformation. In the young pelvis models the deformations were notably greater than those that occurred in the older pelvis models; the CT data showed that the bone densities of all the older patients were lower, generating a lower modulus in the model, thereby reducing the cup deformations. In all pelvis models, the maximum reduction in diameter of the component was found to occur as a result of it experiencing a pinching effect, as predicted in the previous chapter.

5.4 Variation of Cup Orientation in Acetabular Cavity

Following observation of deformations at the optimum cup position, the orientation of the cup within the cavity was varied by $\pm 5^\circ$, $\pm 10^\circ$, $\pm 15^\circ$ and $\pm 20^\circ$, individually in both the directions of abduction and version. The influence of varying the cup position from the surgeon defined optimum on the maximum reduction in diameter was investigated. The two reasons for this investigation were as follows:

- Clinically, different surgeons with differing levels of experience or surgical techniques may orientate the components in various positions, whilst still keeping within the safe zone. This part of the study sought to determine how much of an influence this surgeon variability had on the range of cup deformations.
- The safe zone was originally defined to minimise the risk of factors such as wear and component loosening. The relationship between the safe zone and cup deformation has not previously been reported; the current study sought to determine if the definition of the limits of the angles of abduction and version were appropriate to limit the cup deformation.

The statistical significances of differences in deformations between the young and old pelvis models and between the cup positioned at the limits of the safe zones in both orientations were determined using Student's t-tests.

5.4.1 Results

Figure 5.26 shows the influence of the version and abduction of the cup from the optimum position on the deformation of the cup.

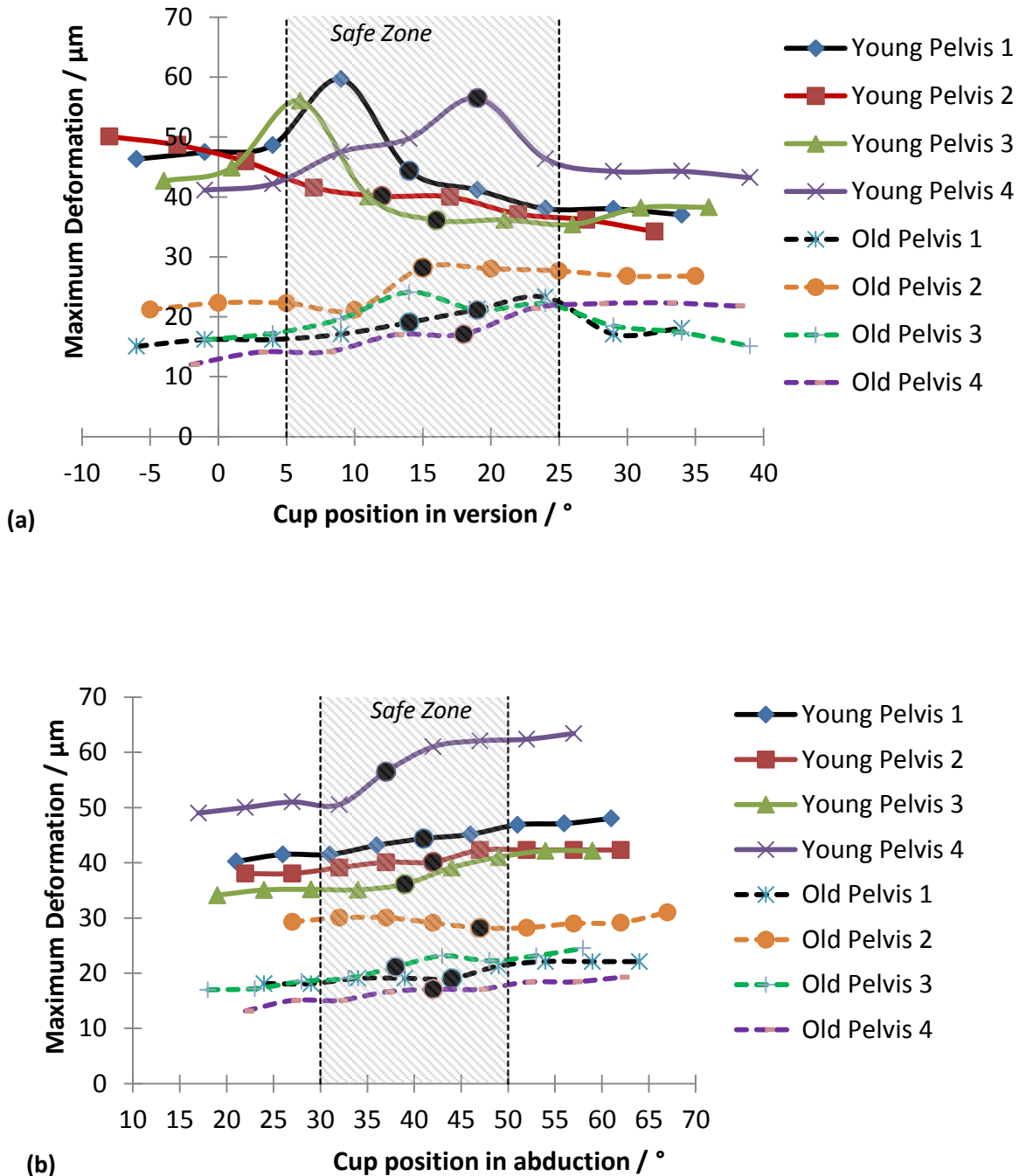


Figure 5.26: Deformation of the cup with position in (a) version and (b) abduction was varied from the ideal as determined by an orthopaedic surgeon (marked as solid circles on curves).

The mean deformation of the cup in the young pelvis models was 44 (34 - 63) μm and was highly significantly larger than the mean deformation of 21 (12 - 31) μm observed in the old pelvis models, $t(142)=19.29$, $p<0.001$. The distribution of deformation values was found to be greater in the young pelvis. With the exception of one young and one old pelvis model, the surgeon defined optimum position resulted in deformations less than or approximately equal to the mean deformations. Unexpected peaks up to 19 μm greater than the mean deformation were observed in the young pelvises at certain orientations within the safe zone and are of interest. When these data points are not considered, the mean deformation was 42 μm and notably the distribution of the values was similar to that of the old pelvis. The absence of similar peaks in the old pelvis models may be an indicator of the age related changes in cup support from the underlying bone. Figure 5.27 shows that when homogenous material properties are used in young pelvis 1, these peaks are also not present. Whilst it was shown in the previous section that physical differences between the precise point of cup support at the rim in the Ischeal and Ilium regions can result in a pinching of the cup, the current results highlight the significance of variations in the apparent density distribution in the bone, which can result in the largest deformations in the pelvis models. It is clear therefore that the cup deformation is as a result of both the anatomy of the underlying bone and also the specific material properties. It was shown in the previous section that a pinch on the cup will still occur with a homogenous material model, however the greatest deformations occur as a coupling of the pinching due to stiffness variability in the acetabulum. These findings also highlight the importance of appropriate definitions of density-stiffness relationships. Many different relationships have been proposed by different authors [Carter and Hayes, 1977; Lotz et al., 1990; Dalstra et al., 1993; Keller et al., 1994] however the ideal situation is to have access to a cadaveric model that can be used to validate the FE results; this is a consideration that should strongly be looked at in future work.

The inclusion of yield stress values based on the apparent density did not notably influence the results of the deformations when compared to using purely elastic material properties. The greatest differences were observed in the young pelvis models where the peak deformations were up to 1.3 μm (<2%) higher in the elastic model than the elastic-plastic model. The differences between the two material models is not considered significant with the simulations parameters used in the

current study, however factors such as increasing the size of the interference may have a greater impact on yielding of the bone in contact with the cup and the definition of the yield stress should therefore be maintained in future models.

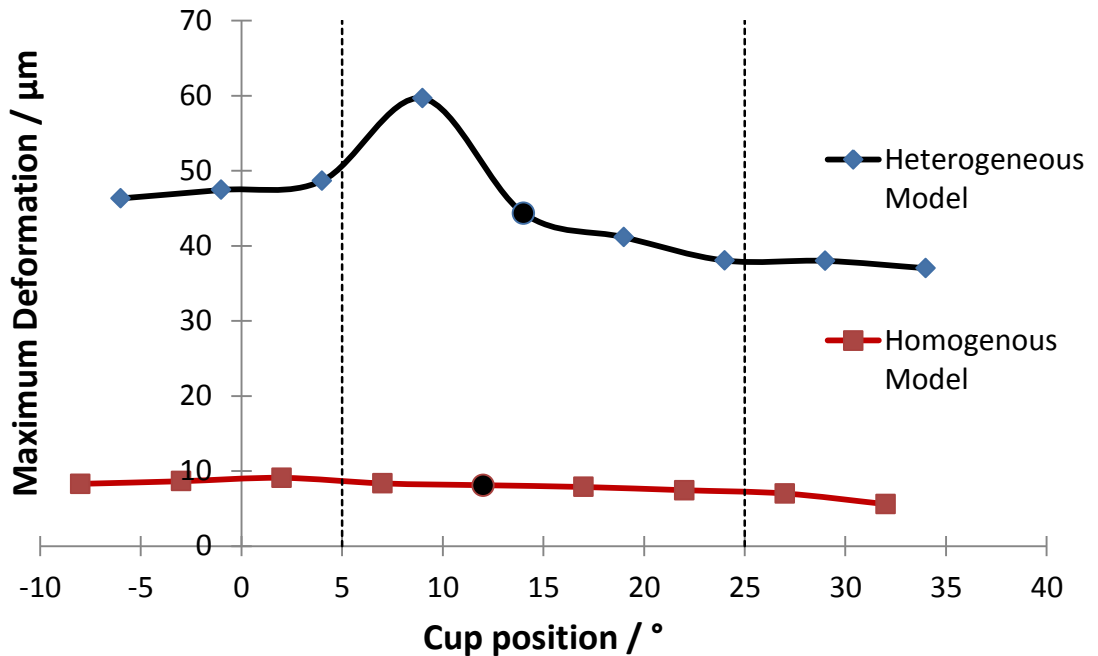


Figure 5.27: Cup deformation for the heterogeneous and homogenous model with different angles of version in young pelvis 1

Deformations were found to be sensitive to variations in cup version between the upper and lower limits of the safe zone in both the young, $t(6)=2.51$, $p<0.05$, and old models, $t(6)=2.64$, $p<0.05$. In general greater deformations were observed with lower cup versions in the young models and with a higher version in the old models. Deformations appeared to increase with increasing abduction however these were not statistically significant in either age group ($p>0.1$). The sensitivity of the cup to changes in version when compared to changing its abduction angle is especially evident when comparing the normalised graphs of the data, Figure 5.28 and 5.29.

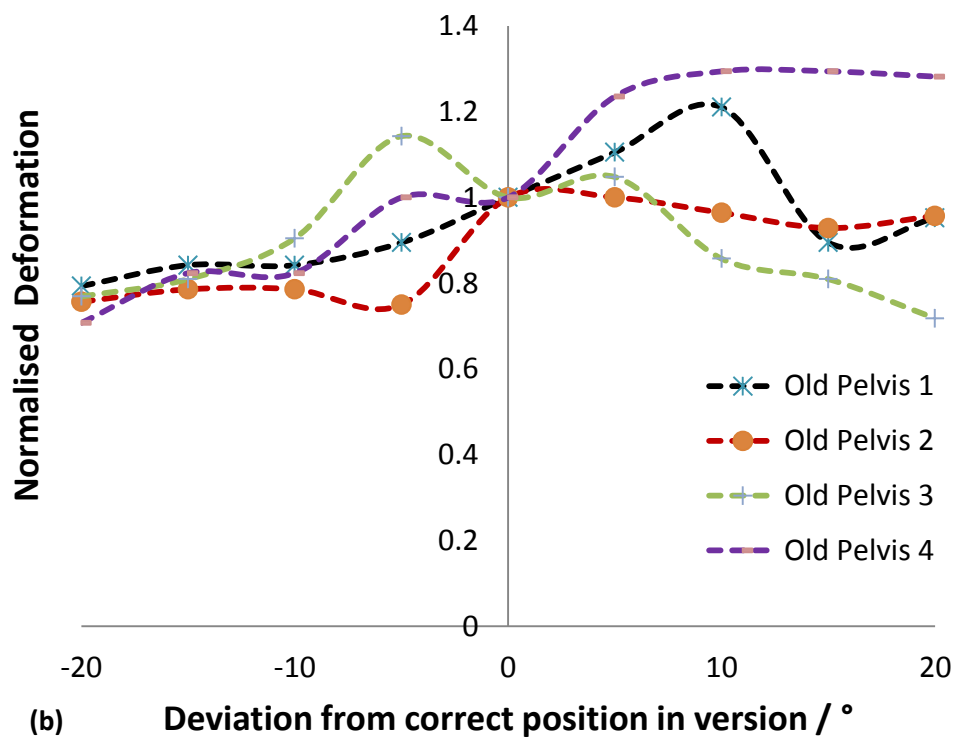
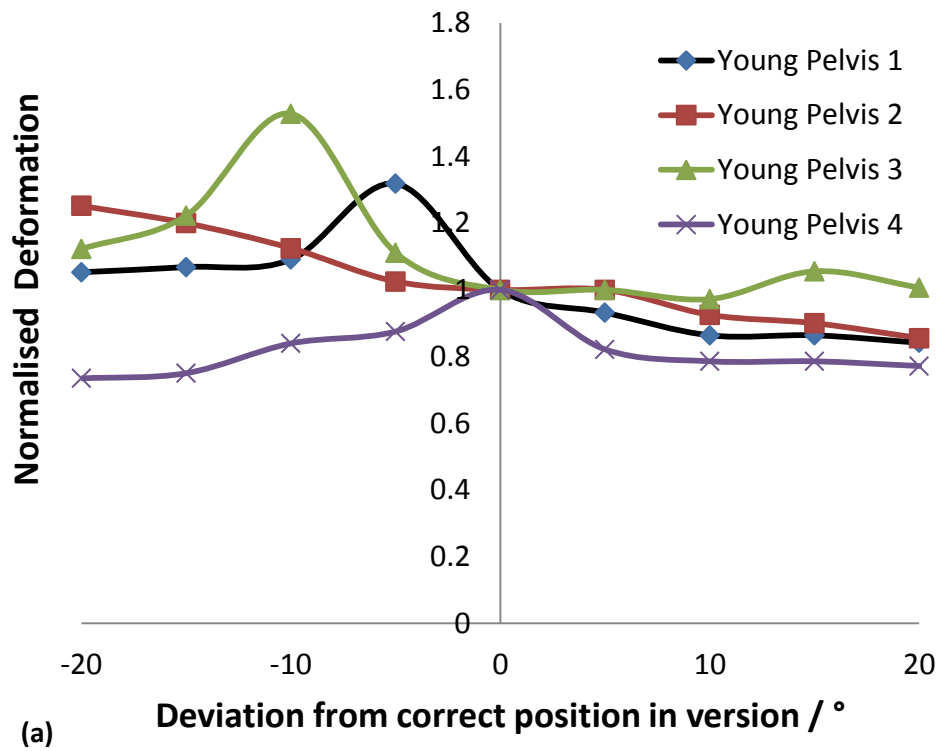


Figure 5.28: Change in the deformation of the cup, normalised to cup deformations in the optimum position, as its position was varied in version in (a) the young pelvis models and (b) the old pelvis models

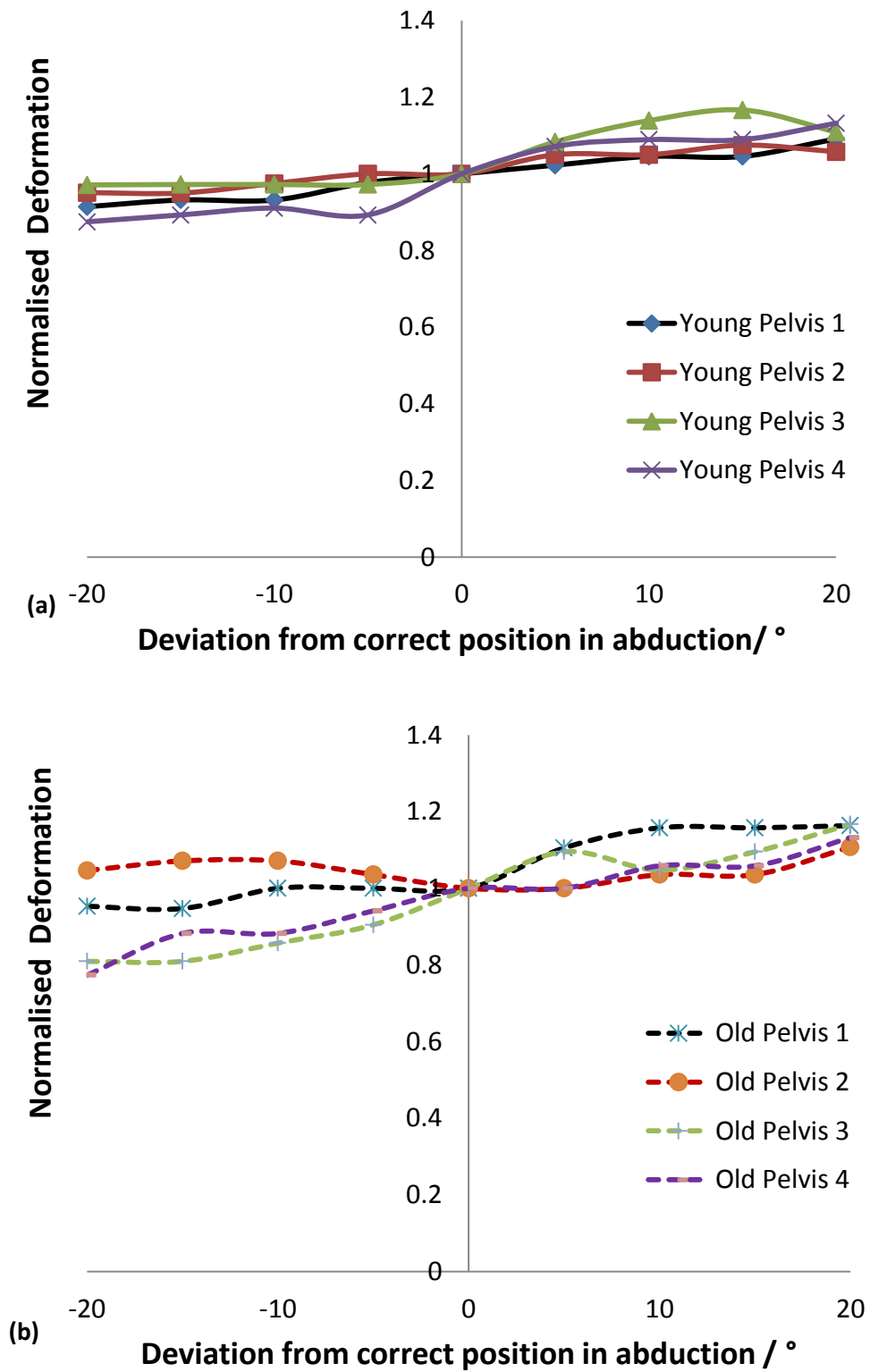


Figure 5.29: Change in the deformation of the cup, normalised to cup deformations in the optimum position, as it position was varied in abduction in (a) the young pelvis models and (b) the old pelvis models

5.4.2 Discussion

The variability in the deformation observed when the position of the cup was changed in the direction of version, particularly between the young pelvis models was notable. This is in contrast to a previous experimental study which did not find these changes in deformation of the acetabular component to occur when the cup was orientated at 0° and 15° with respect to the underlying support [Fritsche et al., 2008]. The peak deformations that were determined in the current study were similar between all the young pelvis models however there were notable differences in the orientation of the component at which they occurred.

In general, a slight increase in the deformation of the component was observed when the abduction angle was increased. However this was not as sensitive to changes in its orientation as for changes in version. When the cup is tilted in version, the stiffer bony regions of the cavity maintain contact with the cup close to its rim. It has been suggested that the greatest deformations occur when there is contact in the region of the rim [Spears et al., 1999]. However when the cup is tilted in abduction, bony support on one half of the cup will always move further away from the rim.

Inevitably the precise positioning of the component in the acetabulum will depend on the individual surgeon [Valle et al., 2005]. Using the example of Young Pelvis 1 from Figure 5.26a, a comparatively small difference of 5° in the cup's position resulted in an increase in the deformation by 14 µm. However the same difference of 5° with Pelvis 2 results in a much smaller change, by only 1 µm. This variation can be explained by considering that the pelvis models had significant differences in terms of the bony support provided to the components which were visibly apparent, particularly at the rim, resulting in variations in the amount and regions of the cup that were in contact with bone. Figure 5.30 shows an example of the cup inserted in the same orientation into two different young pelvis models. It can be seen that whilst there is full bony contact in the ischeal and ilial regions of the pelvis, the sides of the cup are clearly supported by different amounts. In young pelvis 2, the cup rim next to the direction of pinching was exposed and would need to be rotated further in the angle of version to experience a similar degree of cup support as pelvis 1.

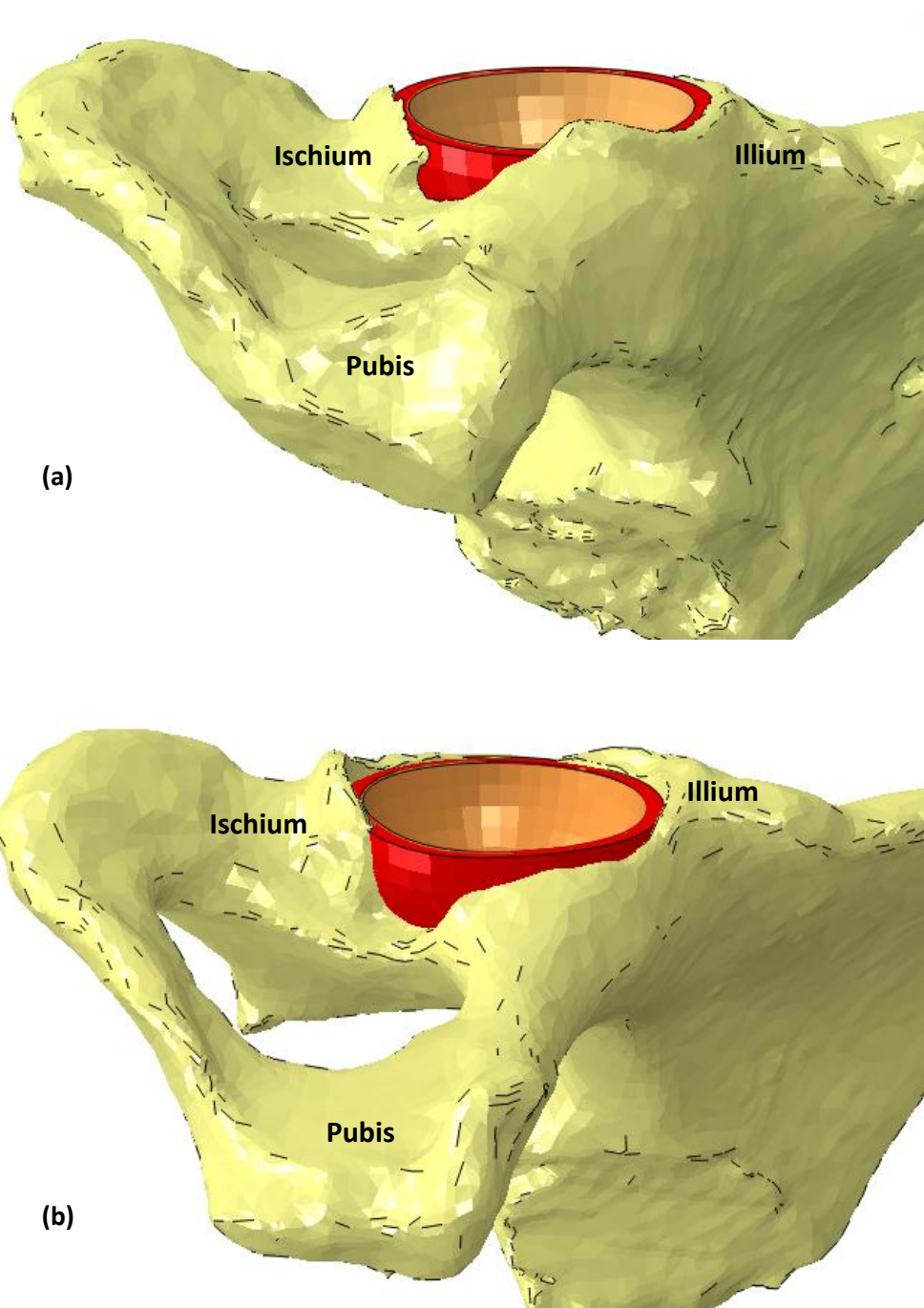


Figure 5.30: Cup impacted in the same orientation into **(a)** young pelvis 1 and **(b)** young pelvis 2. Differences in the support at the rim between the two models are clearly visible.

It is important therefore that a surgeon is aware that the influence of varying cup position on deformation is strongly dependent on both the local anatomy and bone quality of the individual patient [Allan et al., 2007; Clarke et al., 1982]. Whilst foam models can provide a good understanding of cup deformation behaviour clinically, this study highlights the limitations of using polyurethane foam FE studies to predict deformation, which may not be an appropriate representation of patients. Variations

in bone stock, density and support, influenced by age, sex and health [Brinckmann et al., 1981; Tauge, 1989], will result in significant differences in the material properties of the pelvis and can be more accurately represented with FE models developed from CT data.

It was found, with Pelvis 3, that a combination of decreasing the version angle and increasing the abduction angle, resulted in an increase in deformation to 61 μm . In this instance, the version angle was on the lower limit of the safe zone whilst the abduction angle was outside the upper limit by 4°. Whilst this higher deformation was still within the typical clearances for this component [Yew et al., 2006], the consequences of elevated deformations when coupled with other factors may influence component performance. It has been reported that rim loading can occur clinically in thin components orientated at high abduction angles of greater than 55° [De Haan et al., 2008]; these factors may lead to increased wear which may in turn be worsened due to large cup deformations [Markel et al., 2010; Kennedy et al., 1998]. In the current study it was shown that increasing the abduction angle to outside the safe zone, did result in greater deformations, although the highest deformations observed as the version angle was varied were found to occur close to the upper and lower limits of the safe zone. In general positioning the cup in the middle of the safe zone in both orientations resulted in lower deformations. It is of note however that there was little correlation between the optimum cup position and the lowest deformations achievable within the safe zone. This indicates that optimum position is not guided by minimising deformations but rather to minimise wear, edge loading and other factors that may contribute to component failure.

Figure 5.23 shows the typical direction of pinching that occurred on the acetabular components after insertion. These pinch points are in a similar position of approximately 150° to each other as has been reported previously [Krebs et al., 2009] and that was simulated in the previous chapter. In the FE foam model the angle of the cup with respect to the cavity was varied such that it was misaligned in a similar plane to version. Misaligning the cup in this anatomical orientation resulted in the greatest deformations when coupled with the pinching of the stiffer ischeal and iliac columns [Widmer et al., 2002], as opposed to varying the orientation relative to the abduction angle. This suggested that cup deformations may be more sensitive to its position in

version than abduction, and is supported by the results of the current study on more anatomically relevant models.

5.5 Introduction of an Eccentricity in the Cavity during Hand Reaming

During the reaming of the acetabular cavity, the movement of the mechanical reamer may be controlled by either hand by a surgeon or alternatively with the assistance of a robot driven by computational software. It has been shown that hand reaming can result in a deviation from the desired hemispherical cavity [Macdonald et al., 1999] and it has been suggested that this may contribute to higher cup deformations [Ong et al., 2009]. It has also been reported that in some patients a *gothic arch* may be present in which the supra-pubic region is unusually arched, Figure 5.31. When a gothic arch is present, perfect reaming of the acetabulum may still result in a non-hemispherical cavity, creating a gap between the impacted cup and the bone in the region of the gothic arch. This feature however is more common in male patients and was not found to be present in any of the pelvis models available for the current study.

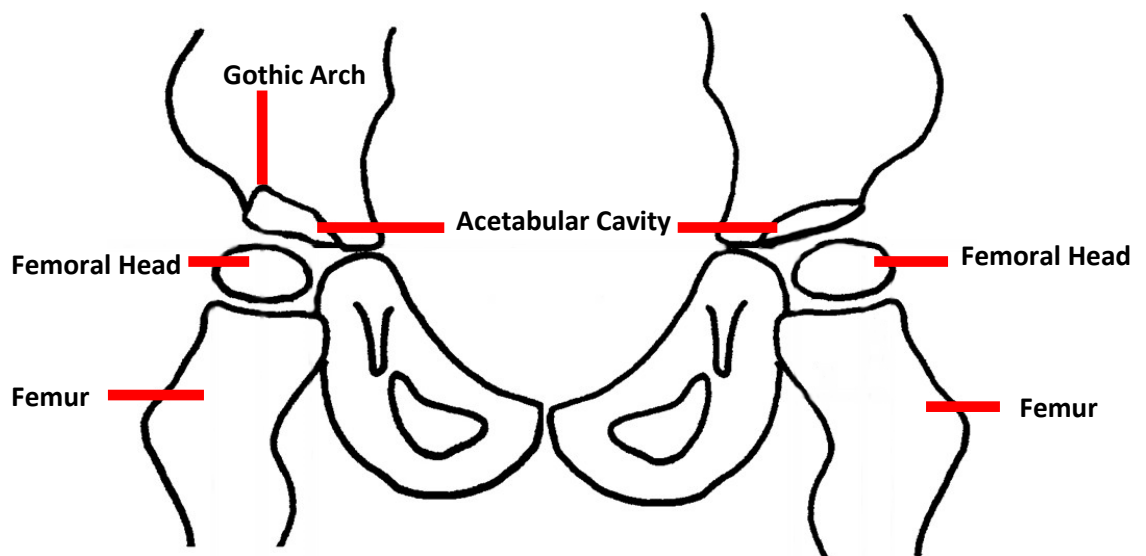


Figure 5.31: Cross sectional schematic showing the presence of a presence of a gothic arch in the acetabulum of the right hemi-pelvis. The absence of the gothic arch is illustrated in the left hemi-pelvis

The influence of introducing an eccentricity into the cavity following reaming was investigated. A single young pelvis model was considered and the stiffer regions of the iliac and ischeal columns were identified by observing the location of the pinch points on the components from earlier simulations. An eccentricity was simulated into the

regions that were less stiff and was achieved by translating the sphere during Boolean subtraction by the desired amount bisecting the pinch points. The acetabulum was reamed to produce an ellipsoidal cavity with the directions of the minor axis located between the iliac and ischeal columns (Figure 5.32) and its length set to 55 mm. The length of the major axis of the ellipse was varied between 55.5mm to 58 mm and the effect of increasing the extent of its eccentricity on deformation was investigated.

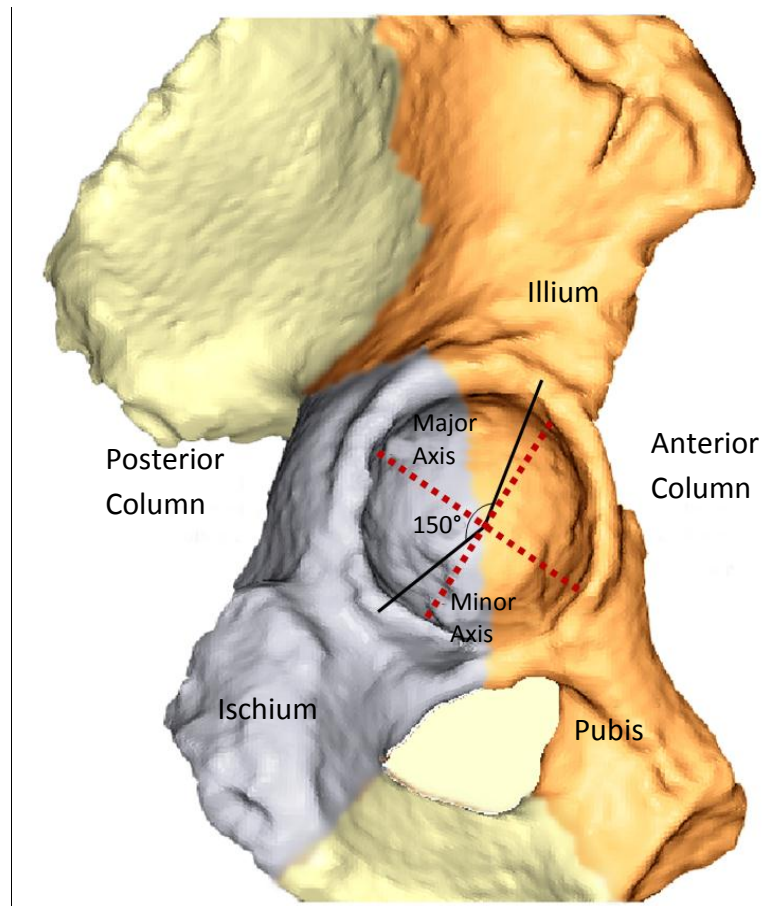


Figure 5.32: The position of the major and minor axis in the ellipsoidal cavity formed during hand reaming

5.5.1 Results

Figure 5.33 shows that increasing the eccentricity of the cavity resulted in greater deformation of the component. The greatest effect was found to occur when the size of the major axis of the ellipse was increased to 1 mm greater than the diameter of the cup, increasing the deformation by 14 μm (approximately 30%). Further increasing the size of the major axis did not considerably alter the deformations.

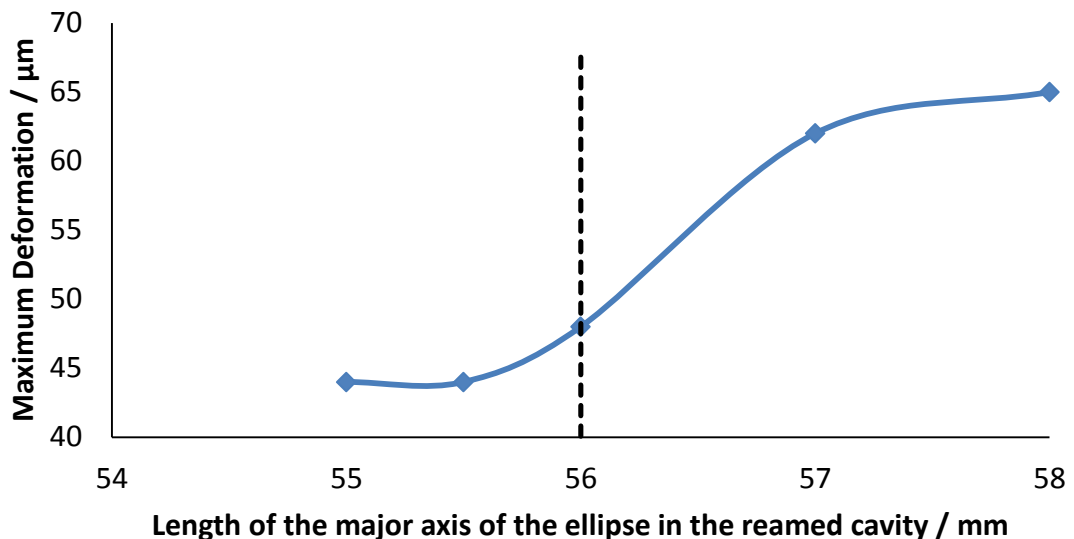


Figure 5.33: Maximum cup deformations observed with increasing deviations from the spherical cavity during hand reaming.

5.5.2 Discussion

The introduction of small eccentricities during hand reaming, which would be unnoticeable in the clinical setting [Macdonald et al., 1999], may contribute further to increased component deformations. The consequences of this would be heightened when using a higher interference fits, thinner components with a lower stiffness and in younger patients with stiffer bony regions. The deviations in the hand reamer simulated in the current study represent a worst case situation in which the length of the minor axis is unchanged. The large increase in deformation is expected as when the major axis is lengthened to larger than the diameter of the cup, the sides of the cup in this region will be completely unsupported by bone. The effect of the pinch along the minor axis between the Ilium and Ischium regions will therefore be heightened. If the minor axis is lengthened during hand reaming, then the pinch effect would lessen, leading to lower deformations.

5.6 Definition of Time Dependent Properties in the Pelvis Cavity

Abaqus allows for experimental data to be entered when defining time dependent material properties when sufficient data relating to the Prony series of the material is not available. Viscoelastic creep properties of cancellous bone were therefore defined in a young pelvis model, using short and long term experimental creep data available for bovine cancellous bone from two different experimental studies [Mano, 2005;

Bowman et al., 1994]. The short term creep time was defined as between 0 and 1000 seconds, and the long term creep was defined as that occurring in a time greater than 1000 seconds. The data from the previous studies was normalised and their log-log curves obtained (Figure 5.34).

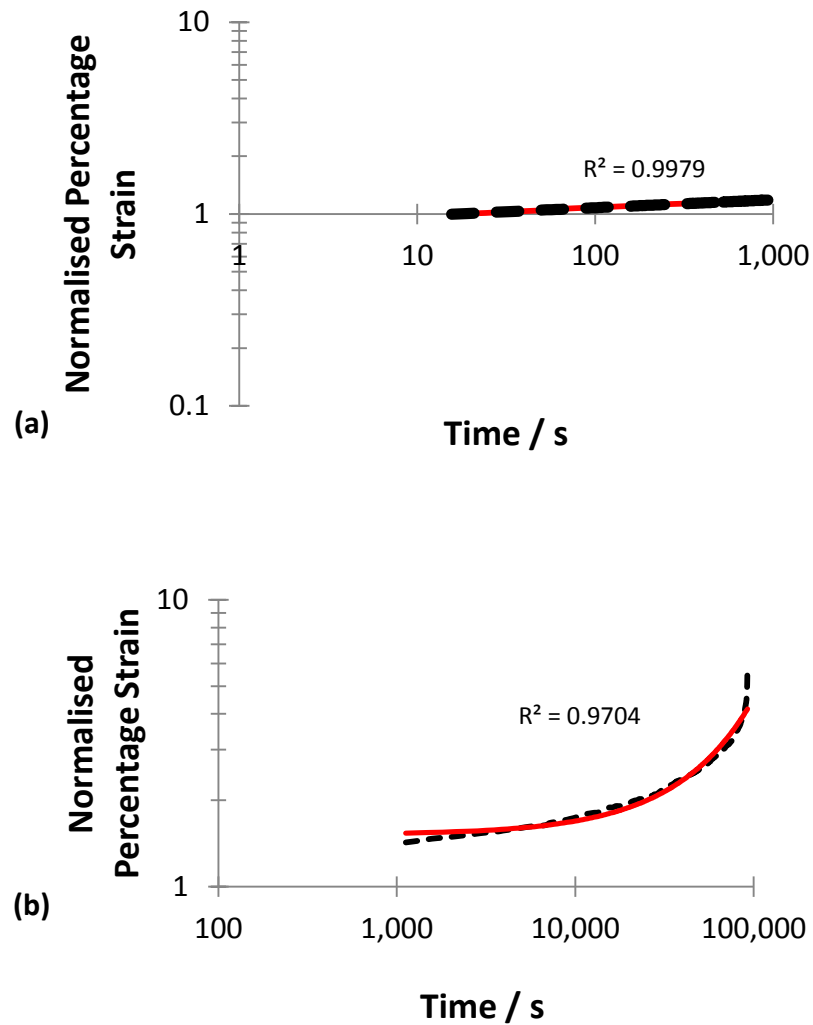


Figure 5.34: Normalised log-log (a) short-term and (b) long-term creep curve (Experimental is black dashed line)

It was found that the normalised short-term creep log-log curve had a very good fit to a power law (Equation 5.7), whilst the normalised long-term creep log-log curve had a very good fit to an exponential curve (Equation 5.8).

$$\varepsilon(t)/\varepsilon_0 = 0.8907t^{0.0415} \quad (t = 0 - 1000) \quad (5.7)$$

$$\varepsilon(t)/\varepsilon_0 = 1.52e^{0.0000109t} \quad (t > 1000) \quad (5.8)$$

Preliminary FE simulations resulted in very good agreement with the experimental data up to 100,000 seconds (approx 27 hours) and were considered as being suitable to evaluate the time dependant cup-bone behaviour up to this time period.

It was noted that however that at the transition from the short term to the long term creep, at time 1000, there was a considerable increase in the value of the normalised strain from equation 5.7, of 1.19 to 1.53 from equation 5.8. In order to compare the effect of this discrepancy between the two equations on the relaxation of the deformation following insertion, the simulation described in the next paragraph was carried out twice:

1. Using the two short term and long term equations together in a single time dependent law.
2. Extrapolating equation 5.8 back to time 0 and removing equation 5.7 from the material property definition.

Time dependent properties were defined to the pelvis model and a single 56 mm Co-Cr cup was inserted in the clinically correct position with an interference fit of 1 mm. After the cup had been fully seated, the model was transferred into a static simulation environment, and a predefined field was created with the final state of the model immediately after impaction. The simulation was then allowed to carry on for a time period of 10^6 seconds and the long-term cup deformation behaviour with the addition of viscoelastic properties was obtained.

5.6.1 Results

Figure 5.35 shows the long term relaxation of the deformation of the cup following impaction. It was observed that there was no difference in the change in deformation in the first 1,000 seconds between using separate equations of the short term and long term creep and using only the long term equation. In this time period the deformation relaxed by only 0.4%. A relaxation by 10% in the deformation of the cup, from 44 μm to 40 μm after a period of approximately 24 hours was observed. A further relaxation of only 0.4% of the deformation occurred after a further 10 days relaxation.

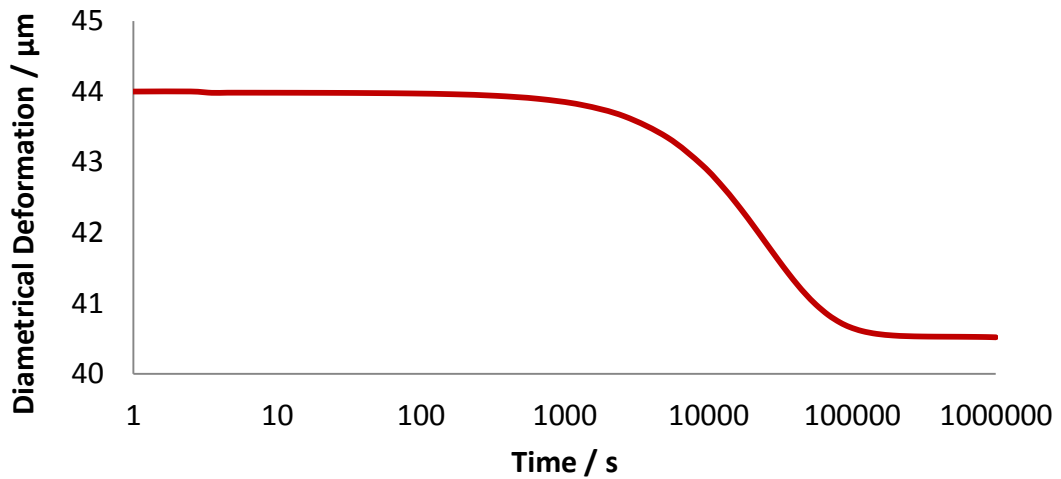


Figure 5.35: Relaxation of the deformation of the 56 mm Co-Cr cup after insertion into a young pelvis model

5.6.2 Discussion

The full extent of the problems caused by cup and shell deformation are currently unknown; a number of previous studies have reported values for cup deformations that may be significant enough to cause joint locking, poor lubrication and poor seating of ceramic and polyethylene cups into metal shells [Hogg et al., 2010]. These studies have made a number of assumptions and simplifications in their models which bring a level of uncertainty to their conclusions. One such simplification has been the omission of time dependency in material models and effect of this on the long term deformation behaviour of the inserted cup [Yew et al., 2006; Jin et al., 2006; Ong et al., 2009; Hogg et al., 2010]. In this study, experimental creep data was defined in a reamed pelvis cavity, where it was found that once the cup was fully seated there was a relaxation of the observed deformation. The reduction in cup deformation appeared to reach a steady state after approximately 24 hours and this finding is in agreement with the study by Deligianni et al. [1994] who found that stress relaxation reached a steady state in approximately 24 hours and with the study by Pawlikowski et al. [2008] who found that their experimental creep curves reached a steady state after approximately 100,000 seconds. The final deformations of approximately 40 μm observed, reduced by approximately 10%, are comfortably within the clearances specified for this cup design. A reduction of approximately 4 μm is similar to the relaxation that was observed experimentally in the previous chapter using Airex foam. Whilst the stiffness of the foam was too low to represent the immediate cup

deformation behaviour in the pelvis, a higher grade of the foam could be used and to model short and long term cup deformation.

Squire et al. [2006] found no change in the deformation of a shell twenty minutes after insertion in vivo. Whilst this is a comparatively short time frame, the results of the current study support the in vivo observations. It may also be the case that the longer term remodelling of the surrounding bone during weight bearing may alter the distribution of forces at the rim, resulting in a further reduction in deformation [Ng et al., 2007].

The suggestion by previous studies [Yew et al., 2006; Jin et al., 2006; Ong et al., 2009; Hogg et al., 2010] that the inclusion of time dependency would result in notably lower deformations appears to be untrue; whilst there is a slight reduction over time, the immediate deformation following impaction will likely be maintained until the patient begins weight bearing.

5.7 Influence of the Material and Geometry of the Acetabular Component

The effect on deformation of impacting a Ti-6Al-4V shell, with a lower modulus than the CoCrMo cup was initially investigated. In the previous chapter a Taguchi Design of Experiment (DOE) was used to demonstrate that the cup diameter and its wall thickness in the polar region were strongly related to the stiffness of the component and the corresponding deformations. These simulations however were carried out using idealised foam models to represent the complex structure of the pelvis. Using the anatomically correct models developed in the current work, the DOE was repeated to confirm whether the component design behaviour observed in the foam models was also present when inserted into the pelvis.

5.7.1 Methods

The geometry of the Ti-6AL-4V shell modelled was such that it had an outer diameter (\varnothing) of 56 mm and depth (d) of approximately 25 mm, and a wall thickness of 3.4 mm at the rim (Tr) and 3.4 mm at the pole (Tp). The shell was inserted into the clinically correct position, as determined by orthopaedic surgeons, in a young and old pelvis and the deformation observed was compared to previous experimental studies carried out with a similar shell design.

Using the DOE the influence of changes in the depth and thickness at the rim and pole on the deformation of the CoCrMo cup, and also the Ti-6Al-4V shell, following impaction was investigated. The cup or shell diameter was not varied in this study as it had previously been established by orthopaedic surgeons that a 56 mm diameter cup was the most appropriate size to use with the pelvis models. Significantly over or under-reaming the cavity to accommodate components of varying diameters would result in variations in the amount of cortical bone that was present below the cup, which could skew the results of the DOE. A diametrical interference of 1 mm was used and a single young pelvis was considered for this part of the study.

The 3 control parameters of the components dimensions were varied between 3 levels (Table 5.3). The Taguchi Orthogonal Array system was used to identify 9 combinations of the parameters, out of a total of 3^3 , to be simulated for the cup and shell, therefore considerably reducing modelling and analysis time. The observed component deformations from each of the simulations were used to calculate the signal-to-noise ratio (S/N ratio) for each of the control parameters as:

$$S/N \text{ Ratio} = 10 \text{ Log}_{10} [\text{Mean of sum of squares of \{measured deformation} - \text{ideal deformation}\}] \quad (5.9)$$

The ideal deformation was considered as being 0 μm and it was considered that the higher the value for the S/N ratio for each parameter, the greater the influence that parameter had on the deformation of the cup or shell.

Table 5.3: Cup and shell parameters used in the pelvis Taguchi DOE

Parameter	Cup Level			Shell Level		
	1	2	3	1	2	3
Thickness at rim /mm	2.5	3.3	4	3.3	4.5	5.5
Thickness at pole /mm	3.3	4.7	6	2.5	3.5	4.5
Depth /mm	17.8	20.2	22.5	20	22.5	25

5.7.2 Results

Impaction of a Ti-6Al-4V shell into a young and an old patient pelvis model resulted in maximum deformations of 248 and 172 μm respectively.

Table 5.4 summarises the S/N ratios obtained when the cup and shell dimensions were varied and inserted into the young pelvis.

Table 5.4: Showing the S/N ratio for the different cup parameters using the Taguchi DOE

	Thickness at Pole	Depth	Thickness at Rim
CoCrMo Cup	3.37	0.25	0.29
Ti-6Al-4V Shell	3.78	0.36	0.19

5.7.3 Discussion

The deformations that occurred in the Ti-6Al-4V shell were considerably larger than those observed with the Co-Cr cups due to their lower material stiffness [Ratner et al., 2004] and also as a consequence of having a much smaller wall thickness at the pole, which has been shown to result in greater deformations [Hothi et al., 2011]. The values are comparable to the deformations of between 10 and 570 μm observed intraoperatively by Squire et al., [2006] using a similar component design, who also reported a relationship between the compressive forces on the component and the quality of the underlying bone. In the current study, differences in deformation of the acetabular shell were largely due to differences in the modulus of the two pelvis models, as expected [Widmer et al., 2002] and is in agreement with an earlier cadaveric study which concluded that there was a strong relationship between bone mineral density and acetabular shell deformation [Markel et al. 2010].

The DOE confirmed the findings from the previous chapter using foam models that increasing the polar thickness resulted in notably lower deformations for both the cup and the shell. Decreasing the diameter was shown in the foam model in the previous chapter to also result in lower deformations and it is expected that this would also be the case in the pelvis. The depth of the components and the rim thickness were the least influential on observed deformation, as indicated by the comparatively lower values for the Taguchi Signal/Noise (S/N) ratio obtained. It is of note that table shows that the titanium shell, which has a lower stiffness than the CoCrMo cup, is more sensitive to changes in its dimensions.

5.8 Conclusions

Using CT data from patients a number of finite element models were developed which showed that patient age, cup orientation and extent of acetabular reaming affected the local cup deformation. The results suggest that even with optimal cup version within the safe zone the chance of high cup deformations, particularly in younger patients may still occur. Excessive deformations in comparison to local clearances may occur as a culmination of a number of contributing factors, such as if a thin-walled, large diameter cup or shell is impacted with a high interference into young patients with high bone densities. Additionally, deformations could be further increased if an ovality of the cavity is introduced during hand reaming. This may help to explain why failures occur in well positioned cups and why high metal ions levels and wear rates can be found in retrievals that were positioned within the safe zone.

Chapter 6

Discussion, Conclusions and Recommendations for Future Work

Large MoM articulations were popular due to their perceived advantages of having a lower risk of dislocation and lower wear rates [Engh et al., 2009]. 15% of all patients receiving a hip replacement in 2009 had either a resurfacing or THR using a large diameter MoM bearing surface [National Joint Registry, 2010]. The short term survival rates of these components were found to be excellent [Lombardi et al., 2004]. However recently the mid to long term clinical experience of MoM components has indicated clinical failure rates being notably greater than expected. The average failure rate for resurfacing implants at seven years is 11.8% whilst it is higher for large diameter MoM total hip replacements at 13.6%, compared with failure rates of 3.3% - 4.9% for other material combinations at seven years [Cohen, 2011]. In addition there is a growing concern related to pseudotumours and metallosis in some patients possibly due to the presence of metal ions generated from the bearing surfaces and wear debris [Haddad et al., 2011].

A range of factors have been suggested as contributing to increased rates of revision procedures, including:

- the design of the components
- surgeon technique, such as in component positioning and impaction
- the sensitivity of individual patients to metal ions and particles.

Analysis of retrieved MoM components following revision surgery has demonstrated that the need for revision is often associated with increased rates of wear at the articulating surfaces [Langton et al., 2010]. This may be an indicator of a poor tribological performance of the bearing, resulting in a greater number of metal ions which can lead to adverse tissue reactions.

Control of manufacturing of these bearings indicates that the departure of roundness of the cup should not be larger than 15 μm [ASTM F2033]. The work presented in this

thesis found that maximum local deformations at the rim of the cup following impaction into a pelvis model, were approximately 65 μm . This would clearly result in a departure of roundness beyond the specified tolerances for sphericity, potentially impacting on the performance of the hip implant by reducing the conformity of the bearing thereby increasing the friction between the surfaces, ultimately resulting in greater wear.

The issue of changes in cup (or head) sphericity due to localised deformation following insertion is closely related to the influence of changes in the clearance between the femoral head and the acetabular cup, which is key in determining optimal joint tribology and wear behaviour. It has been reported [Dowson et al., 2004] that to ensure that optimal mixed lubrication is maintained in hip implants that the diameter of the head should be as large as practical and that the clearances should be minimised to be as low as possible. If the clearance is too large, such that the cup diameter is much bigger than that of the head [Figure 6.1], there will be low conformity of the components, resulting in a smaller contact area, with a thinner lubrication film over this region, resulting in greater friction and wear.



Figure 6.1: Cup diameter much larger than head diameter, which can result in a small contact area [adapted from Wright Medical, 2007]

It was shown in a hip simulator study [Dowson et al., 2004] that there was a strong relationship between clearances as low as 83 μm for a 54 mm cup and low rates of wear. Lower clearances will result in a larger contact area with a thicker lubrication film generated and therefore lower friction and wear. However for head diameters greater than 36 mm, clearances should be a minimum of 70 μm [ASTM F2033] to prevent high torques and possible seizure of the bearing. As with deviations from sphericity, the maximum deformations reported in this thesis suggest that if these

minimum clearances are utilised, then factors such as contact between the cup rim and head and a local transition into boundary lubrication are highly likely, Figure 6.2.

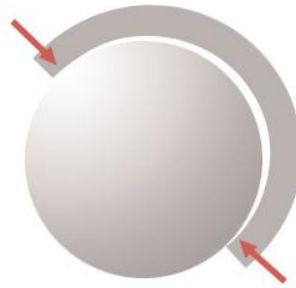


Figure 6.2: Contact between cup rim and head possible due to excessive deformations [adapted from Wright Medical, 2007]

Compensation for this deformation may be to design components with higher pre-insertion clearances which decrease to the optimal size due to cup deformation upon impaction. It has been demonstrated in this thesis that diametrical deformations are influenced by a range of factors including patient specific bone density and variations in surgical technique (for example when positioning the cup). As such patient specific models could be used to predict in each case the extent of deformation that would occur in a patient and therefore by how much to compensate for this in the selection of the cup design. However factors such as bone remodelling or patient weight bearing may result in the relaxation of the deformation over time which could mean that the clearances that were initially optimal may increase with time leading to an increase in friction and wear. It has been reported [Dowson et al., 2004; Rieker et al., 2005] that an increase in the overall bearing clearance from 100 to 300 μm can result in an increase in the wear rates by up to four times. Other studies [McKellop et al., 1996; Chan et al., 1999; Brockett et al., 2008] have also reported an increase in wear rates of up to sixteen times with greater clearances as high as 1.7 mm, and also notable increases in friction and incidences of squeaking between the components. More significantly however is the demonstration in the current thesis that diametrical deformation of the cup will always result in an ovality of the component. This means that as there are localised regions where there is a reduction in the cup diameter due to pinching, there will equally be regions of expansion of the diameter of the cup. As such there will be regions in the implant where the localised clearance is smaller than desired and in other regions where the localised clearance is larger than intended, potentially causing additional problems with fluid film lubrication.

For low wear conditions to be achieved the inserted components must also be seated and orientated correctly such that the centres of the acetabular cup and the femoral head are concentric with each other [Fisher, 2011]. In these situations contact and wear between the two bearing surfaces occurs well within the intended polished regions of the acetabular cup, Figure 6.3.

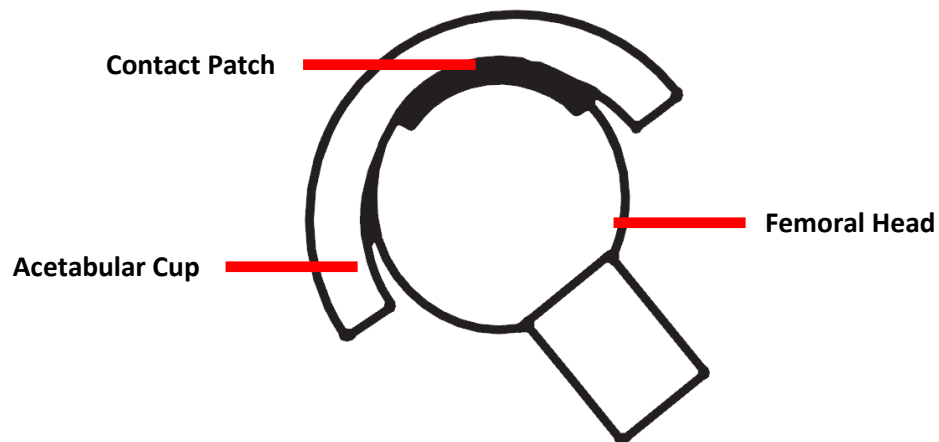


Figure 6.3: Femoral head contact within the polished region of the cup [adapted from Fisher, 2011]

Changes in these ideal articulating requirements could result in the rim (edge) of the acetabular cup coming into contact with the femoral head, Figure 6.4.

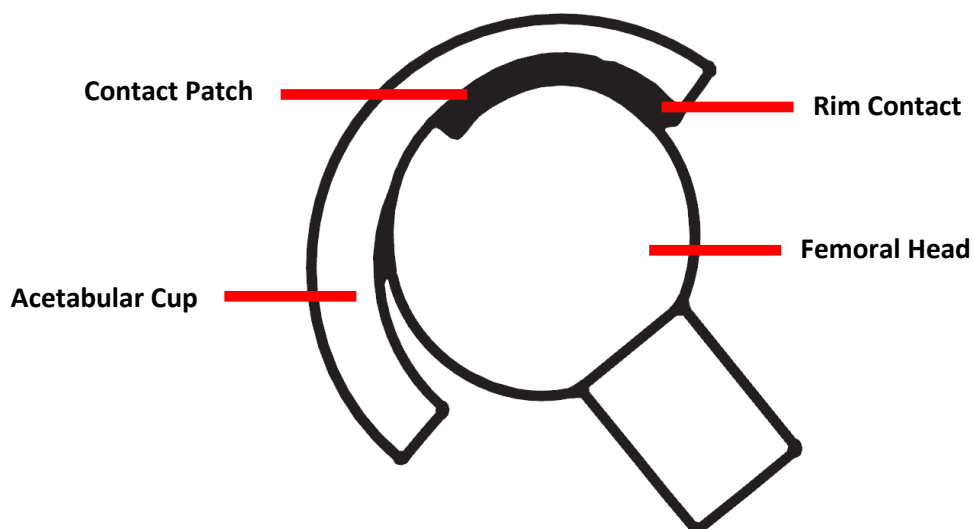


Figure 6.4: Rim of acetabular cup in contact with the femoral head [adapted from Fisher, 2011]

Rim contact can disrupt the distribution of fluid-film lubrication resulting in considerably higher rates of wear [Shimmin et al., 2010]. Rim contact is known to occur for a number of reasons which can all be related to the condition of poor positioning of

the relative position of the head and cup. This can be as a result of surgical error or poor support from the underlying bone causing a shift in the position of either component. It has been reported that 64% of patients requiring revision surgery following metal-on-metal resurfacing arthroplasty, did so because of malpositioning of the acetabular component [De Haan et al., 2008]. It has been shown that a translation of the components by less than 0.5 mm can result in rim contact in order to maintain concentricity [Mak et al., 2002]. Rim contact is also known to occur in acetabular cups orientated at high abduction angles and it has been reported that the particles generated through these wear mechanisms are larger (in the order of microns) than those generated in ideal conditions [Fisher, 2011]. These may be more likely to become embedded in peri-prosthetic tissue and may explain the adverse reactions experienced in some patients. It has been shown in a hip simulator study [Angadji et al., 2007] that at cup abduction angles of 60°, the wear zone of the cup reaches the rim, suggesting that rim contact occurs, interrupting fluid entrainment to the rest of the bearing surface. Additionally there may be high concentrations of stress in these regions which may be further increased due to the deforming forces acting on the cup from the underlying bone. In the study by Angadji et al. [2007] head contact is very close to the rim of the cup when the cup angle was orientated at 50°. However this study did not consider the influence of cup deformation. A local reduction in cup diameter in this situation may have been sufficient to result in rim contact; in the current work deformations greater than 60 µm were able to be generated for a cup inserted into a young pelvis with an abduction angle of 50°.

There are a number of predictable factors that can be used to explain the reasons for high wear and early failure. These, as discussed earlier, can include malpositioning of the acetabular component but may also involve factors such as poor initial seating and fixation of the cup, leading to loosening. However unexpectedly high wear rates and failure have been found to occur in cups that appear to be correctly seated and well positioned in the pelvis [Haddad et al., 2011]. The findings of the current thesis suggest that diametrical cup deformations leading to localised reductions in the clearance between the head and cup may be an important consideration when attempting to explain the poor implant performance observed in some patients. Low clearances may appear to be desirable as they have been shown to reduce wear rates, particularly during the running in phase of the implant [Isaac et al., 2006], due to a better

conformity of the components. However this results in a larger contact area which means that there is a greater chance of rim contact than when larger clearances are used, Figure 6.5 [Underwood et al., 2012].

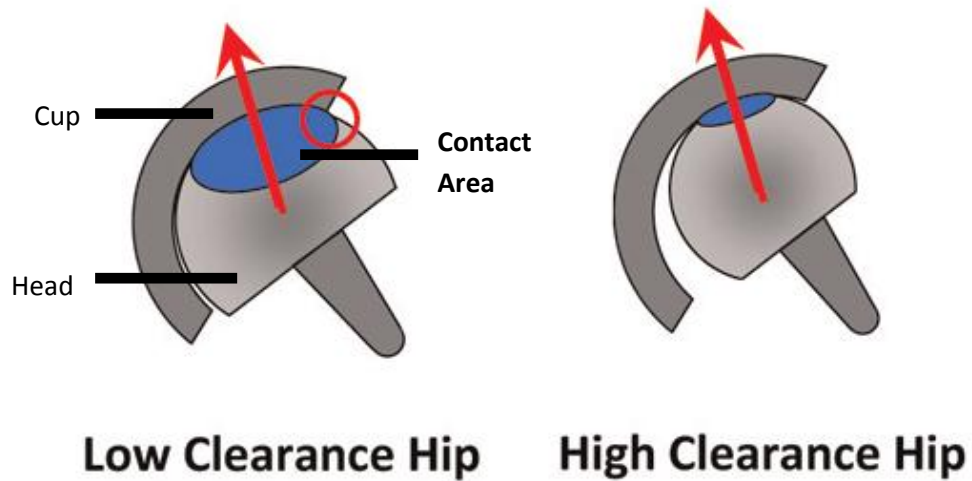


Figure 6.5: Larger contact area with a low clearance increases risk of rim contact [adapted from Underwood et al., 2012]

Hip simulator tests demonstrating improved wear characteristics with low clearances [Dowson, 2004; Brockett, 2007] have not tested the effect of high cup deformations; these implants, which appear to function well in laboratory tests under ideal conditions, may perform poorly in some patients due to the excessive pinching of the cup by the underlying bone resulting in rim contact, higher friction and wear rates and possibly early failure.

Earlier studies that have reported on cup deformations have been limited in their approach as they have largely assumed that cups are impacted such that the poles of the cup and cavity are aligned and that the cavity has been perfectly reamed [Yew et al., 2006; Ong et al., 2009; Hogg et al., 2010]. Additionally they have only considered single factors that may contribute to deformations. This thesis investigated the effect of a range of clinical and design parameters on the extent of cup deformation and tried to ascertain if these deformations are significant enough to alter the performance of MoM implants. A number of finite element models were developed that simulated the impaction of acetabular cups into the acetabulum. These models initially consisted of foam representations of the acetabulum which were used to identify key factors that

controlled cup deformations. Following this, anatomic models of the pelvis were created to simulate cup behaviour which would be likely to be observed clinically. The following summarises the key conclusions relating to the factors influencing cup deformation that were obtained throughout the work of the thesis and which together may aid understanding of why unexplained high wear rates and failures occur.

Method of Impaction

It was important that the impaction of the cup was appropriately modelled using a momentum rather than a static point load as has been extensively reported previously [Yew et al., 2006; Spears, 1999]. The use of clinically relevant impaction momentums, using an appropriate coefficient of friction between the cup and cavity, allowed for a more realistic estimation of the cups position following impaction, in terms of the polar gap remaining, and therefore a better estimation of the deformations that may occur clinically.

Impacting the rim of a CoCrMo cup via a cap between the impactor and cup, as is the case clinically, results in better seating of the component than when it is impacted on its inner polar surface; fewer impacts are required to seat the cup further into the cavity. Locking a rigid cap to the rim such that the entire construct is stiffened leads to notably fewer impacts to insert the component than either free rim or polar impaction. This may be significant to impactor design, allowing easier insertion of the acetabular cup and also minimising the polar gap between the porous surface of the cup and the bone, allowing for improved bone in-growth.

Cup-Bone Interference

Decreasing the diameter of the reamed acetabular cavity relative to the diameter of the acetabular cup makes insertion of the component more difficult. Full seating of the cup with interferences of greater than 2 mm may not be possible unless a large number of high momentum impacts are administered. This increases the risk of the surgeon mis-hitting the component, possibly resulting in the precise position of the cup to be altered. There is also a greater risk of damage to the implant or bone when using high momentum impacts. Cup deformations will be greater when implanted using higher interferences and is a consideration for surgeons, particularly when performed hip replacements on younger patients with stiffer boney support.

Cup Design

Titanium shells will deform by a greater amount than CoCrMo cups due to their lower material stiffness and generally thinner profile. The diameter and polar wall thickness of a cup has a considerable influence on its stiffness and therefore the extent to which it deforms. Larger diameter cups will deform more than cups with a smaller outer diameter. This can be minimised by increasing the thickness of the cup wall at the pole. Conversely, the wall thickness at the rim and the depth of the cup has comparatively very little influence on deformation. It is curious therefore that manufacturers do not appear to stiffen large diameter components to account for the increased deformations that can occur [Springer et al., 2011].

Time Dependency in Bone

It has been suggested by a number of authors [Jin et al., 2006; Yew et al., 2006; Ong et al., 2009] that the viscoelastic properties of bone would result in a relaxation in the deformation of a cup immediately following impaction. The work in the current thesis found that whilst a relaxation did occur, it was relatively small at approximately 4 μm and would not be expected to alter the deformation behaviour of the implant. Other factors such as bone remodelling would play a more significant role in the long term in influencing the change in cup deformation.

Patient Selection

Mont et al. [2007] and Allan et al. [2007] highlighted the importance of patient selection for hip resurfacing procedures, stating that bone mass and stability had a considerable effect on the revision rate. Clarke [1982] highlighted that clinical difficulties may include selecting patients with adequate bone stock and accurately reaming the acetabulum. The density and material stiffness of bone in patients is known to decrease with age. It was demonstrated in the current work using four patients from two distinct age populations that cups deformed by a greater amount when impacted into younger patients compared to older patients. However in patients suffering from osteoporosis, most often in older patients, a larger cup interference (approximately 2 mm) is often used [Callaghan et al., 2006] which may result in deformations closer to those observed in the younger patient models using a comparatively low interference of 1 mm.

Cup Orientation

It has been suggested [Birbeck et al., 2010] that an inexperienced surgeon may tend to position the cup flush with the acetabulum rim. It was also noted [Bosker et al., 2007] that the mean accuracy for cup placement was 11° in relation to the abduction angle. The results of the current study suggest therefore that even small cup misalignments in these situations which may not be noticeable in clinical practice may produce a significant ovality after insertion.

Cup deformations appear to be sensitive to variations in cup orientation in version within the safe zone, particularly for younger patients. Small changes of approximately 5° can increase deformations by up to 40 % in some patients, which could have a significant impact on normal articulation especially when low clearances are already present in the implant. This is in contrast to an experimental study [Fritsche et al., 2008] which did not find a difference in deformations when the cup was positioned at 0 and 15° with respect to the underlying cavity. The work of the current thesis also observed similar deformations at 0 and 15° to the cavity and highlights a limitation of investigating only two variations in orientation as in the previous experimental work. It is likely that the experimental study did not investigate smaller increments in the cup angle due to the practical difficulties of precisely orientating the cup in each position before impaction and ensuring that this orientation was unchanged during and after insertion. This also highlights a clear advantage of using finite element models to understand the effect of subtle changes in test parameters on cup behaviour which cannot be easily performed experimentally.

Even when a surgeon positions the cup to fall within the safe zone [Lewinnek et al., 1978], the cup deformations may still be problematic. The deformations may become significant beyond just monoblock metal cups if ceramic or polyethylene cups are seated into metal shells, causing them to be poorly seated or deforming excessively themselves; Markel et al. [2010] suggested that inaccurately positioning the cup or shell during insertion may lead to increased cup deformations. The occurrence of high deformations within the safe zone indicates that this range of recommended cup orientations is not guided by the consequences of cup deformation but by the minimising the risk of rim contact due to high abduction angles or other factors such as dislocations.

Cup Support

The underlying bony support to an inserted cup will significantly influence the extent of deformation. Cup deformations in the pelvis occur primarily as a result of a pinching between the ilial and ischeal regions, resulting in an ovality of the component. These pinch points are typically located at 150° to each, rather than at 180° as previous studies have modelled [Jin et al., 2006; Yew et al., 2006; Ong et al., 2009; Schmidig et al., 2010]. Variations in support may be due to age related changes in density or physical differences in the precise location of contact between patients.

Non Uniform Reaming of the Acetabulum

Deviations from a perfectly spherical cavity could result in small eccentricities during reaming which would not be noticeable by a surgeon clinically. This has been shown in the current thesis to increase deformations in the inserted cup by up to 30%.

6.1 Significance of Cup Deformation

Optimal minimum clearances have been reported to lie in the region of 80 to 120 µm [Jin et al., 2006]. The work of this thesis found that there is no parameter that individually would result in excessive deformations in comparison to these however it is clear that there are a number of factors, in terms of surgical technique, component design and patient selection which together could create articulation problems and increased wear rates. As a *worst case scenario*, problematic deformations would be most likely to occur if large diameter, thin walled cups are impacted with high interferences (>2 mm) into young patients with healthy, high density bone stock. These deformations could be exacerbated if the cups are unknowingly positioned at orientations in version within the safe zone that result in a greater pinching of the component and if the acetabulum is not perfectly reamed. On the other hand, lower deformations could still contribute to high wear or failure if they serve to compound the effect of other factors. For example if rim loading occurs due to a high cup abduction angle, the occurrence of deformation could increase the concentration of stresses in this region, resulting in accelerated wear rates or the occurrence of failure which may otherwise not have happened. Additionally, the use of low clearances to maintain low wear rates could be negated by cup rim contact occurring with the femoral head due to it experiencing pinching forces. It is recommended therefore that

a surgeon is aware of the primary factors that may most significantly affect the extent to which a cup deforms and is mindful of these during preoperative planning.

6.2 Recommendations for Future Work

The models developed in this thesis provide a resource which could be used in future studies to investigate a range of issues related to cup deformation and also more broadly to hip replacement procedures.

- Whilst the significance of age related changes on cup deformation has been demonstrated, another important consideration is that of gender. Latteier et al. [2011] reported that occurrence of cup revision, aseptic loosening and metal bearing complications were higher in women than men; the role of cup deformation in these differences requires exploration.
- This thesis has highlighted the main factors that will influence deformations however in order to identify the effects of more subtle variations between similar patient groups, it is clear that a larger number of models is required based on a wider population.
- Hip simulator studies that have demonstrated improved wear characteristics with low clearances should be adapted to simulate different levels of pinching of the cup and assess the impact that this has on the behaviour of the implant.
- It has been shown that metal cups can deform more at certain orientations and it is expected that thinner titanium shells would experience greater deformations. Of particular interest would be to investigate the effect of shell deformations on the seating of ceramic and polyethylene liners. This could be extended into modelling the wear of different components that have deformed excessively and compared with similar experimental data.
- Whilst the viscoelasticity of bone does not appear to substantially alter the cup deformations 24 hours after insertion, an important consideration in future

work should be the effect of bone remodelling on the changes in the behaviour of the cup in the long-term, following weight bearing.

- In a broader scope, it would be valuable to obtain experimental data relating to the determination of the optimum cup position in a single cadaveric pelvis model in a controlled environment by a number of orthopaedic surgeons. This data could be analysed to investigate if there was a relationship between the experience or techniques of the individual surgeons and the variation in cup position. The influence of variations in cup orientation on cup deformation could be used to inform surgeon decision making processes during hip replacement procedures.
- The use of cadaveric models would also be valuable to experimentally validate finite element models that had been developed using CT data.
- As the power and efficiency of computational methods increases, it may be feasible in future developments for surgeons to have access to models based on patient specific CT data that can be used during pre-operative assessment to highlight circumstances in which cup deformations could become problematic.

Appendix

Publications and presentations of the work of the thesis

Papers

Hothi HS, Busfield JJC and Shelton JC. 2011. Explicit Finite Element Modelling of the Impaction of Metal Press-Fit Acetabular Components, The Journal of Engineering in Medicine, Proc IMechE, Part H, 225: 301-314.

Hothi HS, Busfield JJC, Shelton JC. 2012. Deformation of Uncemented Metal Acetabular Cups following Impaction: Experimental and Finite Element Study. Submitted to Computer Methods in Biomechanics Biomedical Engineering.

Oral Presentations

Hothi HS, Busfield JJC, Shelton JC. 2010. Impact and Deformation of Press-Fit Metal Cups and Shells, 6th World Congress of Biomechanics, Singapore.

Hothi HS, Busfield JJC, Shelton JC. 2011. Influence of Mis-Alignment on the Deformation of Metal Press-Fit Acetabular Cups, IMechE, Engineers and Surgeons: Joined at the Hip III, London, UK.

Poster Presentations

Hothi HS, Busfield JJC, Shelton JC. 2010. Impact and Deformation of Press-Fit Metallic Hip Replacement Cups and Shells, 17th Congress of the European Society of Biomechanics, Edinburgh, Scotland, UK.

Hothi HS, Busfield JJC, Shelton JC. 2012. Deformation of Press-Fir Metal Acetabular Components following Impaction into Physiologically Relevant Models, Annual Meeting of the Orthopaedic Research Society, San Francisco, California, USA.

References

Adler E, Stuchin SA and Kummer FJ. 1992. Stability of Press-Fit Acetabular Cups, The Journal of Arthroplasty, 7: 295-301.

Allan DG, Milbrandt JC and Naughton, MB. 2007. Metal-on-metal hip resurfacing: The importance of patient selection, 8th Congress of the European Federation of National Associations of Orthopaedics and Traumatology, Florence, Italy: 11-15 May.

Amstutz HC, Dorey F O'Carroll PF. 1986. THARIES Resurfacing Arthroplasty: Evolution and Long-Term Results, Clinical Orthopaedics and Related Research, 213: 92-114.

Amstutz HC, Beaulé PE, Dorey FJ, Le Duff MJ, Campbell, PA and Gruen, TA. 2004. Metal-on-metal hybrid surface arthroplasty: two to six-year follow-up study, The Journal of Bone and Joint Surgery, 86 (A1): 28-39.

Amstutz HC and Le Duff MJ. 2005. Background of metal-on-metal resurfacing, The Journal of Engineering in Medicine, Proc IMechE, 220, H: 85-94.

Angadji A, Royle M, Smith S and Shelton JC. 2009. Influence of cup orientation on the wear performance of metal-on-metal hip replacements Proc IMechE, Part H: J Engineering in Medicine, 223: 449-457.

Archibeck MJ, Berger RA and Jacobs JJ. 2001. Second-Generation Cementless Total Hip Arthroplasty: Eight to Eleven Year Results, Journal of Bone and Joint Surgery, 83A: 1666-1673.

Aspenberg P and Van der Vis H. 1998. Fluid pressure may cause periprosthetic osteolysis. Particles are not the only thing, Acta Orthop Scand, 69(1): 1-4.

ASTM F2033. 2012. Standard specification for total hip joint prosthesis and hip endoprosthesis bearing surfaces made of metallic, ceramic and polymeric materials,

[online] Available at: <http://www.astm.org/Standards/F2033.htm> [Accessed 21/04/2012].

Babisch JW, Layher F, Amiot LP. 2008. The rationale for tilt-adjusted acetabular cup navigation, *The Journal of Bone and Joint Surgery*, 90: 357-365.

Baleani M, Fognani R and Toni A. 2001. Initial stability of a cementless acetabular cup design: experimental investigation on the effect of adding fins to the rim of the cup, *Artificial Organs*, 258: 664-669.

Bandak FA, Tannous RE and Toridis T. 2001. On the development of an osseoligamentous finite element model of the human ankle joint, *International Journal of Solids and Structures*, 38: 1681-1697.

Bauer TW and Schils J. 1999. The pathology of total joint arthroplasty. II. Mechanisms of implant failure, *Skeletal Radiol*, 28(9): 483-497.

Beaule PE, Le Duff M, Campbell P, Dorey FJ, Park SY and Amstutz HC. 2004. Metal-on-metal surface arthroplasty with a cemented femoral component: A 7-10 year follow-up study, *The Journal of Arthroplasty*: 17-22.

Biomet. 2009. ReCap Hip Resurfacing System, [online] Available: <http://www.biometcouk/resource/17148/FLH156%20ReCap%20Optech%202008pdf> [Accessed 21/04/2012].

Birbeck AP and Collins R. 2010. Surgical Prostheses, Intellectual Property Publication No: WO/2010/122281 Publication date: 28/10/2010.

Bordini B, Stea S, De Clerico M, Strazzari S, Sasdelli A and Toni A. 2007. Factors affecting aseptic loosening of 4750 total hip arthroplasties: multivariate survival analysis, *BMC Musculoskelet Disord*, 8: 1-8.

Bosker BH, Verheyen CCPM Horstman WG and Tulp NJA. 2007. Poor accuracy of freehand cup positioning during total hip arthroplasty, Archives of Orthopaedic and Trauma Surgery, 127: 375-379.

Bowsher JG, Nevelos J, Pickard J and Shelton JC. 2003. Do heat treatments influence the wear of large metal-on-metal hip joints? An in vitro study under normal and adverse conditions, 49th Meeting of the Orthopaedic Research Society, New Orleans, USA.

Bowman SM, Keaveny, TM, Gibson LJ, et al. 1994. Compressive creep behaviour of bovine trabecular bone, J Biomech 27(23): 301-310.

Brinckmann P, Hoefert H and Jongen HT. 1981. Sex differences in the skeletal geometry of the human pelvis and hip joint, Journal of Biomechanics, 14(6): 427-430.

Brockett CL, Harper, P, Williams S, Isaac GH, Dwyer-Joyce RS, Jin Z and Fisher J. 2007. The influence of clearance on friction, lubrication and squeaking in large diameter metal-on-metal hip replacement, Journal of Materials Science: Materials in Medicine, 19(4): 1575-1579.

Bronzino JD. 2006. The biomedical engineering handbook, 3rd Edition, CRC Press, USA.

Callaghan J, Rosenberg A and Rubash HE. 2006. The Adult Hip, 2nd Edition, Lippincott Williams and Wilkins, USA.

Campbell P, Beaulé PE, Ebramzadeh E, LeDuff M, De Smet K, Lu Z and Amstutz HC. 2006. A study of implant failure in metal-on-metal surface arthroplasties, Clinical Orthopaedics and Related Research, 453: 35-46.

Carter DR, Hayes WC. 1977. The compressive behaviour of bone as a two-phase porous structure. J Bone Joint Surg Am 59: 954-962.

Chan FW, Bobyn JD, Medley JB, Krygier JJ and Tanzer MD. 1999. Wear and lubrication of metal-on-metal hip implants, *Clinical Orthopaedics and Related Research*, 369: 10-24.

Chang J D and Billau K. 2007. Bioceramics and Alternative Bearings in Joint Arthroplasty, 12th BIOLOX Symposium Seoul, Republic of Korea September 7 - 8, 2007 Proceedings, Steinkopff-Verlag Darmstadt.

Charnley J. 1960a. Anchorage of the Femoral Head Prosthesis to the Shaft of the Femur, *The Journal of Bone and Joint Surgery*, 42B(1): 28-30.

Charnley J. 1960b. Surgery of the Hip Joint: Present and Future Developments, *British Medical Journal*, 19: 821-826

Charnley J. 1964. The Bonding of Prostheses to Bone by Cement, *The Journal of Bone and Joint Surgery*, 46B(3): 518-529.

Charnley J. 1979. *Low Friction Arthroplasty of the Hip: Theory and Practice*, 1st Edition, Springer-Verlag, Germany.

Clarke IC. 1982. Symposium on surface replacement arthroplasty of the hip: biomechanics: multifactorial design choices—an essential compromise? *Orthopaedic Clinics of North America*, 13:681–707.

Clarke SG, Phillips ATM, Bull AMJ and Cobb JP. 2012. A hierarchy of computationally derived surgical and patient influences on metal on metal press-fit acetabular failure, *J Biomechanics*, 45: 1698-1704.

Cohen D. 2011. Revision rates for metal on metal hip joints are double that of other materials, *BMJ*, 344:e1410.

Cohen D. 2012. How safe are metal-on-metal hip implants? *BMJ*, 344:e1410.

Coles JM, Chang DP and Zauscher S. 2010. Molecular mechanisms of aqueous boundary lubrication by mucinous glycoproteins, *Current Opinion in Colloid and Interface Science*, 15(6): 406-416.

Columbia University Medical Centre (CUMC). 2007. Anatomy of a joint, [online] Available at: http://www.cumc.columbia.edu/dept/rehab/musculoskeletal_health/anatomy.html [Accessed 21/04/2012].

Conroy JL, Whitehouse SL, Graves SE, Pratt NL, Ryan P and Crawford RW. 2008. Risk factors for revision for early dislocation in total hip arthroplasty, *J Arthroplasty*, 23(6): 867-872.

Cook SD, Thomas KA, Barrack RL and Whitecloud TS. 1992. Tissue growth into porous-coated acetabular components in 42 patients. Effects of adjunct fixation, *Clinical Orthopaedics and Related Research*, 283: 163-170.

Cornell CN. 2005. Management of acetabular fractures in the elderly patient, *Hospital for Special Surgery*, 1: 25-30.

Curtis MJ, Jinnah RH and Wilson VD. 1992. The Initial Stability of Uncemented Acetabular Components, *Journal of Bone and Joint Surgery*, 74B: 372-376.

Dalstra M, Huiskes R, Odgaard A, and van Erning L. 1993. Mechanical and textural properties of pelvis trabecular bone, *J Biomech*, 26: 523-535.

Daniel J, Pynsent PB and McMinn DJ. 2004. Metal-on-metal resurfacing of the hip in patients under the age of 55 years with osteoarthritis, *The Journal of Bone and Joint Surgery*, 86(B2): 177-184.

De Hann R, Pattyn C, Gill HS, Murray DW, Campbell PA and De Smet K. 2008. Correlation between inclination of the acetabular component and metal ion levels in

metal-on-metal hip resurfacing replacement, *The Journal of Bone and Joint Surgery*, 90B(10): 1291-1297.

De Hann R, Campbell PA, Su EP and De Smet KA. 2008. Revision of metal-on-metal resurfacing arthroplasty of the hip, *The Journal of Bone and Joint Surgery*, 90B(9): 1158-1163.

Dimaano F, Hermida J, D'Lima D, Cowell CW, Kulesha G. 2010. Comparison of the coefficient of friction of porous ingrowth surfaces, 56th Annual Meeting of the Orthopaedic Research Society, USA.

Dollar JV. 2004. Comparative Analysis of Weight Bearing Surfaces in Joint Arthroplasty, *The TM Journal*, 3(11).

Dowson D, McNie CM and Goldsmith AAJ. 2000. Direct experimental evidence of lubrication in a metal-on-metal total hip replacement tested in a joint simulator, *Proc. IMechE* 214(C): 75-86.

Dowson D. 2003. The relationship between steady-state wear rate and theoretical film thickness in metal-on-metal total replacement hip joints, *Tribology Series*, 41: 273-280.

Dowson D, Priest M, Dalnaz G and Lubrecht AA. 2003. Tribological research and design for engineering systems, 1st Edition, Elsevier Science, UK.

Dowson D, Hardaker C, Flett M and Isaac GH. 2004. A hip joint simulator study of the performance of metal-on-metal joints. Part II: Design, *J Arthroplasty*, 19(8): 124-130.

Dowson D. 2006. Tribological principles in mom hip joint design, *IMechE*. 220 161-171.

Ebied A and Journeaux S. 2002. Metal-on-Metal Hip Resurfacing, *Current Orthopaedics*, 16: 420-425.

Engh CA, O'Connor D, Jasty M, McGovern TF, Bobyn JD and Harris WH. 1992. Quantification of implant micromotion, strain shielding, and bone resorption with porous-coated anatomic medullary locking femoral prostheses, *Clin Orthop Relat Res*, 285: 13-29.

Engh CA Jr, MacDonald SJ, Sritulanondha S, Thompson A, Naudie D and Engh CA. 2009. John Charnley award: metal ion levels after metal-on-metal total hip arthroplasty: a randomized trial, *Clin Orthop Relat Res*, 467(1): 101-111.

Engh Jr. CA, Ho H, Engh CA. 2009. Metal-on-metal arthroplasty: Does early clinical outcome justify the change of an adverse local tissue reaction?, *Clin Orthop Relat Res*, 468(2): 406-412.

FDA. 2008. Class 2 recall Durom cup, [online] Available at:
<http://www.accessdata.fda.gov/scripts/cdrh/cfdocs/cfres/res.cfm?id=72744> [Accessed 11/05/2012]

Felippa CA. 2001. Introduction to finite element methods, [online] Available at:
<http://www.colorado.edu/engineering/CAS/courses.d/IFEM.d/> [Accessed 21/04/2012].

Firkins PJ, Tipper JL, Saadatzadeh MR, Ingham E, Stone MH, Farrar R and Fisher J. 2001. Quantitative analysis of wear and wear debris from metal on metal prostheses tested in a physiological hip joint simulator, *Biomed Mater Eng*, 11: 143-157.

Flannery M, Jones E and Birkinshaw C. 2008. Analysis of wear and friction of total knee replacements part II: Friction and lubrication as a function of wear, *Wear*, 265(7-8): 1009-1016.

Fritsche A, Bialek K, Mittelmeier W, Simnacher M, Fethke K, Wree A and Bader R. 2008. Experimental Investigations of the Insertion and Deformation Behaviour of Press-Fit and Threaded Acetabular Cups for Total Hip Replacement, *Journal of Orthopaedic Science*, 13: 240-247.

Furuya K, Tsuchiya M and Kawachi S. 1978. Socket-Cup Arthroplasty, Clinical Orthopaedics and Related Research, 134: 41-44.

Garellick G, Karrholm J, Rogmark C and Herberts P. 2010. Swedish hip arthroplasty register, Annual report, [online] Available at:

www.shpr.se/Libraries/Documents/AnnualReport-2009-EN.sflb.ashx [Accessed 21/04/2012].

Gerard Y. 1978. Hip Arthroplasty by Matching Cups, Clinical Orthopaedic and Related Research, 134: 25-35.

Gohar R and Rahnejat H. 2008. Fundamentals of Tribology, Imperial College Press, UK.

Gordon AC, D'Lima DD and Colwell CW. 2006. Highly cross-linked polyethylene in total hip arthroplasty, Journal of the American Academy of Orthopaedic Surgeons, 14(9): 511-523.

Grant JA, Bishop NE, Gotzen N, Sprecher C, Honi M and Morlock MM. 2007. Artificial composite bone as a model of human trabecular bone: the implant-bone interface, Journal of Biomechanics, 40: 1158-1164.

Green M and Nokes LDM. 1988. Engineering theory in orthopaedics: An introduction, 1st Edition, Ellis Horwood, UK.

Grigoris P, Roberts P, Panousis K and Jin Z. 2005. Hip resurfacing arthroplasty: the evolution of contemporary designs, Proceedings of IMechE, 220, Part H: Journal of Engineering in Medicine: 95-105

Grimes JB. 2010. Reclassification of metal-metal bearings based on operational clearance, 56th Annual Meeting of the Orthopaedic Research Society

Guedes RA, Simoes JA and Morais JL. 2006. Viscoelastic behaviour and failure of bovine cancellous bone under constant strain rate, Journal of Biomechanics, 39: 49-60.

Haddad FS, Thakrar RR, Hart AJ, Skinner JA, Nargol AVF, Nolan JF, Gill HS, Murray DW, Blom AW and Case CP. 2011. Metal-on-metal bearings. The evidence so far, *J Bone Joint Surg Br*, 93: 572-579.

Hall SJ. 2011. Basic biomechanics, 6th Edition, McGraw-Hill Higher Education, USA.

Hamrock BJ and Dowson D. 1978. Elastohydrodynamic lubrication of elliptical contacts for materials of low elastic modulus, *Transactions of the ASME, Journal of Lubrication Technology*, 100: 236-245.

Hart AJ, Buddhdev P, Whiship P, Faria N, Powell JJ, Skinner JA. 2008. Cup inclination angle of greater than 50 degrees increases whole blood concentrations of cobalt and chromium ions after metal-on-metal hip resurfacing, *Hip International*, 18-3: 212-219.

Hart AJ, Sabah S, Henckel J, Lewis A, Cobb J, Sampson B, Mitchell A, Skinner JA. 2009. The painful metal-on-metal hip resurfacing, *The Journal of Bone and Joint Surgery*, 91-B: 738-744.

Hart AJ, Ilo K, Underwood R, et al. 2011. The relationship between the angle of version and rate of wear of retrieved metal-on-metal resurfacings. A prospective, CT-based study. *J Bone Joint Surg Br* 93: 315-320.

Hart AJ, Lloyds G, Sabah S, Sampson B, Underwood R, Cann P et al. 2012a. Why do current generation metal on metal hip arthroplasties fail?, *J Bone Joint Surg Br* 94:65.

Hart AJ, Matthies A, Henckel J, Ilo K, Skinner J and Noble PC. 2012b. Understanding why metal-on-metal hip arthroplasties fail: a comparison between patients with well-functioning and revised Birmingham hip resurfacing arthroplasties, *J Bone Joint Surg Am* 94(4):22.

Havelin L, Engesaeter L, Espehaug B, Furnes O, Lie S and Vollset S. 2000. The Norwegian arthroplasty register: 11 years and 73,000 arthroplasties, *Acta Orthopaedica Scandinavica* 71: 337-353.

Hogg MC and Gilles RM. 2009. Impaction of a press-fit acetabular cup using a dynamic finite element model, 55th Annual Meeting of the Orthopaedic Research Society, USA.

Hogg MC and Gilles RM. 2010. Impaction of a typical press-fit modular acetabular cup using a dynamic finite element method: The effect of cup oversizing and shell wall thickness on cup deformation and shell-liner uncoupling, 56th Annual Meeting of the Orthopaedic Research Society, USA.

Hothi HS, Busfield JJC and Shelton JC. 2011. Explicit Finite Element Modelling of the Impaction of Metal Press-Fit Acetabular Components, The Journal of Engineering in Medicine, Proc IMechE, Part H, 225: 301-314.

Hothi HS, Busfield JJC, Shelton JC. 2012. Deformation of Uncemented Metal Acetabular Cups following Impaction: Experimental and Finite Element Study. Submitted to Comput Methods Biomech Biomed Engin.

Howie DW, Neale SD, Stamenkov R, McGee MA, Taylor DJ and Findlay DM. 2007. Progression of acetabular periprosthetic osteolytic lesions measured with computed tomography, J Bone Joint Surg Am, 89(8): 1818-1825.

Huiskes R. 1993. Failed innovation in total hip replacement. Diagnosis and proposals for a cure, Acta Orthop Scand. 64(6): 699-716.

Isaac GH, Siebel T, Schmalzried TP Cobb AG, O'Sullivan T, Oakeshott RD, Flett M and Vail TP. 2006. Development rationale for an articular surface replacement: a science-based evolution, Proc IMechE, Part H, 220: 253-268.

Jacobs JJ and Craig TL. 1998. Alternative Bearing Surfaces in Total Joint Replacement, American Society of Testing and Materials, 6(4): 198-203.

Jacobsson SA, Djerf K and Wahlstrom O. 1996. Twenty-Year Results of McKee-Farrar versus Charnley Prosthesis, Clinical Orthopaedics and Related Research, 329: S60-8.

Jedemalm A, Nilsson F, Noz ME, Green DD, Gedde UW, Clarke IC, Stark A, Maguire GQ, Zeleznik P and Olivecrona H. 2010. Validation of a 3D CT method for measurement of linear wear of acetabular cups. A hip simulator study, *Acta Aorthop*, 82(1): 35-41.

Jia YM, Cheng LM, Yu GR, Du CF, Yang ZY and Ding ZQ. 2008. A finite element analysis of the pelvis reconstruction using fibular transplantation fixed with four different rod-screw systems after type I resection, *Chinese Medical Journal*, 121(4): 321-326.

Jin ZM, Meakins S, Morlock MM, Parsons P, Hardaker C, Flett M and Issac G. 2006. Deformation of Press-Fitted Metallic Resurfacing Cups Part 1: Experimental Simulation, *The Journal of Engineering in Medicine, Proc IMechE*, 220, Part H: 299-309.

Jones LC and Hungerford DS. 1987. Cement Disease, *Clinical Orthopaedics and Related Research*, 225: 192-206.

Kadir MRA. 2010. Finite element analysis of idealised unit cell cancellous structure based on morphological indices of cancellous bone, *Medical and Biological Engineering and Computing*, 48(5): 497-505.

Karrholm J, Borsen B, Lowenhielm G, Snorrason F. 1994. Does early micromotion of femoral stem prostheses matter? 4-7 year stereoradiographic follow-up of 84 cemented prostheses, *J Bone Joint Surg Br*, 76(6): 912-917.

Keller TS. 1994. Predicting the compressive mechanical behaviour of bone. *J Biomechanics* 27: 1159-1168.

Kennedy JG, Rogers WB, Soffe KE, et al. 1998. Effect of acetabular component orientation on recurrent dislocation, pelvis osteolysis, polyethylene wear and component migration, *J Arthroplasty*, 13: 530-534.

Khairy A. 2005. Tribology, [online] Available at:

http://www.arthroclub.egydoc.com/sites/arthroclub/AC_Files/Articles/article83.pdf
[Accessed 21/04/2012].

Kim YS, Callaghan JJ and Ahn PB. 1995. Fracture of the Acetabulum during Insertion of an Oversized Hemispherical Component, *The Journal of Bone and Joint Surgery*, 77A: 111-117.

Kowalczyk P. 2003. Elastic properties of cancellous bone derived from finite element models of parameterized microstructure cells, *Journal of Biomechanics*, 36(7): 961-972.

Krebs V, Incavo SJ and Shields WH. 2009. The anatomy of the acetabulum: What is Normal?, *Clinical Orthopaedics and Related Research*, 467: 868-875.

Kristiansen B, Jorgensen L and Holmich P. 1985. Dislocation following total hip arthroplasty, *Arch Orthop Trauma Surg*, 103(6): 375-377.

Kroeber M, Ries MD and Suzuki Y. 2002. Impact Biomechanics and Pelvic Deformation during Insertion of Press-Fit Acetabular Cups, *The Journal of Arthroplasty*, 17: 349-354.

Kwong LM, O'Connonr DO and Sedlacek RC. 1994. A Quantitative In Vitro Assessment of Fit and Screw Fixation on the Stability of Cementless Hemispherical Acetabular Component, *The Journal of Arthroplasty*, 9: 1663-170.

Langton DJ, Jameson SS, Joyce TJ, Webb J, Nargol AVF. 2008. The effect of component size and orientation on the concentrations of metal ions after resurfacing arthroplasty of the hip, *The Journal of Bone and Joint Surgery*, 90B: 1143-1151.

Langton DJ, Jameson SS, Joyce TJ, Hallab NJ, Natsu S and Nargol AVF. 2010. Early failure of metal-on-metal bearings in hip resurfacing and large-diameter total hip replacement. A consequence of excess wear, *J Bone Joint Surg Br*, 92(1) 38-46.

Langton DJ, Jameson SS, Joyce TJ, Gandhi JN, Sidaginamale R, Mereddy P, Lord J and Nargol AVF. 2011. Accelerating failure rate of the ASR total hip replacement, *J Bone Joint Surg Br*, 93(8): 1011-1016.

Latteier MJ, Berend KR, Lombardi AV, Ajluni AF, Seng BE and Adams JB. 2011. Gender is a significant factor for failure of metal-on-metal total hip arthroplasty, *The Journal of Arthroplasty*, 26(6): 19-23.

Laursen MB, Nielsen PT and Soballe K. 2007. Bone remodelling around HA-coated acetabular cups, *Int Orthop*, 31(2): 199-204.

Levangie PK and Norkin CC. 2005. Joint structure and function: A comprehensive analysis, 4th Edition, FA Davis, USA.

Lewinnek GE, Lewis JL, Tarr R, Compere CL, Zimmerman JR. 1978. Dislocations after total hip replacement arthroplasties, *Journal of Bone and Joint Surgery*, 60: 217-220.

Liu F, Jin Z, Roberts P and Grigoris P. 2006. Importance of head diameter, clearance and cup wall thickness in elastohydrodynamic lubrication analysis of metal-on-metal hip resurfacing prostheses, *Proc. IMechE* 220(6): 695-704.

Long WT. 2005. The clinical performance of metal-on-metal as an articulations surface in total hip replacement, *Iowa Orthopaedic Journal*, 25: 10-16.

Lotz JC, Gerhart TN and Hayes WC. 1990. Mechanical properties of trabecular bone from the proximal femur: a quantitative CT study, *J Comput Assist Tomogr*, 14: 107-114.

Macdonald W, Carlsson LV, Charnley GJ and Jacobsson CM. 1999. Press-fit acetabular cup fixation: principles and testing, *Proceedings of the Institution of Mechanical Engineers, Part H: Journal of Engineering in Medicine*, 213, 33-39.

Macdonald W, Carlsson LV, Charnley GJ, Jacobsson CM and Johansson CB. 1999. Inaccuracy of acetabular reaming under surgical conditions, *The Journal of Arthroplasty*, 14(6): 730-737.

MacKenzie JR, Callaghan JJ, Pedersen DR and Brown TD. 1994. Areas of Contact and Extent of Gaps with Implantation of Oversized Acetabular Components in Total Hip Arthroplasty, *Clinical Orthopaedics and Related Research*, 298: 127-136.

Mak MM, Besong AA, Jin ZM and Fisher J. 2002. Effect of microseparation on contact mechanics in ceramic-on-ceramic hip joint replacement. *Proc. IMechE* 216: 403-408.

Malchau H, Herberts P, Eilert T, Garellick G and Soderman P. 2002. The Swedish Total Hip Replacement Register, *Journal of Bone and Joint Surgery*, 85(5): 970.

Marieb EN and Hoehn K. 2010. Human anatomy and physiology, 8th Edition, Pearson International Edition, USA.

Markel D, Day J and Siskey R. 2010. Deformation of metal-backed acetabular components and the impact of liner thickness in a cadaveric model, *International Orthopaedics*, 35(8): 1131-1137.

Martini FH and Bartholomew EF. 2000. Essentials of anatomy and physiology, 2nd Edition, Prentice Hall, USA.

Matthews JB, Green TR, Stone MH, Wroblewski BM, Fisher J and Ingham E. 2000. Comparison of the response of primary human peripheral blood mononuclear phagocytes from different donors to challenge with model polyethylene particles of known size and dose, *Biomaterials*, 21(20): 2033-2044.

Matthies A, Underwood R, Cann P, et al. 2011. Retrieval analysis of 240 metal-on-metal hip components, comparing modular total hip replacement with hip resurfacing, *J Bone Joint Surg Br* 93(3): 307-314.

Matthies AK, Henckel J, Skinner JA, Hart AJ. 2011. A retrieval analysis of explanted Durom metal-on-metal hip arthroplasties. *Hip Int* 21(6): 724-731.

Matthies AK, Henckel J, Skinner JA, Hart AJ. 2012. Pseudotumors are common in well positioned, low wearing retrieved metal-on-metal hip arthroplasties, Annual Meeting of the American Academy of Orthopaedic Surgeons, USA.

McEwen HM, Barnett PI, Bell CJ, Farrar R, Auger DD, Stone MH and Fisher J. 2005. The influence of design, materials and kinematics on the in vitro wear of total knee replacements, *J Biomech*, 38(2): 357-365.

McKee GK and Watson-Farrar J. 1966. Replacement of Arthritic Hips by the McKee-Farrar Prosthesis, *The Journal of Bone and Joint Surgery*, 48B(2): 245-259.

McKellop H, Park SH, Chiesa R, Doorn P, Lu B, Normand P, Grigoris P and Amstutz H. 1996. In vivo wear of 3 types of metal on metal hip prostheses during 2 decades of use, *Clinical Orthopaedics and Related Research*, 329: 128-140.

McMinn D and Daniel J. 2005. History and modern concepts in surface replacement, *Proceedings of IMechE*, 220, Part H, *Journal of Engineering in Medicine*: 239-251.

Medical Blog. 2009. Pelvis injuries, [online] Available at:
<http://www.blog-medico.com.ar/noticias-medicina/emergencia/traumatismo-de-pelvis.htm> [Accessed 21/04/2012].

Medley JB. 2008. Tribology of bearing materials, Hip resurfacing: Principles, indications, technique and results, 1st Edition, Saunders Elsevier, USA.

Medley JB, Chan FW, Krygler JJ and Bobyn DJ. 1996. Comparison of alloys and designs in a hip simulator study of metal on metal implants, *Clinical Orthopaedics and Related Research*, 329: 148-159.

Mont MA, Seyler TM, Ulrich SD, Beaulé PE, Boyd HS, Grecula MJ, Goldberg VM, Kennedy WR et al. 2007. Effect of changing indications and techniques on total hip resurfacing, *Clinical Orthopaedics and Related Research*, 465: 63-70.

Mootanah R, van der Linde I, Ingle P, Cheah K, Dowell J and Shelton JC. 2001. An accurate 3-D finite element model of the pelvic bone with geometry and material properties retrieved from CT-scan data, *Computer Simulations in Biomechanics, Proc of ISCSB, LCM Selecta Group*: 81–84.

Morlock M, Schneider E, Bluhm A, Vollmer M, Bergmann G, Muller V and Honl M. 2001. Duration and frequency of every day activities in total hip patients, *Journal of Biomechanics*, 34: 873-881.

Morlock MM, Bishop N, Zustin J, Han M, Ruther W and Amling M. 2008. Modes of implant failure after hip resurfacing: Morphological and wear analysis of 267 retrieval specimens, *The Journal of Bone and Joint Surgery*, 90: 89-95.

Morscher EW. 1983. Cementless Total Hip Arthroplasty, *Clinical Orthopaedics and Related Research*, 181: 76-91.

Najarian BC, Kilgore JE, Markel DC. 2009. Evaluation of component positioning in primary total hip arthroplasty using an imageless navigation device compared with traditional methods, *The Journal of Arthroplasty*, 24(1): 15-21.

Nagle JA. 2011. A quick guide to hip hemiarthroplasty, *OR Nurse*, 5(4): 30-37.

National Cancer Institute (NCI). 2009. Anatomical Terminology, [online] Available at: <http://training.seer.cancer.gov/anatomy/body/terminology.html> [Accessed 21/04/2012].

National Institute for Health and Clinical Excellence (NICE). 2011. Hip fracture. The management of hip fracture in adults, [online] Available at: <http://www.nice.org.uk/nicemedia/live/13489/54919/54919.pdf> [Accessed 12/05/2012].

National Joint Registry (NJR). 2010. National joint registry of England and Wales 7th annual report, [online] Available at: <http://www.njrcentre.org.uk> [Accessed 21/04/2012].

Ng FY, Zhu Y, Chiu KY. 2007. Cementless acetabular component inserted without screws-the effect of immediate weight bearing, *Int Orthop* 31: 293-296.

Ong KL, Rundell S, Liepins I, Laurent R, Markel D and Kurtz SM. 2009. Biomechanical Modelling of Acetabular Component Polyethylene Stresses, Fracture Risk, and Wear Rate following Press-Fit Implantation, *Journal of Orthopaedic Research*, 27(11): 1467-72.

Perez MA, Fornells P, Garcia-Aznar M and Doblare M. 2011. Validation of bone remodelling models applied to different bone types using mimics, [online] Available at: <http://uc.materialise.com/mimics/resources/articles?tid=39> [Accessed 21/04/2012].

Perona PG, Lawrence J, Paprosky WG, Patwardhan AG and Sartori M. 1992. Acetabular micromotion as a measure of initial implant stability in primary hip arthroplasty, *J Arthroplasty*, 7(4): 537-547.

Peters CL and Miller MD. 2006. The cementless acetabular component, *The Adult Hip*, 2nd Edition, Lippincott Williams and Wilkins, USA.

Pilliar RM, Lee JM and Maniopoulos C. 1986. Observations on the effect of movement on bone ingrowth into porous-surfaced implants. *Clin Orthop Relat Res*, 208:108-113.

Poitout DG. 2004. Biomechanics and Biomaterials in Orthopaedics. 1st Edition, Springer, USA.

Ranawat AS and Ranawat CS. 2006. The cemented acetabulum: Rationale and technique, *The Adult Hip*, 2nd Edition, Lippincott Williams and Wilkins, USA.

Rao SS. 2010. The finite element method in engineering, 5th Edition, Butterworth-Heinemann, UK.

Ratner BD, Hoffman AS, Schoen FJ and Lemons JE. 2004. An Introduction to Materials in Medicine, 2nd Edition, California, Elsevier Academic Press: 535.

Rieker CB, Schon R, Konrad R, Liebentritt G, Gnepf P, Shen M, Roberts P and Grigoris P. 2005. Influence of clearance on in-vitro tribology of large diameter metal-on-metal articulations pertaining to resurfacing implants, Orthop Clin North Am, 36(2): 135-142.

Ries MD and Harbaugh M. 1997. Acetabular Strains Produced by Oversized Press-Fit Cups, Clinical Orthopaedics and Related Research, 334: 276-281.

Roy RK. 2001. Design of experiments using the taguchi approach: 16 steps to product and process improvement, 1st Edition, John Wiley & Sons, USA.

Ryan JA, Jamali AA, Bargar WL. 2010. Accuracy of Computer Navigation for Acetabular Component Placement in THA, Clinical Orthopaedics and Related Research, 468: 169-177.

Salzer M, Knahr K, Locke H and Stark N. 1978. Cement-Free Bioceramic Double-Cup Endoprosthesis of the Hip-Joint, Clinical Orthopaedics and Related Research, 134: 80-86.

Sandborn PM, Cook SD, Spires WP and Kester MA. 1988. Tissue Response to Porous-Coated Implants Lacking Initial Bone Apposition, The Journal of Arthroplasty, 3: 337-46.

Sawbones. 2009. Solid Rigid Polyurethane Foam, [online] Available: <http://www.sawbones.com/products/bio/testblocks/solidfoamaspx> [Accessed 21/04/2012].

Sariali E, Lazennec JY, Khiami F and Catonne Y. 2009. Mathematical evaluation of jumping distance in total hip arthroplasty, Acta Orthopaedica, 80(3): 277-282.

Schnurr C, Nessler J, Meyer C, Schild HH, Koebke J and Konig DP. 2009. Is a valgus position of the femoral component in hip resurfacing protective against spontaneous fracture of the femoral neck?, *The Journal of Bone and Joint Surgery*, 91B(4): 545-551.

Sharkey PF, Hozack WJ and Callaghan JJ. 1999. Acetabular Fracture Associated with Cementless Acetabular Component Insertion: A Report of 13 Cases, *The Journal of Arthroplasty*, 14:426-431.

Shetty NR, Hamer AJ, Kerry RM, Stockley I, Eastell R and Wilkinson JM. 2006. Bone remodelling around a cemented polyethylene cup. A longitudinal densitometry study, *J Bone Joint Surg*, 88(4): 455-459.

Simulia. 2010. Abaqus User's Manual, Simulia, USA.

Smith AJ, Dieppe P, Vernon K, Porter M and Blom AW. 2012. Failure rates of stemmed metal-on-metal hip replacements: analysis of data from the National Joint Registry of England and Wales, *Lancet*, 379(9822): 1199-1204.

Spears IR, Morlock MM, Pfeiderer M, Schneider E and Hille E. 1999. The influence of friction and interference on the seating of a hemispherical press-fit cup: a finite element investigation, *Journal of Biomechanics*, 32: 1183 – 1189.

Springer BD, Griffin WL, Fehring TK, Suarez J, Odum S and Thompson C. 2008. Incomplete Seating of Press-Fit Porous-Coated Acetabular Components, *The Journal of Arthroplasty*, 23(6): 121-126.

Springer BD, Habet NA, Griffin WL, et al. 2012. Deformation of 1-piece metal acetabular component, *J Arthroplasty* 27(1): 48-54.

Squire M, Griffin WL, Bohannon M, Peindl RD and Odum S. 2006. Acetabular Component Deformation with Press-Fit Fixation, *The Journal of Arthroplasty*, 21: 72-77.

Smith SL, Dowson D and Goldsmith AAJ. 2001. The effect of femoral head diameter upon lubrication and wear of metal-on-metal total hip replacements, Proc. IMechE 215(H): 161-170.

Smith & Nephew. 2010. Surgical technique: Acetabular system, [online] Available at: www.aura-group.cz/pdf/R3-operacni-manual.pdf [Accessed 19/05/2012].

Standring S. 2004. Gray's anatomy: The anatomical basis of clinical practice, 39th Edition, Churchill Livingstone, UK.

Stiehl JB, MacMillan E and Skrade DA. 1992. Mechanical Stability of Porous-Coated Acetabular Components in Total Hip Arthroplasty, The Journal of Arthroplasty, 6:295-300.

Sundfeldt M, Carlsson LV, Johanson CB, Thomsen P and Gretzer C. 2006. Aseptic loosening, not only a question of wear: a review of different theories, Acta Orthop, 77(2): 177-197.

Tauge RG. 1989. Variation in pelvic size between males and females, American Journal of Physical Anthropology, 80: 59-71.

Thompson MS, Flivik G, Juliusson R, Odgaard A and Ryd L. 2004. A comparison of structural and mechanical properties in cancellous bone from the femoral head and acetabulum, Proceedings of the IMechE, Part H: Journal of Engineering in Medicine, 218: 425-429.

Tortora GJ and Derrickson B. 2006. Principles of anatomy and physiology, 11th Edition, John Wiley and Sons, USA.

Treacy RBC, McBryde CW, Shears E and Pynsent PB. 2011. Birmingham hip resurfacing. J Bone Joint Surg Br, 93: 27-33.

Trentani MD and Vaccarino F. 1978. The Paltrinieri-Trentani Hip Joint Resurface Arthroplasty, *Clinical Orthopaedics and Related Research*, 134: 36-40.

Tsai S and Pawar V. 2010. A bi-layer foam block model to evaluate deformation of a modular metal-on-metal acetabular liner design, 56th Annual Meeting of the Orthopaedic Research Society, USA.

Turner CH, Rho J, Takano Y, Tsui TY and Pharr GM. 1999. The elastic properties of trabecular and cortical bone tissues are similar: results from two microscopic measurement techniques, *Journal of Biomechanics*, 32: 437-441.

Udofia I. 2007. The initial stability and contact mechanics of a press-fit resurfacing arthroplasty of the hip. *J Bone Joint Surg Br* 89: 549-556.

Underwood RJ, Zografos A, Sayles RS, Hart A and Cann P. 2012. Edge loading in metal-on-metal hips: low clearance is a new risk factor, *Proc. IMechE* 226(3): 217-226.

US Food and Drug Administration (FDA). 2012. Metal-on-metal hip implants, [online] Available at:

<http://www.fda.gov/MedicalDevices/ProductsandMedicalProcedures/ImplantsandProsthetics/MetalonMetalHipImplants/default.htm> [Accessed 21/04/2012].

Valle AGD, Padgett DE, Salvati ED. 2005. Preoperative planning for primary total hip arthroplasty, *J Am Acad Orthop Surg* 13(7): 455-462.

Van der Vis HM, Aspenberg P, Marti RK, Tigchelaar W and Van Noorden CJ. 1998. Fluid pressure causes bone resorption in a rabbit model of prosthetic loosening, *Clin Orthop Relat Res*, 350: 201-208.

Wagner M and Wagner H. 1996. Preliminary Results of Uncemented Metal-on-Metal Stemmed and Resurfacing Hip Replacement Arthroplasty, *Clinical Orthopaedics and Related Research*, 329: S78-S88.

Wan Z, Malik A, Jaramaz B, Chao L and Dorr LD. 2009. Imaging and navigation measurement of acetabular component position in THA, *Clinical Orthopaedics and Related Research*, 467: 32-42.

Weber BG. 1996. Experience with the Metal Total Hip Bearing System, *Clinical Orthopaedics and Related Research*, 329: S69-S77.

West C and Fryman JC. 2008. Cadaveric measurement of impact force on total hip arthroplasty surgical instrumentation, American Society of Biomechanics Conference Abstract, [online] Available:
<http://www.asbweborg/conferences/2008/abstracts/173pdf> [Accessed 21/04/2012].

Wheless CR. 2011. Acetabular component position, [online] Available at:
http://www.whelessonline.com/ortho/acetabular_component_position [Accessed 21/04/2012].

Which Medical Device (WMD). 2011. Pinnacle acetabular cup system, [online] Available at:
<http://www.whichmedicaldevice.com/by-manufacturer/86/254/pinnacle-acetabular-cup-system#product-description> [Accessed 19/05/2012].

Widmer KH, Zurfluh B, and Morscher EW. 2002. Load transfer and fixation mode of press-fit acetabular sockets, *The Journal of Arthroplasty*, 177: 926-935.

Williams PA, Yamamoto K, Masaoka T, Oonishi H and Clarke IC. 2007. Highly crosslinked polyethylenes in hip replacements: Improved wear performance or paradox?, *Tribology Transactions*, 50(2): 277-290.

Won CE, Hearn TC and Tile M. 1995. Micromotion of Cementless Hemispherical Acetabular Components, *The Journal of Bone and Joint Surgery*, 77: 484-489.

Wright Medical. 2007. Metal-on-metal articulation and wear, [online] Available at:

www.surfacehippy.info/metalonmetalfaq.pdf [Accessed 21/04/2012].

Wright Medical Technology. 2009. Lineage acetabular cup system, [online]
Available at: <http://www.wmtcom/downloads/techniques/lineageceramicstpdf>
[Accessed 21/04/2012].

Wroblewski BM, Taylor GW and Siney P. 1992. Charnley Low Friction Arthroplasty: 19-25 Years Results, *Orthopaedics*; 15: 421-424.

Yew A, Jin ZM, Donn A, Morlock MM and Isaac, G. 2006. Deformation of Press-Fitted Metallic Resurfacing Cups Part 2: Finite Element Simulation, *The Journal of Engineering in Medicine, Proc IMechE*, 220, Part H: 311-319.

Zimmer.2008. Surgical technique, [online] Available at:
http://www.zimmer.com/web/enUS/pdf/surgical_techniques/Metasul_LDH_Large_Diameter_Head_with_Durom_Acetabular_Component.pdf [Accessed 19/05/2012].